JUNE 2015 Ph.D. in CIVIL ENGINEERING MUTHANNA ADIL NAJM

UNIVERSITY OF GAZİANTEP

GRADUATE SCHOOL OF

NATURAL & APPLIED SCIENCES

MODELLING AND ANALYSIS OF INTERFACE IN COMPOSITE BOX GIRDER BRIDGES

Ph.D. THESIS

IN

CIVIL ENGINEERING

BY

MUTHANNA ADIL NAJM

JUNE 2015

Modelling and Analysis of Interface in Composite Box Girder Bridges

Ph.D. Thesis

in

Civil Engineering

University of Gaziantep

Supervisor

Prof. Dr. Mustafa ÖZAKÇA

Co -Supervisor

Assist. Prof. Dr. Talha EKMEKYAPAR

by

Muthanna Adil NAJM

June 2015

T.C

REPUBLIC OF TURKEY

UNIVERSITY OF GAZİANTEP

GRADUATE SCHOOL OF NATURAL & APPLIED SCIENCES

CIVIL ENGINEERING DEPARTMENT

Name of the thesis: Modelling and Analysis of Interface in Composite Box Girder Bridges

Name of the student: Muthanna AdilNAJM

Exam date: June 11, 2015

Approval of the Graduate School of Natural and Applied Sciences

Prof. Dr. Metin BEDİR
Director

I certify that this thesis satisfies all the requirements as a thesis for the degree of Doctor of Philosophy.

Prof. Dr. Mustafa GÜNAL
Head of Department

This is to certify that we have read this thesis and that in our consensus/majority opinion it is fully adequate, in scope and quality, as a thesis for the degree of Master of Science/Doctor of Philosophy.

Assist. Prof. Dr. Talha EKMEKYAPAR
Co-Supervisor

Prof. Dr. Mustafa ÖZAKÇA
Supervisor

Examining Committee Members:	Signature
Prof. Dr. Hacı Murat ARSLAN	....
Prof. Dr. Mustafa ÖZAKÇA	....
Prof. Dr.Abdulkadir ÇEVİK	....
Assoc. Prof. Dr. Mustafa ŞAHMARAN	....
Assist. Prof. Dr.Nildem TAYŞİ	....

I hereby declare that all information in this document has been obtained and presented in accordance with academic rules and ethical conduct. I also declare that, as required by these rules and conduct, I have fully cited and referenced all material and results that are not original to this work.

Muthanna Adil NAJM

ABSTRACT

MODELLING AND ANALYSIS OF INTERFACE IN COMPOSITE BOX GIRDER BRIDGES

NAJM, Muthanna Adil
Ph.D. in Civil Engineering
Supervisor: Prof. Dr. Mustafa ÖZAKÇA
Co- Supervisor: Assist. Prof. Dr. Talha EKMEKYAPAR
JUNE 2015, 207 pages

The role of composite box bridges in the interchanges of modern highway systems has become more and more popular for functional, economic and artistic considerations. This type of structure, guides to an efficient transverse load distribution due to excellent torsional stiffness of the part. Further utilities and services can be readily provided within the boxes. In this thesis as a first approach a study of the effect of shear connector's numbers and distribution on the behaviour of composite box girder bridges is submitted. Additionally, several finite element models are developed to assessed against the results acquired from a field test. A number of factors are considered, and confirmed through available experimental results, especially full shear connections, which are obviously essential in composite box girder. A good representative for shear connectors of suitable finite element type is considered. Preparatory results signalize that number of shear studs can be obviously reduced to facilitate adoption of a new arrangement in design of composite box girder bridges with full makeup. The parametric investigations are performed along with the composite box girder model to appraise the effects of several important parameters on the behaviour of the girder. The outcomes from this study would enable bridge engineers to design composite box girder bridges more reliably and economically. Referable to the complexity of the three-dimensional interaction between shear connector and concrete, there is little success in numerical modelling of the push-out test in literature. A three-dimensional finite element model with multiple elements was counseled to simulate shear connector based on static loading. The interaction between the steel connector and concrete will cause the main significance of the global behaviour of the structural element. The geometry and material nonlinearities of headed stud, steel beam were included in the finite element model. Contact regions between the concrete and steel elements are simulated using surface to surface and embodiment techniques. Shear capacity for studs are obtained and results compared with various codes of practices such as EC4, AISC and BS and BS5950. The proposed model was used to estimate the load-slip curve and to analyse important phenomena of the mechanical behaviour of connectors that are usually difficult to evaluate through tests.

Key Words: Partial interaction, Shear Connector, Finite element method, Composite box girder, Full interaction.

ÖZET

KOMPOZIT KUTU KIRIŞ KÖPRÜLERIN ARAYÜZEY MODELLEME VE ANALIZ

NAJM, Muthanna Adil
Doktora Tezi, Inşaat Mühendisliği Bölümü
Tez Yöneticisi: Prof. Dr. Mustafa ÖZAKÇA
Yardimci Tez Yöneticisi: Yrd. Doç. Dr. Talha EKMEKYAPAR
June 2015, 207 sayfa

Kompozit kutu kiriş köprülerin fonksiyonelliği, ekonomik olması ve görselliği sebebiyle otoyol geçiş bölgelerindeki rolü gittikçe önem kazanmaktadır. Bu tip bir yapı burulma rijitliğinin çok iyi olması sayesinde enine doğrultudaki yük transeferini çok iyi şekilde yapar. Bu tip yapılar sayesinde daha başka faydalar ve servis koşulları sağlanır. Bu tez çalışmasında öncelikle kesme saplamasi bağlantılarının sayısının ve dağılımının kompozit kutu kiriş köprülerin davranışına etkileri ile ilgili bir çalışma yapılmıştır. Sonra, değişik sonlu eleman modelleri kurularak bu modellerin doğruluğu literatürdeki laboratuvar test sonuçları ile karşılaştırılmıştır. Göz önüne alınan belirli faktörler deney sonuçları ile doğrulanıp özellikle kutu kiriş köprüler için önemli olan tam kesme modele bağlantıları üzerine odaklanılmıştır. Kesme saplamasi bağlantıları için uygun sonlu eleman modelleri değerlendirilmiştir. Sonuçlar kesme saplamasi bağlantısı sayısının kutu kiriş köprü tasarımlarında yeni düzenlemeler yapılması için azaltılabileceğini işaret etmektedir. Kompozit kutu kiriş modeli üzerinde değişik parametrelerin etkilerini belirlemek için parametrik çalışmalar yapılmıştır. Bu çalışmanın sonuçları köprü mühendislerinin daha güvenilir ve ekonomik kompozit kutu kiriş tasarımları oluşturabilmesini sağlayabilecektir. Kesme saplamasi bağlantıları ile betonun üç boyutlu karmaşık etkileşimi sebebiyle literatürde bu bağlantılar için yapılan testlerin nümerik modelleri çok başarılı değildir. Bu çalıbase modelada kesme saplamasi bağlantıları için statik yükler göz önüne alınarak üç boyutlu sonlu elemanlar modelleri kurulmuştur. Çelik kesme saplamasi bağlantısı ile beton arasındaki etkileşim yapının genel davranışını önemli ölçüde etkileyebilecek düzeydedir. Sonlu elemanlar modellerinde çelik kiriş ve kesme saplamasi bağlantısı için geometrik ve malzeme davranışında lineer olmayan özellikler dahil edilmiştir. Sonlu elemanlar modellerinde beton ve çelik etkileşimi yüzey kontak elemanları kullanılarak sağlanmıştır. Kesme saplamasi bağlantılarının elde edilen kesme saplamasi kapasiteleri EC4, AISC, BS ve BS5950 gibi değişik tasarım şartnameleriyle karşılaştırılmıştır. Önerilen model yük-kayma eğrisini elde etmede ve bu tip testlerde gerilmelerin dağılımını ölçmede yaşanabilecek zorluk gibi kesme saplamasi bağlantılarının mekanik davranışını analizinde kullanılmıştır.

Anahtar Kelimeler: kıbase modeli kesme saplamasi, kesme saplamasi bağlantısı, sonlu eleman modelleri, Kompozit kutu kiriş, tam kesme saplamasi

ACKNOWLEDGEMENTS

I would like to express my special appreciation and thanks to my advisor Professor Dr. Mustafa ÖZAKÇA, who have been a tremendous mentor for me. I would like to thank him for encouraging my research and for allowing me to grow as a research scientist. His advice on both research as well as on my career have been priceless.

I would like to express sincere gratitude to my co-supervisor Assist. Prof. Dr. Talha EKMEKYAPAR for his patience, guidance and support throughout this study.

I would also like to thank my committee members, for serving as my committee members even at hardship, and for brilliant comments and suggestions.

I would also like to express sincere thanks to the FTE /Technical College of Mosul for providing me with a Graduate Scholarship for the duration of my Ph.D. program. I take this opportunity to express gratitude to all of the college members for their help and support.

Sincere thanks are also due to the staff of the civil engineering of the University of Gaziantep in assisting me in my study.

A special thanks to my family. Words cannot express how grateful I am to my father spirit Prof. Dr. Adil NAJM that his words lead me to get certificates, and my mother Feryal, for all of the sacrifices that you've made on my behalf. Your prayer for me was what sustained me thus far. Also to all my brothers and sisters.

I am greatly indebted to my wife, All'a for their strong encouragement during the years of my study.

TABLE OF CONTENTS

LIST OF FIGURES

LIST OF TABLES

LIST OF SYMBOLS

Scalars

K	The slop of the load- slip curve for the connectors.
E_c	Elastic modulus in compression and tension.
Q_x	The longitudinal shear force on a connector at distance *x* from the web center.
q	Design longitudinal shear due to global and local loadings per unit length.
b_w	Half the distance between the centerlines of adjacent webs.
p	Percentage of reduction %.
x_2	Span length X (0.025).
ε_c	The strain in the lower edge of the concrete.
ε_s	The slip of the upper part of the steel part.
Uc	The slip in the concrete.
$\Delta\varepsilon$	The slip strain is the rate of change of slip along the beam.
a & b	Constants of idealized load/slip function of a shear connector.
Q	The shear load on a shear connector.
γ	The slip at the interface.
P_u	The shear resistance of a headed stud.
$\emptyset$	Resistance factor for shear connectors.
d	Diameter of the studs.
Fu	Ultimate tensile strength of the stud.
$f c$	Compressive strength of concrete cylinders.
γ_v	The partial safety factor.
α	Factor =0.2 (H/d+l).

H	Height of the studs.
ε_{yc}	Average values of yield strain.
f_{yc}	Yield stress.
S_1	Distance before reduction.
S_2	Initial distance from the edge of top flange without reduction.
S_3	Cumulative uniform spacing.
L	Span length.
Dc	Concrete depth.
TW	Web thickness.
HW	Web depth
HR	Haunch ratio.
TF	Flange thickness.

CHAPTER 1

INTRODUCTION

1.1 General

Box girders are used in the growth of urban expressways, evenly in banded, and long-span bridges. Box girders have a higher flexural limit and torsional inflexibility, and the closed shape diminishes the uncovered surface, making them less exposed to erosion. Box girders likewise provide base modelooth and aesthetically satisfying structures.

The role of composite bridges in the interchanges of modern highway systems has become more and more popular for functional, economic and artistic considerations. This case of structure, guides to an efficient transverse load distribution due to excellent torsional stiffness of the part. Further utilities and services can be readily provided within the boxes.

Compared with its non-composite counterpart with the same components, a composite bridge tends to have greater stiffness, higher load capacity against material damage. Consequently, a composite section is generally base modelaller compared to alternative designs to sustain the same load, thus resulting material and weight saves. Compared with reinforced concrete construction, composite construction allows the use of prefabricated units and has the advantage of providing facilities for the support of soffit shuttering.

The obvious difference between concrete and composite box girders is the need to provide shear connectors and the necessary labour involved. Compared with reinforced concrete, a composite bridge deck incurs the subsequent cost of steel maintenance, i.e. painting.

In spite of predominance of such bridges, codes of practice, such as BS5400, AASHTO do not provide detailed provisions for their analysis and design. This is especially the case for multicellular and composite box girders. In most cases the codes recommend that the loading effects which cannot be predicted by the elements or engineers beam theory, such as shear lag effects, warping stresses due to torsion and distortion, transverse stresses due to distortion, effects of pre-stressing, temperature, creep and shrinkage, should be considered and theoretically sound principles should be applied in their determination.

1.2 Composite Box Girder Bridges

A composite box section typically consisting of two webs, two top flanges, a bottom flange and shear connectors connected to the top flange at the interface between concrete deck and the steel part. The exemplary portions of composite box girder bridges are shown in Figure 1.1. The top flange is generally accepted to be adequately braced along the hardened concrete deck for the strength limit state. The flange should be widely enough to allow sufficient bearing for the concrete deck and to permit sufficient space for welding of shear connectors. The bottom flange is formatted to counter bending effects. Since the bottom flange is typically wide, longitudinal stiffeners are often required in the negative bending regions. Web plates are designed primarily to convey shear forces and may be placed perpendicular or bent to the bottom flange.

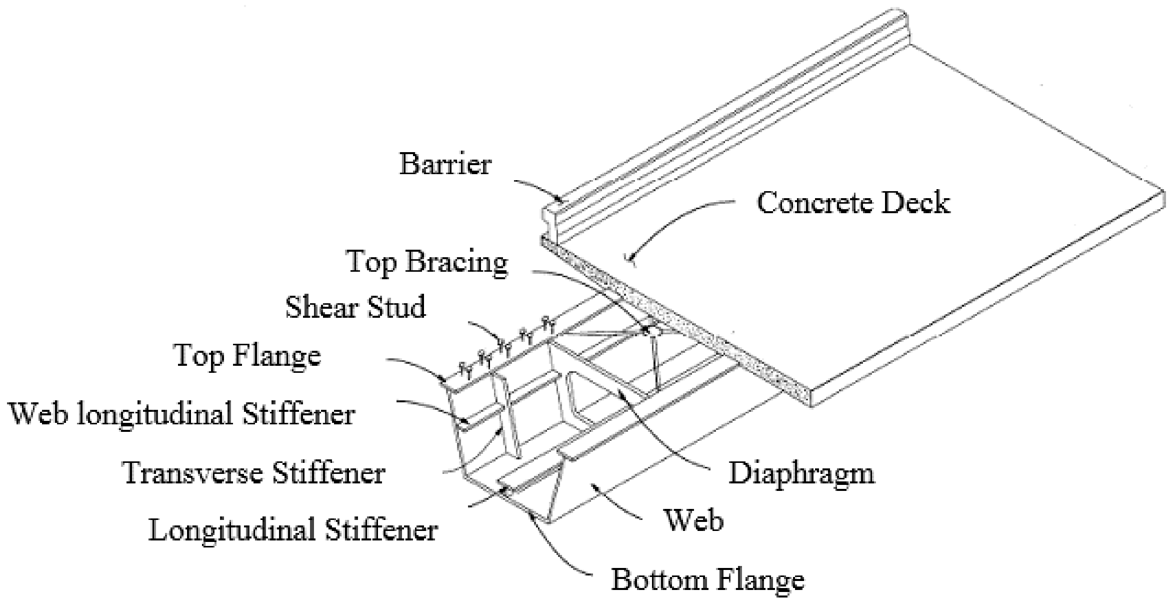

Figure 1.1 Typical components of a composite box girder [1].

In composite bridges, box girders are oftentimes chosen over I-girders because of their pleasing appearance, offering a base modelooth, uninterrupted cross section. Bracings, web stiffeners, utilities and other structural and nonstructural components are usually hidden from view within the steel box girder, resulting in the box girders clean appearance. Additionally, composite box girder bridges offer advantages over other superstructure types in terms of span range, stiffness, durability, and future maintenance. Steel box girders can potentially be more economical than steel plate I-girders in long span applications due to the increased bending strength offered by their wide bottom flanges, and they require less field work due to handling fewer pieces. Steel box girders can also be suitable in short span ranges as well, especially when aesthetic preferences preclude the use of other structure types.

The increased torsional resistance of a closed composite steel box girder result in an improved lateral distribution of loads. For curved bridges, warping, or lateral flange bending, stresses are lower in box girders, when compared to I-girders, since the torsional stiffness of a box girder is much larger than the torsional stiffness of an I-girder. The exterior surfaces of box girders are less susceptible to corrosion since there are fewer details for debris to accumulate in comparison to an I-girder structure. For box girders, stiffeners and most diaphragms are located within the box girder and so protected from the environment. Additionally, the interior surface of the box girder is protected from the environment, further reducing the likelihood of deterioration. Box girder bridges tend to be easy to inspect and maintain since much of the inspection can occur from inside the box girder, with the box serving as a protected walkway.

These advantages led to an increase in the use of box construction that exceed the growth of knowledge of their structural behaviour, which the inescapable results that there were several failures in steel bridges, in the period 1969 to 1971.

There followed a phase of intensive research into the problems so revealed, leading to new design rules in respect of plates, construction tolerance, residual stresses, and local stresses in diaphragms and near bearings. Many existing structures had to be strengthened to meet the new standards, and design calculations became more complex.

1.3 Types of Composite Box Girder Bridges

Two types of steel box girders are available: steel-concrete composite box girders (i.e., steel box composite with concrete deck) and steel box girders with orthotropic decks. Composite box girders are mostly employed in medium span (30 to 60 m) bridges, and steel box girders with orthotropic decks are predominantly used for longer span bridges.

Composite box-girder bridges commonly have individual or multiple cells as indicated in Figure 1.2 a single cell box girder given in Figure 1.2 (a) is simple to analyse and depend on the torsional stiffness to load eccentric loads. The required flexural stiffness is independent of the torsional stiffness [1].

A single box girder with multiple cells shown in Figure 1.2 (b) is economical for extremely long spans. Multiple webs reduce the flange shear lag and also share the shear forces. The bottom flange creates symmetrical deformations and better load distribution between neighbouring girders. The boxes in multiple box girders shown in Figure 1.2 (c) are relatively base modelall and tight together, making the flexural and torsional stiffness very high. The torsional stiffness of the single box is generally less significant than its relative flexural stiffness.

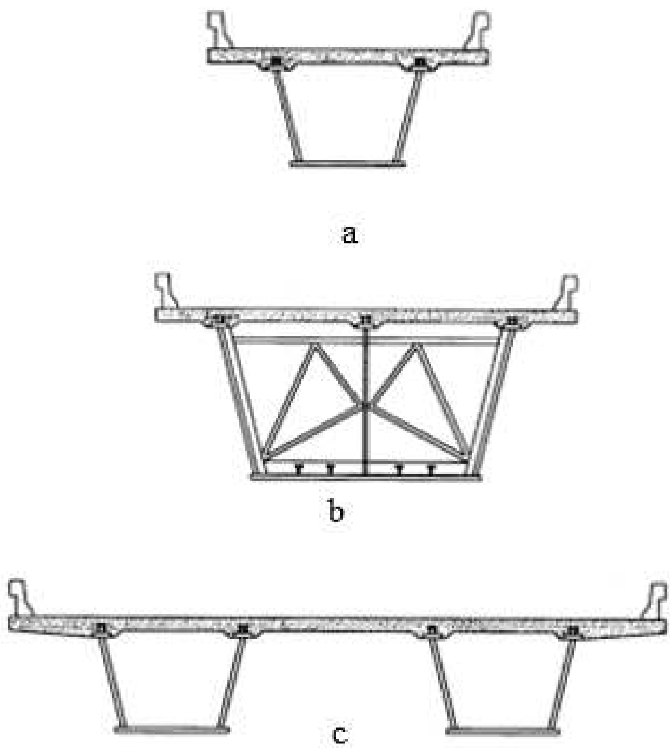

Figure 1.2 Typical cross sections of composite box girder.
(a) Single cell box, (b) Multiple cell box, (c) Multiple boxes [1].

Box girder decks have been subdivided into those where the top plate of the box is initially of steel, later forming part of a composite slab, and those where the composite box is formed by an open-top steel trough, and concrete slab. Both types have been used for spans ranging from 20 to 75 m. In the problem of erection closed or hybrid boxes are normally used. Both types of construction have been widely used. The open top box makes use of the torsional and flexural stiffnesses of the concrete deck slab efficient, and needs fewer shear connectors, because in closed boxes they are provided across the whole width of the top plate to resist local loads and in some bridges to stabilise the plate. During fabrication access for welding is better, and less steelwork is needed in the final structure.

The advantages of the closed-top box in construction and erection. The open-top box has negligible torsional stiffness and inadequate lateral restraint for its top flanges until the deck slab is complete, so extensive temporary bracing is needed. The closed box provides permanent formwork for part of the deck slab, and its interior can be hermetically sealed to reduce corrosion. These last two problems have been solved in open-top boxes by using corrugated metal decking or thin steel membrane as permanent formwork.

Rectangular and trapezoidal boxes are other types of composite box girder bridges. The spacing of webs at the top of the box is related to the design of the concrete deck and the method used to provide load distribution. The need to stabilise the top flange during erection has little influence on the shape of box chosen, but in continuous decks the bottom flange can be more highly stressed near supports, if it is made as narrow and thick as possible. This also reduces the loss of effective cross-section due to shear lag, and leads to the use of trapezoidal boxes.

1.4 Main Components of Box Girders

Composite box bridge main girder are large structural steel members fabricated, except in the case of a few base modelall span bridges in which they can be hot-rolled standard steel sections. In their longitudinal direction, flange width is generally constant, whilst flange thickness and web depth and thickness are variable. Connectors, usually studs, are fixed to the upper faces of the top flanges. These connectors inhibit bridge slab movement (sliding and uplift) with respect to the steel frame, thereby ensuring composite behaviour of the system. The simplest box girder decks comprise a concrete slab and a U-shaped steel frame. The latter is made of longitudinal plates forming the external U (from top to bottom. 2 top flanges. 2 webs and a bottom flange).

1.4.1 Shear connectors

Shear connectors are required on the top flange for composite action, to provide the necessary shear' transfer between the steel girder and the concrete slab. The shear flow varies along the length of the girder, being highest near the supports. For economy, it is customary to vary the number and spacing of connectors to provide just sufficient shear' resistance. The most commonly used form of connector is the headed stud.

1.4.2 Web

Box girder webs are composed of plate sections of constant thickness. They are usually inclined with respect to an axis perpendicular to the bottom flange and are normally stiffened by flat bars or T sections. Webs may be inclined or vertical. The inclination of the web plates to a plane normal to the bottom flange should not exceed 1 to 4 according to codes. For the case of inclined webs, the distance along the web shall be used for checking all design requirements.

1.4.3 Stiffeners

Stiffeners consist of longitudinal, transverse, and bearing stiffeners. They are practiced to prevent local buckling of plot elements, and to administer and transfer concentrated loads.

1.4.4 Bracings

Steel composite box girders are usually constructed on three steel sides and a composite concrete deck. Before the hardening of the concrete deck, the top flanges may be subject to lateral torsion buckling. Top lateral bracing shall be planned to resist shear flow and flexure forces in the department prior to curing of the concrete deck.

1.4.5 Diaphragms

Internal diaphragms or cross frames are usually offered at the conclusion of a bridge and interior supports within the braces. Internal diaphragms not only provide warping restraint to the box girder, but improve distribution of live loads, depending on their axial stiffness which prevents twisting. Because rigid and widely spaced diaphragms may introduce undesirable large local forces, it is generally good practice to offer a heavy number of diaphragms with less stiffness than a few very rigid diaphragms [1]

1.4.6 Steel flanges

Flange size depend of course on the configuration of the cross section and the moments to be carried. A first estimate of size can be based on very simple approximations and these can be quickly refined to a better initial selection suitable for use in the detailed design.

1.4.7 Concrete deck

The slab depth of a box girder composite bridge is constant in the longitudinal direction and most often variable in the transverse direction (usually between 24 and 40 cm). It is made of reinforced concrete, slab integrality with its supporting steel frame is ensured by connectors welded to the top flange of the box main girders. It is constructed after installing the steel frame, either by casting in situ or by assembling slab segments precast on site or at a casting yard.

1.5 Composite Actions

It should be noted that the composite box girder bridge in the above section can be considered composite only if the various components are connected to act as a single unit. The structural performance depends on the extent to which composite action can be achieved. This is illustrated in Figure 1.3, which shows the reduction in both deflection and strains due to composite action. The presence of interface slip (shown as displacement of the vertical marks between the two parts) can also be observed from the Figure 1.3. It follows that rigid connection on the interface tend to eliminate slip and hence ensure composite action.

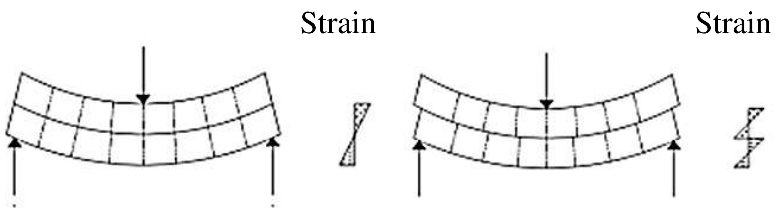

(a) Non composite structure (b) Composite structure

Figure 1.3 Composite and non-composite beams under equal loads.

In practice, such connections are provided by shear connectors embedded in both components. If there is no shear connection or friction on the interface, the upper beam cannot deflect to a greater extent than the lower one, so each carries the freight per unit length as if it an isolated beam of second moment of area, and the analysis and design transacts by elementary beam theory. Otherwise full and partial interaction theories.

1.6 Characterization of Connection Details

Shear connections in composite beams are obviously essential. The nature of composite action induces large shear forces at the interface between the steel and concrete. Traditionally, these shear forces are carried by means of a shear stud welded to the steel, which is then embedded in the concrete deck. When a cast-in-place deck is used, embedding of the shear studs is simple. Shear studs are shop-welded and the deck is poured around them. However, if the deck is prefabricated, pockets are left in the precast slabs that correspond to the location of the shear studs on the steel. These pockets are then filled with a non-shrink grout, which hardens the composite action. The design of the shear studs, as well as the properties of the grout used, can have large effects on the response of the entire section.

The deformations, stress distributions and modes of failure of composite box girder depend on the behaviour of the shear connection between the steel and concrete elements. The behaviour of this bond is represented by the relationship between the interface longitudinal shear-load and slip.

The connection between the two components of a composite member is an important parameter, which may significantly affect the behaviour. Horizontal shear resistance is generally the ruling criterion for composite box girder, and with this in mind, connectors may be classified as either “rigid” or “flexes”.

1.7 Full Interaction Theory

In order that the steel beam and the slab act as a composite structure, the connectors must have adequate strength and stiffness. If there are no horizontal or vertical separations at the interface (i.e. No slip or uplift), the connectors are described as rigid, full interaction can be said to exist under these idealized circumstances. In full interaction an infinitely stiff shear, connecting joins two of the structures together. The two members then behave as one. Slip and slip strain are zero, and it can be assumed that plane sections remain plane. This case is known as full interaction. Except in design with partial shear connection (see section 1.8), design of composite beams and columns in practice is depends on the assumption that full interaction is achieved.

The provision of shear connection increases both the strength and the stiffness of a beam, and in practice leads to a reduction in the size of the beam required for a given load, and usually to a reduction in its cost. When the interface connection is sufficiently rigid, the strain difference due to slip may be neglected in the calculation of stresses and deflections. Accordingly, the strain distribution over the depth of the composite section consists of a continuous straight line. The normal elastic calculations can be used, assuming that concrete has the same elastic modulus (E) in compression and tension (uncracked).

1.8 Partial Interaction Theory

All connectors are flexible to some extent, and therefore the partial interaction always exists. For most connectors used in practice, failure of vertical separation is unlikely and any uplift would have only a negligible effect on the behaviour of the composite box girder bridges. It is therefore sufficient to consider only slip in the study of the effects of partial interaction. The role of partial interaction design in determining the number of shear connectors in a composite box girder bridge is now rare. From tests carried out on full-scale composite beam it has been found that discrete flexible connectors give rise to non-linear connection behaviour.

The partial interaction state enables the designer to reduce the number of connectors used to tranbase modelit shear between slab and beam. Consequently, the degree of connection may be designed that the size of the steel beam found because of construction loading will be just adequate for the composite stage loading. The ultimate load, which the beam can carry in its final service condition, is then based not on the yield strength of the steel but on the capacitance of the shear connection.

This has implications when looking at the stiffness of the composite beam, as the reduced connection also gives up a reduced stiffness. In summation, as the shear connection is the critical design parameter, the strength, deformation and cumulative slip deformation along the beam become important [2].

The results of push tests show that even at the base modelallest loads, slip is not zero. It is thus necessary to recognize how the behaviour of a beam is changed by the presence of slip. This is best exemplified by an analysis based on elastic theory. It contributes to a differential equation that has to be worked out for each case of loading, and is therefore too complex for use in design offices. Even so, the partial interaction theory is useful, it provides a starting spot for the evolution of simpler methods predict the behaviour of beams at working load, and finds application in the calculation of interface shear forces due to shrinkage and differential thermal expansion.

1.8.1 Slip calculations

The slip can be defined as the longitudinal differential displacement at the interface between concrete and steel plate. Headed studs are generally used as the shear connectors, which can be classified as flexible connectors, interface slips which represent the slip between concrete and steel, cannot be completely prevented. The interaction between the steel and the concrete is; therefore, incomplete, producing a different strain at the interfaces [3].

The shear flow at the interface is related to the number and spacing of shear connectors provided between the two materials, and the properties of the shear connectors such as the shear stiffness (K). shear stiffness can be defined as the slop of the load- slip curve for the connectors. In the other words, shear stiffness is the load per connector required to produce a unit slip and this is assumed to be constant for the elastic range. This load slip curve should ideally be found from tests on composite structures, merely in practice a simpler specimen is necessary.

The layer slip under external action is the main property, which determines the calculation methods used for the design of composite structures and calculation of stresses and strains.

Most of the effects on shear connectors have been received from several cases of push-out. Figure 1.4 depicts a typical load slip relationship for 19 mm shear connectors in a composite construction.

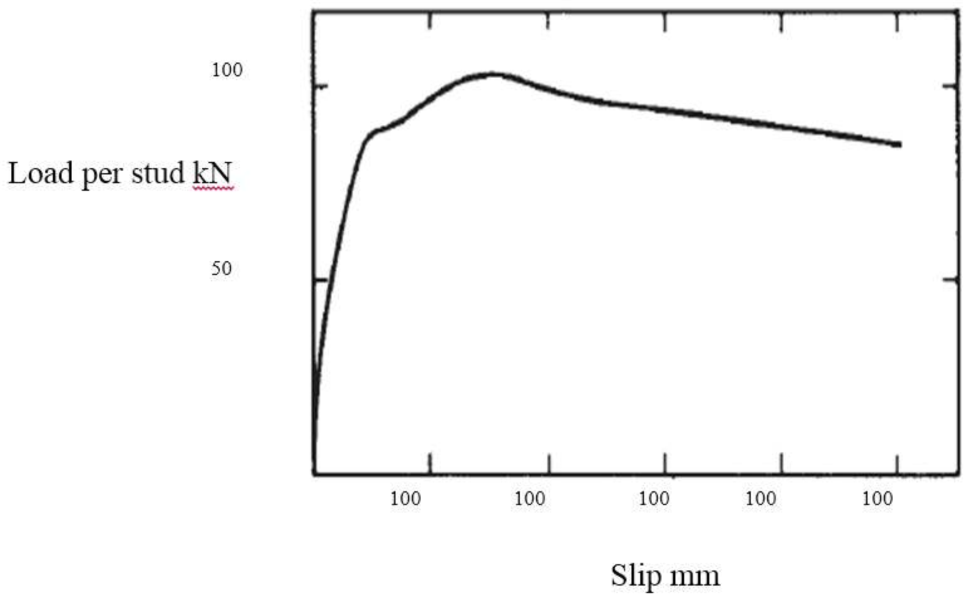

Figure 1.4 Typical load slip curve from 19 mm stud connectors in a composite structure.

1.8.2 Definition of stud connector strength and the push-out tests

The most important characteristics of a connector, is the capability to sustain shear forces and tension forces either separately or in a combined form. Yet standard tests are available to measure one of these forces only, which are push-out test and pull-out test. The attribute of a shear connection, most relevant to design, is the relationship between the tranbase modelitted shear force and the slip at the interface. The flanges of a short length of steel box section are connected to two base modelall concrete slabs.

1.9 Analysis Methods for Box Girders

Meanwhile, many numerical analysis methods have been developed over the past decades for the analysis of the composite box-girder bridges. These methods include the planar grid method, the space frame method, the finite strip method, the finite difference method, the FE method, and the closed form method. These methods are the basis for the computer programs that are presently used for research as well as design. However, the FEM has been proven to be the most accurate technique to model and analyse bridges. It has been credited as a powerful tool for presenting solutions to complex structures.

Finite Element (FE) is a method for numerical solution of field problems. A field problem requires determination of the spatial distribution of one or more dependent variables. Mathematically, a field problem is identified by differential equations or by an entire formulation. Either description may be applied to formulate FEs. Individual FEs can be seen as base modelall parts of a social system. Components are joined at points called nodes and the assemblage of elements is sent for a FE structure.

In the study, some methods with several levels of rigour are available for analysis. These range from the elementary or engineer's beam theory to complex shell FE analyses; other methods of analysis utilize folded plate and finite strip methods. While some of the latter methods are general and accurate, their usage in early stages of design may not be justified. This is particularly true about the FE method, which involves a large quantity of effort and tends to make inordinate quantities of output whose interpretation can be time consuming. The more sophisticated methods also obscure the significance of the contribution of individual structural actions to the over-all resistance of the box girder. For instance, it is not comfortable in a FE analysis to keep apart the effect of torsional and distortional warping on normal stresses from that of extension and bending. This too applies to folded plate and finite strip analyses.

The actual variation in the region crossed by an element is almost certainly more complicated, hence a FE analysis provides an approximate answer. In more and more engineering situations today, we see that it is necessary to obtain approximate numerical solutions to problems, rather than exact closed-phase solution. Of all the available analysis methods, the FE method is considered to be the most powerful, versatile and suitable numerical tool to solve a complex continuing problem. The method has become an important and frequently indispensable part of engineering analysis and design.

Recent development in computer technology makes it possible to use FE computer programs, practice in all branches of engineering. A complex geometry such as that of composite box girder bridges can be readily modelled using the FE technique. The method is likewise capable of dealing with different material properties, relationships between structural elements, boundary conditions, as well as statically or dynamically applied loads. The linear and nonlinear structural response of such bridges can be prophesied with good accuracy using this method.

The FE method has become a staple for expectation and simulating the physical behaviour of complicated engineering systems. The commercial FE analysis programs have gained common acceptance among engineers in industry and researchers at universities and government laboratories. Therefore, academic, engineering departments include graduate or undergraduate senior-level courses that cover not only the theory of FE method, but also its applications using the commercially available FE analysis programs.

1.10 Design Codes Used for Box Girder Bridges

British Standard (BS) 5400 covers the design and construction of composite box bridges: steel, concrete and composite bridges. The Standard comprises codes of practice for design and Specifications for design loadings, construction materials and workmanship. A Limit State design basis is used in the codes. Part 5 of BS 5400 covers the design of composite box bridges in section seven, it deals with general principles and the details of the interaction between steel and concrete elements. The connectors at any cross section are assumed all of the same type and size. The design of the shear connectors between each steel web and its associated concrete flange should be considered for each web separately. The design longitudinal shear due to global and local loadings per unit length of girder at the serviceability limit state for the web considered, calculated assuming full interaction between the steel plate and the concrete slab.

American Association of State Highway and Transportation Officials (AASHTO) provided Shear Connectors in section 6.10.10 to be in regions of negative flexure in curved continuous bridges because torsional shear exists and is developed in the full composite section along the entire bridge.

EUROCODE 4 established for design of composite steel and concrete structures, the EN 1994 Part 2 deals with composite bridges. EN 1994-2 discussed rules for bridges in seven parts and the objectives of the fifth part about the connection at the steel–concrete interface are the full interaction required for bridges, elastic resistance design of the shear connectors and shear connectors locally added due to concentrated longitudinal shear force (for instance, shrinkage and thermal action at both bridge deck ends or cable anchorage)

1.11 Objectives & Aims of the Study

The failures all arose from inadequate attention to the details of design, erection of steelwork, or the connection details essentially the shear connectors, and did not cast any doubt on the fundamental soundness of steel or composite box girders.

Due to these problems, researchers and designers have been practicing an innovative form of theories to analyse composite box girders. An extended study of the applications of partial interaction theory has been provided in this field. The accuracy of the stresses calculated by the more advanced version of the theory is adequate for practical applications. Furthermore, the method clearly and elegantly accounts for each character of structural action and for its relative importance in the overall conduct of the composite box. It is also efficient and, once programmed in the computer, requires minimal input data and computer time. To date, however, existing applications have been limited to full interaction theory in composite box girders, and temperature and time dependent effects, such as prestressing, creep and shrinkage, and slip calculations, shear lag, and warping stresses have not been integrated into this theory for composite box girders. The extended versions of thin-walled beam theory and elementary beam theory are not applied to curved, haunched and skew composite box girders in its existing form; modifications are needed for its extension to the latter situations.

The aim of the dissertation is to study the purpose and execution of composite box girder bridges using FE method.

The overall goal of the thesis is to acquire a working knowledge of the bridge system at hand. This was thought to have been accomplished when the following objectives were satisfied:

- Few theoretical studies dealt with the incomplete interaction between steel and concrete in a composite box girder bridges. The intention of this theoretical work is to look into the behaviour of composite box girder bridges with partial interaction between components.

- Develop a 3D FE model with the ability of predicting the structural response of composite box girder bridges.

- This study includes an investigation of the possibilities and shortcomings of ANalysis SYStem for static problems (ANSYS), a Commercial program for FE analyses for modelling composite box girder bridges with complete and incomplete interactions.

- Determine global system response and behaviour of composite box girder bridges with complete and incomplete interaction systems due to loads.

- Determine localized behaviour of joints and connections in the system.

- Investigate the key geometric parameters of the bridge superstructure that affect behaviour at the service load.

1.12 Layout of Dissertation

The contents and arrangement of this study are described to achieve the aforementioned objectives, the first step toward completing the study was to compile and study existing literature on related topics. This literature review can be found in Chapter 2 of this thesis. This chapter also presents a literature review of the earlier analytical and experimental work on steel box girder bridges with composite action.

Developing 3D FE composite box girder bridge models using the commercially available FE computer program "ANSYS" with full interaction theory can be found in Chapter 3. Chapter 3 also highlights the comparing of the FE model predictions with the experimental findings of the laboratory tested bridge models for various load cases to verify the FE model and provide information about the linear and nonlinear response of box girder bridges.

Once the literature review was performed, the possible variations of the model to be studied were pared down using a rating model, which accounted for factors such as: shear connectors, numbers and location of these studs, push out test, hautching ratio, dimensional detail variations, and element type. This can be found in Chapter 4. Chapter 4 also highlights information on section details, the selection of analysis tools, parametric studies, and detailed studies of joints and connections. A new 3D modelling to perform composite box girder bridges with partial interaction theory using the same software is presented in Chapter 5. Lastly, summary and conclusions are presented in Chapter 6.

CHAPTER 2

LITERATURE REVIEW

2.1 General

A literature and survey review of current, complete superstructure systems have been guided to identify the interaction behaviour of composite box girder spans. The review considered available information at the conceptual, research, or implementation stage. As a reference, a brief account of full interaction is discussed and then more emphasis is placed on partial interaction in composite action.

Composite concrete deck over steel box girder bridges are considered more efficient than steel I-girder bridges. They are characterized by high torsion resistance when compared to I-girders, thus enhancing the transverse live load distribution. A significant incidental advantage is the significant decrease in the transverse moment in the deck slab due to better load sharing between closed boxes and less differential deflection between adjacent girders. Box girders have high flexural amplitude and torsion hardness, and the closed form reduces the exposed external, making them less susceptible to corrosion.

This chapter presents a summary of the literature review pertained to (i) the interactions between components and codes of practice for box-girder bridge design, and (ii) the modelling of composite box girder bridges.

2.2 Numerical Works on Composite Box Girder Bridges

The analysis and design of composite box girder bridges is very complicated for many reasons such as the existence of curvature, the interaction between the girder and concrete deck, and the torsional and distortional warping. Except in analysis and design with partial shear connection, all calculations of composite box girder bridges in the field are based on the assumption that complete interaction is achieved.

2.2.1 FE analytical method.

Kim and Williamson [4] presented a detailed FE modelling method for evaluation the redundancy of twin steel box-girder bridges. It was taken for granted that the enactment of a truck live load triggers the sudden break of one girder. Because of the possibility of localized damage in some bridge components, the proposed computational models incorporate material nonlinearity to represent cracking and crushing of concrete and steel yielding. In summation, the proposed FE models are capable of capturing deck haunch separation by taking in a stud connection failure model. This failure mode was first mentioned during testing of a full-scale bridge that let in a girder with a full-depth fracture. Analytical results show that typical twin steel box-girder bridges likely have greater redundancy than the current provisions indicate and that stud connection failure could significantly affect the redundancy of steel box-girder spans.

The stress analysis of a long-span cable stayed bridge using FE analysis compared very well with a full-scale static experimental loading performed by Lertsima et al. [5]. Yamaguchi et al. [6] in 2005 conducted a 3D nonlinear FE analysis of plate-girder bridge and dry shrinkage and pre-stressing are obtained. The dynamic interaction between a heavy truck and highway is shown by the FE analysis by Kwasniewski et al. [7].

Nonlinear FE analysis of Svinesund Bridge, which links Norway and Sweden were developed. Multi- response objective function was introduced by Schlune et al. [8], which allow combing different types of measurements to obtain a solid basis for parameter estimation. Fan and Helwig [9] presented an analytical study on the distortional behaviour of box girder with a tapered web cross-section shape. They discussed typical torsional loads on curved box girders, and they studied distortion components of these applied torsional loads. The distortion components from different torsional loads on trapezoidal box girders are I identified and used to derive expressions for the brace forces in the internal cross frames for quasi-closed box girders. The outcomes from the approximate equations for brace forces due to cross sectional distortion are verified by 3D FE analyses.

A pragmatic approach to the distortion analysis of steel box girders presented by Hsu et al. [10]. Equivalent beam on elastic foundation method is an enhancement of the beam on elastic foundation method, which has been widely utilized in design practice. Using this method on closed box girder analysis provides a simplified process to account for the distortion of the cross section for the consequence of fixed or flexible interior diaphragms and continuity over the musical accompaniments. The methodology, numerical examples, and stiffness matrix are also represented in this work.

Analytical equations were formulated by Kim and Yoo [11] to compute the brace forces developed in bracing members by taking into account bending and torsional actions of tub girders with single stroke type lateral bracing systems. Brace forces in both diagonals and struts can be estimated by these new equations more accurately than with the other operations. Member forces due to twisting and torsion computed using the new equations were compared with those measured by 3D FE analyses, and excellent correlation was found. The trapezoidal steel box may be at their critical point during construction because the non composite steel section must bear both the wet concrete and the entire building load. A lateral bracing system is normally set up at the top flange level to make a quasi-closed box, thereby increasing the torsional stiffness during construction. Typical lateral bracing includes a single stroke type and a crossed-diagonal type.

Software has been developed by Popp and Williamson [12] to investigate the overall behaviour of steel trapezoidal box-girder bridges during the construction phase. The software explicitly accounts for partially-composite behaviour between the girder and the large number of cards. In summation, the developed program utilizes a FE-based procedure in which the precise geometry of the cross-section is discretized for the purposes of analysis. Former research has shown that such an approach is needed to accurately forecast the response of trapezoidal box-girder bridges under construction loads. The effects of the current survey have demonstrated that lateral torsional buckling of the entire girder, which is not currently a limit state for design, must be seen. The developed software is utilized to investigate the failure of the bridge in Marcy. Calculated results are shown to correspond with observations from the forensic investigation.

Williamson et al. [13] provided an overview of the detailed FE simulations performed for full-scale testing of a twin steel box-girder bridge. The simulation models include inelastic material behaviour and nonlinear geometry, and they account for the complex interaction of the shear studs with the concrete deck under progressing levels of damage. In addition, the contribution of the bridge rail, including the presence of expansion joints, has been successfully modeled in the FE analyses carried out for this study. These simulation models have been validated using base modelall-scale laboratory tests and results obtained from full-scale tests on a twin steel box-girder bridge. A brief description of the test program and the FE models developed for this research.

2.2.2 Two dimensional finite element modelling.

The studies conducted by El-Lobody and Lam [14] and Chung and Sotelino [15] used Two Dimensional (2D) FE modelling to predict the stress and deflection of steel-concrete composite girders. A beam-truss model is introduced by Nie and Zhu [16] for the design analysis of composite box-girder bridges. An integrated research program for beam-truss models, including modelling, execution, analysis, and application, has been performed to exploit this research and design tool. Beam truss models of composite box-girder bridges are carried out, and then corresponding model strategies are developed based on classical shear–flexible grillage analysis. The calculation accuracy of the beam-truss models is then verified through comparative studies on the morphological behaviour of straight and curved composite, simply affirmed, and continuous box-girder bridges obtained using elaborate beam-truss FE models. Numerical analyses include modal analysis; static analysis under gravity load, prestressing load, and lane live load; and whole-process analysis considering the building method and the long-term behaviour of concrete. Finally, beam-truss models are used for the analysis of field trials on two actual composite boxes-girder bridges, one square and the other curved. It is resolved that the beam-truss model provides a dependable instrument for the design, analysis of composite box-girder spans.

Sennah et al. [17] gave an extensive parametric study, using an experimentally calibrated FE model, results from tests on five box girder bridge models verify the FE model. Grounded on the outcomes from the parametric study simple empirical formulas for maximum shears (reactions) are risen that are suited for the design position. A comparison is made with AASHTO and CHBDC formulas for straight bridges.

The total construction works of multi-span composite steel box-concrete continues girder bridge having different cross-section was studied by Zhang [18] by using spatial FE method. The element creation technique was created to simulate the total flexural process of composite steel box-concrete continuous girder bridge. The analysis results display that when the middle span of composite steel box-concrete continuous girder bridge is longer and its cross section size is limited, the strength requirement of the negative moment region at middle support cannot be satisfied by using the conventional measures such as forced top-pier displacement, internal prestressing on bridge deck, etc. The load carrying capacity and spanning ability of a composite steel box-concrete continuous girder bridge can be increased, which will bring greater integrated economic benefits.

2.2.3 Three dimensional finite element modelling.

A Three Dimensional (3D) solid FE model was created by Chang and Robertson [19] using ANSYS to study thermal loadings. Considering longitudinal strains, modal analysis, and deformations, this model simulated a three span, 220-meter concrete bridge developed to supplant an existing six span concrete bridge spanning the Kealakaha Stream. Ryu et al. [20] submitted a 3D FE model in which the concrete slab and the steel girder were modelled with shell elements.

Seaman [21] at the same year employed 3D FE analysis to investigate the static and dynamic responses of continuous curved composite box girder bridges. Lei Zheng [22] developed several 3D FE models using ANSYS to propose new distribution factor equations of the live load moment and shear for open-box girder bridges. The structural behaviour of bridge deck slabs under static loads in composite bridges in terms of a non-linear 3D FE model with software ABAQUS was presented by Zheng et al. [23].

A 3D FE simulation of the composite box-girder bridge with corrugated steel webs was performed by Song et al. [24]. Jaturong et al. [25] presented a 3D FE analysis model of composite steel-concrete bridges to simulate the actual bridge behaviour, Thai trucks are loaded at possible locations of the bridge to obtain the maximum stresses on the bridge. A 3D FE model of an inner and external tendon concrete, simple-supported composite box girder bridge with corrugated steel webs was established by He et al.[26] utilized the means of the composite element method. The mechanical behaviour of the structure with different inner and external tendon parameters were analysed, including the organisation of the inner and external tendon, the tensile force, the status of the anchorage point and the length of the diversion period. The conclusions indicate that the normal stresses of the sections between two diversion points in the mid-span only depend on the tensile force, while those between the anchorage point and the diversion point change with the parameters. It is proposed the reasonable ratio of the external tendon to be 30%~40% of this bridge, and the prestressing force should be no less than 60% of characteristic value of tensile force.

Samaan et al. [27] used the FE method to model the bridges as 3D structures. The vehicle axle used in the analysis was simulated as a couple of concentrated forces moving along the concrete deck in a circumferential path with a constant velocity. The effects of bridge forms, loading positions, and vehicle speed along the impact factors were studied. Bridge configurations included span length, bridge-to-radius of curvature ratio, number of lanes, and number of corners. The result of the volume of the vehicle along the dynamic reaction of the bridges is also looked into. The information generated from the parametric study and the deduced expressions for the impact factors would enable bridge engineers to design curved continuous composite multiple-box girder bridges more reliably and economically.

2.2.4 Finite strip method.

A finite strip analysis of the influence of bracing systems on open section box girders is presented by Branco and Green [28] and compared with test results calculated using a one-quarter scale model with the analysis. The influence of ties, distortional bracing, torsion boxes, and top chord bracing on the behaviour of torsionally open box girders is tested. The simplified design method is also presented whereby the bracing forces and the stresses arising from the distortion of the section can be computed.

The influence of bracing on the deformation of composite bridges during service is examined by Branco and Green [29]. A linear elastic finite strip analysis was developed and results are compared with experimental studies from a model and a prototype bridge. The effectiveness of transverse web stiffeners and distortional bracing in preventing distortional stresses is studied. Transverse web stiffeners are effective in resisting distortion of completed girders, and distortional bracing is not essential for stiffened girders. For unstiffened girders, bracing is essential if additional longitudinal stresses due to distortion are not included in design. Interconnecting bracing between boxes is found to be effective in reducing transverse slab moments.

The semi-analytical finite strip method of analysis is used by Bradford and Wong [30] to study the local buckling of composite box sections in negative bending consisting of a concrete deck connected to a steel trough. Design charts are produced to determine the local buckling coefficient for the web. It is then shown how this local buckling coefficient may be used to calculate the web width-to-thickness ratio that delineates the boundary between the section classifcations of semi-compact and slender.

2.2.5 Optimization method

Shape optimization techniques based on the FE method have been used for many years with some success in the design of structures and structural components. Hinton and Rao [31] [32] investigated the optimum structural design of prismatic folded plate and shell structures using the finite strip method with strain energy minimization as an objective and allowed the cross sectional shape and thickness to be varied. For a similar class of structures under going free vibration, Özakça et al. [33] [34]have demonstrated the use of the FS method in Shape optimization.

The size, shape and topology optimization of composite steel box girders using particle swarm optimization method were studied by Ghasemi and Dizangian [35]. The advantage of using the particle swarm optimization compared to gradient-based techniques lies in the fact that the discrete spaces can be optimized in a simple manner. This algorithm was written in Python language in the FE analysis software, ABAQUS, environment as a script file. The objective function is the minimization of the total weight of the structure under strength and serviceability constraints, enforced by penalty functions. All design requirements correspond to AASHTO compared to a conventional feasible design, the optimum solution showed a 55% reduction of structural weight In this study.

Musa and Diaz [36] described the use of excel solver to find the minimum weight for a composite trapezoidal box cross section for a two-lane bridge. Design aid tables were generated for structural steel grades 250, 345, 485, and 690 MPa, and different spans varying from 3.0–100 m.

An integrated metaheuristic based optimization procedure is proposed by Kaveh et al. [37] for discrete size optimization of straight multi-span steel box girders with the objective of minimizing the self-weight of girder. The metaheuristic algorithm of choice is the Cuckoo Search algorithm. The optimum design of a box girder is characterized by geometry, serviceability and ultimate limit states specified by AASHTO. Size optimization of a practical design example investigates the efficiency of this optimization approach and leads to around 15% of saving in material.

The practicality of optimization applied to a complex structural design problem is examined by Surtees et al. [38] using the steel box girder bridge a case for study. An automated procedure as to generate, appraise and cost differing layouts a stiffened, open or closed steel box for girder with composite concrete deck is described.

2.2.6 Parametric study

The coming of a raw and improved material specification, high performance steel, has prompted by Price [39] and focused on a two-girder bridge system concept which addresses a number of key issues and owner criteria, including cost, reliability, redundancy, replace ability and durability. Samaan et al. [27] presented results from a parametric study on the impact factors for several curved continuous composite multiple-box girder spans. Reflections for the impact factors for tangential flexural stresses, bending, shear forces and reactions are deduced for AASHTO truck loading.

Samaan et al. [40] presented the results of an extensive parametric study, utilizing a FE method, in which the structural responses of 240 models of two-equal-span continuous curved box-girder spans of various geometries were investigated. The parameters taken in this study included span-to-radius of curvature ratio, span length, number of lanes, number of boxes, web slope, number of bracings, and truck loading type. Established on the information generated from this field, empirical formulas for load distribution factors for maximum longitudinal flexural stresses and maximum deflection due to dead load as well as AASHTO live loading were deduced. An illustrative design example is exhibited.

An extensive parametric study using the FE method in which 120 bridges of various geometries were analysed by Sennah and Kennedy [41]. The parameters studied are: number of cells, number of lanes, span length, and cross bracings. Results from testing a simply supported three-cell bridge model is employed to confirm the analytical modelling. Founded on the parametric study, moment and shear distribution factors are deduced for such bridges subjected to AASHTO truck loadings as well as dead freight. Saint-Venant torsional stiffness for composite cellular cross sections used in this work is also looked into. Recommendations to enhance the torsional stiffness are formulated. An illustrative design example is presented.

Sennah et al. [17] gave an extensive parametric study, using an experimentally calibrated FE model, in which simply supported straight and curved prototype bridges are analysed to determine their shear distribution characteristics under dead load and under AASHTO live loadings. The parameters studied in their study are span length, number of steel boxes, the number of traffic lanes, bridge aspect ratio, degree of curvature, and numbness and stiffness of cross bracings and of top-chord systems.

The dynamic characteristics of curved composite multi-cell (contiguous boxes) bridges, continuous over two and three spans was summarized by Sennah and Kennedy [42]. An extensive parametric study, using the FE method, was conducted to evaluate the key parameters that may affect the natural frequencies and the corresponding mode shapes for this type of bridge. These parameters are end-diaphragm thickness, number of cross-bracings, aspect ratio, span-to-depth ratio, degree of curvature, number of cells, and span-to-span ratio. The effect of cracking of the concrete deck slab in the vicinity of interior supports is also investigated. Results obtained from tests on a 1/12 scale two-span continuous curved composite three-cell bridge model are used to substantiate the analytical modelling. Based on the data generated from the parametric study, empirical formulas for the dominant frequency are deduced. An illustrated design example is presented. A study is also conducted to determine the dynamic deflections caused by a moving truck over the bridge with a view to improve human discomfort and perception to vibration. The use of cellular-shaped cross sections for highway bridges, especially on curved alignments, is an economical solution because of the high flexural and torsional strength of such sections.

Cheung and Foo [43] presented the results of a parametric study on the relative behaviour of curved and straight box-girder bridges and on the development of a simplified design method for the combined longitudinal moment of curved bridges. The combined moment includes the effects of flexure, torsion, and distortion. Three simply supported concrete-steel composite bridge models, including single-cell, twincell, and three-cell box girders and subjected to loadings as specified in the

CHBDC, were analyzed using the finite strip method. The parameters considered in the study include types of cross section; types, locations, and magnitudes of loads; span lengths; and radius of curvature. Preliminary analysis of the results suggests that the behaviour of horizontally curved box-girder bridges is dependent on a variety of parameters, but most importantly on the span-to-radius ratio. Empirical relationships for combined longitudinal moment between curved and straight box-girder bridges are also proposed.

The deformation behaviour of single and multicell steel and concrete box girders is studied by Chapman et al. [44] by reference to specific examples which incorporate variations in wall thickness, loaded length, stiffener size, diaphragm spacing, shape of section, curvature, and support positions are considered in their study.

2.2.7 Dynamic analysis

The dynamic impact factors for horizontally curved steel box-girder bridges was presented by Schelling et al. [45]. The dynamic impact is presented as a subroutine of the span length and the first fundamental frequency. The results are discussed and compared with the impact provisions as given in the previous AASHTO specifications and the Canadian Highway Bridge Design Code (CHBDC). It is reasoned that the impact functions previously specified by AASHTO exhibit shortcomings and do not apply for a big percentage of the inventions.

A dynamic measurement program was carried out by Cheung [46] on a number of steel-concrete composite box-girder bridges with different span lengths and number of spans The program involved the multi-point measurement of strain and acceleration at selected locations in the bridges due to normal traffic and special test vehicles The data acquired are used to determine bridge dynamic characteristics such as natural frequencies, modal shapes, impact factors and damping ratios For the bridges tested, the average impact factor is about 15 to 16 percent.

2.2.8 Behaviour of the composite box girder

Numerous studies have been directed by Ko et al. [47] on the shear buckling and flexural behaviour of the composite box-girder with corrugated steel webs. However, the torsional behaviour is not fully understood yet, and it needed to be investigated. Prior study of the torsion of the composite box-girder with corrugated steel webs has been developed by assuming that the concrete section is cracked prior to loading. A composite box-girder with corrugated steel webs has been used in civil engineering practice as an alternative to the conventional pre-stressed concrete box-girder because of several advantages, such as high shear resistance without vertical stiffeners and an increase in the efficiency of pre-stressing due to the accordion effect.

A full-depth fracture in one girder, simplified analytical methods have been developed by Samaras. et al. [48] and are presented. A crack-critical bridge is a structure that is expected to break down after the bankruptcy of an essential tension component. In the positive bending moment region, the bottom flanges of a twin steel box-girder bridge are seen to be fracture-critical elements. Bridges with fracture-critical components are taken to undergo stringent hands-on inspections at least every two years. These reviews, which often call for lane closures, are labour intensive and costly. There have been multiple cases of crack-critical bridge s that have had a failure in one of their fracture-critical elements without breaking up, which hints that current provisions may not accurately account for the inherent redundancy that exists in various crack-critical bridge structural systems. The proposed methodology has been validated against data from full-scale tests and provides a convenient way for predicting response.

Fan and Helwig [49] presented results from a FE study on the bending behaviour of trapezoidal box girder systems during construction. The results show that large forces can develop in the horizontal truss system due to vertical bending of the box girder. For truss systems with a single diagonal, the forces induced from bending result in large lateral bending stresses in the top flanges of the box. Expressions to estimate the bending forces in the lateral truss system as well as the lateral bending stresses in the top flange are developed. A numerical example illustrates the use of the expressions.

Gara et al. [50] proposes a simplified method of analysis for the design of twin-girder and single-box steel-concrete composite bridge decks. Its main advantages rely on the use of the real width of the slab for the whole bridge length when performing the global analysis, i.e. without modifying the deck geometry based on the effective width method, and its ability to evaluate the normal longitudinal stress distribution on the slab by means of a cross-sectional analysis considering the internal actions obtained from the global analysis. The proposed approach is capable of handling different loading conditions, such as constant uniformly distributed loads, envelopes of transverse actions due to traffic loads, support settlements and concrete shrinkage.

The method proposed by Peiretti [51] for the analysis of the behaviour of composite cross-sections subject to normal forces is briefly explained. This procedure allows the modelling of the behaviour in ultimate limit state, as well as in previous strain situations (moment curvature diagram). An experimental program designed to test this approach, is also presented, as well as some of the results obtained so far. Evans et al. [52] presented extensions of the harmonic method to consider girders of more general and complex multicellular, composite cross sections. The proposed extensions allow the basic simplicity of the approach to be retained so that the method is still regarded as an ideal design aid. The accuracy of the method is established by comparison with results obtained from a FE analysis and from a careful series of experiments; values from BS5400 are also included in the comparison.

Kwak et al. [53] investigated the effect of slab concrete placing sequence on the transverse cracking of slab decks theoretically, using developed algorithm. Bending moments and the corresponding tensile strains influencing the cracking behaviour were calculated both in the construction stage and in the service stage. The effect of drying shrinkage was considered in terms of the ultimate shrinkage strain, and it was found to be much more important than the concrete casting sequences. Based on the ACI Code, the ultimate shrinkage strain was expressed as a function of concrete slump and relative humidity, while the other remaining factors such as unit weight of cement and air content were assumed in accordance with the typical values in mixed concrete.

2.2.9 Warping stresses

A computer program for simulating the behaviour of curved box girders is developed by El-Tawil and Okeil [54] to conduct an investigation of warping-related stresses in 18 existing box girder bridges in Florida. Forces are evaluated from analyses that account for the construction sequence and the effect of warping loading is considered following the AASHTO load resistance factor design provisions. The differences between stresses obtained taking into account warping and those calculated by ignoring warping are used to evaluate the effect of warping. Another study was undertaken to investigate load distribution factors promoted by current specifications. Single girder and detailed grillage models were created for a variety of bridges and analyzed using the computer program. The distribution factor results were compared with those obtained using the equations recommend by AASHTO in the commentary of the guide specification for horizontally curved bridges. Results show that the recommended equation overestimates the distribution factor by an average of about 15 percent. By considering differences between stresses obtained taking into account warping and those calculated by ignoring warping, it is shown that warping has little effect on both shear and normal stresses in the bridges considered, suggesting that there could be a large subset of bridges where the warping effect is base modelall enough to be ignored in structural calculations.

2.2.10 Temperature effects

Alliy [55] presented a study of the temperature effects of a composite box girder bridge. It has been found that an accurate assesbase modelent of the temperature distribution within a bridge deck is necessary for the computation of thermal stresses. Also, to predict accurately longitudinal bridge movements associated with temperature changes a good knowledge of the relationship between the mean bridge temperature and ambient shade air temperature is necessary.

2.2.11 Shear lag

A method is proposed by Kristek and Ahmad [56] for shear lag analysis which can be applied to steel and composite box girders of various cross-sectional types. The proposed method uses harmonic analysis and allows the determination of shear lag effects from simple calculations. Examples of such calculations are given and the accuracy of the proposed method is illustrated by comparisons with results obtained from other sources.

The elastic shear lag behaviour has been extensively submitted by Lin and Zhao [57] and considered in structural design while the study of inelastic shear lag is limited. Knowing that flanged flexural members likely have plastic deformation at their ultimate limit state, a least-work based method was developed for modeling inelastic shear lag behaviour. An effective modulus was formulated and the Poisson's ratio following the theory of plasticity was used in the inelastic shear lag model. The analytical method was verified using laboratory tests of two steel box beams. Comparison with experimental data indicates the proposed variation method can accurately predict the plastic normal strain distribution and the deflection of steel box beams.

Considering three longitudinal displacement functions and uniform axial displacement functions for shear lag effect and uniform axial deformation of thin-walled box girder with varying depths, a simple and efficient method with high precision to analyze the shear lag effect of thin-walled box girders was proposed by Zhou et al.[58]. The governing differential equations and boundary conditions of the box girder under lateral loading were derived based on the energy-variational method, and closed-form solutions to stress and deflection corresponding to lateral loading were obtained. Analysis and calculations were carried out with respect to a trapezoidal box girder under concentrated loading or uniform loading and a rectangular box girder under concentrated loading. The analytical results were compared with numerical solutions derived according to the high order finite strip element method and the experimental results. The investigation shows that the closed-form solution is in good agreement with the numerical solutions derived according to the high order finite strip method and the experimental results, and has good stability. Because of the shear lag effect, the stress in cross-section centroid is no longer zero, thus it is not reasonable enough to assume that the strain in cross-section centroid is zero without considering uniform axial deformation.

The shear lag phenomenon in steel box girder bridges is studied by Moffatt and Dowling [59] by means of the FE method of analysis. Some of the results of this study provided background for the preparation of the Merrison shear lag rules, and the rules are discussed in the light of these results. Suggestions are then made on how the rules could be simplified for inclusion in a Code of Practice.

The governing differential equations and the corresponding boundary conditions of steel-concrete composite box girder with consideration of the shear lag effect meeting self-equilibrated stress, shear deformation, as well as rotational inertia were introduced by Zhou et al. [60]. Therefore, natural frequency equations were obtained for the boundary types, such as simple support, cantilever, continuous girder and fixed support at two ends.

2.2.12 Fatigue loading

Acoustic emission sensors were installed by Hendy and Chakrabarti [61] to determine if the predicted fatigue activity was actually occurring and elastic shell FE modelling was undertaken for an improved determination of stresses. Plastic redistribution was considered to demonstrate adequate ultimate limit state performance and an analysis was undertaken with potential fatigue damage modelled to prove the structure would not collapse with such damage at the ultimate limit state. In situ strain monitoring was undertaken to calibrate the FE results, improve the predicted fatigue life and allow preparation of a long-term strategy for managing and monitoring fatigue activity using a damage tolerant approach.

2.2.13 Full interaction connection

Abbu et al [62] presented numerical predictions of vertical displacements in composite box girder bridge, they considered several factors, and confirmed through available experiments especially full shear connections which are obviously essential in composite box girder.

Abbu et al. [63] presented 3D numerical models of composite box girder bridges to simulate their actual structural behaviour, with emphasis on the girder-deck interface. Additionally, a prediction of several FE models is assessed against the results acquired from a field test. A number of factors are considered, and confirmed through experiments, especially full shear connections, which are obviously essential in composite box girder. A good representation for shear connectors by suitable element type is considered. Numerical predictions of vertical displacements at critical sections fit fairly well with those evaluated experimentally The agreement between the FE models and the experimental models show that the FE model can aid engineers in design practices of box girder bridges. Preliminary results indicate that number of shear studs can be significantly reduced to facilitate adoption of a new arrangement in modeling composite box girder bridges with full composition.

Abbu et al.[64] examined the stress patterns obtained using static 3D FE modelling. Comparisons are made between stresses obtained for the deck concrete of the composite box girder bridge, from the shell element model and solid element model. Several factors are considered, and confirmed through experiments especially full shear connections which are obviously essential in composite box girder. Numerical predictions of both vertical displacements and normal stresses at critical sections agree fairly well with those evaluated experimentally.

Composite box girder bridges analysed by Abbu et al. [65] with solid and shell elements using 3D FE analyses and their behaviour is investigated. The parametric investigations are performed on the composite box girder model to evaluate the effects of several important parameters on the behaviour of the girder. The results from this study would enable bridge engineers to design composite box girder bridges more reliably and economically.

2.2.14 Partial interaction connection

The difficulty of the structural section of the composite box girder bridges, and the complexity of the partial interaction theory, caused that the researchers avert merging between composite box girder and partial interaction theory in one study. The established design methods for reinforced concrete and for structural steel give no help with the basic problem of connecting steel to the concrete. The force applied to this connection is mainly, but not entirely, longitudinal shear.

Continuous steel-concrete composite box girder are widely used in bridge constructions; therefore the structural behaviour of composite box girder with interlayer slip is a significant subject. Numerical studies and experimental tests in this field are very lack and information about the efficiency of shear connection when the slab is under longitudinal shear are really few.

Lu et al. [66] submitted a paper named ’A theoretical model of deflection for composite box girder considering interface slip’, but they investigated the effects of shear slip on the deflection of composite beams. A theoretical formulation of the deflection for composite beams considering interface slip was derived. Further, the exact closed form characteristic equations for composite beams with interlayer slip are derived for the boundary conditions. Numerical simulations of simply supported beam subjected to different load cases were conducted. The analytical solutions show an excellent agreement with the numerical results. Finally, the proposed method was extended to analyse the deflection of the different pitch of shear connector composite beam and to some extent validate the mechanical sensitivity.

The difficulties of modeling the vertical flexure of mechanically fastened wooden ship hulls as that of box beams, a mainstay of naval architecture when applied to iron and steel ships, can largely be overcome by factoring the incomplete composite action of timber components in terms of a reduced shear modulus, an increased shear lag, and a reduced sectional area in tension (owing to butt joints). Sample computations on a large wooden hull indicate that its deflection can be limited to about twice that of a completely composite hull if stiff fasteners (drift pins) are used by Milner and Peczkis [67] at a much greater density than is typical of traditional construction. The lengths of timber pieces become severely limiting only if they are below 1⁄5th of hull length. The methodology has broad application to the preliminary design of many-piece timber box beam structures in general.

The behaviour of wide composite box girders having incomplete interaction was studied by Moffatt and Dowling [68] using FEs. Linkage elements' with a finite stiffness were used to connect the concrete slab to the steel plate forming the flange of a box girder. The FE model was validated against experimental results. The aim of the investigation was to study the effect of both the distribution and the flexibility of the shear connectors on the longitudinal bending behaviour. It was found that when the connectors were placed directly over the web, both stresses and deflections were little affected by the connector flexibility. The results of the study provided background for the formulation of design rules included in the draft Unified Bridge Code, and the rules are discussed in the light of these results.

Details are given by Moffatt and Lim [69] of several FEs which are especially suitable for use in the analysis of composite box girder bridges having complete or incomplete interaction. Model test results are utilized as a base for establishing the accuracy of the elements, which are then utilized to study some effects of shear connector distribution on the elastic behaviour of composite box girder spans.

The representing differential mathematical statements and boundary conditions of the composite box girders under horizontal loading were determined by Zhou et al. [70] using energy-variation method. Based on the consideration of longitudinal warp caused by shear lag effects on concrete slabs and bottom plates of steel beams, shear deformation of steel beams and interface slip between steel beams and concrete slabs, The closed-form solutions for stress, deflection and slip of box beams under lateral loading were obtained, and the comparison of the analytical results and the experimental results for steel-concrete composite box beams under concentrated loading or uniform loading verifies the closed-form solution.

A 3D FE model was proposed by Abbu et al. [71] to study the behaviour of shear connectors allowing for the concept of partial shear connection in both sagging and hogging moment regions. Behaviour of stud connected steel-concrete composite girders is numerically studied. Focus of the study is to develop and validate a 3D FE model. Suitable contact elements combined with the constraints are used to describe interaction among the concrete slab, steel beam and studs. Besides, the appropriate value of friction coefficient is also used for interaction between concrete and steel. The investigation focuses on the evaluation of partial shear connection in composite structures. The proposed 3D FE model is able to simulate the overall flexural behaviour of simply supported composite beams subjected to either concentrated or uniformly distributed loads. This covers: load deflection behaviour, longitudinal slip at the steel–concrete interface. The reliability of the model is demonstrated by comparisons with experiments and with alternative numerical analyses.

2.3 Experimental Works on Composite Box Girder Bridges

Experimental studies and field studies of composite box girders that are reported are relatively few. However, they are extremely important and have served to assess the adequacy of the analytical theories. Generally, field studies, although expensive to carry
out, provide invaluable data on the actual performance of such bridges.

2.3.1 Experimental works considering full interaction with no slip

The elastic response of a curved composite box girder bridge model was evaluated experimentally by Cheung et al. [72] and confirmed analytically using the FE method. Analytical predictions of both vertical displacements and normal stresses at critical sections compared fairly well with those evaluated experimentally. The isoperimetric thin shell element employed in the analysis proved to be versatile and provided an accurate representation of the various structural components of a curved box girder bridge. The experimental and analytical model studies on the horizontally curved box girder bridge have led to a number of important findings.

Composite beams with corrugated steel webs represent a new innovative system, which has emerged in the past decade for short and medium span bridges. The system usually combines the usage of corrugated steel plates as webs and prestressed concrete slabs as flanges for plate or box girders. Bridges that have been recently built with this hybrid system are outlined by Sayed-Ahmed [73], which focuses on the advantages of using corrugated steel webs as opposed to traditional flat webs. The flexural behaviour and bearing resistance of girders with corrugated steel webs is briefly discussed. The flanges of the new system solely provide the flexural strength of the beam with no contribution from the corrugated web. On the other hand, the corrugated web provides the shear capacity of the system. Thus, the shear behaviour of girders with corrugated webs is explicitly discussed focusing on the different failure and (or) buckling modes that affect the design of the corrugated steel web plates. Design charts for such webs are constructed based on the different interaction equations of failure. The torsion-warping behaviour of composite box girders with corrugated steel webs is also discussed. A structural system which combines the usage of external prestressing and corrugated steel webs has recently been used for different bridge composite girders. It was evident that there is no interaction between the flexural and the shear behaviour of beams with corrugated steel web. The web solely provides the shear strength of the cross section, which is controlled by buckling. Three modes of buckling exist in the case of corrugated webs: local buckling mode, global buckling mode, and an interaction mode. The critical shear stress for local buckling can be based on the classical isotropic plate theory. Shear stress for each mode have been presented. The interaction between the three buckling modes and the yield failure criterion of the steel was explicitly studied. Post-buckling shear strength of beams with corrugated steel webs was found to be significantly dependent on the corrugation panel width. This post-buckling strength may range between 10% and 80% of the total ultimate shear strength of the beam. When corrugated webs are used for composite box girders, a unique torsional–warping interaction behaviour results. The corrugated webs were assumed to be pin connected to the concrete slabs of the box girder and thus the behaviour may be simplified.

In order to design continuous composite bridges with full-depth precast decks, an experiment was executed by Ryu et al. [20] with a steel box-girder bridge model having two spans of 10 m each. Because there is no reinforcement at the transverse joints except prestressing tendons, a design criterion for the prevention of cracking at the joints is not to allow tension at the joints under service loadings. A major interest is in the behaviour of a composite section in a negative moment region. Therefore the elastic and inelastic behaviour of the model was carefully observed to provide proper design bases. In particular, cracking load, crack width and moment curvature of composite sections were investigated. The validity of the stiffness of the concrete slab in the negative moment region is discussed in terms of serviceability and ultimate limit states. After cracking at the joints, the flexural behaviour of a beam was observed carefully to estimate tension stiffening effects of the tendon and moment redistribution. Test results showed that uncracked section analysis for the concrete slab in a negative moment region could be used for serviceability, and a cracked section for ultimate limit states.

The experimentally observed behaviour of five, one-twelfth scale. wide-flange single-cell composite steel-concrete box girders with both box- and trough-shaped steel sections is described by Dalen and Narasimham [74] and compared with the behaviour predicted by a folded plate analysis. The folded plate method accurately predicts the elastic strains in such girders when subjected to uniformly distributed load but seriously underestimates the elastic deflections. Aspects of the design of single-cell composite box girders where existing standards result in satisfactory structural behaviour are identified.

The folded plate method can be used to calculate stresses in a wide-flange single-cell composite box girder bridge with a box or a trough section, and with a shear connection designed by conventional means. The maximum discrepancies between the analytical and experimental magnitudes of the longitudinal strains were 10% for the steel strains at the bottom of the box or trough and 15% for the longitudinal concrete strains on the top of the composite plate. Vertical deflections are grossly underestimated by the folded plate method. Discrepancies between experimental and analytical deflections as large as 35% were observed. Some of this discrepancy is ascribed to the fabrication techniques used in the models, but a discrepancy of 13% remains unexplained. It is concluded that the folded plate underestimates deflections of a box girder section by approximately 13%. For the dimensions of the models tested, no conclusive difference in the general structural behaviour was observed between specimens with a steel box section and a steel trough section with the same flexural stiffness.

Bracing systems are usually installed within the girder during construction to increase the torsional and distortional stiffness of the open section. The influence of these bracing systems on open box behaviour is discussed by Branco and Green [75] using finite strip analysis results and a one-quarter scale girder model test data. The distortional bracing were found effective in preventing distortion, with web stiffening found to be more effective than interior cross bracing. Horizontal bracing at the flange level was considered to reduce twisting of the section. This bracing can take the form of either torsion boxes or top chord bracing, both being effective.

Temperature distribution in composite box girder bridges is predicted by Dilger et al. [76] from the diurnal variation of the solar radiation to which the structure is exposed. Parametric studies are conducted in order to find the extreme temperature differences developed. Selected cases of temperature distributions are used as input for analyses to find temperature-induced stresses in a two span continuous structure.

Huang [77] presented the results of full-scale static and dynamic load testing of a curved box girder bridge. Two florida department of transportation test trucks with a total weight of up to 117 tons provided the static loading. One florida department of transportation test truck with a total weight of 52.7 tons applied the dynamic loading. Two different theoretical mechanical models were developed to evaluate the test results. The agreement between test and analytical results supports the expectation that actual bridge responses can be well predicted through theoretical analysis with limited experimental data. The influence of barriers, effective width of concrete slabs and impact factors are discussed.

Experimental results on a 20 m continuous composite bridge model with precast decks were presented by Shim et al. [78]. Internal tendons and external tendons were used to prevent cracking at the joints. Judging from the inelastic behaviour of the bridge model, external prestressing in negative moment regions could offer better performance in terms of cracking and flexural stiffness. Simple plastic analysis was carried out to estimate the ultimate flexural capacity of the continuous bridge, and the incremental prestress of external cables after cracking was estimated.

The performance of steel-concrete composite structures depends significantly upon the bond characteristics of connection between concrete and steel plates. A new type of shear connectors was developed by Tategami et al. [79] using perforated steel plates, commonly known as perforbond. An experimental investigation was conducted to study the shear strength characteristics of such connections, considering several test parameters. This paper describes the results of the experimental investigation. Further, based on the experimental results, prediction equations are proposed to calculate the shear strength of perforated steel plates and effects of confinement due to penetrating steel.

He et al. [80] presented a type of composite box girder with corrugated webs and concrete filled steel tube slab to overcome cracking on the web and reduce self-weight. Utilizing corrugated steel web improves the efficiency of prestressing introduced into the top and bottom slabs due to the accordion effect. In order to understand the loading capacity of such new composite structure, experimental and numerical analyses were conducted. A full-scale model was loaded monotonically to investigate the deflection, strain distribution, loading capacity and stiffness during the whole process. The experimental results show that test specimen has enough loading capacity and ductility.

Experimental and analytical studies of two-span continuous composite bridges with open box girder section were conducted by Ryu and Chang [81]. Cracking, yielding and ultimate loads were evaluated and compared with the test results for design of continuous composite bridges with precast decks. To evaluate yielding loads of continuous bridges, an uncracked section method considering moment redistribution which is defined in EUROCODE 4, was considered. In calculation of ultimate strengths, full or partial shear connection and sectional classes which were defined in EUROCODE or AASHTO LRFD specifications were considered. Also, through numerical analysis considering material nonlinearities, moment–curvature relationship and moment redistributions were estimated.

To have a better understanding of the torsional mechanibase model and influencing factors of PC composite box-girder with corrugated steel webs, ultimate torsional strength of four specimens under pure torsion were analyzed by Ding et al. [82] with model test method. Monotonic pure torsion acts on specimens by eccentric concentrated loading. The experimental results show that cracks form at an angle of 45o to the member's longitudinal axis in the top and bottom concrete slabs. Longitudinal reinforcement located in the center of cross section contributes little to torsional capacity of the specimens.

An experimental box girder having nominally identical cantilever sections was constructed by Korol et al. [83] to model the geometry of a pier girder of the Hunt Club–Rideau Bridge structure in Ottawa. The one-fourth scale model did not, however, replicate the varying depth of the prototype. The objective was to determine whether a deliberate reduction in the gross heat input for welds attaching longitudinal stiffeners to the flange plates for one end of the girder could augment the carrying capacity of a statically loaded box girder. The results from the two tests are such as to suggest that inward bent transverse stiffeners may account for a greater reduction in strength than do the imperfections of local plate panels of compression flanges.

The degree of geometrical imperfections existing in the plate panels of six in situ steel box girder bridges located throughout Canada is reported by Korol et al. [84]. The purpose of a continuing investigation is to establish the extent to which strength and performance of Canadian box girders in multispan bridges are sensitive to imperfections. The 95% fractals obtained from the imperfection measurements of webs and bottom flanges are shown to vary considerably from one bridge to another but, in general, tend to decrease with increasing plate thickness.

Research on the fatigue behaviour of horizontally curved, steel bridge elements was conducted at Fritz Engineering Laboratory by Daniels et al. [85]. The multi-phase investigation spanning nearly five years was performed which included, analysis and design of five large scale horizontally curved steel twin plate girder assemblies and three large scale horizontally curved steel box girders, primarily for fatigue testing, and special analytical studies of the influences on fatigue of stress range gradient, heat curving, "oil canning" of webs and the spacing of internal diaphragms in curved box girders, fatigue tests, to 2,000,000 cycles, of each of the above eight curved test girders, additionally ultimate strength tests of three of the curved plate girder assemblies and two of the curved box girders following the fatigue tests (composite reinforced concrete slabs were added to two of the three curved plate girder assemblies and to both curved box girders) and finally development of design recommendations suitable for inclusion in the AASHTO bridge design specifications.

Daniels et al. [86] presented the results of the ultimate strength tests of one curved non-composite plate girder assembly, two curved composite plate girder assemblies and two curved composite box girders. The primary objectives of the research reported herein are: to determine the load-deflection behaviour of large size curved plate girder assemblies and curved box girders which are loaded to ultimate strength, and to compare the experimental behaviour with analytic predictions. The study is of very limited scope and is intended only as a pilot study of the ultimate strength of curved plate and box girders.

The ultimate strength behaviour of box girders when subjected to simultaneously applied bending and torsional loads was investigated by Heins and Humphreys in 1977 [87]. The study was conducted by experimentally testing several straight box girder models. Both non-composite and composite girders were tested. The results were compared to expected behaviour based on available analytical methods. From the test results a non-dimensional interaction curve was developed to expedite the load factor design of box girders. Simple relationships are also presented to relate straight box girders to curved box girders. With these relationships, the interaction curves can be applied to curved box girder designs. Application of these relationships are given by a design example.

The experimental program conducted by Sennah and Kennedy [41] involved the laboratory testing of five 1/12 linear scale composite concrete slabs on steel three-cell bridge models. These models were tested under eccentric and concentric loading conditions. For each loading case the following were measured: deflections of the bottom flanges, longitudinal strains in the steel top and bottom plate flanges, longitudinal strains in the concrete deck slab, and the support reactions.

The time-dependent behaviour of composite steel girder bridges was investigated by Kwak et al. [53] both theoretically and experimentally. The layer approach was used as an analytical model to determine the equilibrium conditions in a section, and to effectively consider the different material properties across the sectional depth. The effect of creep was studied in accordance with the first-order algorithm based on the expansion of a degenerate kernel of compliance function. In addition, the shrinkage effect of concrete was accounted for by the volume change of the concrete slabs. To verify the analytical results, field tests were performed on two actual bridges under construction. Strain values on the top and bottom flanges were monitored 30 days after the deck concrete had been placed. Analytical results compared well with the experimental results. The ultimate shrinkage strain recommended in the specifications can be significantly different from the actual rate of drying shrinkage, depending on field conditions such as concrete slump, the ambient temperature, and the relative humidity.

Two continuous composite girders, both of which had two 9 m long spans with 300 mm extension at each edge support and were 0.55 m high, were designed by Xu et al. [88] to study the mechanical properties in concrete crack, formation of sectional plastic hinge, load-carrying capacity, etc. One was a conventional composite girder and the other one was designed with double composite action in the negative flexural region. Moreover, evaluations of concrete crack width, based on different design codes, and cracking moment were compared with test results and agreed with each other. It indicated double composite action made concrete crack development slower in service load stage. The evaluation of sectional bending–carrying capacity of conventional composite girder in the negative flexural region based on the mechanical model with full plastic section of Euro Code 4 and an analogous method was found to evaluate that of double composite girder. The evaluation results coincided with test results proved the summation which can be drawn from test results.

Chang and Im [89] investigated the behaviour of composite box-girder bridges subject to environmental thermal effects such as solar radiation, air temperature and wind speed. It is based on the statistical analysis of measured temperature data which were recorded hourly in a newly constructed composite box-girder bridge for about 20 months continuously. Major thermal loading parameters that characterize the temperature profile are defined, and the seasonal behaviour of the parameters is described in detail. The experimental results are compared to the specifications suggested in the design codes for thermal loads. In addition, a series of heat transfer analyses using the two-dimensional FE method is conducted in order to generalize the results to bridges with different cross-sections.

Androus [90] consisted of an experimental and a theoretical investigation. The experimental investigation included testing up-to-collapse three bridge models. While the theoretical investigation used a FE software to examine the behaviour of 225 different bridges to extract stress distribution factors for maximum bending stresses that occur at the mid span.

2.3.2 Experimental works considering partial interaction and slip

In Composite box girder bridge systems, the box steel girder is designed to act compositely with the concrete deck to form a closed box for live loading. During the construction stage, however, the behaviour is not well understood. The usual practice of assuming the system to be non-composite during construction requires more researches.

Field studies have Composite box girders with live loading, and girders during construction was evaluated during the design of curved steel trapezoidal box girder bridges by Topkaya et al. [91]. Stresses due to construction loading can reach up to 60-70 percent of the total design stress for a given cross section. Laboratory tests were performed to investigate the shear transfer between the concrete deck and steel girder at early concrete ages (hours, not weeks).

2.4 Behaviour and Properties of Shear Connectors

Shear connectors have been provided to ensure the mechanical interaction between the steel profile and the concrete slab required to develop the composite action. They are really the most common devices.

A few researchers deal with the 3D FE modelling of stud shear connectors. It is widely known that laboratory tests require a great amount of time, are very expensive and, in some cases, can even be impractical. On the other hand, the FE method has become, in recent years, a powerful and useful tool for the analysis of a wide range of engineering problems.

A FE model developed by Lam and El-Lobody [92] to simulate the load-slip characteristic of the shear stud without head in a solid RC slab. The model takes into account the linear and nonlinear material properties of the concrete and shear stud. The FE results compared well with the results obtained from the experimental push-off tests and specified data from the codes.

Bursi et.al [93] investigated The seibase modelic performance of moment-resisting frames consisting of steel–concrete composite beams with shear connection, 3D FE models of the substructures set with the ABAQUS code and based on shell elements are established in order to evaluate different modeling assumptions and local effects, non-linear spring elements are adopted to trace the behaviour of shear connectors as well as the bond-slip between the slab and reinforcing bars.

Queiroz et.al. [94] presented investigation focuses on the modeling of composite beams with full and partial shear connection using the software ANSYS. A 3D model is proposed, in which all the main structural parameters and associated nonlinearities are included (concrete slab, steel beam and shear connectors). And nonlinear springs is used to represent the shear connectors.

Two-dimensional FE models employing plane stress elements are established by Wang and Chung [95], in order to examine the structural behaviour of simply supported composite beams with large rectangular web openings. Shear connectors with non-linear deformation characteristics are incorporated into the models through the use of both vertical and horizontal springs.

Sakr and Sakla [96] presented an uniaxial nonlinear FE procedure for modeling the long-term behaviour of composite beams at the serviceability limit State, the nonlinear load–slip relationship of shear connectors as well as the creep, shrinkage, and cracking of concrete slab are accounted for in the proposed FE procedure. An analytical model to simulate the time-dependent behaviour of composite beams is presented in this study.

An accurate nonlinear FE model of the push-out specimen developed by Nguyen and Kim [97] to investigate the capacity of large stud shear connectors embedded in a solid slab. The material nonlinearities of concrete, headed stud, steel beam and rebar were included in the FE model.

A FE model was created using ANSYS for each of the connections tested in the laboratory by Julander [98]. The results from the model were compared to the tested results to better understand the cracking behaviour of the connections. A preliminary FE model that when compared and matched with the tested results gives more information on the cracking behaviour of each connection was also created. LINK8 elements are line elements with three translational degrees of freedom were used to model the steel plate, welded rebar, and shear studs.

The simulation of the nonlinear structural behaviour of timber-to-concrete composite beams made with screws is presented by Oudjene et.al. [99], the screws were modeled using one-dimensional beam element, while the timber and concrete members were modeled, in detail, using 3D solid elements.

Tahmasebinia et.al. [100] presented a probabilistic study to evaluate the influence of material uncertainties on the numerically simulated structural response of composite steel–concrete floors consisting of concrete slabs cast on steel profiled sheeting and connected to steel beams by means of shear connectors. The numerical analyses are performed using a 3D FE model with all components of the composite member being modelled by means of solid elements developed using the commercial software ABAQUS.

Gattesco and Giuriani [101] studied the behaviour of the connectors in four specimens, two of them were subjected to monotonically increasing loading while the others were submitted to cyclic loading. For this purpose a direct shear test is proposed. These tests gave useful information both on the shape of the load-slip curves and on the damage accumulation at the end of each cycle.

Shim et al. [102] evaluated Ultimate slip capacity and strength for large studs through the push-out tests on large stud shear connectors, beyond the limitation of current design codes, static behaviour was investigated also.

A lot of push-out tests of shear studs embedded in normal strength concrete were conducted by Shim et al. [103]. Experimental push out tests were used to evaluate both the shear stud capacity and the load-slip curve of the connector

Mirza and Uy [104] studied the behaviour of shear connection in composite beams with both solid and profiled sheeting slabs subjected to axial and shear forces. They developed a 3D FE half symmetric model with shear studs placed at two levels

Kwak and Hwang [3] introduced a numerical model to simulate bond-slip behaviour in composite beam bridges. Based on a linear bond stress-slip relation along the interface, the slip behaviour is implemented into a FE formulation.

Pavlović et al. [105] submitted different alternatives for shear connectors (bolts and headed studs) are analysed to gain better insight in failure modes of shear connector in order to improve competiveness of prefabricated composite structures.

Guezouli and Lachal [106] proposed an accurate and efficient 2D nonlinear FE model to investigate the mechanical behaviour of the shear connection between prefabricated concrete slab and steel girder in composite bridges. A numerical investigation is carried out to study the influence of the friction coefficient on the load– slip behaviour of the specimen and the distribution of internal deformations and forces in the specimen.

2.5 The Push out Test

Because full-scaled push-off tests remain a costly and time-consuming option, numerical procedure that can predict the nonlinear response and the ultimate load capacity of the push-off test developed in this study in order to replace most of the experiments once the verification of the numerical method has been established from selective, well-controlled experimental results.

A total of twelve push-out tests carried out BY Shen and Chung [107] to obtain the shear resistances of the shear studs in standard push-out tests where the shear studs are under direct shear force. The load-slippage curves of the test specimens are analyzed rationally to provide two standardized load-slippage curves to describe the structural behaviour of the connections during the entire loading ranges.

Push-out tests conducted by Xue et al. [108]to investigate the different behaviour between single-stud and multi-stud connectors. A new expression of stud load-slip relationship was proposed.

The push-out test configuration suffered some changes in time, related with the specimens' geometry and the materials used. Various authors tested push-out specimens with different slab, reinforcement and stud dispositions, Slutter and Fisher [109] examined the fatigue resistance on 46 stud connector specimens by beam tests. All the specimens' slabs had the same geometry, with 680×500×150 mm3, including the same distribution 13mm in diameter, 4 transversal and 3 longitudinal rebars were disposed. The concrete flange was casted in horizontal position, as in a real structure. Mainstone and Menzies in 1967 [110] performed fatigue tests on push-out specimens, using stud shear connectors. Stud dimensions were 19 mm in diameter and 100 mm in height.

Ollgaard et al. [111] determined the static strength (nominal shear resistance) of stud shear connectors embedded in both normal-weight and lightweight concrete slabs. Johnson and Oehlers [112] reported several variables that influence push-out strength including "the thickness of the steel flange; the shank cross section, height, tensile strength, and position of the studs and the properties of the concrete.

Roderick and Ansourian [113] reported on 4 push out tests with one level load and three tests with multi-level load. The studs presented 19 mm in diameter and 100 mm in height. Hallam [114] reported on 13 tests using headed studs with 19 mm in diameter and 76 mm in height. Nothing is said about the rebar properties or the welding procedure. The push-out specimens built with two studs on each side. And during the tests, the concrete slabs were prevented from separation by a steel rod.

Faust and Leffer [115] reported push-out tests performed with headed studs embedded in lightweight aggregate concrete. The specimens tested under cyclic loading. Four headed studs with 22 mm diameter and 125 mm height welded on the flanges of the steel section. The fatigue endurance of the shear connection applied in composite bridges with precast decks has been reported by Shim et. al [116]. The standard push-out specimens built. The studs had 19 mm in diameter and 150 mm in height. The specimens performed with a 20 mm bedding layer to estimate the fatigue endurance in a precast deck.

Badie and Tadros [117] reported on fatigue tests performed with large shear studs in steel bridge girders. The diameter of the steel studs was 31.8 mm. these kinds of studs had about twice the static ultimate strength than the 22.2 mm studs, so fewer studs were required along the height of steel girder. Lam and El-Lobody [92] presented four Test Specimens of push out test with deferent concrete strength, an effective numerical model using the FE method ABAQUS to simulate the push-off test was proposed.

Jin-Hee Ahn et.al [118] reported on fatigue experiments of studs welded on steel plate for a new bridge deck system. Nine specimens fabricated according to the standard push-out specimen. The concrete slabs connected to 9 mm steel plates by means of four welded stud shear connectors with 16 mm diameter and 125 mm height.

2.6 Haunched Composite Box Girder Bridge

Steel box girders are often used for medium and long span continuous bridges. In the negative moment regions over the interior supports, the bottom flange of the box girder is subjected to compressive forces. Because the bridge bending moment is normally highest at the piers and the compressive strength of steel bottom flange plates are relatively low on account of buckling, thick steel plates with longitudinal stiffeners are necessary. For long span continuous box girders, a haunched profile is also often necessary so as to keep the compressive stresses in the compression flange within safe limits.

For multi span highway and railroad bridges, haunched continuous steel box girders are often used as main load-carrying members. The use of haunches at the interior supports provides a variation of negative moment strength similar to that of the design requirements, therefore enhancing the structural efficiency of the design.

Preliminary analyses of several bridge designs submitted by Yen et al. [119] that reveal thepossibility of reducing or eliminating haunches, with significant ramificationson efficiency of design as well as on economy of fabrication and erection. Tests of base modelall panel and box girder specimens show that with the use of concrete, the controlling mode of failure changes from the overall buckling of the bottom flange steel plate panel to local buckling between transverse anchor lines. The concrete slab shares in carrying compression force in the flange. Design guidelines are presented to insure the development of full yield strength of the steel plate and the full composite action of the materials. Proposed modifications to the AASHTO Specifications are included.

The economy of a haunched profile is affected by a large number of parameters, including the span length, the span ratio, the midspan depth, the shape and size of haunches, and the configuration and thickness of the flanges; All of these must be considered to achieve the proper design regarding the adoption and geometry of the haunches. Huang et al. [120] presented the results of a parametric study in which the costs of haunched and constant-depth continuous steel box girders are compared. Wide ranges of the parameters listed in the preceeding paragraph are included. The relative cost comparison is made based" on equal stresses in the bottom flange of the box girder. Practical guidelines are developed for the selection of the haunched profile.

2.7 Summary

More than 100 references about composite box girder bridge and the interface between it components are submitted. As noted above there is a gap in the partial interaction section even some researchers worked in this line but no one of them deal with the problem directly. Some of them used doubled I-girder analysis instead of box girder and some used composite beam ignoring box section. All of other researchers used full interaction theory when they modeled composite box girder in their numerical works even those who used the partial interaction theory in their analytical works. In recent years, some severe problems have developed in the deck of each bridge. There are areas of visible damage created from the separation between concrete and steel. When this happens, huge potholes have formed resulting from the destruction of the cast concrete. Inspectors have observed movement in the deck panels when trucks travel across the structure. In order to answer the question as to possible causes of the damage on the bridge, an accurate computer model of the section of the composite box girder bridge was generated. The slip calculations according to partial interaction between components are estimated. This will lead to resolving whether the bridge is performing at the level for which it was designed. The computer model will allow for a more thorough investigation of different conditions the bridge may undergo.

CHAPTER 3

FULL INTERACTION INTERFACE CONNECTION

3.1 General

Composite structures consist of two different materials joined together in such a manner that the resultant intensity of the composite system is more than the strength of the two materials added together. Due to this composite construction can make best utilization of each of the component materials. In steel and concrete composite box girder, concrete is assumed to hold most of the compression load while steel takes all the tensile stress. The two materials in the composite structure need to be firmly held together to arrive at the structure rigid and stiff. Steel and concrete composite structures, the two materials are kept together by means of headed shear connectors.

A box girder usually appears lighter than a conventional girder deck because it is both more slender and its inclined webs make it seem more slender than a twin girder deck for a given deck depth. Web inclination of the box girder effectively means that its bearing devices are always significantly closer together than those of a conventional girder deck are: this allows more compact pier designs.

The role of composite structures is increasingly present in civil construction works. Composite box girder consisting of two layers, both joined by metal devices known as shear connectors. The main functions of these connectors are to allow for the joint behaviour of the girder-deck, to restrict longitudinal slipping and uplifting at the element's interface.

Composite box girder are not new and have been used successfully tor many years in bridge construction. A simple girder analysis, modified by modular ratio techniques, has generally been used, assuming that there is full interaction between the steel and concrete. Such interaction is almost impossible to achieve as the connection is rarely stiff enough to provide complete interaction and some slip between concrete and steel is inevitable. The determination of the shear force between concrete and steel assuming full interaction is possible, and the simple expression of shear is quoted in many elementary texts. However, the accuracy of full interaction method is questionable as the connectors are often discrete and rarely act in a linearly elastic manner.

3.2 Composite Box Girder Bridges with Full Interaction Connection

Steel–concrete composite box girder generally consist of steel box girder, concrete and reinforcement. Shear connectors usually utilized to develop the composite action between steel and concrete. In steel, concrete composite members, the natural bonding, friction, and mechanical interlocking actions of shear connectors have a significant influence on the degree of interaction. It known that the degree of interaction between steel and concrete influences the shear flow and strain distribution. In addition, it has an impact on the structural performance, such as strength, stiffness, and failure mode. The degree of interaction in steel, concrete composite systems can evaluated as fully-interaction, partial-interaction, and no-interaction.

Full interaction analysis of composite box girders is based on the following assumptions: both steel and concrete are linearly elastic materials.

- Concrete subjected to tensile strain is cracked and ineffective in resisting load.
- The shear connection between the concrete and steel is sufficiently stiff to ensure that slip is negligible.
- Plane sections remain plane.
- These used essentially for effective shear transfer and consequently.
- Ensure full interaction for the complete composite action of box girder.

A global analysis is required to establish the maximum forces and moments at the critical parts of the bridge, under the variety of possible loading conditions. Local analysis of the deck slab usually treated separately from the global analysis. For proper and efficient evaluation of bending and torsion effects, it is necessary to use computer analysis. Programs are available over a wide range of sophistication and capability: the selection will usually depend on the designer's computing facilities. However, for global analysis of what is fundamentally a simple structure, quite simple programs will usually suffice. For the type of box girders considered in this study, there will normally be sufficient intermediate cross-frames or diaphragms to restrain distortion effects and to ensure that simple global analysis will be adequate. In the event of needing to investigate box girders, which provided with very little distortion restraint, more detailed analysis may needed, perhaps even involving the use of FE programs.

According to British Standard (BS) [121] the connectors at any cross section are assumed to be all of the same type and size. The design of the shear connectors between each steel web and its associated concrete flange should considered for each web separately. The longitudinal shear force Q_x on a connector at distance (x) from the web center line can be determined from BS [121]

$$Q_x = \frac{q}{n}\left[K\left(1-\frac{x}{b_w}\right)^2 + 0.15\right] \qquad 3.1$$

Where q is the design longitudinal shear due to global and local loadings per unit length of girder at the serviceability limit state for the web considered and calculated assuming full interaction between the steel plate and the concrete slab. The symbol n represents the number of shear connectors. K is a coefficient determined from some charts and b_w is equal to half the distance between the centerlines of adjacent webs or for portions projecting beyond an outer web. In other words b_w is the distance from the centerline of the web to the free edge of the steel flange.

3.3 Analysis Approach

Modelling and analysis of steel-concrete composite box beam combine many of the challenges encountered in steel structures and reinforced concrete structures, plus specific issues owing to the interaction and load sharing between structural steel and reinforced concrete components, shear lag and shear deformation. An important aspect of the structural analysis process is the selection of the mathematical model and associated analysis method. Few absolute guidelines are available for the selection of an analysis method. The number of permutations resulting from various combinations of complicating physical features and mathematical models is virtually boundless. This decision should be based on an evaluation of the nature and complexity of the structure, a thorough understanding of the expected behaviour, and knowledge of the capabilities and limitations of the various analysis options. Selection of a suitable analysis method is key to accurate and complete analysis results that are calculated to an appropriate level of refinement.

3.3.1 Analysis dimensionality

All bridges are 3D systems. However, depending upon its complexity, the actual system can potentially be mathematically reduced to a two-dimensional or one-dimensional model. Some bridges may be effectively modelled directly using a one-dimensional model, e.g., a straight I-girder bridge with moderate or no skew. A one-dimensional model considers an individual girder outside the context of the system and the model transverse distribution of live load using an empirically based approach.

In some cases, a system can be reduced from 3D to a 2D grillage (grid) model. This model can include the effect of girder eccentricity and cross frame stiffness in an indirect and/or approximate manner. The other cases a 3D analysis approach, which includes the depth of the system in the model and associated cross frames, etc., is appropriate.

3.3.2 Categories of steel girder bridges

The choice of analysis method is directly influenced by the nature and complexity of the structure as well as the analysis objectives and the resources available. In general terms, the behaviour of straight girders is less complicated than curved girders. Often straight girders can be analyzed using relatively simple methods. Alternately, curved girders experience torsional effects, both locally within each girder as well as globally through the entire superstructure. This complex behaviour often suggests the need for more rigorous analysis.

Either adding skew to a straight or curved girder bridge complicates the behaviour and associated analysis required to capture it. Compared to a non-skewed bridge, increased differential deflection between girders in a skewed bridge results from the adjacent girders and their supports being at different longitudinal positions. The connection of adjacent girders by cross frames affects the loads in both the girders and the cross frames. This behaviour is influenced by various geometric parameters including girder spacing, length of bridge, radius of curvature, and skew angle. Quantifying these effects often requires a more refined analysis than would be required for a non-skewed bridge.

Box-shaped girders are generally considered more complicated structures than I-shaped girders. Box-shaped girders have more pieces and parts than I-shaped girders, and these work together as a structural system in more complicated ways than simple I girder plus cross frame systems. The analysis of box-shaped girders by modelling them as line elements requires a number of simplifying assumptions and several additional calculations at the end of the analysis to determine all of the individual member load effects.

3.3.3 Complicating factors

In addition to the various levels of complexity inherently associated with different structure types, other factors can also complicate the analysis of any steel girder bridge. In some cases, these complicating factors can be addressed outside the analysis, perhaps by some simple supplemental hand calculations; in other cases, these factors may suggest the need for using a more rigorous analysis method. Some of these factors include:

Variable web depth (haunched girders) more simplified analysis methods either do not allow for non-prismatic girder cross sections, or require simplifying assumptions to model the section properties and leave the calculation of stress resultants in nonparallel flanges to the designer. While the approximations introduced in stiffness modelling typically have a negligible effect on the final results of the stiffness analysis used to determine load effects, the more important aspect of modelling non-prismatic girders is the use of the associated section properties in the computation of stresses due to the load effects and the associated resistances. However, such variations must be included in the computations of stresses and resistances.

Unusual substructures (integral substructures, flexible substructures such as deformable shear connectors or straddle bents, or multiple fixed piers) configurations can noticeably affect the structural response of superstructure elements. For example, if a slip in shear connectors for composite bridges is occurring which provides different vertical stiffness at the behaviour, the load distribution to the girders be affected. Likewise, shear lag present additional stiffness and loading complexity.

3.3.4 Girder modeling

How to approach the modelling of individual girders depends greatly on the type of analysis method being used and whether girders are considered individually or the entire superstructure system is modelled. In the case of most of the simplified analysis methods, however, the typical approach is to model a single girder, rather than modelling the entire multiple girder cross section.

For such an analysis, the designer must determine appropriate cross-sectional properties. The non-composite steel girder cross-sectional properties are generally easy to quantify as the dimensions of the girder are clearly and unambiguously identified. For the composite case, the problem becomes slightly more complex, with an important parameter being the "effective width" of the composite deck. The AASHTO LRFD specifications [122] offer explicit guidelines for effective width estimates.

Keep in mind that simply using deformable connectors do not ensure that the stresses offer good restraint to the bridge. Most designers and owner-agencies neglect any restraint from deformable connectors in superstructure design. For this reason, most engineers have concluded that the connectors to be rigid and that the girder and deck can be assumed to behave as a one part.

3.4 Finite Element Approach

Of all the available analysis methods, the FE method is believed to be the most vigorous, versatile and suitable numerical tool to resolve a complex continuing problem. The method has become an important and frequently indispensable part of engineering analysis and intent.

Recent development in computer technology makes it possible to use FE computer programs, practice in all branches of engineering. A complex geometry such as that of composite box girder bridges can be readily modelled using the FE technique. The method is also capable of dealing with different material properties, relationships between structural components, boundary conditions, as well as statically or dynamically applied loads. The linear and nonlinear structural response of such bridges can be predicted with good accuracy using this method.

The FE method has become a staple for predicting and simulating the physical behaviour of complex engineering systems. The commercial FE analysis programs have gained common acceptance among engineers in industry and researchers at universities and government labs. Thus, academic, engineering departments include graduate or undergraduate senior-level paths that encompass not just the theory of FE method, but also its applications using the commercially available FE analysis programs.

FE analysis, also called the FE method is a method for numerical solution of field problems. A field problem requires determination of the spatial distribution of one or more dependent variables. Mathematically, a field problem is described by differential equations or by an integral expression. Either description may be applied to formulate FEs. Individual FEs can be visualized as base modelall pieces of a structure. Elements are connected at points called nodes and the assemblage of elements is called a FE structure.

Although 3D FE modelling is probably the most involved and time consuming, it is still the most general and comprehensive technique for static and dynamic analyses, capturing all aspects affecting the structural response.

There are three ways to make a model in any FE program for solid modelling. The first method is directly (manual) generated, in this method we specify the location of nodes and define which nodes make up an element. This method is used for simple problems that can be modelled with line elements (links, beams, pipes) and for objects made of elementary geometry (rectangles) but not recommended for complex solid structures.

The second method is importing geometry, in this method the geometry created in a CAD system like Autodesk Inventor and saved as an import file such as an IGES, DFX files, but inaccuracies occur during the import, and the model may not import correctly.

The last method is solid modelling approach, in this method the model is created from simple primitives (rectangles, circles, polygons, blocks, cylinders, etc.) and boolean operations are utilized to combine primitives.

3.4.1 Three dimensional finite element modelling

Typically, the most analytically complicated level of analysis is 3D analysis. Like a grid analysis, a 3D analysis is a FE modelling technique. Instead of limiting the model to a 2D grid of nodes and line elements, a 3D analysis models the superstructure in detail (flanges, webs, deck, bracing members, and so forth). Commercial applications are available to perform part or all of a 3D analysis. Such applications are available which build a 3D model of a composite box girder bridge and run a live load analysis using either influence surface or live load generator methods.

One of the best uses of brick elements is to model the deck, where the girders are modelled with shell or frame elements located eccentrically with respect to this deck. Shell elements can adequately model the load distribution to the girder and shear lag (effective flange) effects with finer meshes. However, modelling the deck stresses or flexural bending in a deck is difficult. Significant arching action, cracking, slip cannot be properly modelled with most shell elements in readily available applications. For a detailed analysis of deck stresses, brick elements are likely required.

Because all of the components of the bridge are directly modelled, a 3D analysis has the advantage of being rigorous and internally consistent among all portions of the structure. A 3D analysis directly models the stiffness characteristics, and direct analysis results are available for all elements of the structure. Complex structural configurations are modelled in detail, rather than approximating the overall stiffness parameters with estimated single values.

For example, to model a steel box girder in a 3D analysis, the bottom flange is modelled with separate elements, as are the two webs, the two top flanges, the internal cross frames and the top flange lateral bracing. In contrast, in a grid analysis the entire box girder (flanges, webs, internal cross frames and top flange lateral bracing) is modelled as a single line element, with the stiffness of all associated complex framing approximated using simplified calculations or empirical estimates. This detail and rigor in a 3D model theoretically leads to analysis that is more accurate results. Many designers find 3D analysis results much less intuitive and harder to visualize and understand. As a result, the risk of inadvertent mistakes or misinterpreted analysis results is greater.

3.4.2 Finite element modelling with ANSYS

ANSYS is a FE analysis program used for solid modelling; it has extensive capabilities in structural analysis. The solid model consists of key points/nodes, lines, areas and volumes with increasing complexity in that order. Careful thought needs to be put into the model before building the entire model. Once the model is meshed, volumes, areas, or lines cannot be deleted if they are connected to existing meshed elements. The aspect ratio and type of mesh must also be decided depending on the size and shape of the complete solid model.

ANSYS contains many solid FEs to choose from, each having its own specialty. First, the type of analysis must be chosen which ranges from the structural analysis, thermal analysis, or fluid analysis. Once the type of analysis is determined, an element type needs to be chosen, ranging from beam, plate, shell, 2D solid, 3D solid, contact, couple-field, Specialty, and explicit dynamics. Each element has unique capabilities and consists of tetrahedral, triangle, brick, 10 nodes, or 20 node FEs in both 2D and 3D analysis. [123]

Structural mechanics solutions from ANSYS provide the ability to simulate every structural aspect of a product, including linear static analyses that simply provides stresses or deformations, modal analysis that determines vibration characteristics, through to advanced transient nonlinear phenomena involving dynamic effects and complex behaviours.

All users, from designers to advanced experts, can benefit from ANSYS structural mechanics solutions. The fidelity of the results is achieved through the wide variety of material models available, the quality of the elementary library, the robustness of the solution algorithms, and the ability to model every product from single parts to very complex assemblies with hundreds of components interacting through contacts or relative motions.

ANSYS structural mechanics solutions also offer unparalleled ease of use to help product developers focus on the most important part of the simulation process understanding the results and the impact of design variations on the model. ANSYS is a FE analysis software package. It uses a preprocessor software engine to create geometry. Then it uses a solution routine to apply loads to the meshed geometry. Finally, it outputs desired results in post-processing [123].

3.5 Description of Collecting Experimental Bridge Models

Ryu et al. [20] presented test results of a two-span continuous composite box girder bridge in 2003. Figure 3.1 depicts the geometrical configuration of the bridge model in conjunction with boundary conditions. The numerical evaluation in the present study is undertaken to simulate behaviour of this model. The height of the steel section was 800 mm and the thickness of the precast concrete slab was 150 mm. The slab width was 1470 mm, as shown in Figure 3.1.

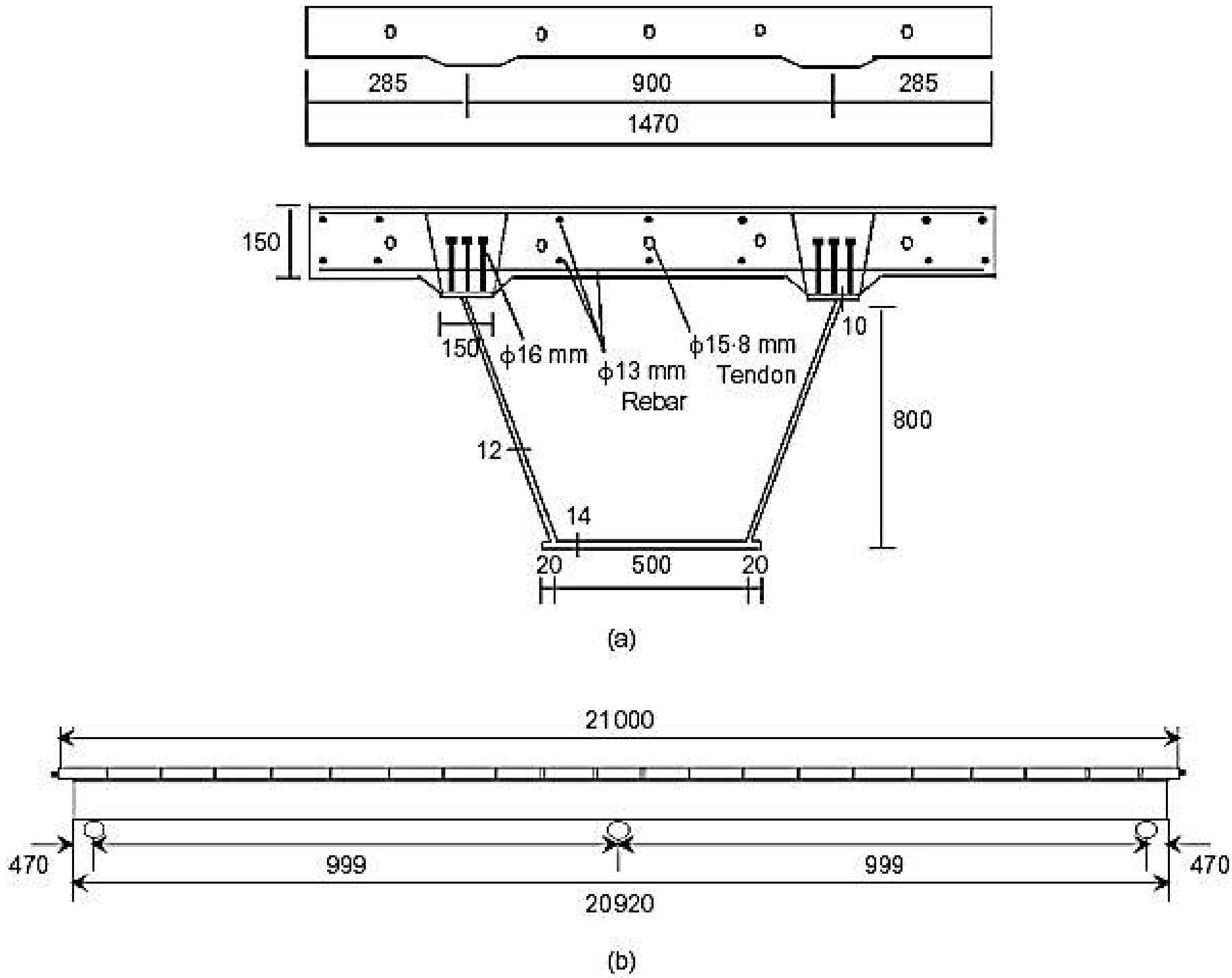

Figure 3.1 Continuous bridge model: (a) cross-section; (b) plan view (in mm) [20].

Twenty-one precast panels 980 mm long were installed on the top flange of the steel girder. Each precast panel has six blocks-outs for stud shear connectors that are installed on the top flanges of the steel girder to achieve full shear connection. The thicknesses of the upper flange, web and lower flange were 10 mm, 12 mm and 14 mm respectively.

3.5.1 Material properties

Yield stress and ultimate tensile strength of steel material used to build box section are 240 MPa and 520 MPa, respectively. Elastic modulus of steel is 190 GPa. 28 days compression strength of concrete used to build the deck portion is 35.5 MPa, the average value of all the precast concrete panels for 28 days compressive strength is 35.3 MPa. Elastic modulus of concrete is 30 GPa.

3.5.2 Experimental model loading

In experimental study of Ryu et al. [20], two concentrated loads were applied in the mid-spans of the composite bridge by an MTS closed-loop electrohydraulic testing system of 2000 kN capacity, as shown in Figure 3.2. Static tests for observation of the elastic behaviour of the model were performed with 250 KN values for each span. Displacements of the continuous beam were measured at each mid-span with linear variable differential transformers (LVDTs). In this thesis, the load with 250 KN values for each span is used.

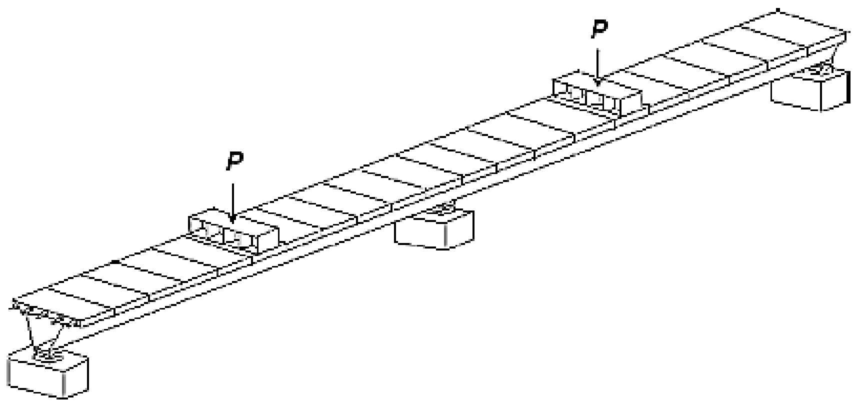

Figure 3.2 Bridge loading [20].

3.6 Description of Numerical Bridge Models

3.6.1 Loading test for finite elements models

In certain engineering problems, the behaviour of some of the unknown degrees of freedoms may be known. For example, certain points (nodes) may be expected to have the same displacement in a certain direction. One can take advantage of this behaviour and enforce it in order to achieve an accurate solution with minimum computational resources. If a particular degree of freedom at several nodes is expected to have the same unknown value, these degrees of freedoms can be coupled.

Coupling is a way to force a set of nodes to have the same Degree Of Freedom (DOF) value. Similar to a constraint, except that the DOF value is usually calculated by the solver rather than user-specified. A coupled set is a group of nodes coupled in one direction (i.e, one degree of freedom).

The coupling is realized with CP command, the value of the degree of freedom is coincident for all the points to be coupled. Beside command CP, the other two CP commands, CPINTF and CPCYC, are utilized frequently. CPINTF is used to couple the nodes at the same location, but CPCYC is used to couple the nodes of the symmetrical model, furthermore, it can be applied to couple the nodes with given distance. Single point load applied for FE models and point loading was simulated by applying a concentrated load at a total of line nodes that are coupled constrained on the midspan of each span for the FE models of composite box girder bridges.

3.6.2 Description about the elements used in the model

The FE modelling and analysis performed in this study were done using a general purpose, multi-discipline FE program, ANSYS, which has an extensive library of truss, beam, shell and solid elements. The brief description of the elements used in the models are presented below:

3.6.2.1 SHELL181 element description

SHELL181 is suitable for analysing thin to moderately-thick shell structures. It is a four-node element with six degrees of freedom at each node: translations in the x, y, and z directions, and rotations about the x, y, and z-axes. SHELL181 may be used for layered applications for modelling composite shells or sandwich construction. The accuracy in modelling composite shells is governed by the first-order shear-deformation theory (usually referred to as Mindlin-Reissner shell theory). The following Figure 3.3 shows the geometry, node locations, and the element coordinates system for this element. The element is defined by shell section information and by four nodes (I, J, K, and L) [124].

3.6.2.2 SOLID185 element description

SOLID185 is used for 3D modelling of solid structures. It is defined by eight nodes having three degrees of freedom at each node. There are translations in the nodal x, y, and z directions. The element capable to analysis plasticity, hyperelasticity, stress stiffening, creep, large deflection, and large strain. It also has the mixed formulation capability for simulating deformations of nearly incompressible elastoplastic materials, and fully incompressible hyperelastic materials. The following Figure 3.4 shows the geometry, node locations, and the element coordinate system for this element [124].

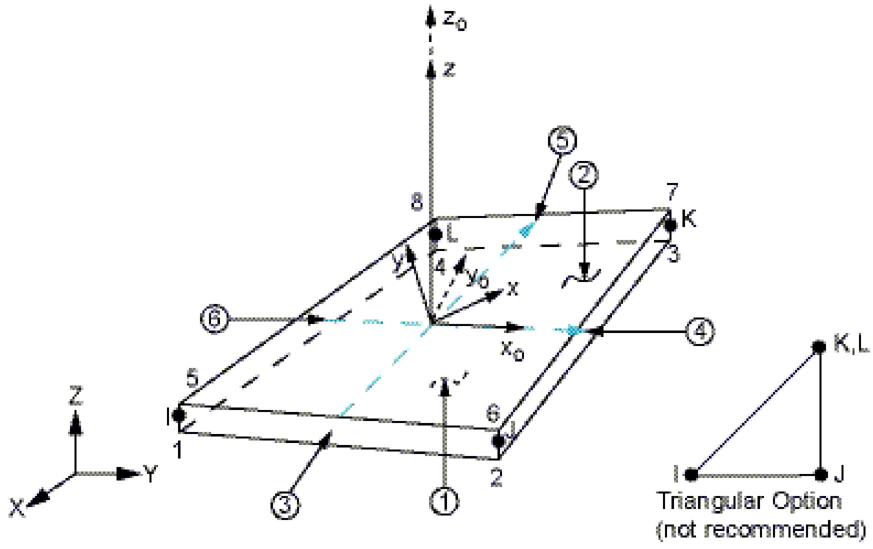

Figure 3.3 SHELL181 geometry [124].

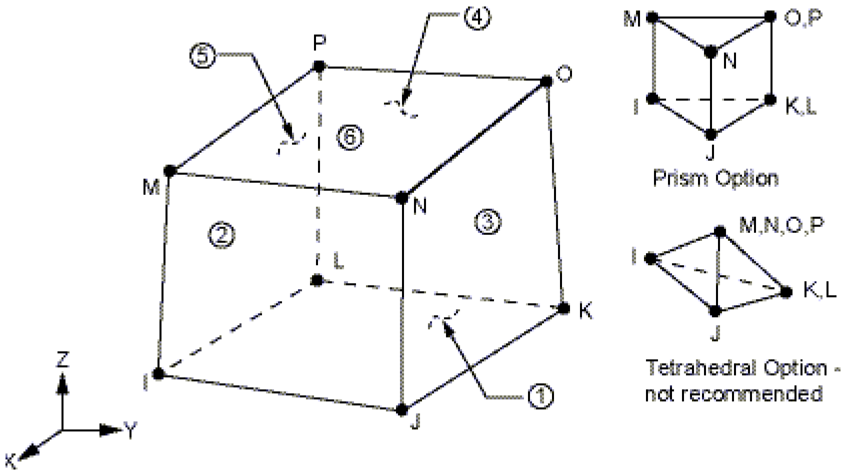

Figure 3.4 SOLID185 geometry[124].

3.6.2.3 MPC184 element description

MPC184 comprises a general class of multipoint constraint elements that apply kinematic constraints between nodes. The elements are loosely classified here as "constraint elements" (rigid link, rigid beam, etc.)

The MPC184 general joint is a two-node element. By default, no relative degrees of freedom are fixed. By specifying as many relative The following Figure 3.5 shows the geometry, node locations and the element coordinate system for this element [124].

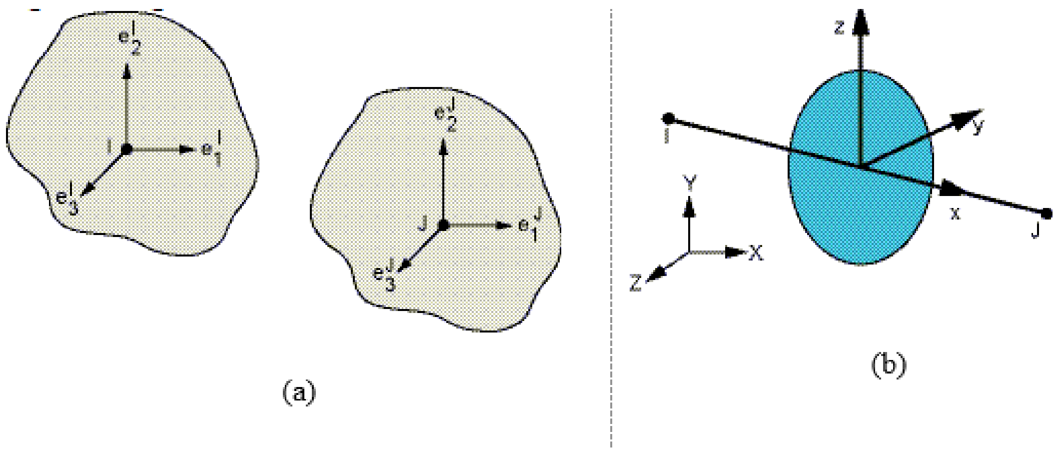

Figure 3.5 MPC184 element (a) General joint geometry, (b) Rigid link geometry [124].

The MPC184 rigid link/beam element can be used to model a rigid constraint between two deformable bodies or as a rigid component used to tranbase modelit forces and moments in engineering applications. This element is well suited for linear, large rotation, and large strain nonlinear applications.

3.7 Finite Element Models

Composite box girder bridge models were simulated using a commercial FE program ANSYS. Since the materials were stressed in elastic limits in the study of. Ryu et al [20]. Linear analysis of bridge models is undertaken in present study. The slab and the box girder were connected by rigid links because full interaction between slab and steel girder was assumed. Figure 3.6 and 3.7 present FE model 1 and 2 respectively, which are developed using SHELL181 shell elements in both concrete deck and steel box girder portions. Point load is applied in model 1 as shown in Figure 3.6. The model 2 differs from model 1 in having different loading at mid-spans in order to represent line loading. The vertical translation degrees of freedom of the nodes across the width of the deck are coupled as shown in Figure 3.7.

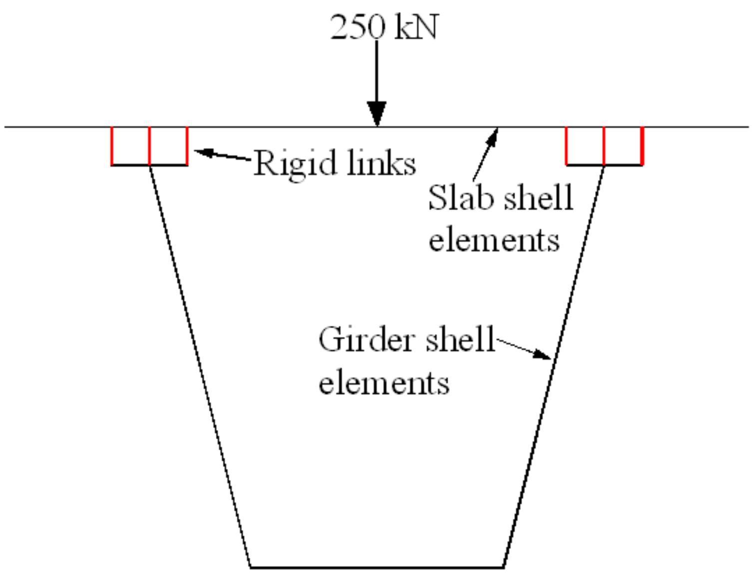

Figure 3.6 FE Model 1.

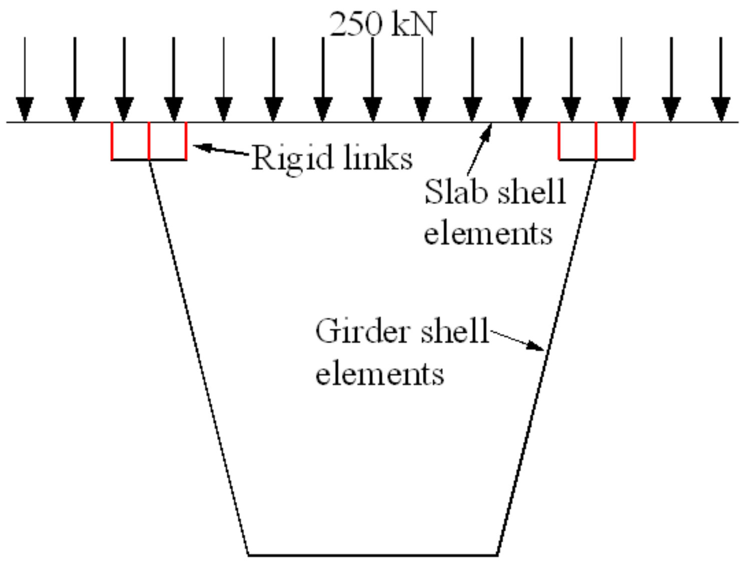

Figure 3.7 FE Model 2.

Thickness of concrete deck portion is considerable compared to steel and other geometrical details.

Another convenient way to represent this thickness is to adopt 3D brick elements. Since the cross section is prismatic, employing 3D brick elements would not cause complicated modelling approach. In order to evaluate the performance of this modelling technique against shell models and test results models 3 and 4 are developed using eight nodes brick elements. Brick elements are just used to model concrete deck portion of the bridge where shell elements still represent the steel box portion as with models 1 and 2. The loading condition, which makes models 1 and 2 different, also creates the difference between models 3 and 4. Figures 3.8 and 3.9 present the details of models 3 and 4.

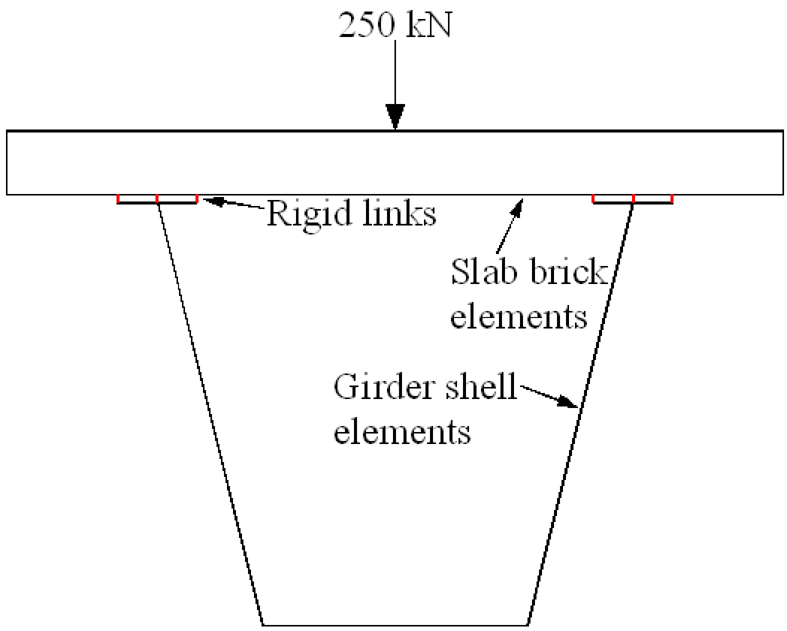

Figure 3.8 FE Model 3

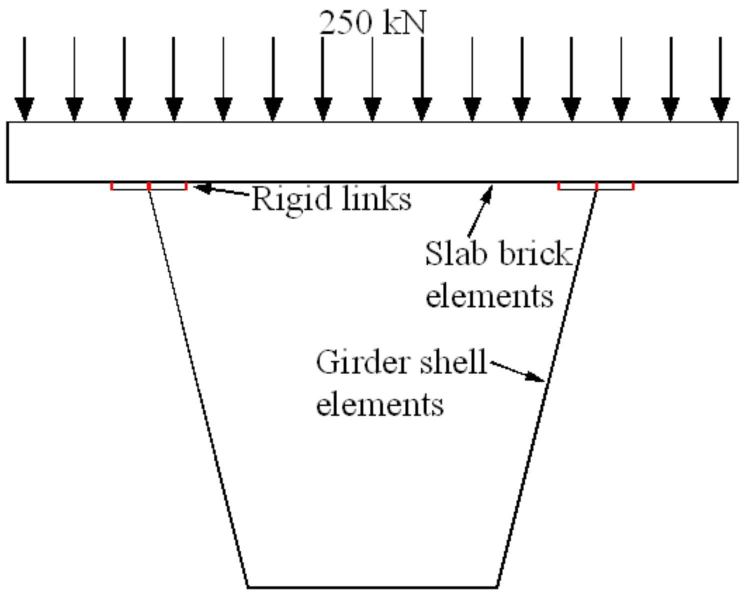

Figure 3.9 FE Model 4.

3.7.1 Finite element models without reduction of shear connector

In this study, the top concrete flanges were divided into thirty-four square elements for an appropriate aspect ratio of the elements and four divisions for each top steel flange.

The bottom flanges were divided into ten elements and webs were divided into twenty square elements. The longitudinal two spans were divided into 160 elements.

Two models are made using Shell 181 Elements-which are four-node elements with six degrees of freedom at each node-, for steel webs, concrete top flange, and the steel bottom flange. The plate thicknesses and the material properties are required input for Shell181. In addition, another two models are made using Shell181, for steel bottom flanges and webs. While solid185 elements are used for 3D modelling of concrete top flanges. They are defined by eight nodes having three degrees of freedom at each node. The mpc184 rigid element is used to model a rigid constraint between two bodies, steel and concrete in this case which are used to tranbase modelit forces and moments in all above models. Boundary conditions are handled in such a way to represent, simply supported conditions of test specimen.

The study was based on the following assumptions;

- The precast concrete slab deck is composite with the top steel flange of the cell.
- All materials are elastic and homogeneous.
- The concrete deck slab is considered uncracked.

3.7.1.1 Results for deflections in models 1-4 without reduction

The results of the ANSYS FE analysis using model 1-model 4 are shown in Table 3.1 and Figures 3.10-3.12 together with the loading-test results and the design values. It is observed that the design, analysis tends to overestimate the stress and the vertical displacement measured in the loading test. The differences at the mid-span of Model 4 are as much as 0.2 mm or 8 % in the vertical displacement.

Obtaining displacements and stresses from the FE, ANSYS models can be utilized in understanding the composite box bridge behaviour. In addition, it can also be used to compare the stress profiles. In modelling the bridges using ANSYS, a FE model was created using the command prompt line input other than the Graphical User Interface (GUI) can be used. During the static test done by Ryu et al. in the elastic range of loading, the flexural stiffness of the composite bridge showed linear elastic behaviour. Midspan deflections from the analysis were compared to the test results. In the experimental test, the midspan deflection was 2.52 mm and in the analysis performed by same researchers it was 2.76 mm at a load of 250 kN. Deflections results obtained from ANSYS FE models Model 1 to model 4 can be observed in figures below and they are summarized in Table 3.1:

Table 3.1 Deflection results for ANSYS models.

Model	**Midspan deflection (mm)**	**Deflection near end support (mm)**	**Deflection near central support (mm)**
Model 1	2.96	0.33	0.33
Model 2	2.57	0.29	0.29
Model 3	3.04	0.31	0.31
Model 4	2.56	0.28	0.28

It is interesting to note that in the case of Model 4 (which had a steel box girder with shell 181 elements and concrete deck with solid 185 elements and point load with constraint nodes along the line of that load) the best result comparing with experimental test had obtained, so the focusing will be on Model 4 to make comparison with experimental data submitted by Ryu et al. [20]. There is very good agreement between the two sets of results, whereas in the case of other models show some deviation. Midspan deflection from the FE analysis was compared with the test results as shown in Figure 3.11. In the test results, the deflection was 2·52 mm and in the analysis, it was 2·56 mm at a load of 250 KN.

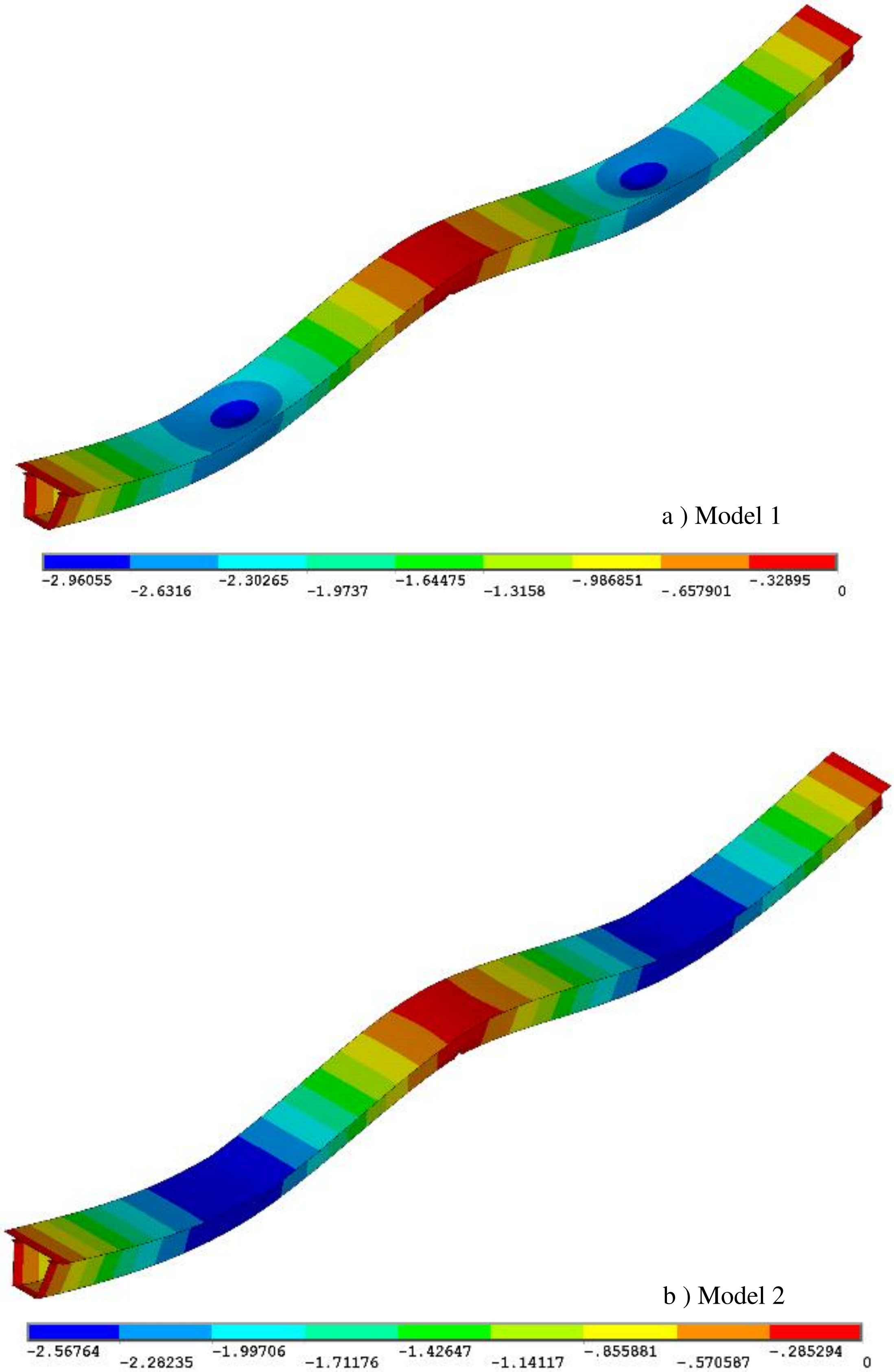

Figure 3.10 Deflections of numerical models

(Magnification factor=400) a) Model 1, b) Model 2, c) Model 3, d) Model 4

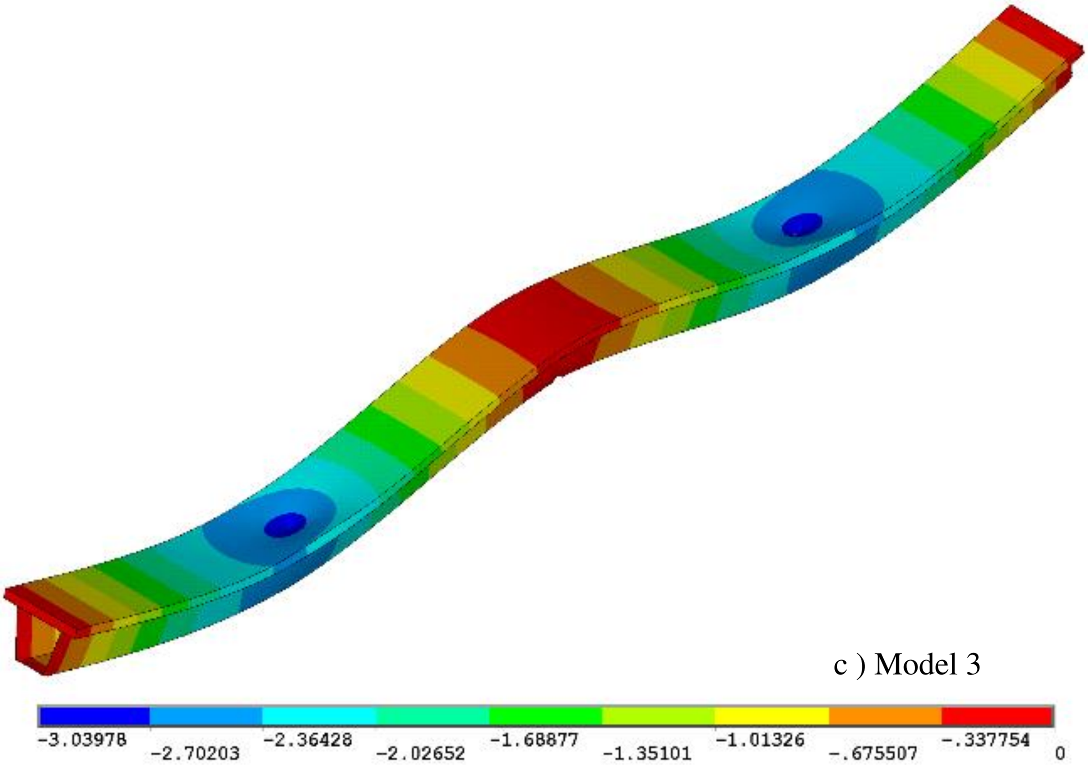

c) Model 3

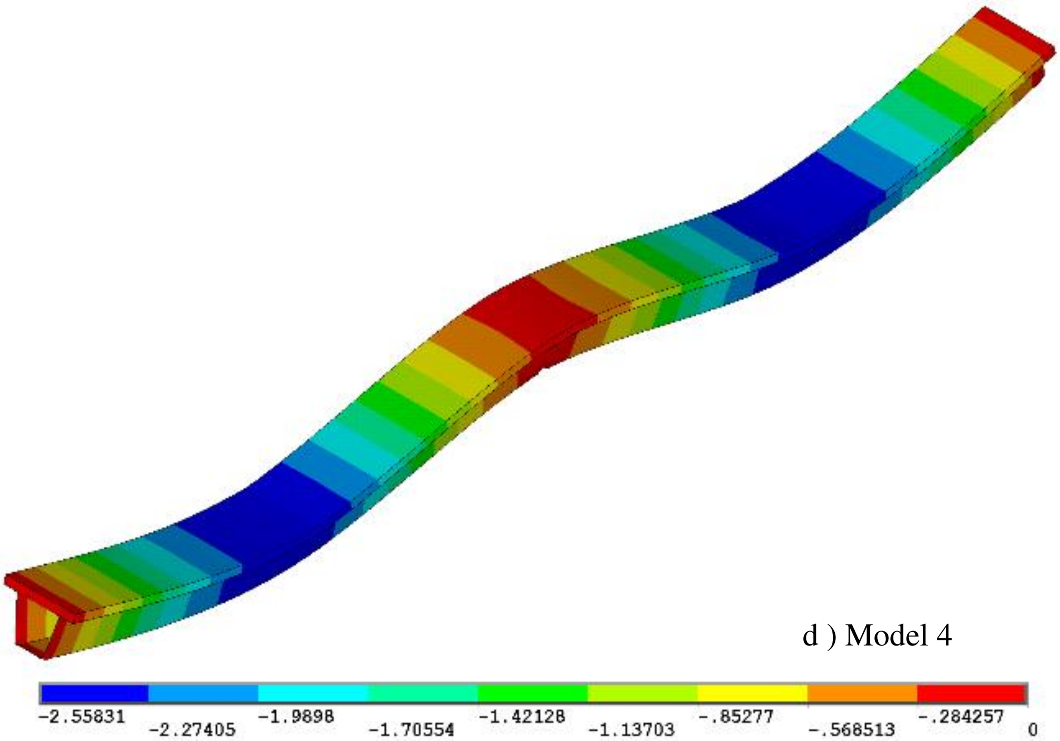

d) Model 4

Figure 3.10 (Continue) Deflections of numerical models
(Magnification factor=400) a) Model 1, b) Model 2, c) Model 3, d) Model 4

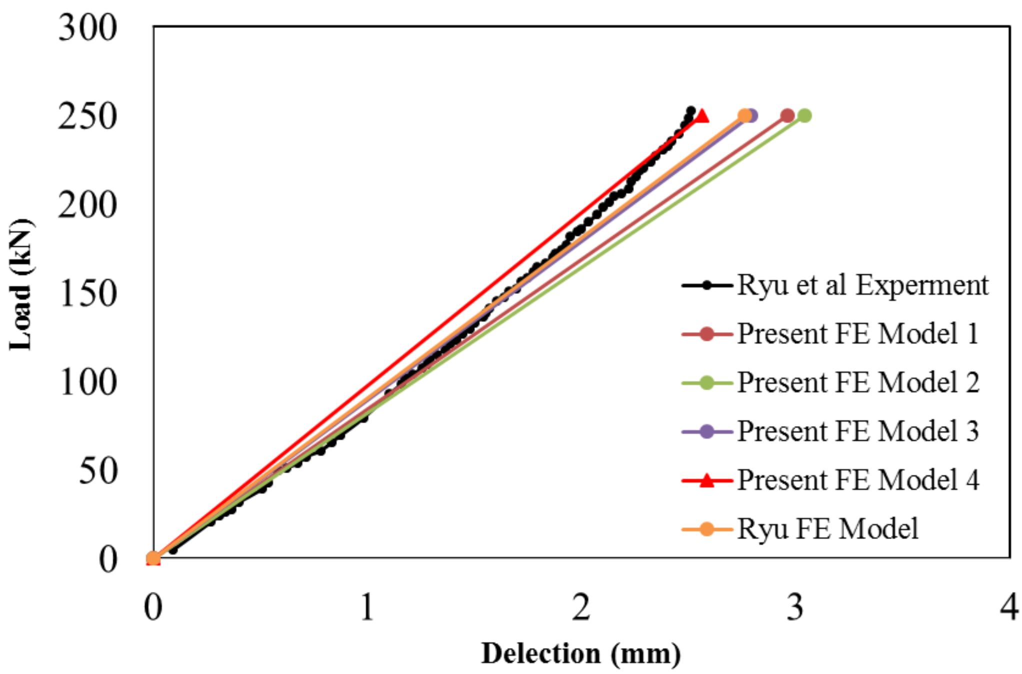

Figure 3.11 Load- Displacement curve for ANSYS and test results

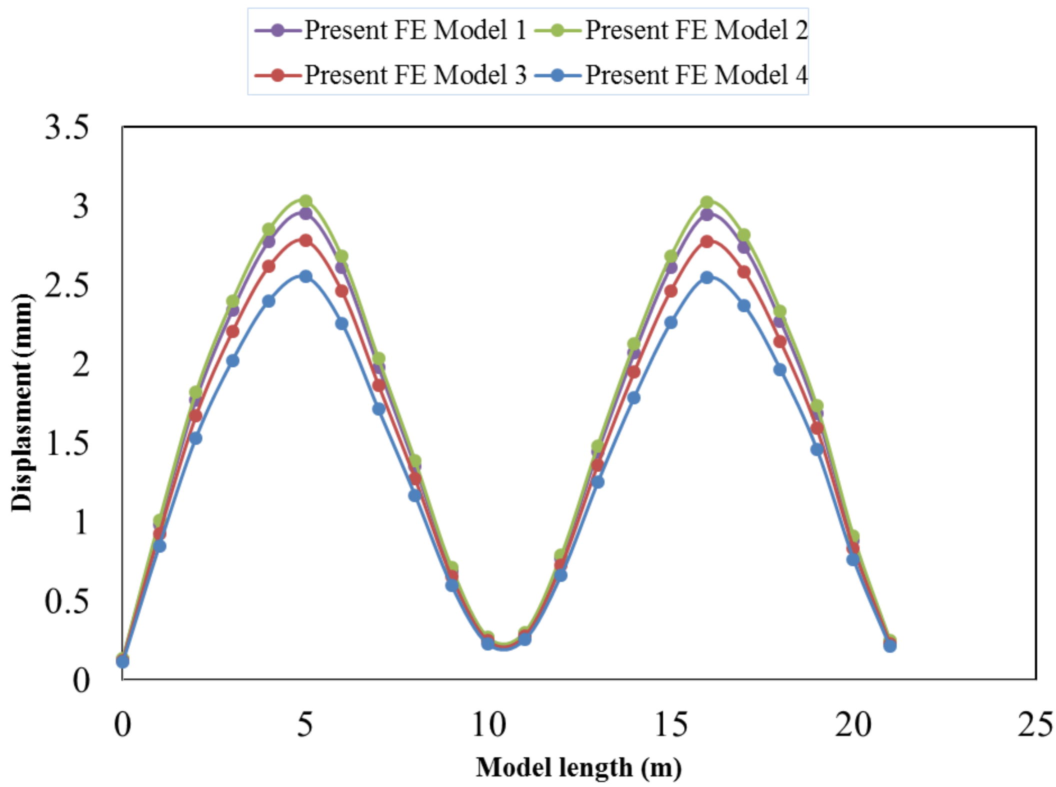

Figure 3.12 Displacement profile of model 4

3.7.1.2 Results for stresses in models 1-4 without Reduction

The results of the ANSYS FE analysis for stresses using model 1-model 4 are shown in Table 3.2 and Figure 3.13 together with the loading-test results and the design values. Stresses results obtained from ANSYS FE Model 1 to Model 4 can be observed in figures below and they are summarized in Table 3.2:

Table 3.2 Von Mises Stress results for ANSYS models

Model	Midspan Stress (N/mm^2)	Stress near end support (N/mm^2)	Stress near central support (N/mm^2)
Model 1	35.3914	0.01795	79.6083
Model 2	35.4098	0.01889	79.6483
Model 3	32.7389	0.01052	73.6493
Model 4	32.7524	0.01061	73.6797

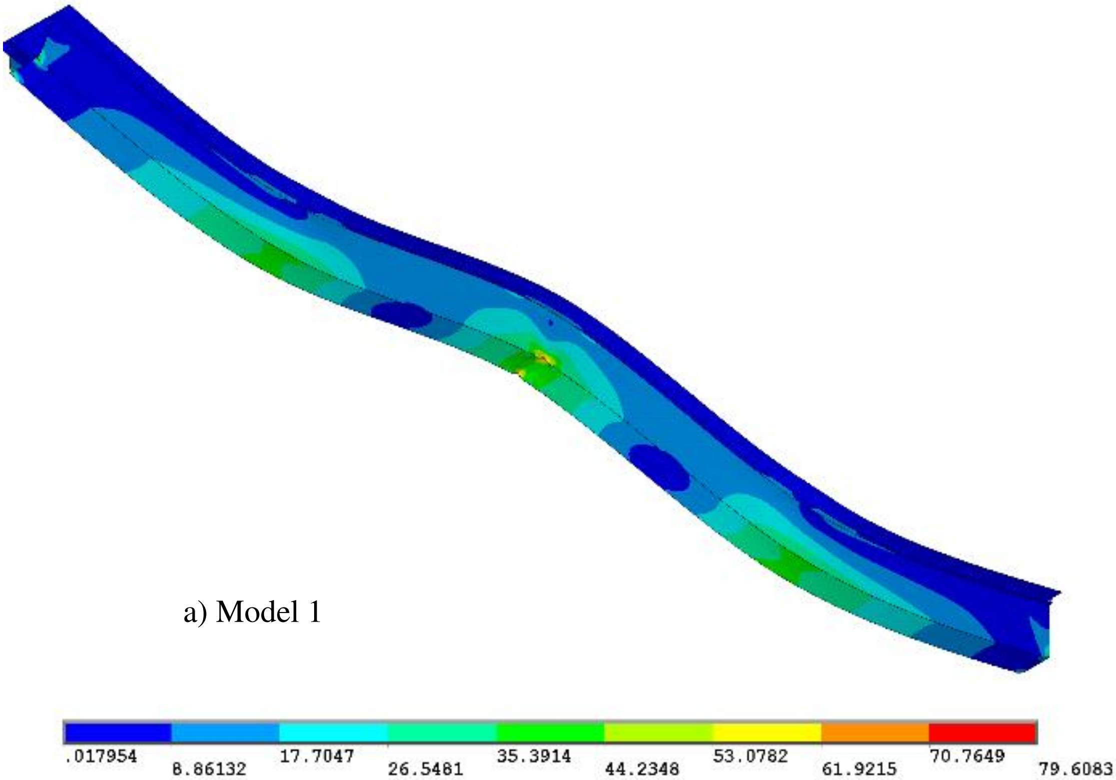

a) Model 1

Figure 3.13 (Continue) Von Mises Stresses of numerical models. (Magnification factor=400) a) Model 1, b) Model 2, c) Model 3, d) Model 4

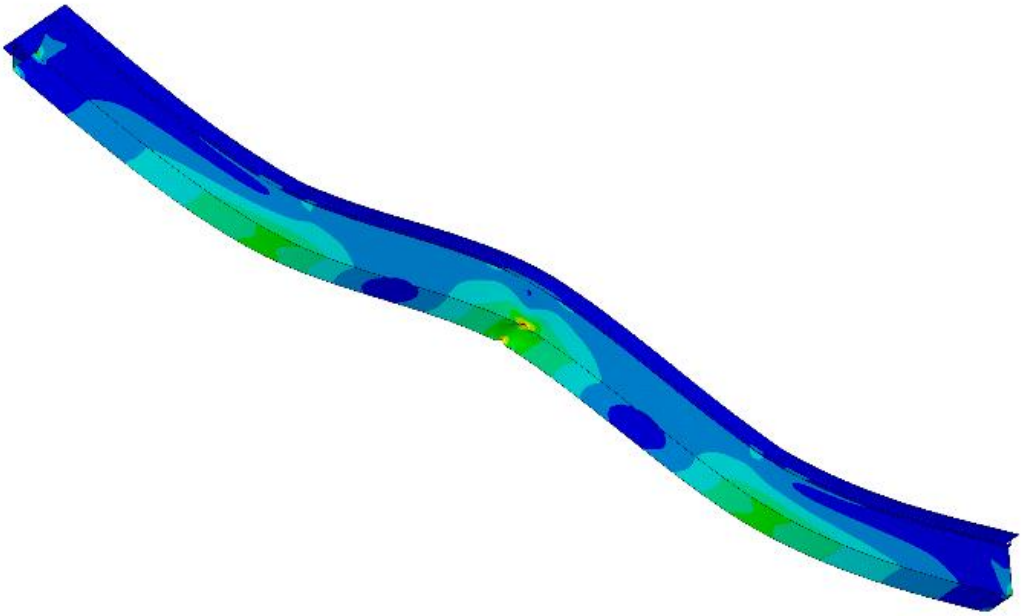

b) Model 2

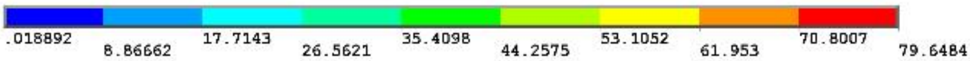

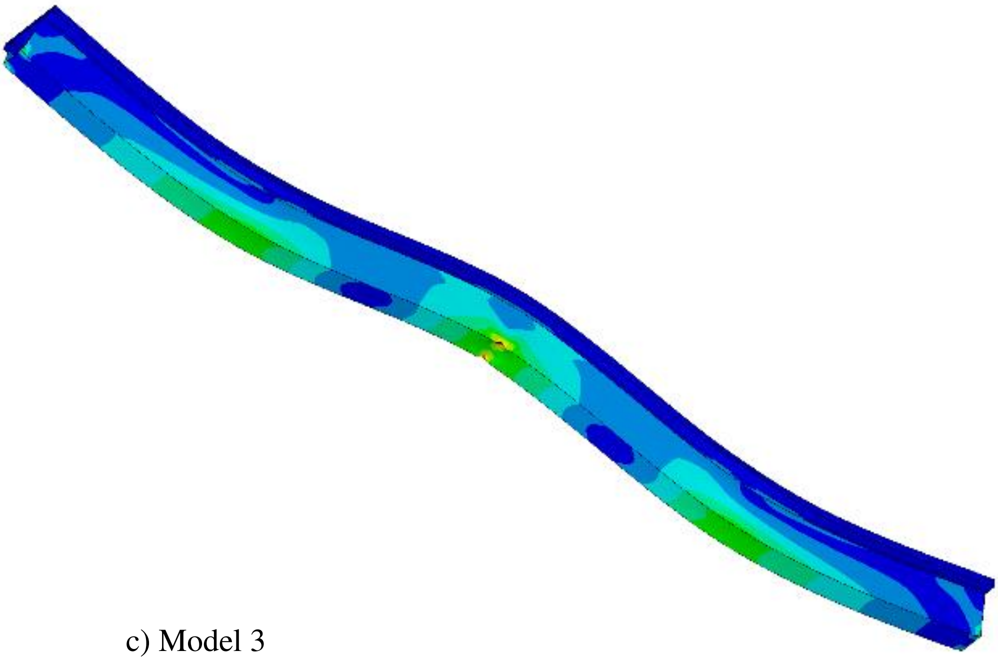

c) Model 3

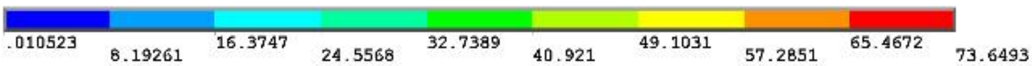

Figure 3.13 (Continue) Von Mises Stresses of numerical models.

(Magnification factor=400) a) Model 1, b) Model 2, c) Model 3, d) Model 4

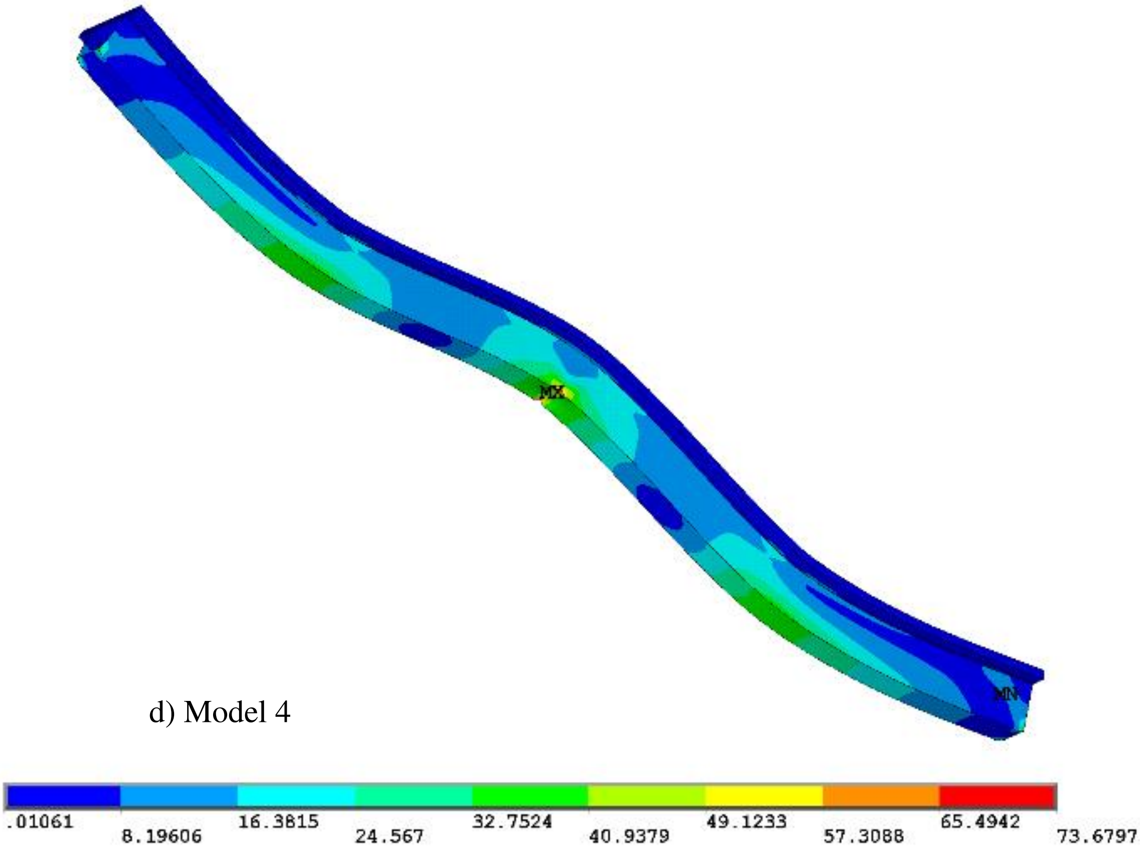

d) Model 4

Figure 3.13 (Continue) Von Mises Stresses of numerical models.
(Magnification factor=400) a) Model 1, b) Model 2, c) Model 3, d) Model 4

3.7.1.3 Results Discussion for Models 1-4 without Reduction

Obtaining displacements and stresses from the FE, models can be utilized in understanding the composite box bridge behaviour. In addition, it can also be used to compare the stress profiles. During the static test done by Ryu et al. [20] in the elastic range of loading, the flexural stiffness of the composite bridge showed linear elastic behaviour. Mid-span deflections from the analysis were compared to the test results. In the experimental test, the mid-span deflection was 2.52 mm and in the analysis performed by same researchers it was 2.76 mm at a load of 250 kN.

Mid-span deflection obtained from the FE analysis in this study for model 4 was compared with the test results. In the test results, the deflection in the analysis was 2·56 mm and it was better than previous researchers. It is interesting to note that in the case of model 4 (which had a steel box girder with shell 181 elements and concrete deck with solid 185 elements and point load with constraint nodes along the line of that load) the best result comparing with experimental test had obtained.

The computational results for model 4 of the mid-span stress distribution (section A&C) in Figure 3.14 on the top plate and bottom plates at the mid-span cross section are shown in Figure 3.15. In these figures, the vertical axis represents normal stress with units of MPa and the horizontal axis is the transverse direction of the cross section of the bridge. Section A shows the maximum stress of the entire bridge cross section, which has maximum compressive stress on the top plate and a maximum tensile stress on the bottom plate in the left span. Section B that represents mid-support stress distribution of the model 4 in Figure 3.16 has the maximum stress in the right span and the maximum compressive stress on the bottom plate in this span. However, on the left span, the maximum compressive stress is on the bottom plate as shown in Figure 3.16.

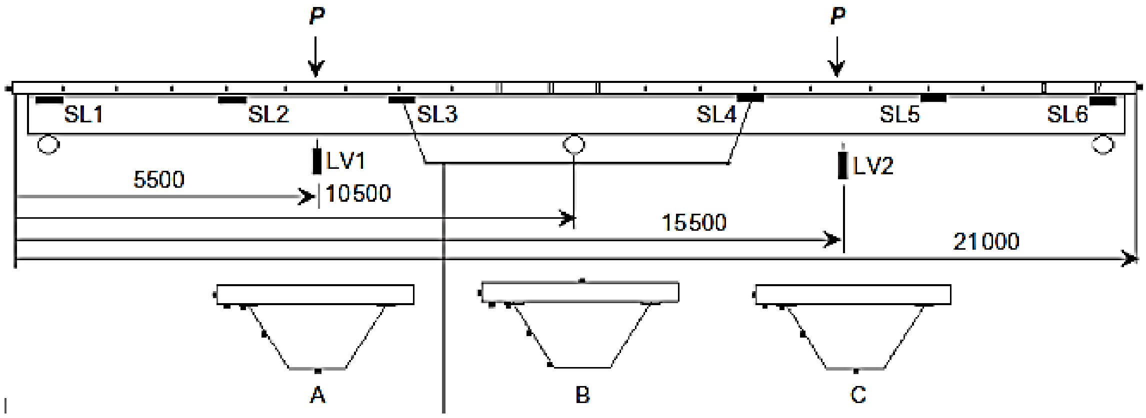

Figure 3.14 Sections along the bridge [20]

(A & C): The mid-span section - (B): Mid-support section

From Figures (3.14-3.16), it can be seen that the actual behaviour of the steel box girder under load can be quite accurately obtained by using the FE modelling methodology. That means that the results of the computational method are reliable and therefore can be used to analyse this kind of structure with good accuracy.

Through comparing the values of experiment and FE analysis between the top and bottom plates, it is shown that the shear lag effect is larger on the top plates and base modelaller on the bottom plates. In particular, the effect of shear lag is larger on the part of flange in this section. As a result, it can be concluded that the effects of shear lag have much to do with the wide-span ratio.

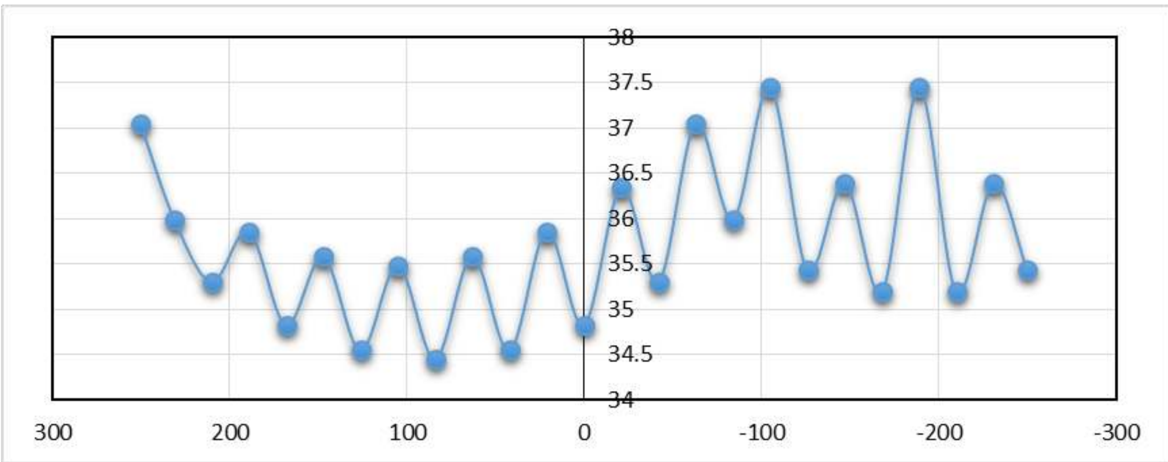

(a) Calculated results for bottom flange (steel)

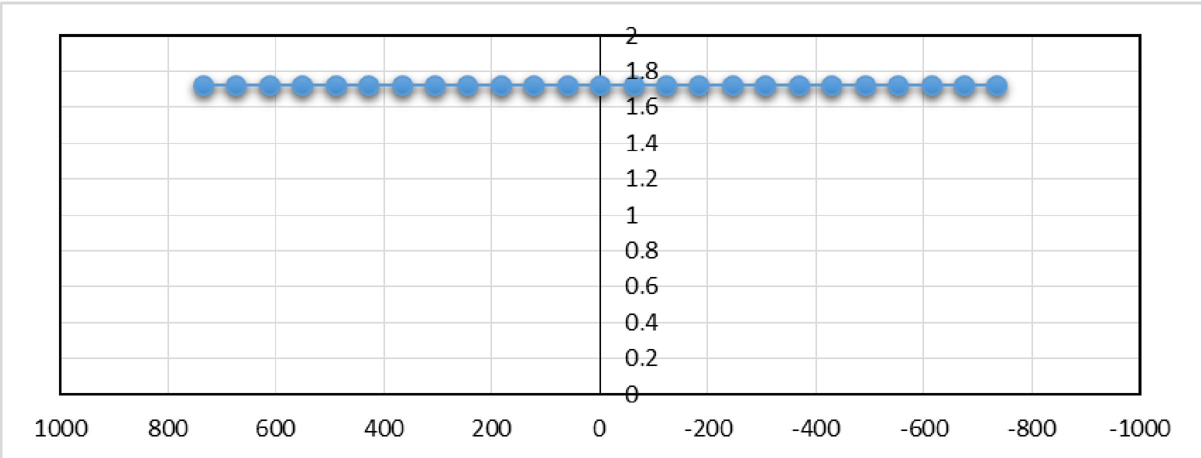

(b) Calculated results for bottom flange (concrete)

Figure 3.15 Longitudinal stress distribution at section A for Model 4

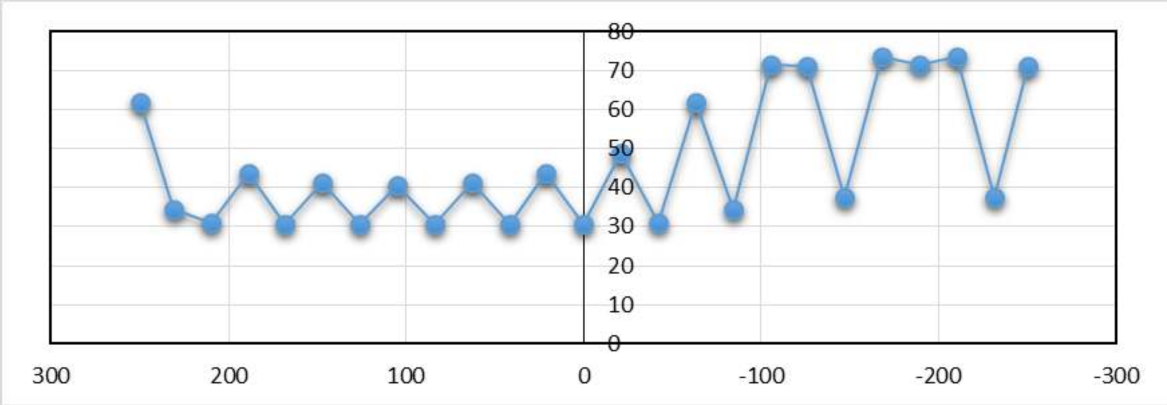

(a) Calculated results for bottom flange (steel)

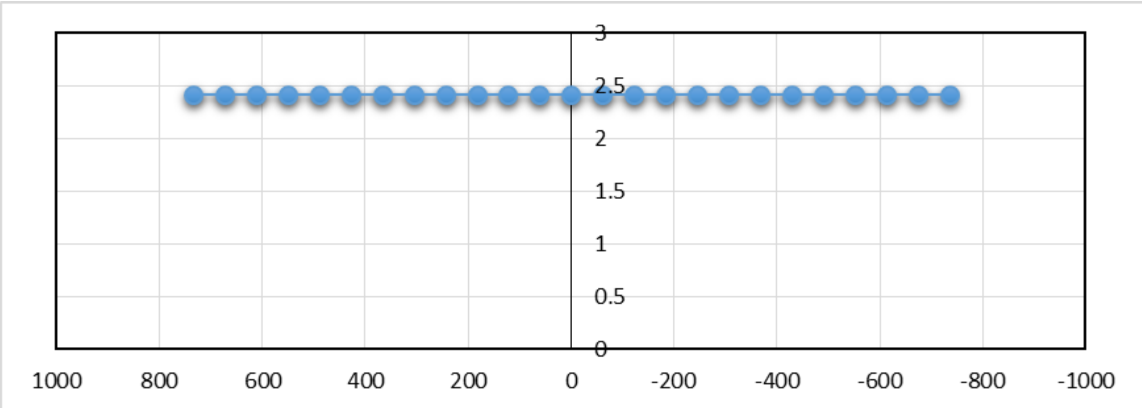

(b) Calculated results for bottom flange (concrete)

Figure 3.16 Longitudinal stress distribution at section B for model 4

3.7.2 Finite element models after reduction of shear connectors

It is now consented that the two portions of any composite structure are joined together by an infinitely rigid shear connecting. The two members then behave as one. Slip and slip strain are everywhere zero, and it can be assumed that plane sections remain plane. This situation is known as full composite interaction. All design of composite structures in practice is established on the assumption that full interaction is achieved.

In general according to BS 5400-5 [121], the spacing of the connectors should be not greater than 600 mm or three times the thickness of the slab or four times the height of the connector, including any hoop, which is an integral part of the connector, whichever is the least. Except that, connectors may be placed in groups, with the group spacing greater than that specified for individual connectors, provided consideration is given in design to the non-uniform flow of longitudinal shear and of the greater possibility of slip and vertical separation between the slab and the steel member.

In order to study the effect of stud spacing and distribution, the previously presented models of the composite box girder in Figures (3.6-3.9) with different shear stud distributions is considered, as shown in Figure3.17. Several extreme cases, 10% to 80% percentage of reduction, considered as well. The first reduction applies to the shear connectors in the transverse direction to model 2 and 4 with 10%, 20%, 30%, 40%, 50%, 60%, and 80% percent, as shown in Figure 3.17 below.

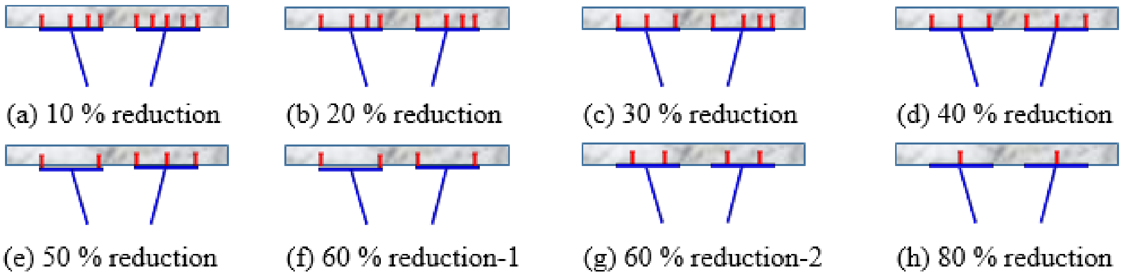

Figure 3.17 Transverse reductions of shear connectors

In every single case above two models created one is duplicated as the model 2 and one more is alike as model 4, sixteen models are resulted with the clear difference caused by reduction for each case.

The second reduction applies to same models two and four because these two models acquired the best results compared with the other two models. Additionally, sixteen models modelled but with longitudinal reduction by 5%, 10%, 20%, 30%, 40%, 50%, 60%, and 80% percentage of connectors reducing.

These reductions are completed according to a plan of removing shear connectors at specified distances on the upper flange of the bridge. The procedure of this plan arranged for 5% by removing the first line of 10 connectors at initial distance 525 mm from the beginning of the highest flange and seven lines of 70 connectors (10 for each line) every 2625 mm from the beginning of the top flange as shown in Figure 3.18 (b). Other

Reductions are increased cumulative with spacing 131.25 mm adding to the spacing of 5%; therefore, reduction as shown in the Figure 3.18 (a-i).

Figure 3.18 Longitudinal reduction of shear connectors at top flange.

3.7.2.1 Results and Discussion for Models 1-4 with Shear Connectors Reduction

In construction practice, the stud spacing or “pitch” is usually around 250 mm to 300 mm, with three to five studs in each row. In the mid-span portion, the spacing may be increased to 600 mm and all these values within BS standards[125]. In order to study the effect of stud spacing and distribution, the previously presented model with different shear stud distributions is considered, as shown in Figures 3.17 and 3.18.

Since models 4 and 2 exhibited the best performance, in this section we consider them to study the reduction of shear connectors. The transverse and longitudinal reduction for shear connectors are performed. The results of midspan deflection are listed in Table 3.3, Figures 3.19, and 3.20.

Table 3.3 Deflection results for ANSYS models 2 & 4 after reduction in connectors

Percentage of reduction%	**Midspan deflection (mm) after transverse reduction**		**Midspan deflection (mm) after longitudinal reduction**	
	Model 2	**Model 4**	**Model 2**	**Model 4**
0	2.568	2.559	2.568	2.558
5	-	-	2.568	2.569
10	2.568	2.559	2.586	2.567
20	2.569	2.561	2.633	2.598
30	2.571	2.562	2.690	2.640
40	2.572	2.563	2.765	2.697
50	2.611	2.634	2.851	2.769
60	2.652	2.706	2.951	2.863
60*	2.585	2.618	-	-
80	2.586	2.618	3.215	3.134

- Not tested

*Centered distribution of connectors.

It is possible to infer from Table 3.3 that the decrease of the number of connectors implies an increase of the vertical displacement, noting that all characteristics of shear connectors are fixed and reducing the number of shear studs is a major factor in determining the economic and practicality of the proposed modification. A simple study was performed to determine the needed shear stud to develop hybrid action in ANSYS. It was determined that full composite action can be achieved with fewer shear stud connectors as compared to existing state of the practice. The results of this study are presented here. From the results, in transverse reduction the deference between the cases (f) and (g) in Figure 3.17 is diagnosed clearly with percentage difference 2.56%

in model 2 and 3.3% in model 4, as noted these two values represent the same percentage of reduction but with different spacing between the connectors..

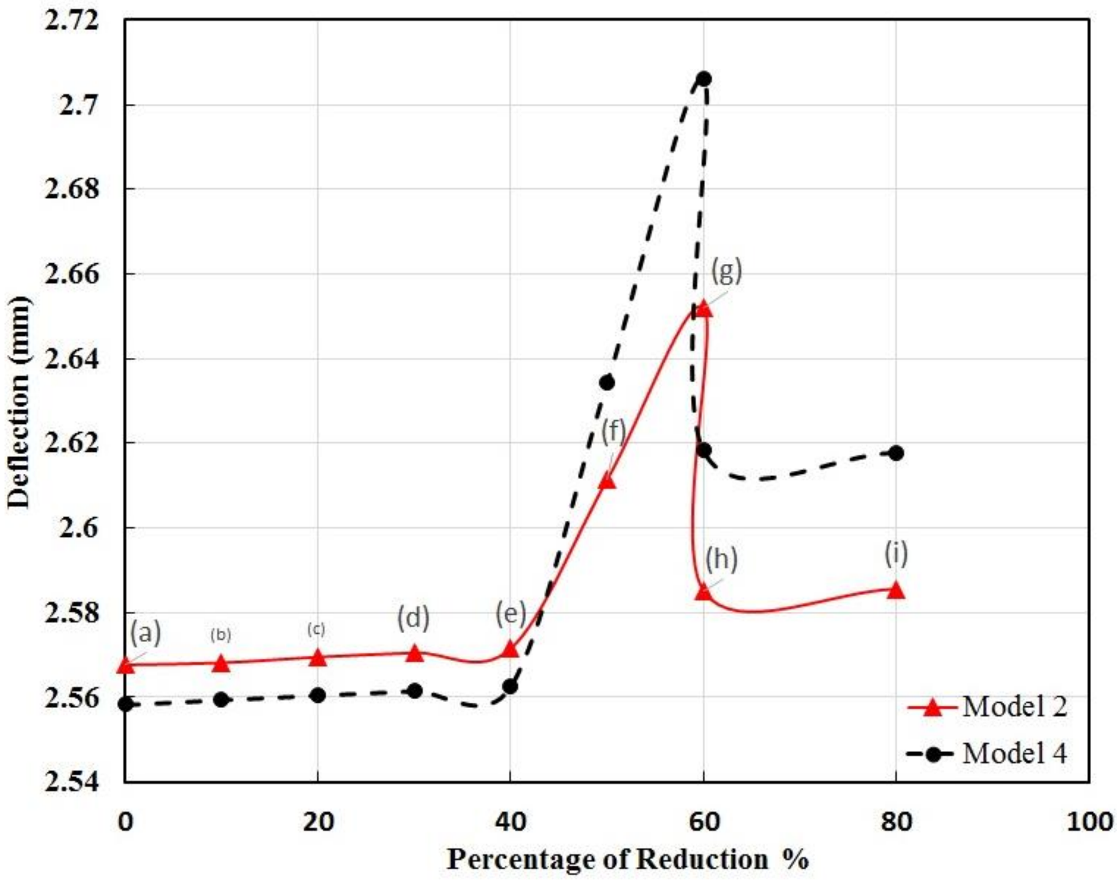

Figure 3.19 Transverse reduction percent vs. vertical displacement

Furthermore, very interesting differences accrued between the cases in Figure 3.17 (f) and (h), when the case (h) deformed less than (f) even with 28% more reduction and resulting percentage difference 2.5% in model 2 and 3.3% in Model 4. The other cases of reduction from the same Figure 3.17 (a) to (d) show an increase in deflection while shear connectors decrease with percentage of difference 0.045% in Models 2 and 4, this percentage increases from case (e) to (f) in Figure 3.10 to become 1.54% in Model 2 and 2.7% in Model 4. Figure 3.19 shows these differences graphically.

The longitudinal reduction in shear connector numbers applied with uniform steps, according to the FE modelling the bridge divided along its span to 160 divisions, there is a line of (10) MPC184 elements at each division, which represent the shear connectors of the composite bridge.

The shear connectors are reduced according to simple equations to get a uniform procedure of longitudinal reduction of shear connectors, these equations explained with the cases of reduction in Figure 3.18, and the equation for the distance before reduction is:

$$S_1 = x_1 = L/n \text{ ....3.2}$$

Where:

x_1 = Spacing between shear connectors without reduction.

L = Length of model.

n = Number of divisions in FE model.

Moreover, the second equation is used to keep the initial distance from the edge of top flange without reduction of shear connectors, the equation is:

$$S_2 = x_2 + \left[\left(\frac{p}{10}\right) \times x_1\right] \text{ .... 3.3}$$

Where:

p = Percentage of reduction %

$x_2 = L \times (0.025)$

The last equation represents the cumulative uniform spacing that is used to reduce the number of shear connectors longitudinally, and the equation is:

$$S_3 = x_3 + \left[\left(\frac{p}{10}\right) \times x_1\right] \text{....................................3.4}$$

Where:

p = Percentage of reduction %

When there are longitudinal reductions from 5% to 60% percent, there is about 0.4 to 0.7 %, increasing in percentage difference occurred in both models 2 &4 in deflection results, thus increasing occurred when the reduction changed from 5% to 10% and from 10% to 20% and so on. Further, there is a 5.0% percentage difference when 80 % reduction is present.

The set of equations formulated above is suitable for any kind of composite box girder bridge when reduction of shear connectors applied, the behaviour of composite components is still as they before reduction that mean full interaction between portions is kept. The complication of modelling composite box girder bridge with partial interaction between steel and concrete leads us to use such equations to model partially interacted shear connectors, but two important notes must consider first one the slip calculation is ignored, and the second is knowing which percentage of reduction is more accurate to represent the incomplete interaction situation. These equations in some stages of reduction may will be useful to model composite box girder bridges with partial interaction between components and reasonable results without complicated procedures.

Consequently, these equations when they used to modelled composite box girder with incomplete interaction between steel and concrete only general behaviour depends on deflection calculations is obtained, also a new study is required for performance the exact percentage of reduction can be used to represent the partial composition. Calculations of midspan deflection in models 2 &4 are graphically presented in Figure 3.20 below.

From the results listed above the effect of longitudinal reduction appears more efficacious than the transverse reduction, also a set of equations is obtained from a longitudinal reduction of shear connectors. These equations are very easy to use and to model composite box girder bridge with the non-complete number of shear stud and full interaction between steel and concrete. Table 3.3 below shows the whole results for models with reduction of shear connectors.

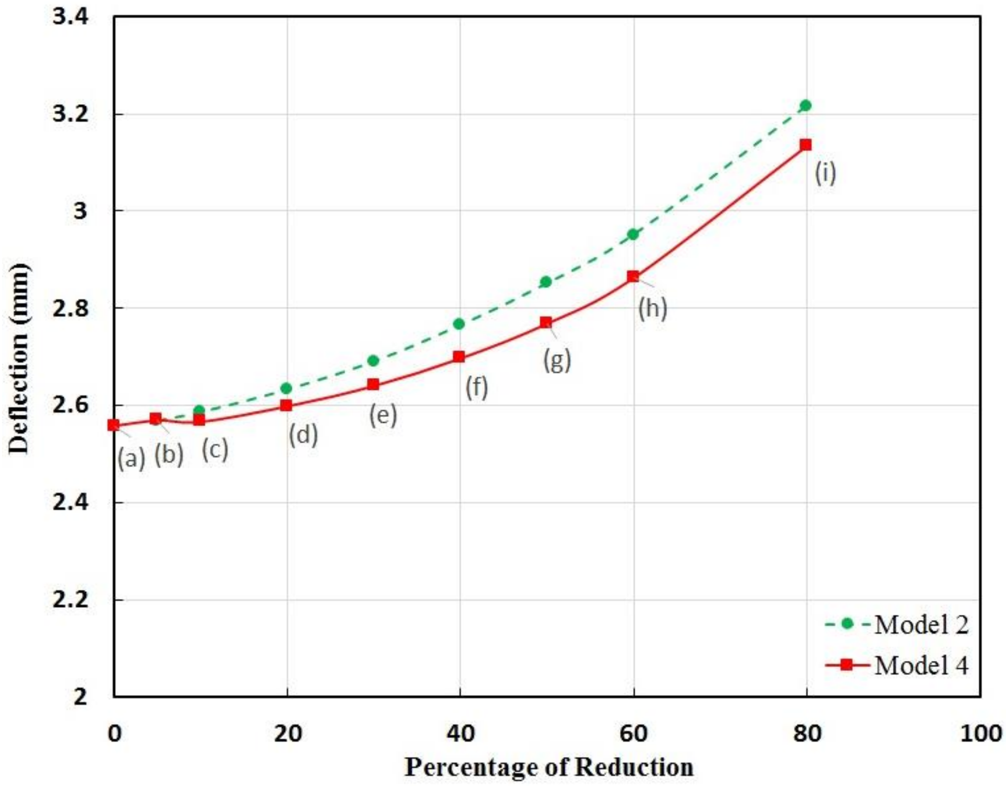

Figure 3.20 Longitudinal reduction percent vs. Vertical displacement

Deflection results for model 2 after reduction for some percentage of reduction are given below in Figure 3.21 (a-f).

Deflection results for model 4 after reduction for some percentage of reduction are given below in Figure 3.22 (a-f).

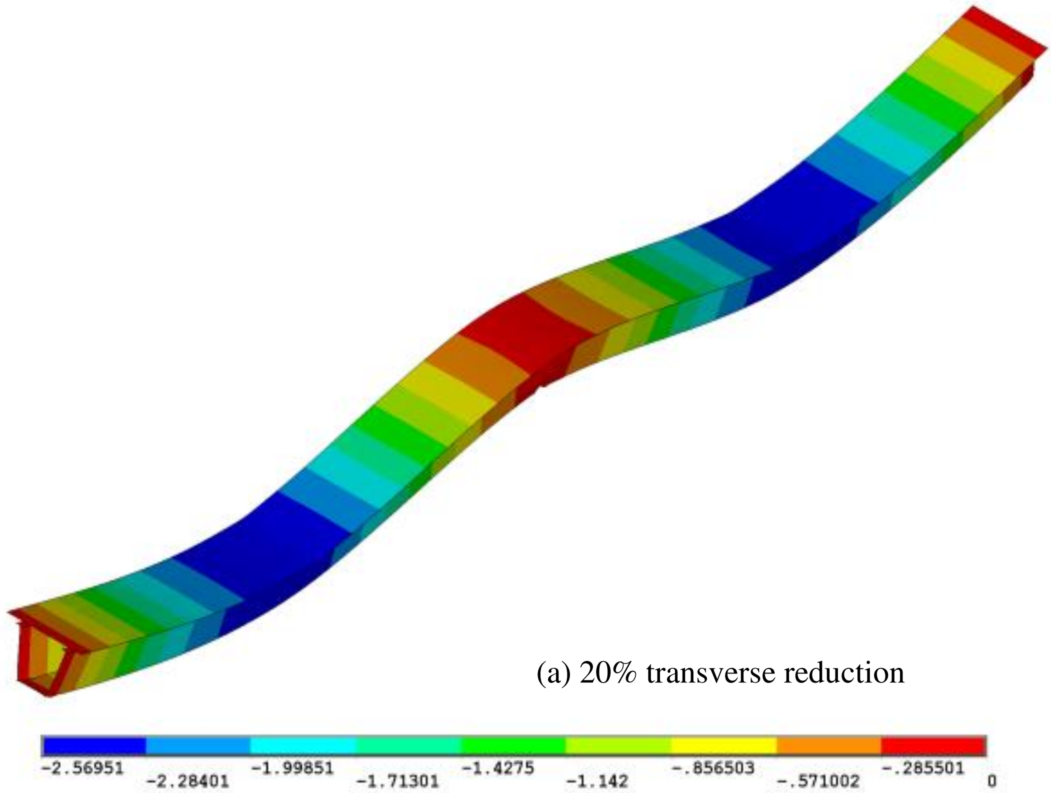

(a) 20% transverse reduction

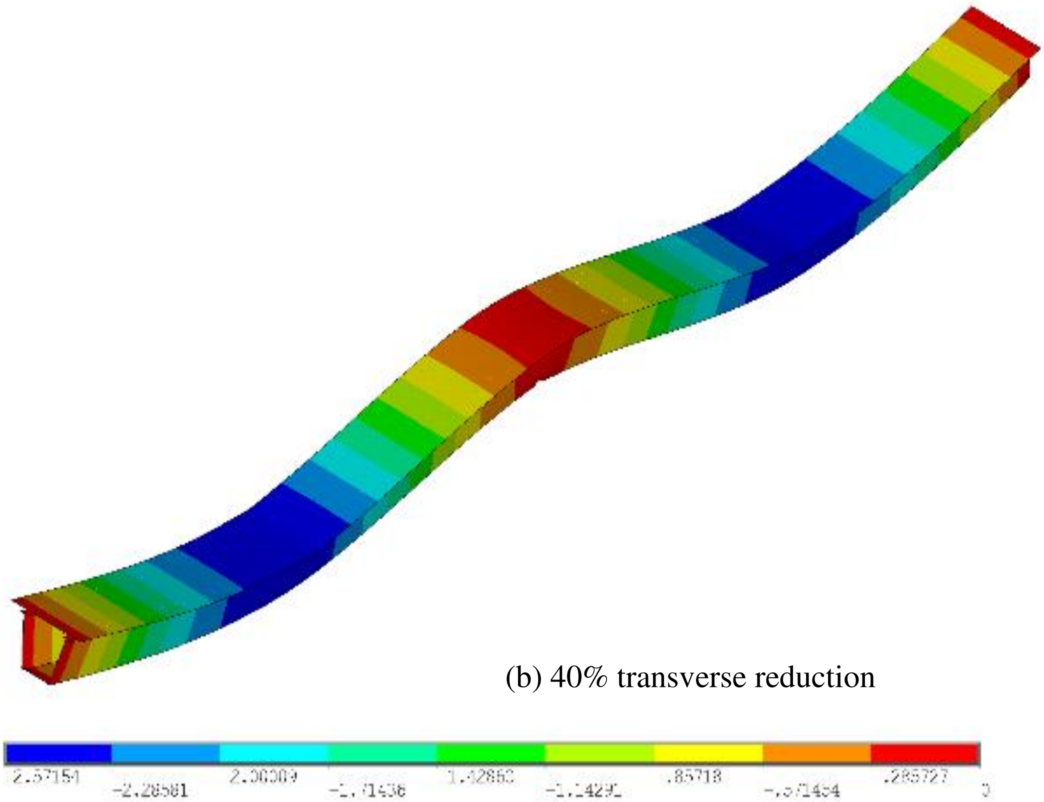

(b) 40% transverse reduction

Figure 3.21 Deflections of numerical Model 2.

(Magnification factor 400)

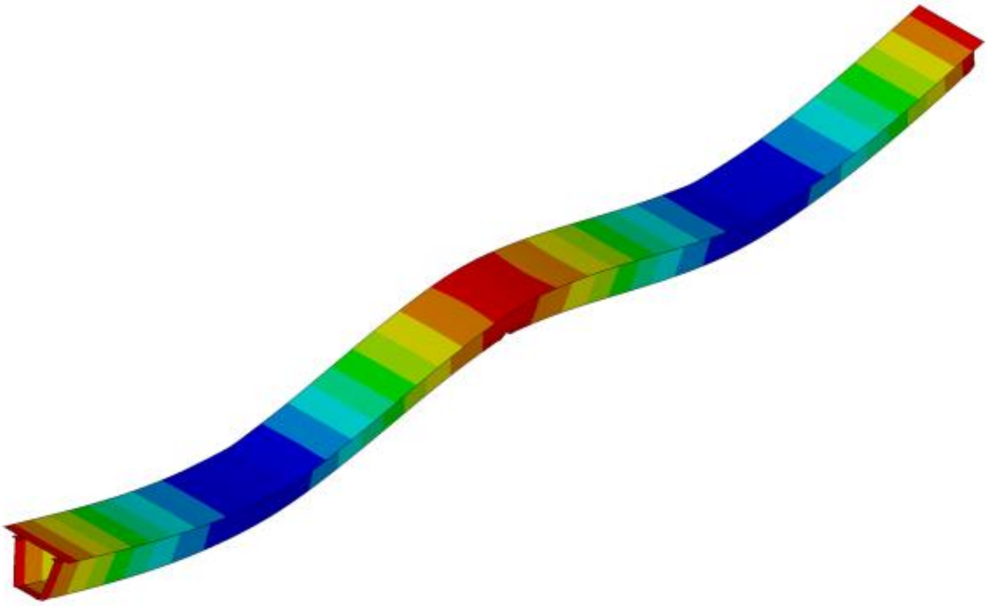

(c) 60% transverse reduction

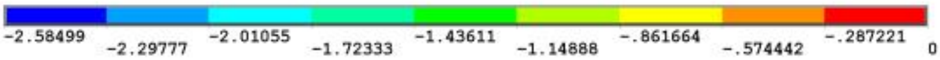

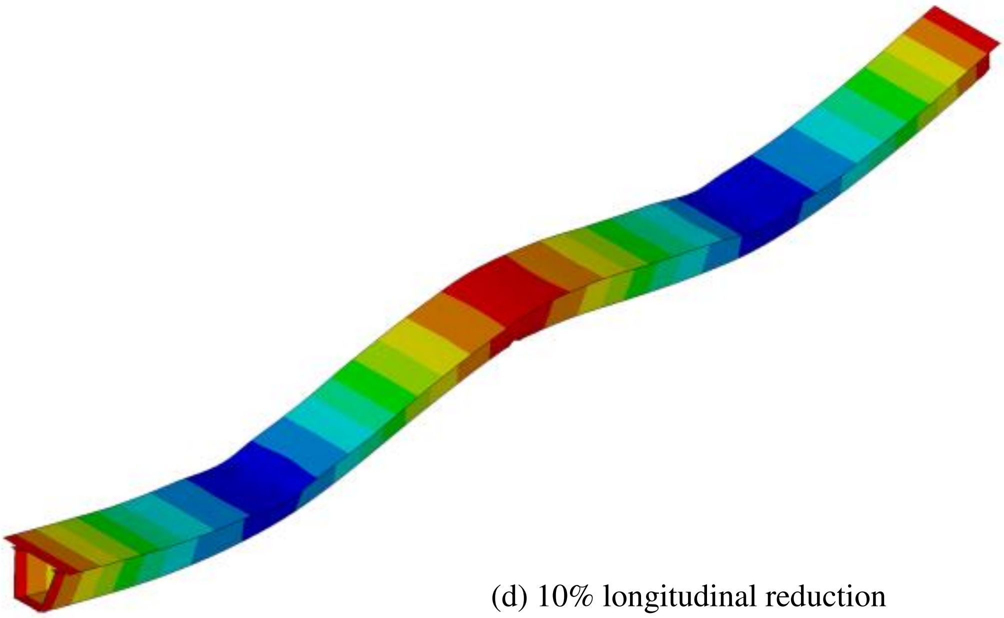

(d) 10% longitudinal reduction

Figure 3.21 (continued) Deflections of numerical Model 2.
(Magnification factor 400)

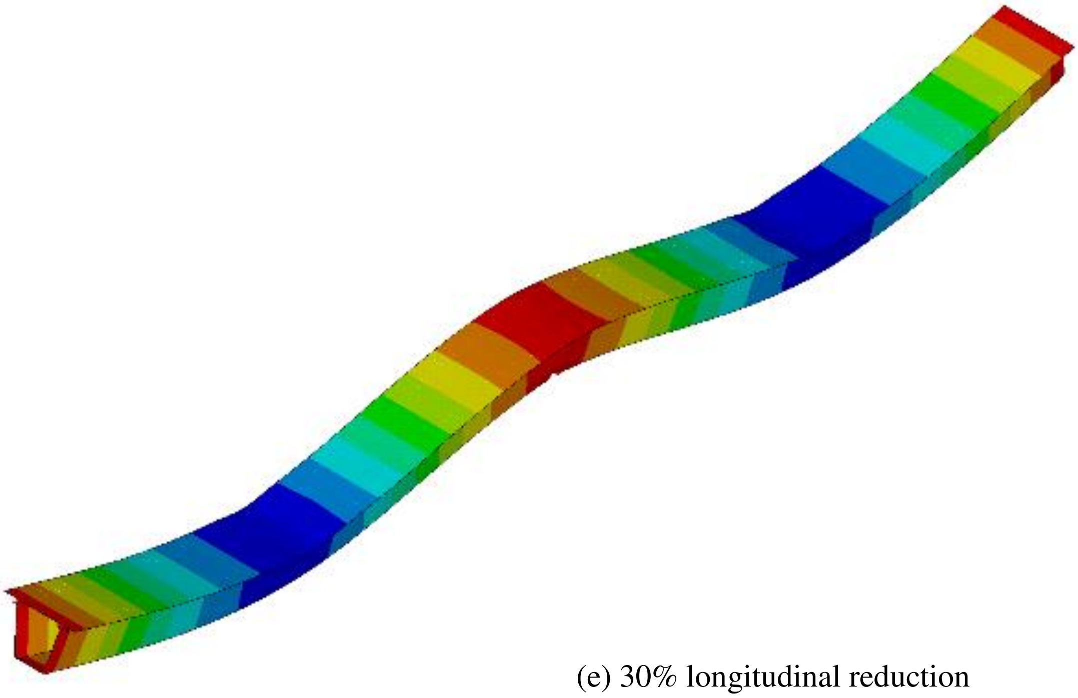

(e) 30% longitudinal reduction

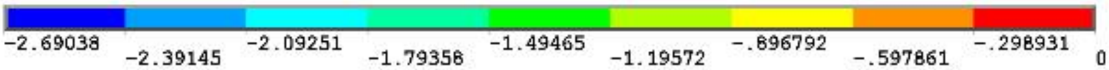

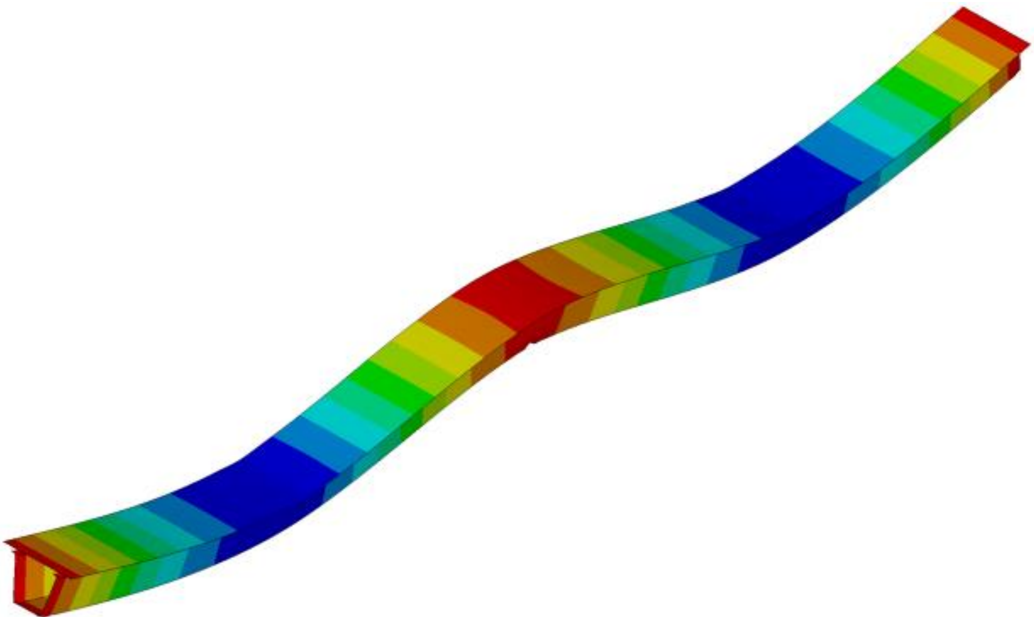

(f) 50% longitudinal reduction

Figure 3.21 (continued) Deflections of numerical Model 2.

(Magnification factor 400)

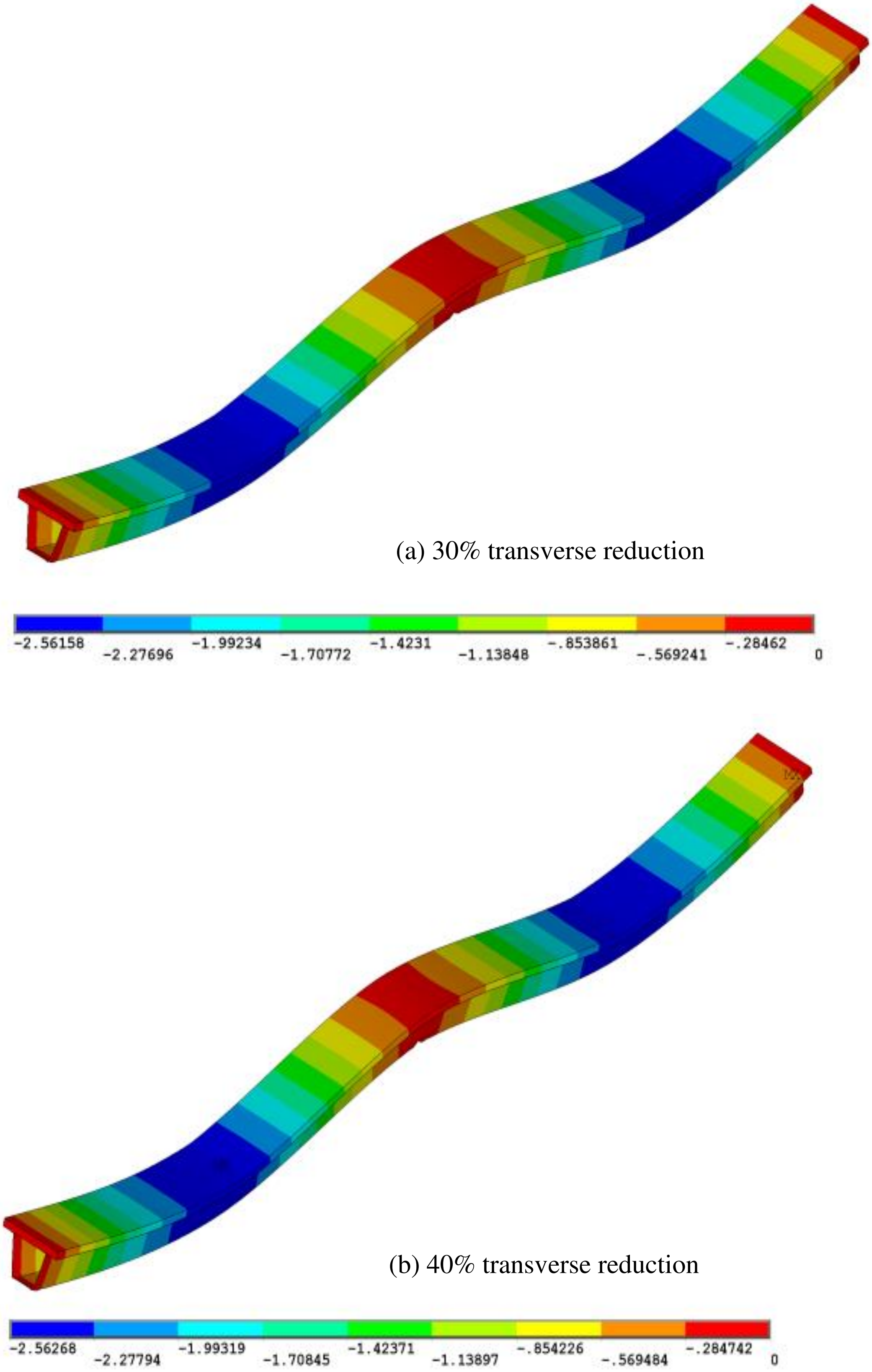

(a) 30% transverse reduction

(b) 40% transverse reduction

Figure 3.22 Deflections of numerical Model 4.

(Magnification factor=400)

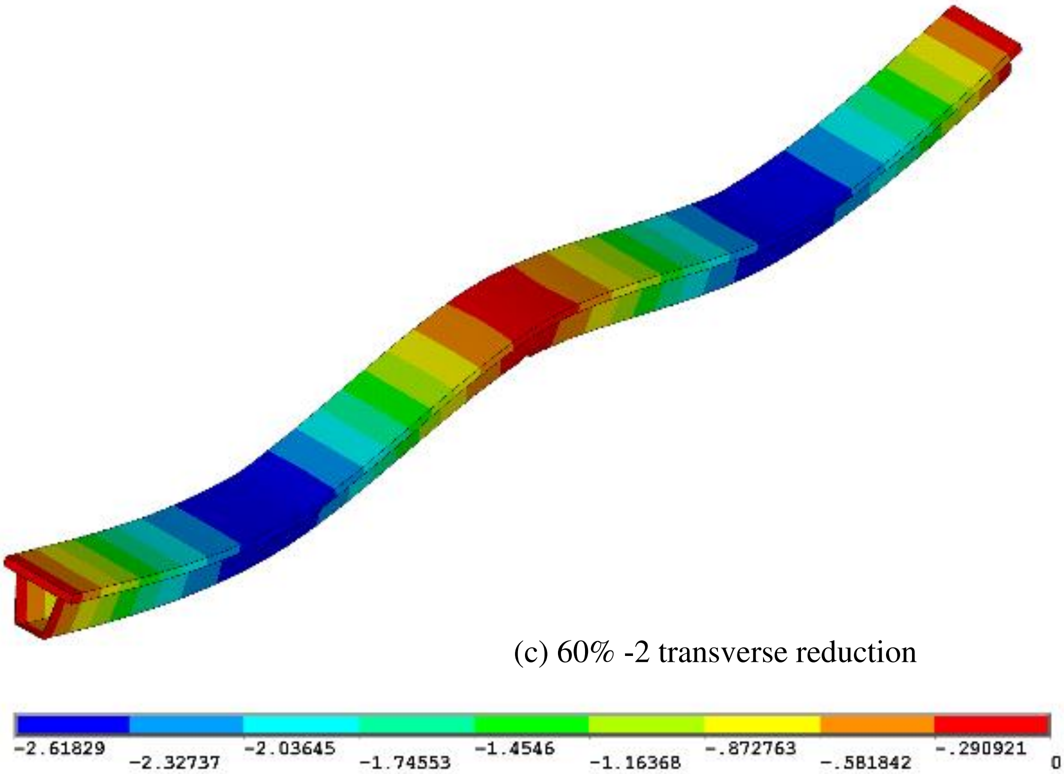

(c) 60% -2 transverse reduction

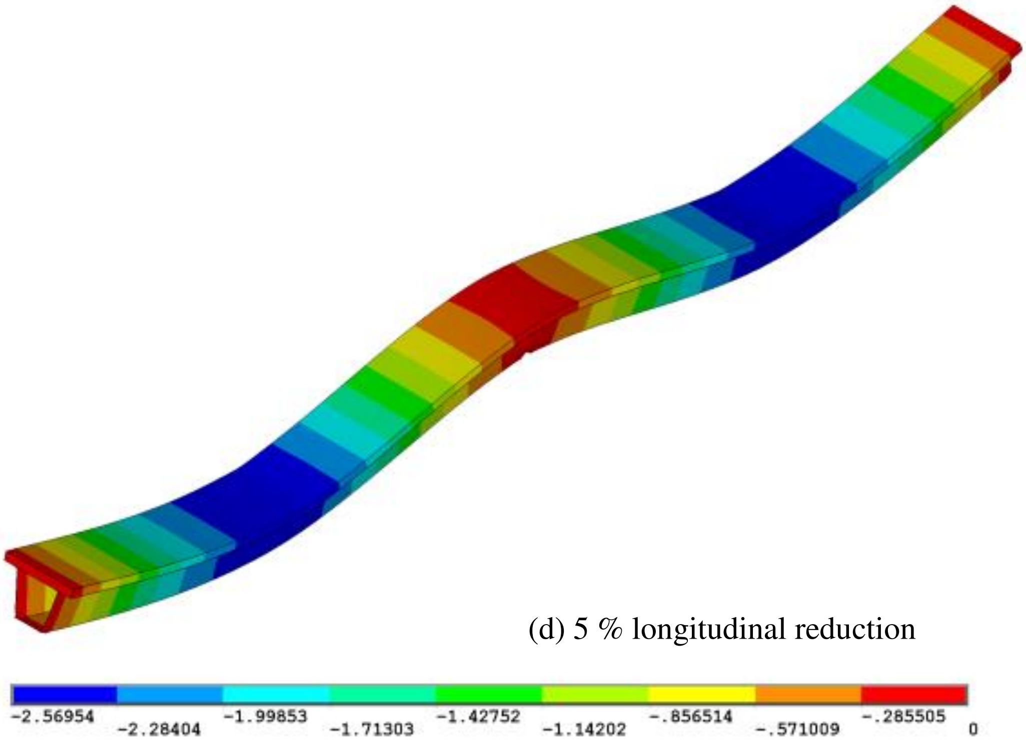

(d) 5 % longitudinal reduction

Figure 3.22 (continued) Deflections of numerical Model 4.
(Magnification factor=400)

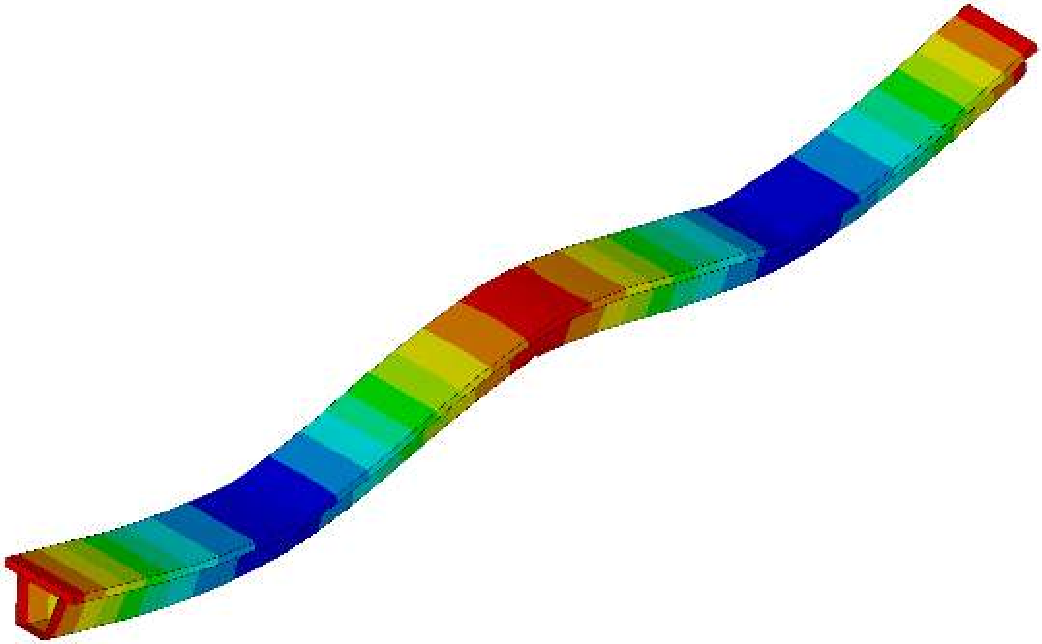

(e) 50 % longitudinal reduction

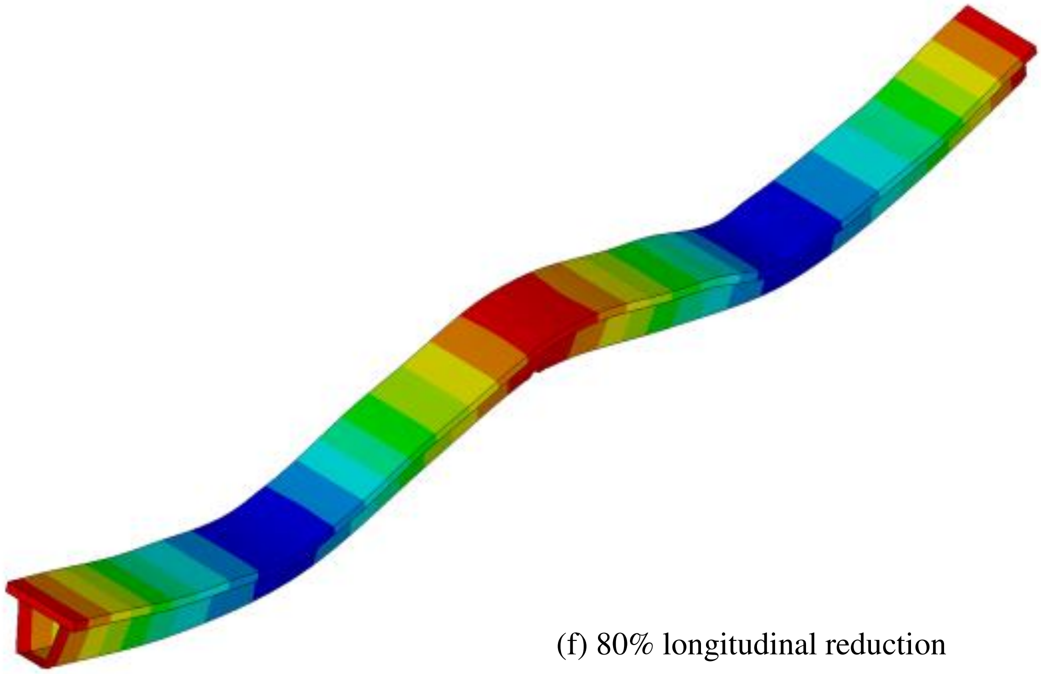

(f) 80% longitudinal reduction

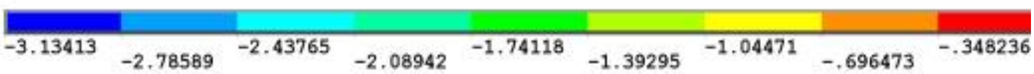

Figure 3.22 (continued) Deflections of numerical Model 4.
(Magnification factor=400)

3.8 Summary

The theoretical 3D FE models developed herein, can predict quite well the elastic behaviour as well as the mode shapes of continuous composite single box girder bridges. This study includes an investigation of the possibilities and shortcomings of (ANSYS), a Commercial program for FE analyses for modelling a 3D FE model capable of predicting the structural response of composite box girder bridges with complete interactions.

A 3D FE model capable of predicting the structural response of composite box girder bridges is developed and this study includes a number of factors, which are considered, and confirmed through experiments, especially full shear connections, which are obviously essential in composite box girder. A good representative for shear connectors of suitable element type is considered. Numerical predictions of vertical displacements at critical sections fit fairly well with those evaluated experimentally. The agreement between the FE models and the experimental models show that the FE model can aid engineers in design practices of box girder bridges.
A new technique to model shear connectors has been adopted; this technique relies on the use of a rigid links MPC element which is used first time in this study to represent shear connectors. This kind of element is perfect to model shear connectors also its ability to simulate complicated composite box girder and can be used as a practical modelling technique for long span composite bridges.

Finally, and for the first time FE modelling of the reductions in all directions for shear connectors in composite box girder bridges was studied. New equations are suggested to represent the reductions in such structures.

CHAPTER 4

EFFECTS OF DIMENSIONAL DETAILS ON BEHAVIOUR OF COMPOSITE BOX GIRDER BRIDGES

4.1 General

The study of bridges in general and composite box girder bridges in particular, requires considerably more information than is contained in codes. A sound understanding of bridge behaviour at all stages of loading is essential. Analysis and design of composite box girder bridges is complicated by many factors including composite interaction between the concrete deck and steel girder, local buckling of the thin steel walls making up the box, torsional warping, interaction between different kinds of cross-sectional forces, and the effect of horizontal bridge curvature on both local and global behaviour.

Analysis and design of box girder bridges are very complex because of its 3D behaviours consisting of torsion, distortion and bending in longitudinal and transverse directions. To assess the performance of a composite box girder bridge, engineers require structural analysis models capable of representing the complex behaviour that occurs under such conditions.

In the winter of 1967, the Silver Point Bridge in Point Pleasant, West Virginia suddenly collapsed into the Ohio River. The investigation of the failure determined that the fracture of a single eye-bar connecting the bridge's suspension chain released the primary load path, which resulted in the total collapse of the structure. This event demonstrated that the failure of individual members could have a significant influence on the stability of an entire bridge structure, and it led to a reconsideration of code and safety requirements for bridges. compositel box girders are often used for medium and long span continuous bridges. In the negative moment regions over the interior supports, the bottom flange of the box girder is subjected to compressive forces. Because the bridge bending moment is normally highest at the piers and the compressive strength of steel bottom flange plates are relatively low on account of buckling, thick steel plates with longitudinal stiffeners are necessary.

For long span continuous box girders, a haunched profile is also often necessary so as to keep the compressive stresses in the compression flange within safe limits. For multispan highway and railroad bridges, haunched continuous steel box girders are often used as main load-carrying members. The use of haunches at the interior supports provides a variation of negative moment strength similar to that of the design requirements, therefore enhancing the structural efficiency of the design.

The economy of a haunched profile is affected by a large number of parameters, including the span length, the huanch ratio, the midspan depth, the shape and size of haunches, and the configuration and thickness of the flanges and webs; all of these must be considered to achieve the proper design regarding the adoption and geometry of the haunches.

This chapter presents the results of a parametric study in which the costs of haunched and constant-depth continuous steel box girders are compared. Wide ranges of the parameters listed in the preceding paragraph are included. The relative cost comparison can be made based on equal stresses in the bottom flange of the box girder. Practical guidelines are developed for the selection of the haunched profile.

4.2 Base Model

Composite box girder bridge models were simulated using a commercial FE program. Since the materials were stressed in elastic limits in the study of previous chapter. linear analysis of bridge models are undertaken in present study. The slab and the box girder were connected by rigid links because full interaction between slab and steel girder was assumed.

The FE model was made using shell elements-which are four-node elements with six degrees of freedom at each node-, for steel webs, and the steel bottom flange. While solid brick elements are used for 3D modelling of concrete top flanges. Eight nodes having three degrees of freedom at each node define them. The plate thicknesses and the material properties are required input for shell element. The rigid element are used to model a rigid constraint between two bodies, steel and concrete in this case which are used to tranbase modelit forces and moments in all above models.

Figure 4.1 presents FE base model, which is developed using shell elements in steel box girder portions and solid brick for concrete deck. Pervious chapter evaluated performance of this modelling technique against shell models by using eight nodes brick elements. Brick elements are just used to model concrete deck portion of bridge where shell elements still represent the steel box portion. Thickness of concrete deck portion is considerable compared to steel and other geometrical details. The convenient way to represent this thickness is to adopt 3D brick elements. Since the cross section is prismatic, employing 3D brick elements would not cause complicated modelling approach.

The vertical translation degrees of freedom of the nodes across the width of the deck are coupled as shown in Figure 4.1 Coupling is a way to force a set of nodes to have the same DOF value. Similar to a constraint, except that the DOF value is usually calculated by the solver rather than user-specified. A coupled set is a group of nodes coupled in one direction. Boundary conditions are handled in such a way to represent simply supported conditions of test specimen. This type of loading examined in previous chapter and gave more accurate results than the point load.

In this study, the top concrete flanges were divided into thirty-four square elements for an appropriate aspect ratio of the elements and four divisions for each top steel flange. The bottom flanges were divided into ten elements and webs were divided into twenty square elements. The longitudinal two spans were divided into 160 elements.

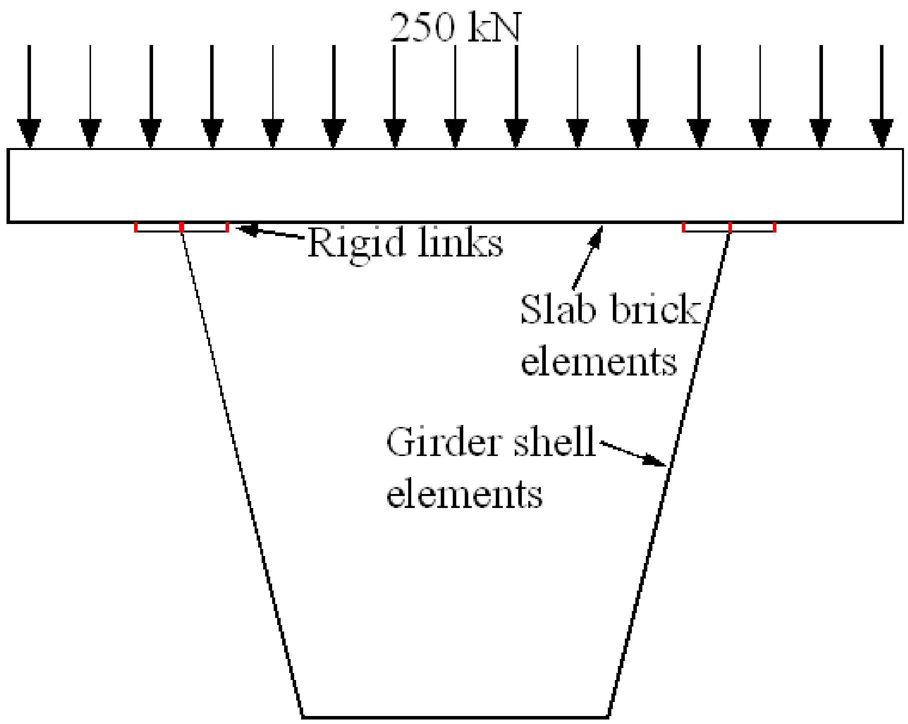

Figure 4.1 FE model of base model

4.3 Variations of Cross Section Parameters

The structure analyzed is a steel box girder bridge continuous over two spans, with span lengths of 10 m for each span. It's out-to-out width is 1.47 m. The thickness of web plates is 12 mm. The factors which may influence the strength of the steel-concrete composite box girders include the following:

- Thickness and width of steel plate for flange and web.
- Thickness of concrete slab.
- Spacing of shear connectors.
- Strength and weight of concrete.
- Amount of reinforcement, if needed.
- Spacing of longitudinal stiffeners, if needed.
- Shrinkage and creep of concrete under long term compression.
- Haunching Ratio.

For the objectives of this study, the most important dimensions are the depth of the boxes and the thickness of the bottom flange steel and web. Many factors influence the performance and economy of a continuous steel box girder. The more significant factors include the span length, depth of the structure at midspan, shape and size of haunches, and thickness of the web and flange plates. In this study, a well-designed continuous steel box girder highway bridge, designated herein as the base model design is used as the basis for the examination of the effect of each of these design parameters.

The parameters examined in this study include the Effects of concrete deck depth (DC), web plate depth (DW), web plate thickness (TW) and the effect of bottom flange plate thickness (TF). Each of the parameters enumerated earlier were modified to generate alternate analysis to be compared with the base model condition. Only one parameter was changed at a time with one-third decreasing and increasing. DC, DW, TW and TF were modelled with same concrete deck depth, web plate depth, Web plate thickness and bottom flange Plate thickness dimensions respectively of base model, while DC1, DW1, TW1 and TF1 were modelled with one-third decreasing in concrete deck depth, web plate depth, Web Plate Thickness and bottom flange Plate thickness dimensions of base model respectively.

Finally, DC2, DW2, TW2 and TF2 were modelled with one-third increasing in concrete deck depth, web plate depth, Web plate thickness and bottom flange plate thickness dimensions respectively of base model. For each change in a parameter, the resulting box girder was analyzed. Comparison of the results with those from the base model provided insight into possible alternate analysis incorporating the selected changes. In addition, the base model analysis was analyzed for a constant span length also in this parametric study. In this section the effect of span length was ignored and the cross section parameters only are considered.

4.4 The Interaction of Variations of Cross Section Parameters

To study the effect of various bridge parameters on the response of composite box girder bridges, a parametric study was performed which focused on the combination of variation of span length, concrete deck thickness, and web thickness. Three bridge cross-section shapes were considered at each parameter and will chick with other parameters. For this purpose a program using ANSYS Parametric Design Language (APDL) is created to study the behaviour of the structure, that contain five loops with three values for each parameter and eighty one models were obtained. The section geometry remains the same for various bridge span lengths, with the exception of the overall section depth. The values of parameters are listed in table 4.1.

Table 4.1 Parameters values for continuing box girder (all units are in mm).

Parameters	Span length (L)	Concrete Depth (DC)	Steel Web Depth (DW)	Web Thickness (TW)
Value 1	14000	100	532	8
Value 2	21000	150	800	12
Value 3	28000	200	1068	16

4.5 Haunching Ratio

The role of continuous thin-walled steel box girders as the principal load carrying members for bridge superstructures has gained considerable popularity. The haunches are often applied to hold the large negative bending moments over the interior supports. The function of the haunches, not only yields a structurally efficient design, but also results in an aesthetically pleasing profile. Nonetheless, because haunches also require more complicated assembly procedures and possibly higher fabrication costs, they should not be applied arbitrarily.

The haunch depths were expressed in terms of a Haunch Ratio,(HR), which was specified as the ratio of the uttermost depth of the interior support to the minimum depth at Midspan. Steel haunched box girders are often used in simply supported and continuous bridges, framed buildings for economic and aesthetic reasons. However, there is little experimental data available for predicting the behaviour of the haunched box girder. Moreover, no rational and economical design method has yet been established in most design specifications. In this study, the effect of haunch on the behaviour mechanibase model of the haunched box girder was investigated.

Haunch girders in this thesis are defined as girders being stiffened at two ends with a tapered triangular box Section. The tapered section is usually cut from a similar section. Haunch girders are designed by assuming a rigid moment connection between the girders and piers. Depth and duration of a haunch are chosen so that they result in an economical method of transferring moment into the pier and in a reduction of girder depth to a practical minimum. Haunch composite box girders in which steel girders are designed to work in conjunction with a concrete slab of definite width could result in shallow girders, provide a sufficient rotation capacity of the association that will permit a redistribution of the moment and thus mobilize a full sagging capacity of the girder resulting in an economical purpose. Furthermore, haunch systems could also provide a long unobstructed space for services and increase the speed of construction.

One of the common scenarios in steel construction is open for services. Haunch composite girders may offer continuity at the support and hence increase the structural performance of the system as a continuous girder.

In the continuous bridge design, most of the approaches are based on either elastic or plastic design. In the elastic analysis, a structure is analysed based on elastic global analysis and a moment envelope is obtained to design the structure. The design has to satisfy both the ultimate and serviceability limit states. Moment redistribution allows for the structure and the percentage of moment redistribution depends on section classification. The second approach, plastic analysis is valid when critical cross-sections are capable of developing and sustaining their plastic resistance until the sections have fully yielded for a mechanic base model of plastic hinges to be present.

The internal forces and moments in a continuous haunch composite beam may generally be determined using either a Global elastic analysis or Plastic hinge analysis. Global elastic analysis of elastic analysis may be used for determining the forces and moments in continuous girders. The assumption used in the global elastic analysis is that the stress-strain relationship of the material is linear elastic but the tensile strength of concrete is neglected. This assumption is valid for first-order and second-order elastic analyses, even though section capacity is evaluated based on plastic resistance.

4.6 The Interaction of Variations of Cross Section Parameters and Haunching Ratio

The eigen functions of a continuous composite bridges are derived from numerical method. The top flange, the vertical variable depth web strip and the bottom flange shell strip are formulated by mixing these roles in the longitudinal direction with appropriate FE shape functions in the transverse direction in order to analyse continuous, haunched box-girder bridges. For this purpose a program using ANSYS Parametric Design Language (APDL) was written. This program has five loops with five values of first loop which represents haunch ratio HR and three values for the rest loops which represent the length L, the concrete depth DC, the box web depth DW, and the web thickness TW.

The base model design has a haunch ratio of one. In this work, the haunch ratio varied from 1.0 to 3.0. A haunch ratio of 1.0 represents a constant depth girder which is analysed in section 4.4. Nevertheless, it should be stressed that this does not necessarily suggest a uniform cross-section Variation of web plate or flange plate thicknesses will cause the moment of inertia of the cross-section to vary on the bridge, resulting in a non-prismatic constant depth design.

The parameters studied in this survey include the following:

1. Depth at Midspan DC.

2. Thickness of web plate TW.

4. Span Length L.

5. Depth of plate web DW.

For haunch, the division of members into FE's may take on a substantial part. A haunch is an ingredient of a varying cross-section, on the other hand, is an ingredient of a constant cross-section. Thus, the result of the varying cross-section (most frequently of a varying depth of the cross-section) must be mollded by means of a finer FE mesh. Thither is a great divergence in the precision of results for very course division and for considerably fine division. Nevertheless, the conflict between the considerably fine division and extremely fine division is virtually negligible.

For a continuous composite girder, the negative bending at internal supports is generally significantly less than the resistance in positive bending in the Midspan region. Therefore, the introduction of a haunch may be an option to overcome the shortcoming because it will increase the hogging section capacity. In addition, if necessary, tension reinforcement could be added, thus increasing the hogging capacity. It is important to find out the factors that affect the design of haunched composite girders so that the structural system will be utilized more efficiently.

The geometry of the models was defined according to a box girder section conducted in chapter three. Five different linear tapering geometries were obtained by keeping constant the haunch ratio HR at each loop and changing the parameters according to five loops with three values for each parameter as illustrated in section 4.4.

To study the effect of various bridge parameters on the response of composite box girder bridges, a parametric study was performed which focused on the combination of a variety of haunch ratio HR, span length, concrete deck thickness, flange thickness and web thickness. Three bridge cross-section shapes were considered at each parameter and will check with other parameters. Four hounded and five models are created to study the behaviour of the structure, which is mean [5X3X3X3X3] parameters. The values of parameters are listed in table 4.2

Table 4.2 parameters values for continuing box girder (all units are in mm)

Parameters	Haunch Ratio (HR)	Span length (L)	Concrete Depth (DC)	Steel Web Depth (DW)	Web Thickness (TW)
Value 1	1.6	14000	100	532	8
Value 2	1.8	21000	150	800	12
Value 3	2.2	28000	200	1068	16
Value 4	2.5	---	---	---	---
Value 5	3.0	---	---	---	---

FE models for the prediction of Stresses and deflections of the composite haunch box girder are established. The effects of the parameters mentioned previously with respect to stress, deflection are studied. The results can be used to develop analytical and design guidelines for composite box girder haunch bridges.

4.7 Numerical Results and Discussions

4.7.1 Results for Variations of Cross Section Parameters

The results of the FE Analysis (FEA) using base model, DC, DW, TW, TF, DC1, DW1, TW1, TF1, DC2, DW2, TW2, and TF2 are shown in Table 4.3 and Figures 4.2-4.10 together with the loading-test results and the design values. It is observed that the design, analysis tends to overestimate the stress and the vertical displacement measured in the loading test. Obtaining displacements and stresses from the FE models can be utilized in understanding the composite box bridge behaviour. In addition, it can also be used to compare the stress profiles. In the elastic range of loading, the flexural stiffness of the composite bridge showed linear elastic behaviour. Mid-span deflections from the analysis were compared with the test results submitted in chapter three. In the experimental test, the mid-span deflection was 2.52 mm and in the analysis performed by same researchers it was 2.76 mm at a load of 250 kN. Mid-span deflection from base model analysis was compared with the test results. Deflections results obtained from FE models with different parameters can be observed in figures below and they are summarized in Table 4.3:

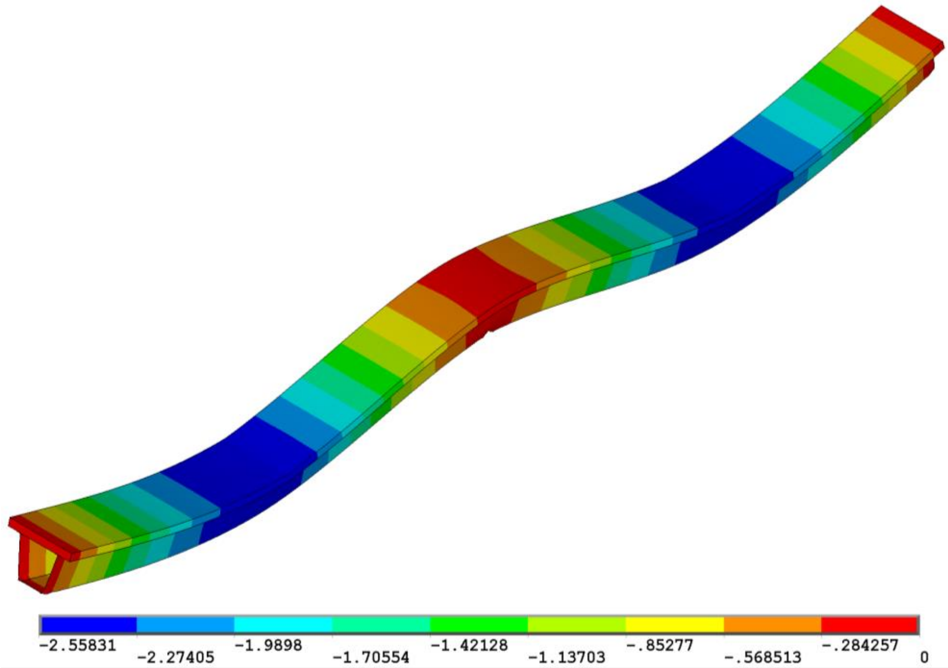

Figure 4.2 Deflections of numerical models base model, DC, DW, TW, TF (Magnification factor=400)

Table 4.3 Deflection results for FE models

Model Name	Dimension details after change (mm)	Midspan deflection (mm)
	Concrete Deck Thickness	
DC	150	2.558
DC1	100	3.005
DC2	200	2.240
	Depth on Steel Box Web	
DW	800	2.558
DW1	533.33	5.166
DW2	1066.67	1.579
	Steel Box Web Thickness	
TW	12	2.558
TW2	8	3.487
TW2	16	2.073
	Steel Box bottom Flange Thickness	
TF	14	2.558
TF1	9.33	2.547
TF2	18.67	2.569

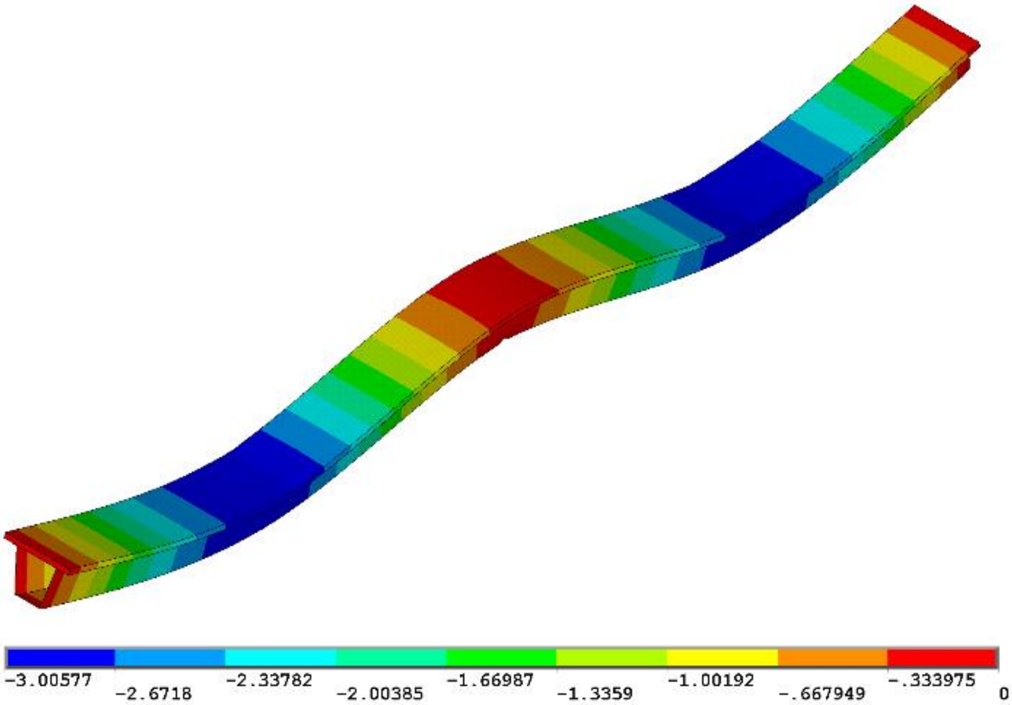

Figure 4.3 Deflections of numerical model DC1

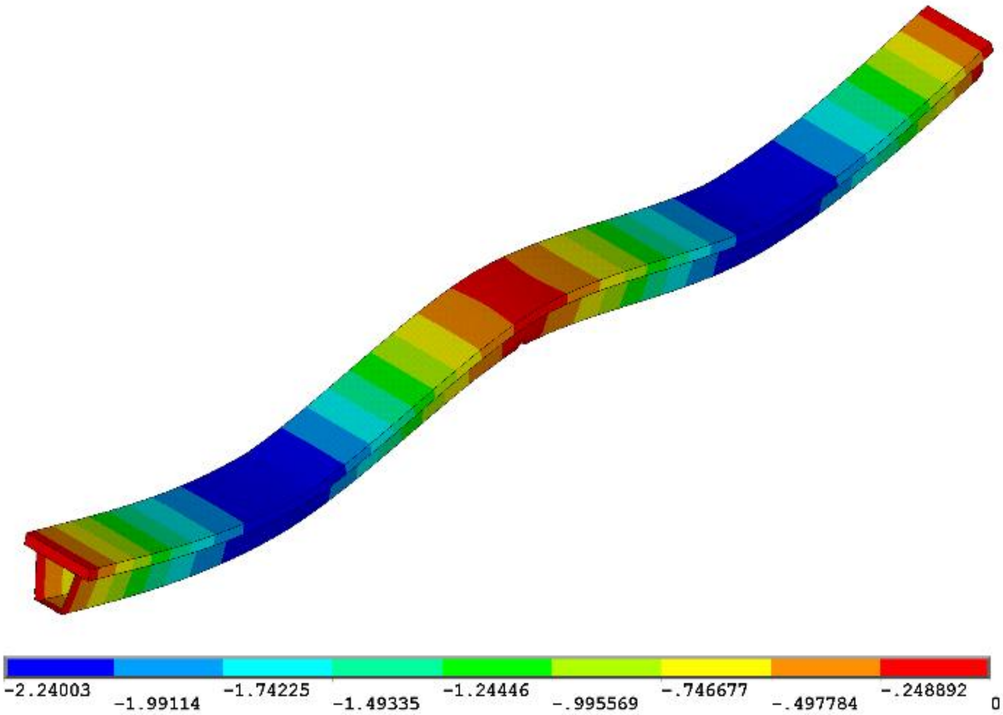

Figure 4.4 Deflections of numerical model DC2

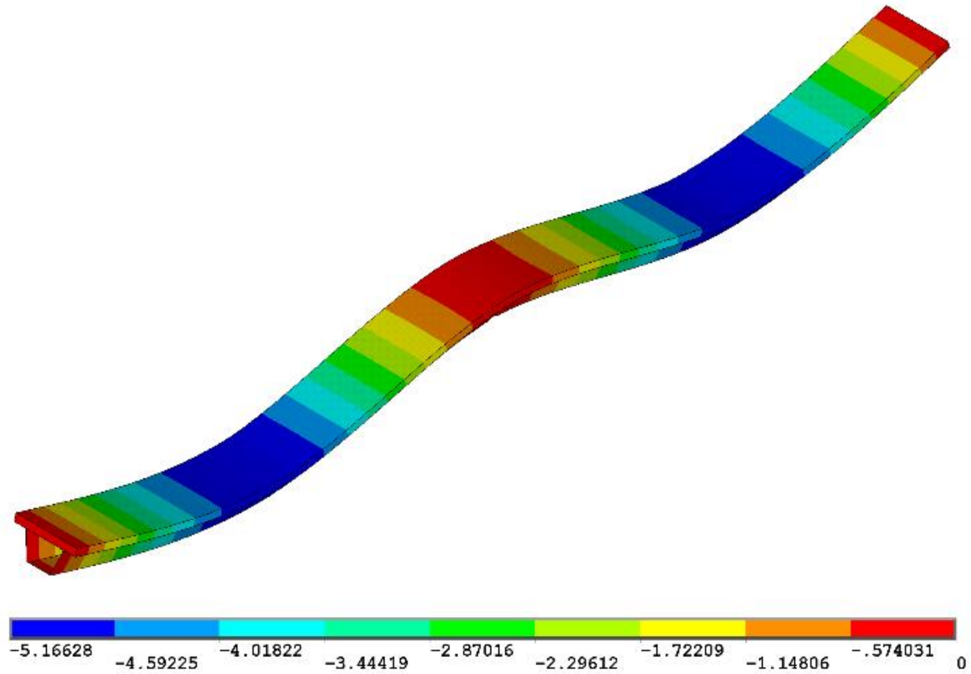

Figure 4.5 Deflections of numerical model DW1

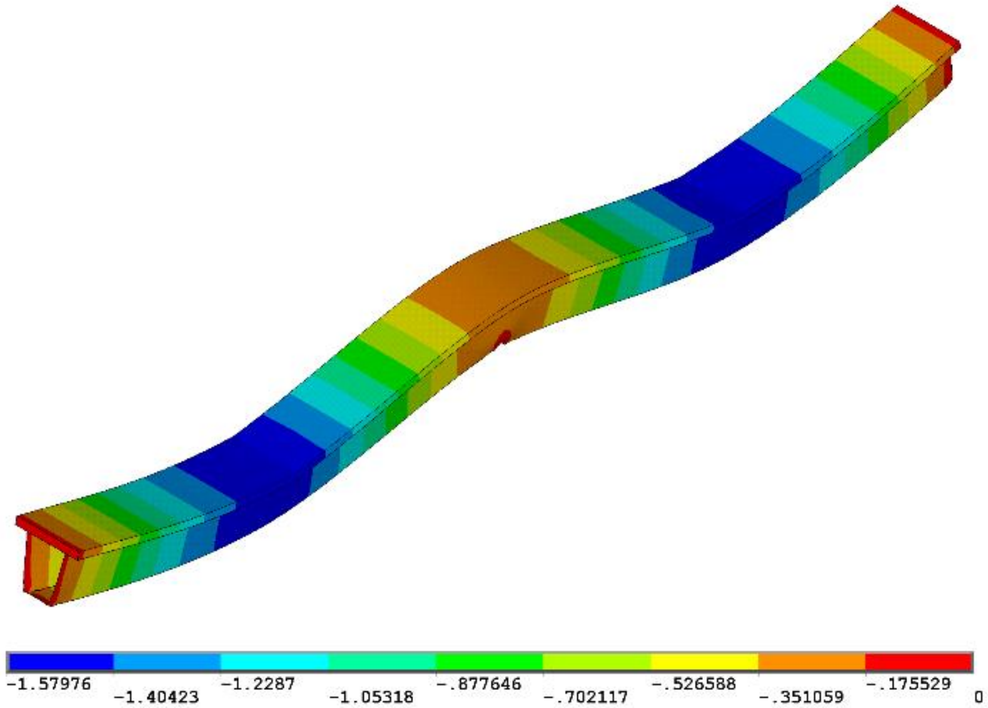

Figure 4.6 Deflections of numerical model DW2

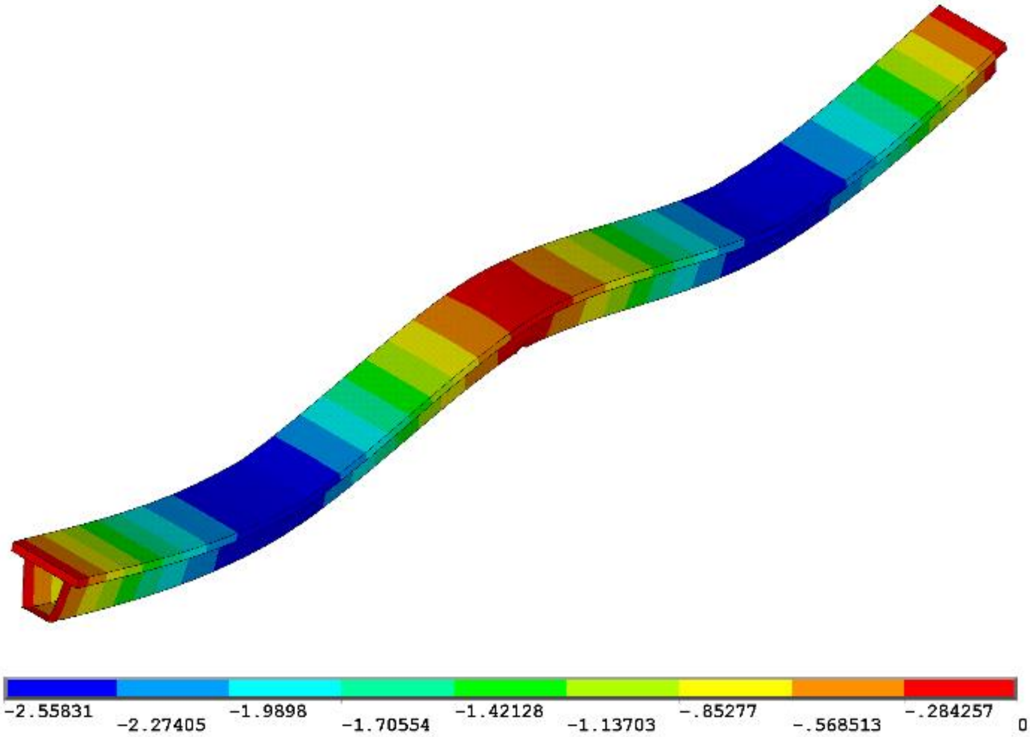

Figure 4.7 Deflections of numerical model TW1

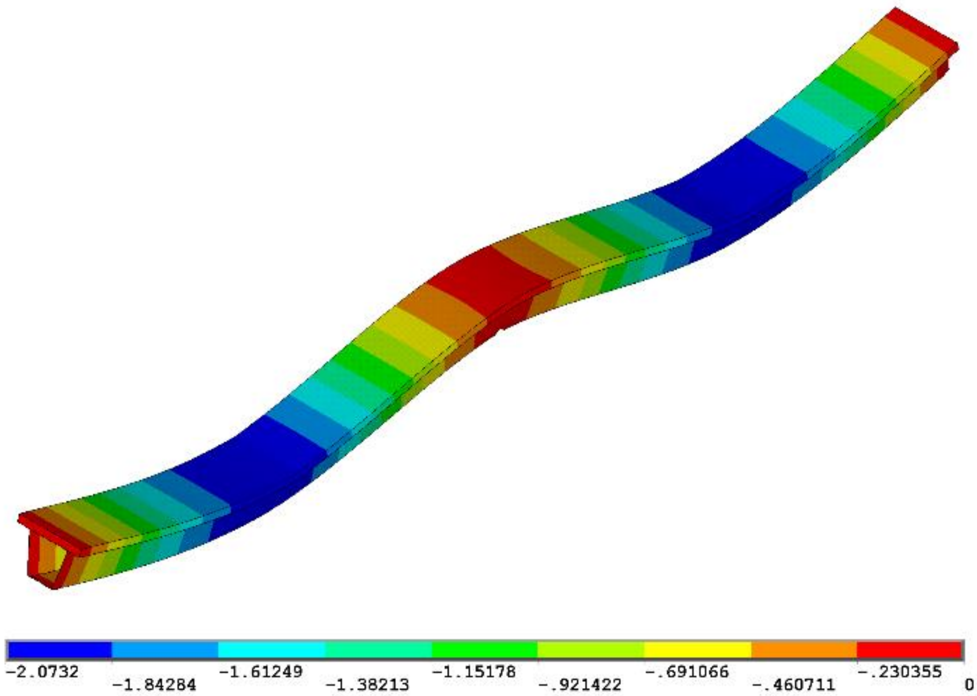

Figure 4.8 Deflections of numerical model TW2

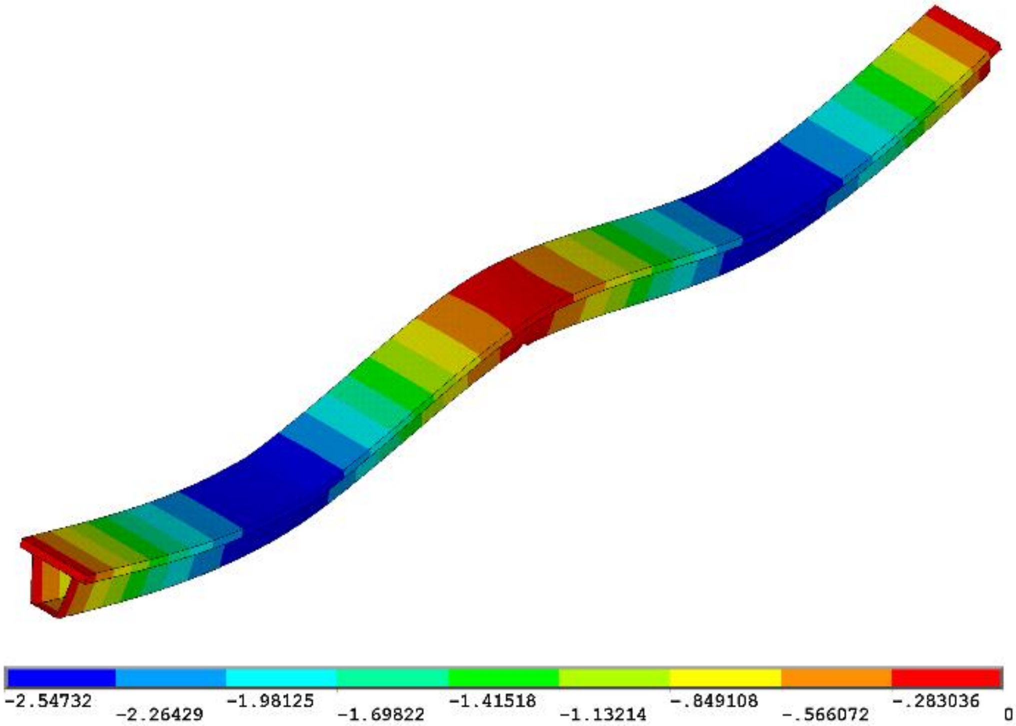

Figure 4.9 Deflections of numerical model TF1

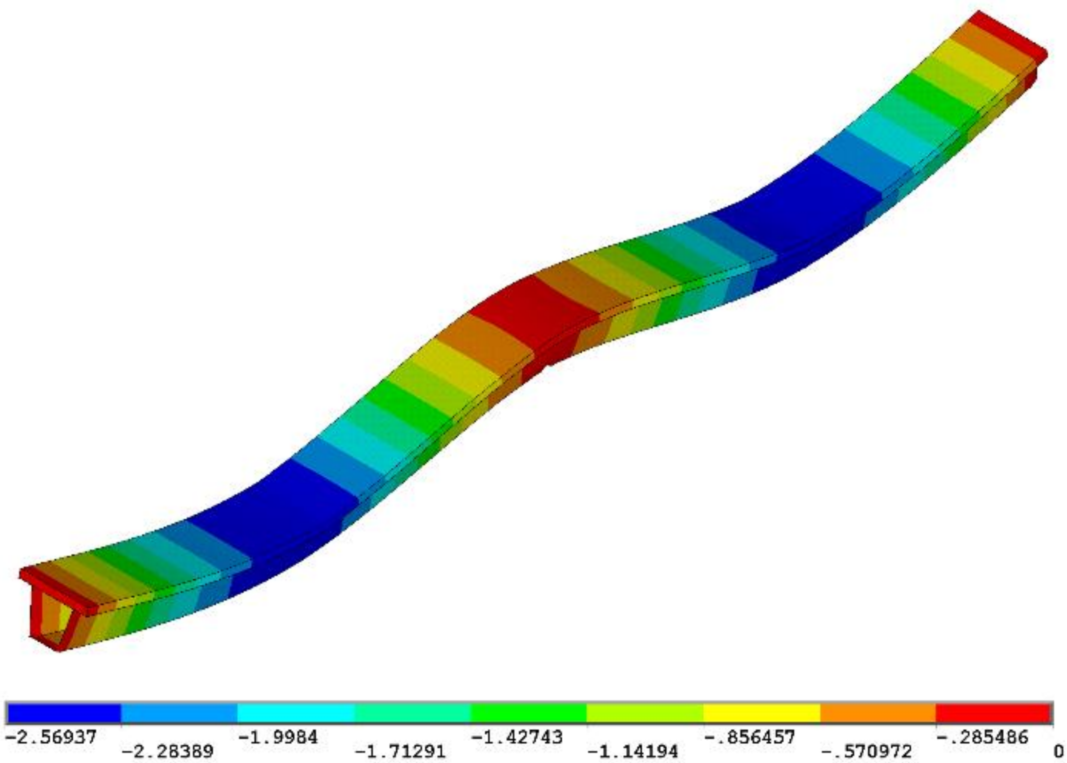

Figure 4.10 Deflections of numerical model TF2

4.7.1.1 Effect of Concrete Deck Depth

The curve in Figure 4.11 (a) shows the effect of the concrete deck depth, DC, on the deflection in the flange of the continuous box girder. With all other design parameters held constant, an addition of depth results in an increase of deflection and at both locations, and frailty versa. However, Figures 4.3 and 4.4 show clear differences with Figure 4.2, DC1 and DC give 16 % of percentage difference while DC2 gives about 13%.

4.7.1.2 Effect of Web Plate Depth

The major effect caused when the depth of the steel box web changed, as noted from table 4.3 and Figures 4.5 and 4.6 DW1 and DW give 67.5 % of percentage difference while DW2 gives about 47 %. These values differently effect on the behaviour of the composite box girder bridge mainly. With all other design parameters held constant, an increase of depth results in an increase of deflection as shown in Figure 4.11 (b).

4.7.1.3 Effect of Web Plate Thickness

Figures 4.7 and 4.8 show the deflections magnitudes for a series of FE models, which have varying from 8 to 16 mm uniform thickness throughout the two continuous spans. The deflections in the base model, with web thickness 12 mm, are also faced in the Figure 4.2 3 for comparison. Clearly, the use of thicker web results in lower deflections. TW1 and TW give 30 % of percentage difference while TW2 gives about 21%. Nevertheless, thicker web plates would require less transverse stiffeners, and would likely result in a lower price.

4.7.1.4 Effect of bottom flange Plate Thickness

Analyses made for a series of FE Models, with a uniform web thickness throughout the integral structure, but with flange plates identical to the base model case. The resulting bottom flange deflections are depicted in Figure 4.11 (d). For all the different uniform web thicknesses from 9.33 in to 18.67 mm, but slight changes occurred in deflection values. The change of bottom flange thickness affects the section modulus of the box girders very little, therefore changing the flange deflections very little. Figures 4.9 and 4.10 show the diversion results in the cases of bottom flange thickness is changed, TF1 and TF give 0.43 % of percentage difference while TF2 gives about 0.42 %.

Table 4.3 shows the results obtained from FE models with the effectiveness of several parameters, same results presented with a 3D contour plot for nodal solution in Figures 4.3 to 4.10. Using the obtained data, a linear regression curve between the FE results and the deflection was calculated from a new equation 1 obtained as shown in Figure 4.12 The following equation for the deflection with the effective parameters illustrated above was proposed:

$$D = 9.76 - 0.0067\,(DW) - 0.00091\,(DC*TW) \qquad 4.1$$

Where D, is a deflection due to four parameters listed above and DW, is the depth of the steel box web. The parameter Dc represents the depth of the concrete deck, finally Tw, is the thickness of the steel box web. All units are in mm.

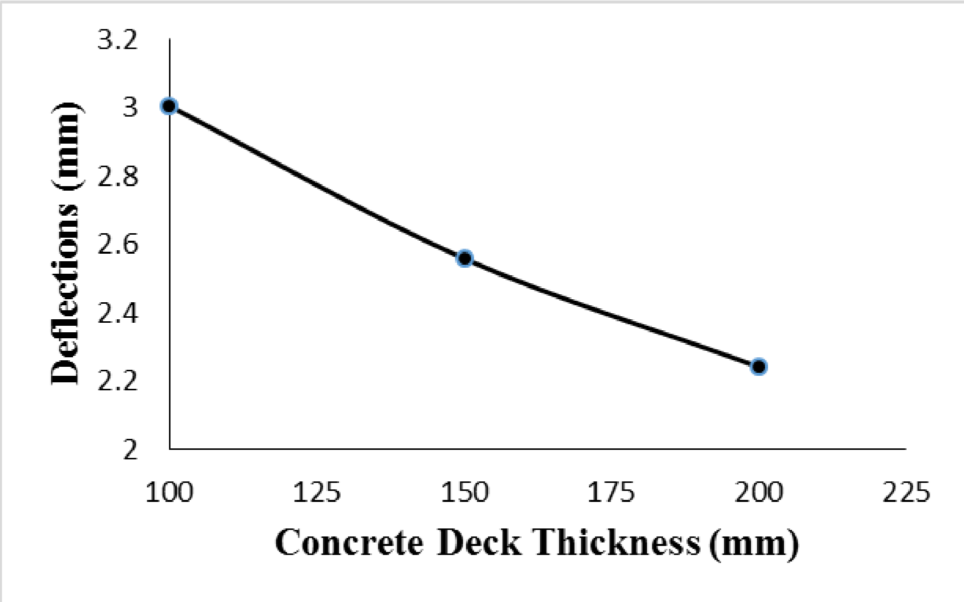

(a) Deflection Vs. concrete deck thickness

Figure 4.11 Variations of deflection value due to dimensions change

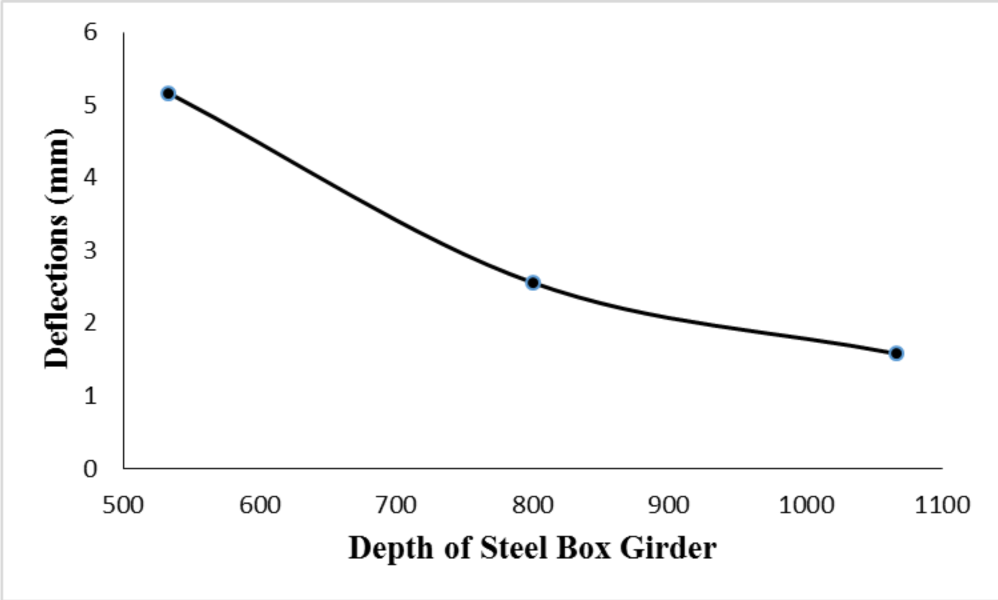

b) Deflection Vs. Box girder depth

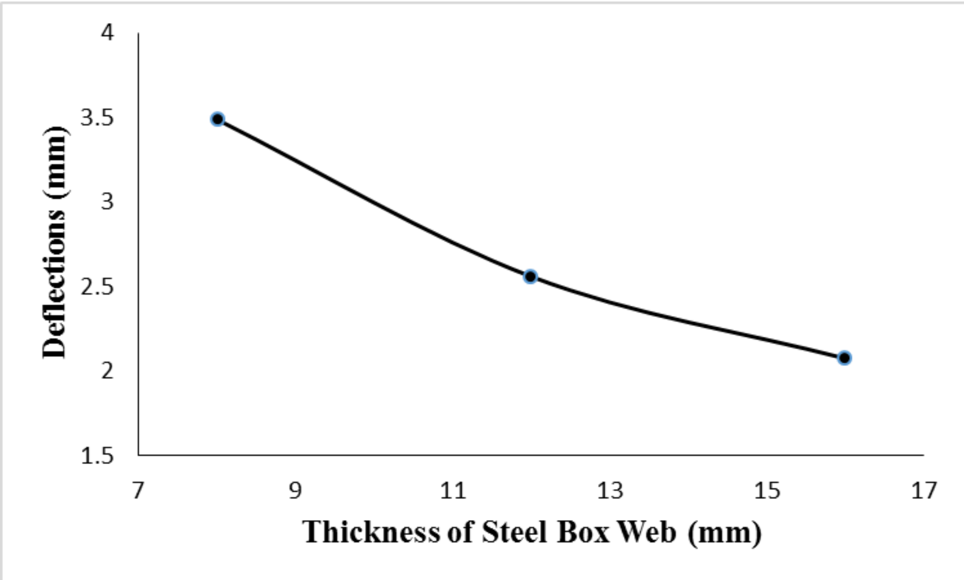

(c) Deflection Vs. Box girder web thickness

Figure 4.11(continued) Variations of deflection value due to dimensions change

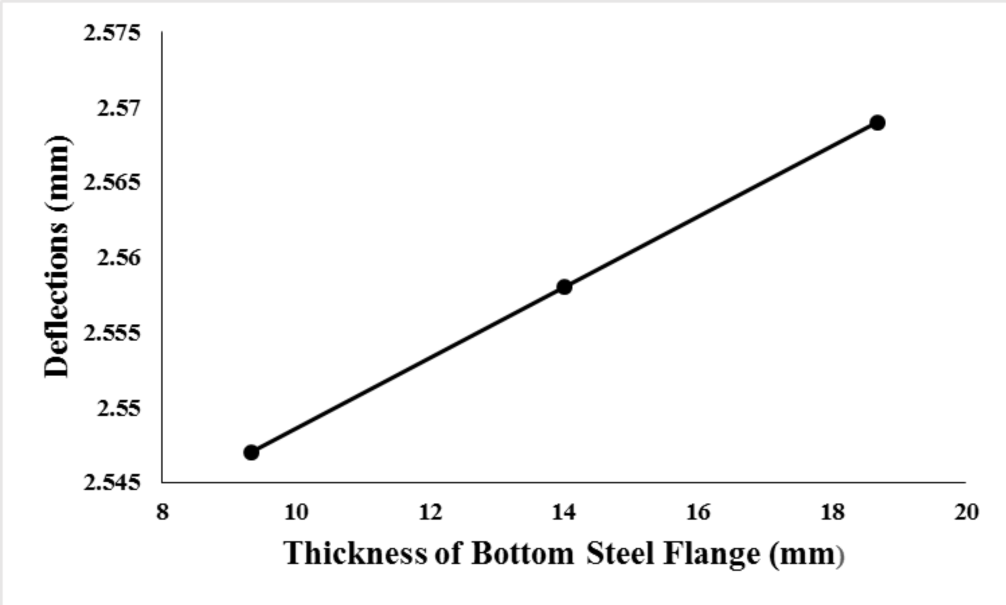

(d) Deflection Vs. bottom steel flange thickness

Figure 4.11 (continued) Variations of deflection value due to dimensions change

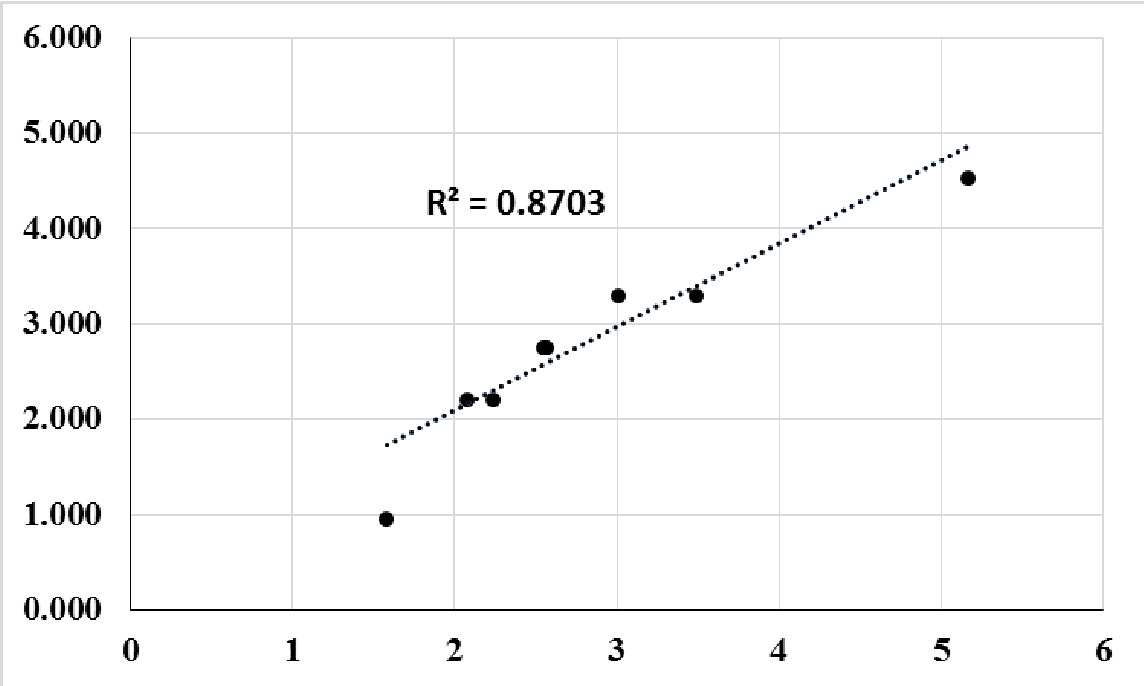

Figure 4.12 Linear regression for deflection in the composite box girder bridge

4.7.2 Results for the Interaction of Variations of Cross Section Parameters

Results of a parametric study for the stresses and deflections in the bottom flange of the box girder are limited to thirteen nodes, which are lying in the Midspan of the lower bottom flange. And because of the symmetry only one span is considered. In this study the effect of the flange thickness is ignored according to its low effect Inferred from the previous section.

The nodes are named N1 to N13 which represent the results of deflections and stresses for the twelve elements in the bottom flange, and they arranged as shown in Figure 4.13 below. In the previous section, the parameters are studied separately without interrupted between them, but in this section the combination between parameters which are changed is considered.

To study this case a program is written using ANSYS Parametric Design Language (APDL) to represent the parameters by leaps and nestling between these loops to get eighty models with different dimensions for each run.

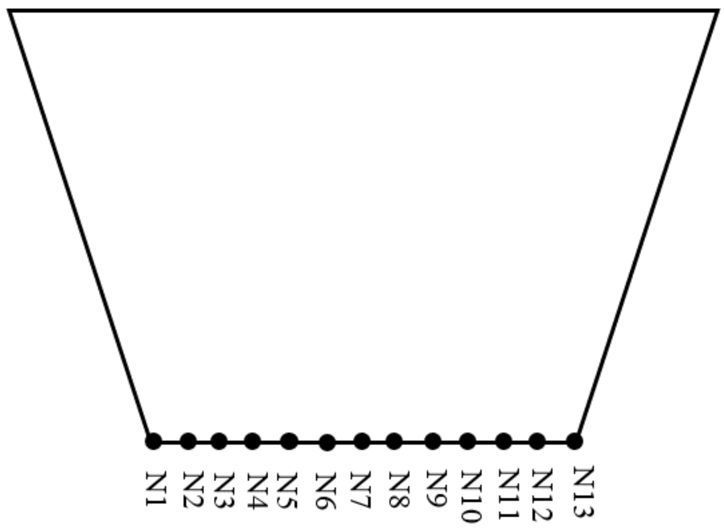

Figure 4.13 Nodes location at the midspan of the second span

The effects of the Combination of Variety of Cross Section dimensions on both of deflections and stresses are listed below in Appendixes A and B respectively. The shaded row in both tables with number 41 represents the base model result that the other results will compare with it. As noted from the results listed in the tables below, it is difficult to indicate the effect of each parameter and also it's difficult to know which parameter has more effect than the others, for this reason a statistical analysis is obtained using Minitab programs.

Minitab uses the general linear model approach with three types of ANOVA models to perform Gage R&R studies: the random-effects model, the mixed-effects model, and the nested design model. The random-effects model is the default. The mixed-effects or the nested design model is used if any factors are fixed or nested. The final selected model only includes the main effects' terms, the significant highest order interactions, and the relevant interactions in between. Minitab calculates the ANOVA table for the appropriate model. That table is then used to calculate the variance components, which appear in the Gage R&R tables.

Table 4.4 Factor Information

Factor	Type	Levels	Values
HW	random	3	532; 800; 1068
DC	random	3	100; 150; 200
TW	random	3	8; 12; 16
L	random	3	14000; 21000; 28000

Table 4.5 Variance Components for deflection results

Source	VarComp	%Contribution (of VarComp)
Total Gage R&R	17.2025	98.46
Repeatability	2.8481	16.30
Reproducibility	14.3544	82.16
TW	0.9008	**5.16**
L	8.0106	**45.85**
HW	5.4430	**31.15**
DC	0.2692	**1.54**
Total Variation	17.4716	100.00

Table 4.6 Variance Components for stress results

Source	VarComp	%Contribution (of VarComp)
Total Gage R&R	732.846	98.52
Repeatability	55.567	7.47
Reproducibility	677.279	91.05
TW	179.028	**24.07**
L	209.116	**28.11**
HW	289.135	**38.87**
DC	11.022	**1.48**
Total Variation	743.868	100.00

Minitab outputs two tables for Gage R&R Expanded. The first table contains the Variance Components (VarComp) column and the %Contribution of VarComp column. Percent contribution (%Contribution) is established on the estimates of the variance factors. Each value in VarComp is divided by the Total Variation, and then multiplied by 100. High %Contribution is considered really safe. When %Contribution for Part-to-Part is high, the system can distinguish between parts.

Minitab also displays columns with percentages based on the standard deviation (or square root of variance) of each part. These columns, labelled %StudyVar and %Tolerance, typically do not add up to 100%. Because the standard deviation uses the same units as the part measurements and the allowance, it allows for meaningful comparisons.

From the bolted number its Cleary that the length is most influential to deflection results and web depth is the most factor effected to the stress. The primary event of the three layers of a component in a balanced design is estimated by the three factor level mean minus the overall mean. For the unbalanced case, Minitab uses the regression model to calculate the effects estimated for each factor and level. To create the graph for a factor, Minitab plots main effects for each level of the factor. As shown below in Figures 4.14 and 4.15.

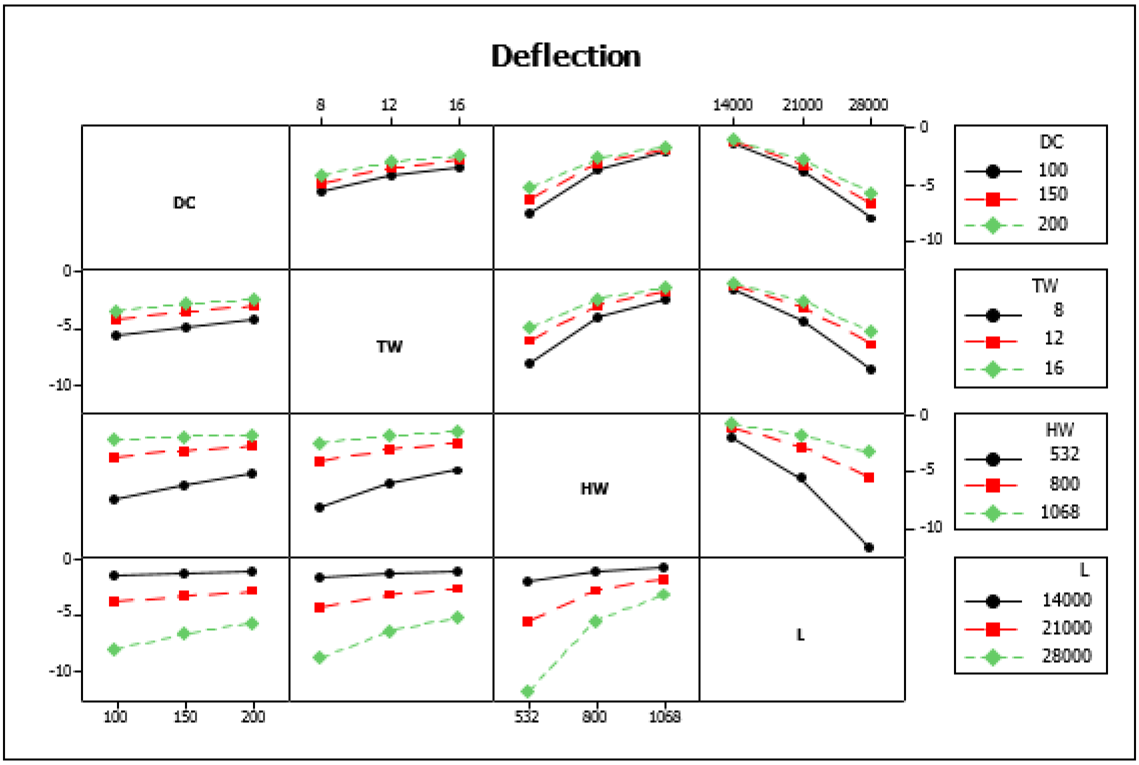

Figure 4.14 Main effects curves for deflection results.

Figures 4.16 and 4.17 show the model which has dimensions with the minimum various results for deflection and stress respectively from base model while Figures 4.18 and 4.19 represent the model which has dimensions with the maximum various results for deflection and stress respectively from base model. Figures (4.20-4.23) show the models with nearest results to the base model.

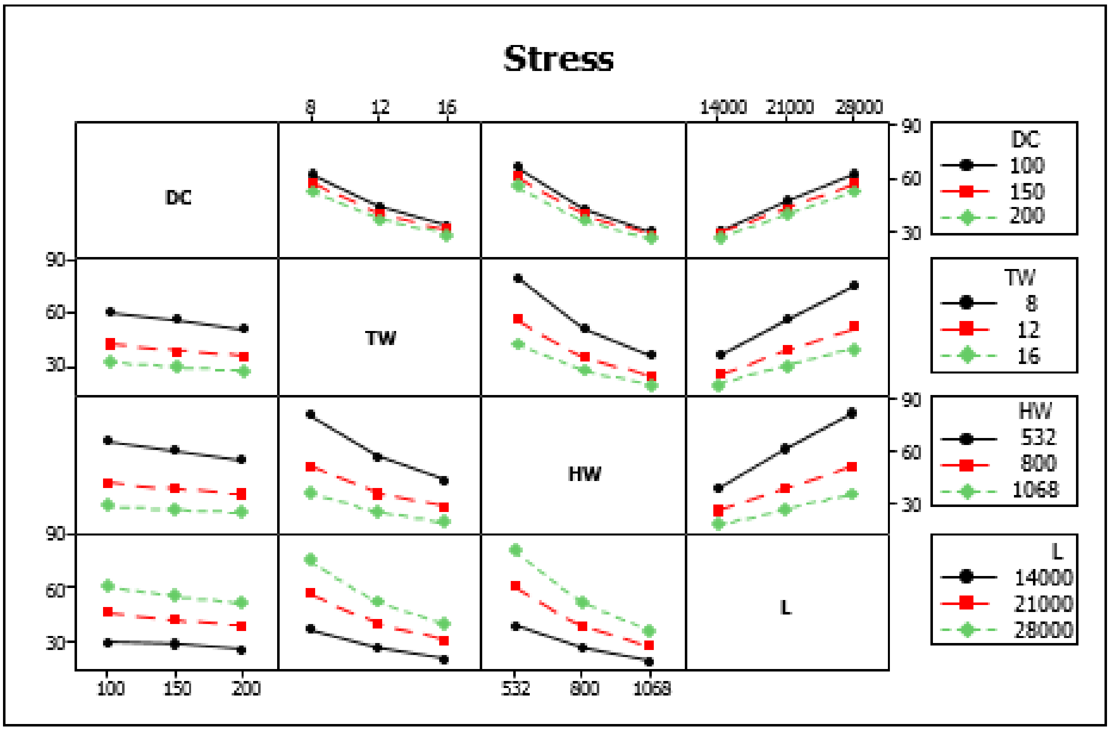

Figure 4.15 Main effects curves for stress results.

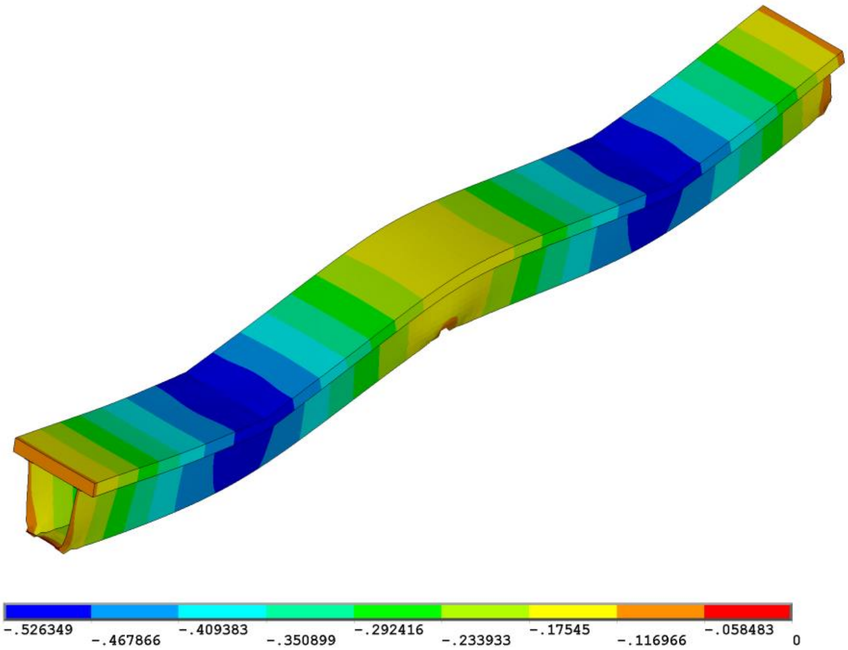

Figure 4.16 the model with dimensions in row (79) in Appendix A for deflection.

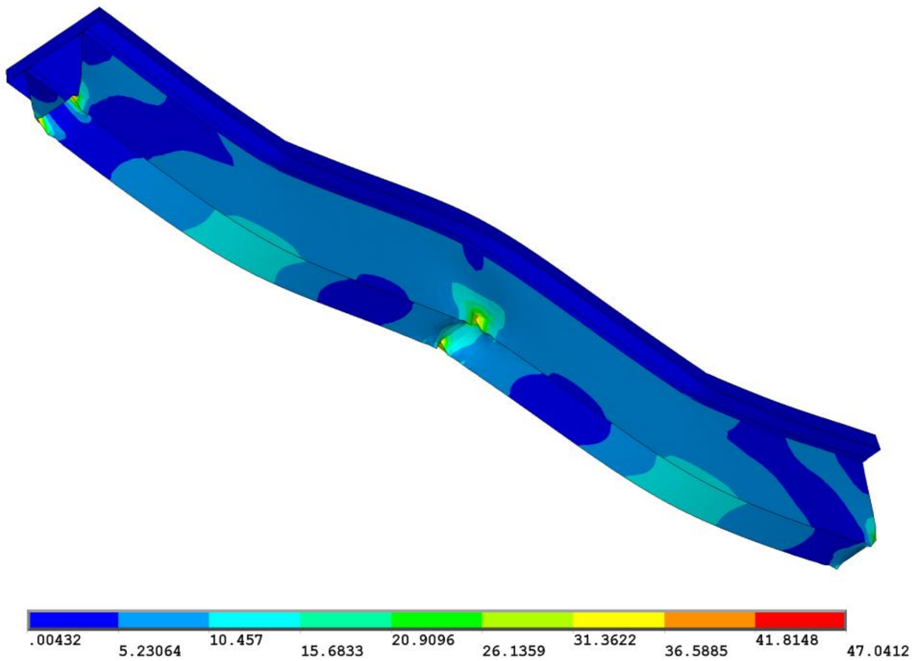

Figure 4.17 the model with dimensions in row (79) in Appendix B for stress.

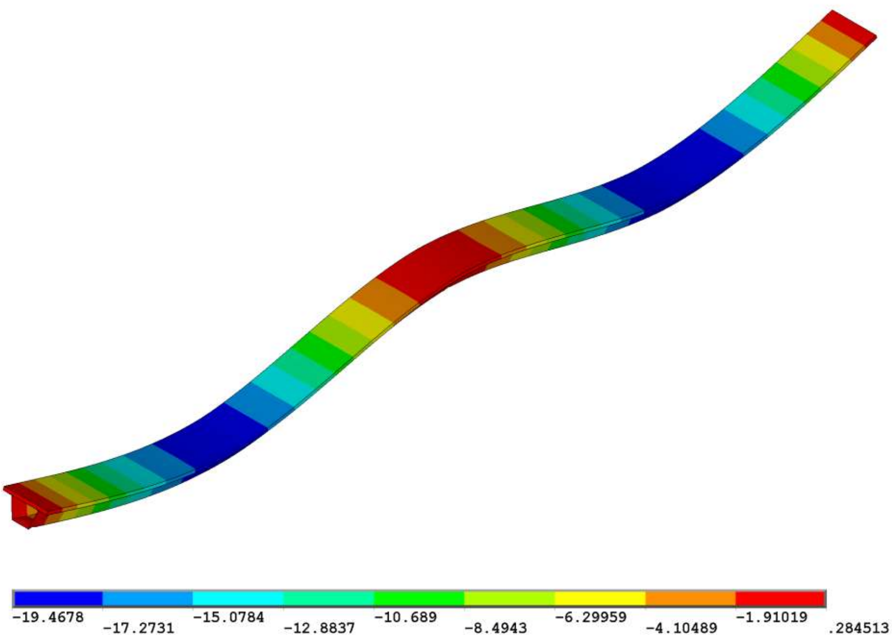

Figure 4.18 the model with dimensions in row (3) in Appendix A for deflection.

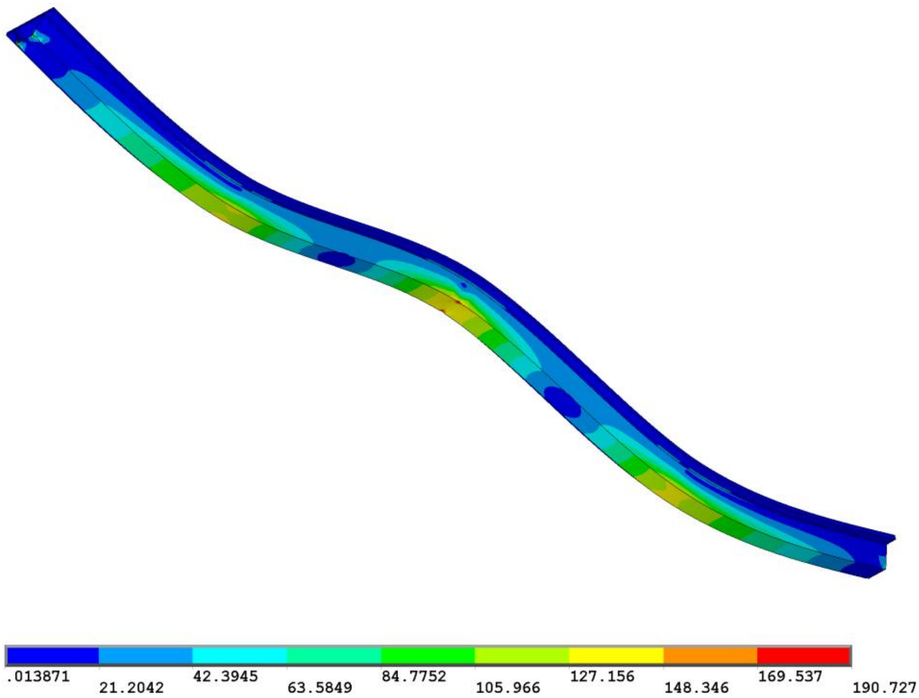

Figure 4.19 the model with dimensions in row (3) in Appendix B for stress.

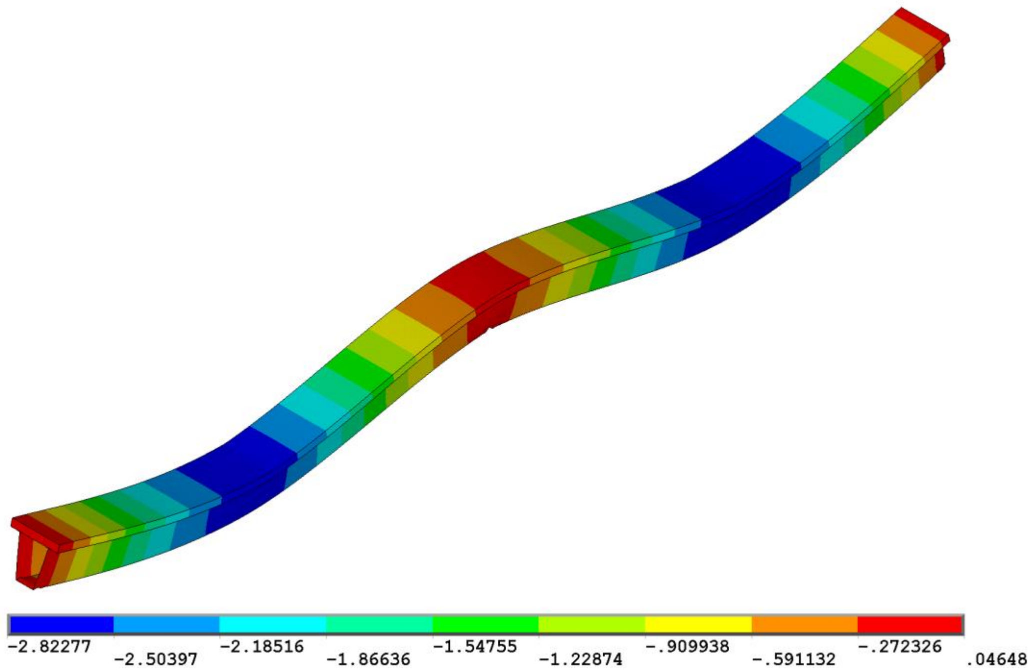

Figure 4.20 the model with dimensions in row (72) in Appendix A for deflection.

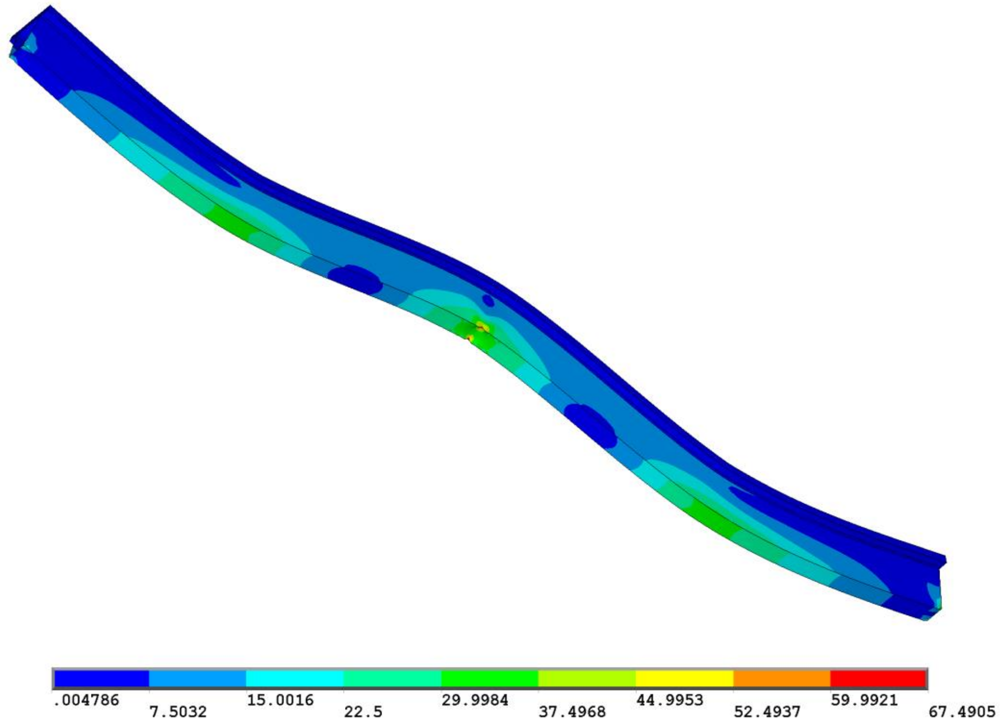

Figure 4.21 the model with dimensions in row (72) in Appendix B for stress.

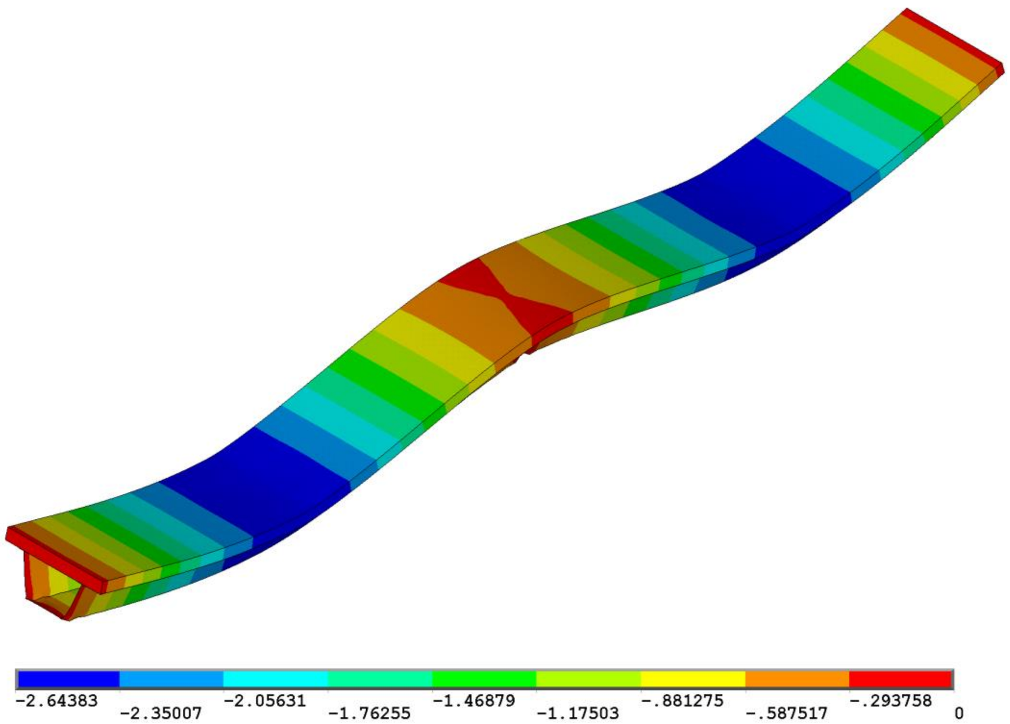

Figure 4.22 the model with dimensions in row (28) in Appendix A for deflection.

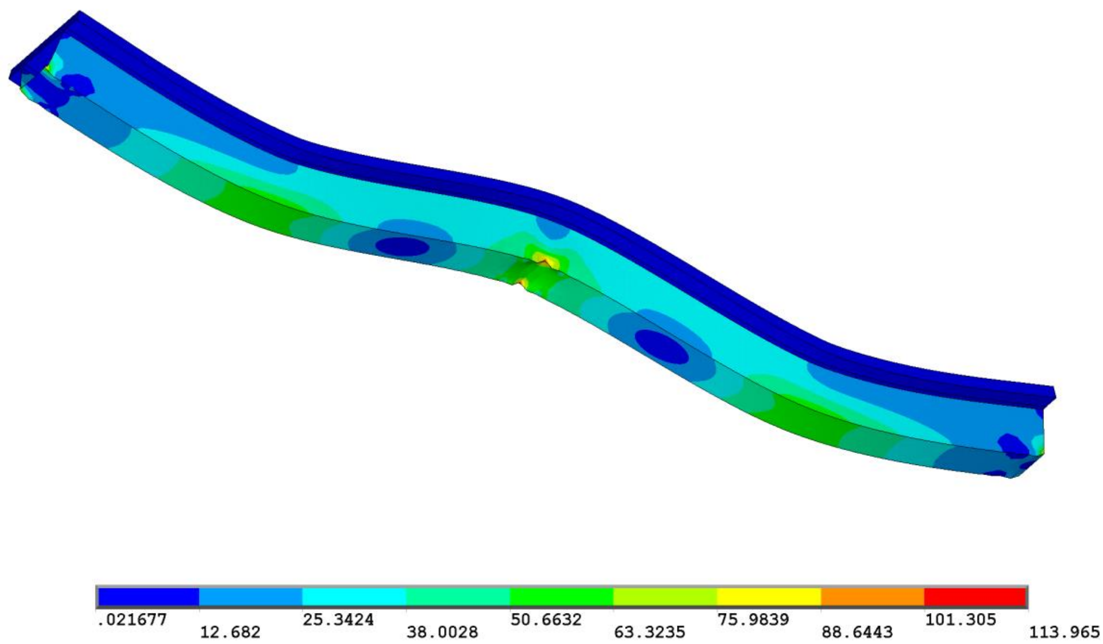

Figure 4.23 the model with dimensions in row (28) in Appendix B for stress.

As noted from Figures above (4.16-4.23) and from results in Appendixes A and B, that the sets of dimensions in the rows 79,3,72, and 28 have special numbers. Rows 79 and 3 represent the maximum various and the minimum various value, respectively compared with the set in the shaded row 42 which represents base model with percentage of difference 151.4% for row 3 and 136% for row 79. At the other hand the set of dimensions in row 72 have longer length and greater values of concrete depth, and steel box web depth also the set have the nearest result to the base model. The percentage difference between a set of row 72 and base model is 4.7%. Finally, the percentage difference between base model and the set of dimension in row 28 is 1.6%, which mean that this model has the closed result to the base model. This set of dimension has same concrete depth as base model but all other values of web thickness, web depth, and length have the lowest values 8,532 and 14000 respectively. The percentage difference between base model and row 3 for stress values is 109.8% and for row 28 is 44.2% and for row 72 is 16.5% and for row 79 is 100%.

4.7.3 Results for the Interaction of Variations of Cross Section Parameters and Haunching Ratio

Results of a parametric study on the effects of haunch dimensions and thickness of steel web plates with the concrete slab depth and span length of the bottom flange are listed in tables 4.9 and 4.10. In these tables, results of a parametric study for the stresses and deflections in the bottom flange of the box girder. The same procedure submitted in the previous section is followed here except the addition of Haunch Ratio (HR) as another factor.

ANalysis Of VAriance (ANOVA) is similar to regression in that it is used to investigate and model the relationship between a response variable and one or more predictor variables. Nevertheless, analysis of variance differs from regression in two ways: the predictor variables are qualitative (categorical), and no assumption is drawn close to the nature of the relationship (that is, the model does not include coefficients for the variables). As a result, analysis of variance expands the two-specimen t-test for testing the fairness of two populace intends to a more broad invalid theory of looking at the equity of more than two methods, versus them not all being equivalent. A few of Minitab's ANOVA procedures, nevertheless, permit models with both subjective and quantitative variables.

Interactions Plot creates a single interaction plot for two components or a matrix of interaction plots for three to nine agents. An interaction plot is a plot of means for each level of a divisor with the level of a second factor held constant. Interaction plots are useful for evaluating the presence of interaction.

Interaction is present when the response at a factor level depends upon the levels of other ingredients. Parallel lines in an interaction plot indicate no interaction. The greater the departure of the lines from the parallel state, the higher the degree of interaction. To utilize the interactive plot, information must be usable for all combinations of grades.

Table 4.7 Factor Information

Factor	Type	Levels	Values
HR	random	5	1.6; 1.8; 2.2; 2.5; 3.0
HW	random	3	532; 800; 1068
DC	random	3	100; 150; 200
TW	random	3	8; 12; 16
L	random	3	14000; 21000; 28000

Table 4.8 Variance Components for deflection results

Source	VarComp	%Contribution (of VarComp)
Total Gage R&R	70.1574	80.68
Repeatability	26.7932	30.81
Reproducibility	43.3642	49.87
TW	2.0858	**2.40**
L	29.0027	**33.35**
HW	12.0434	**13.85**
DC	0.2322	**0.27**
HR	16.7982	**19.32**
Total Variation	86.9555	100.00

Table 4.9 Variance Components for stress results

Source	VarComp	%Contribution (of VarComp)
Total Gage R&R	118.093	78.97
Repeatability	45.004	30.10
Reproducibility	73.089	48.88
L	42.880	**28.68**
DC	4.585	**3.07**
TW	9.285	**6.21**
HW	16.340	**10.93**
HR	31.442	**21.03**
Total Variation	149.535	100.00

From the bolted number it's clear that the length is the most effective to deflection and stress results and HR is also has high effected to the stress and deflection. The main effect of the three levels of a factor in a balanced design is estimated by the three factor level mean minus the overall mean and five levels for HR. For the unbalanced case, Minitab uses the regression model to estimate the effects Calculated for each factor and level. To create the graph for a factor, Minitab plots main effects for each level of the factor. As shown below in Figures 4.30 and 4.31

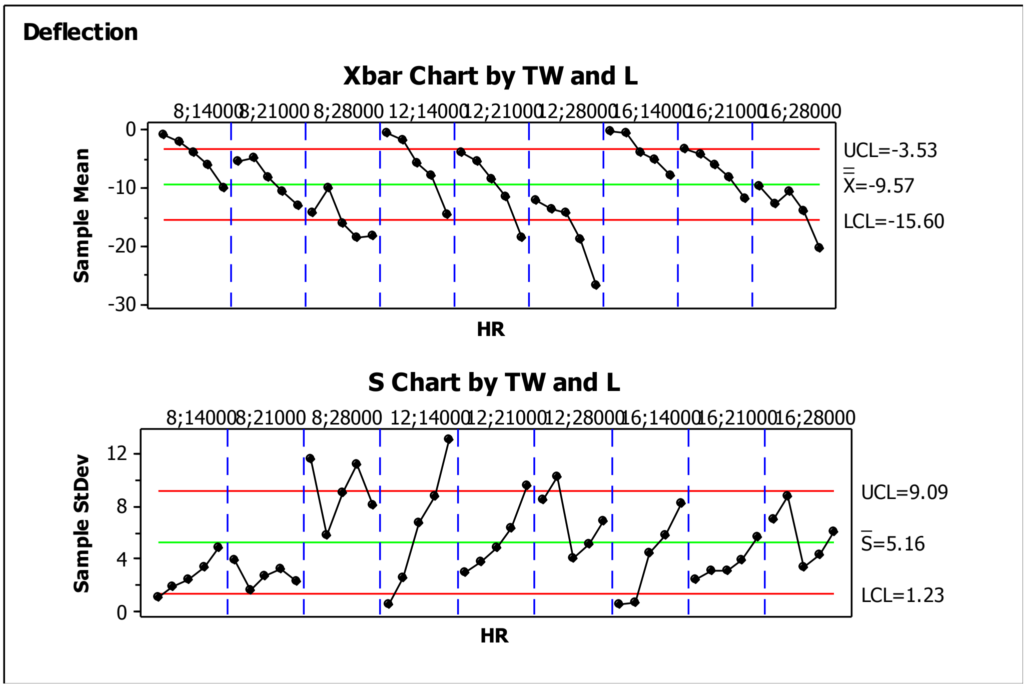

Figure 4.24 Xbar and S charts by TW and L

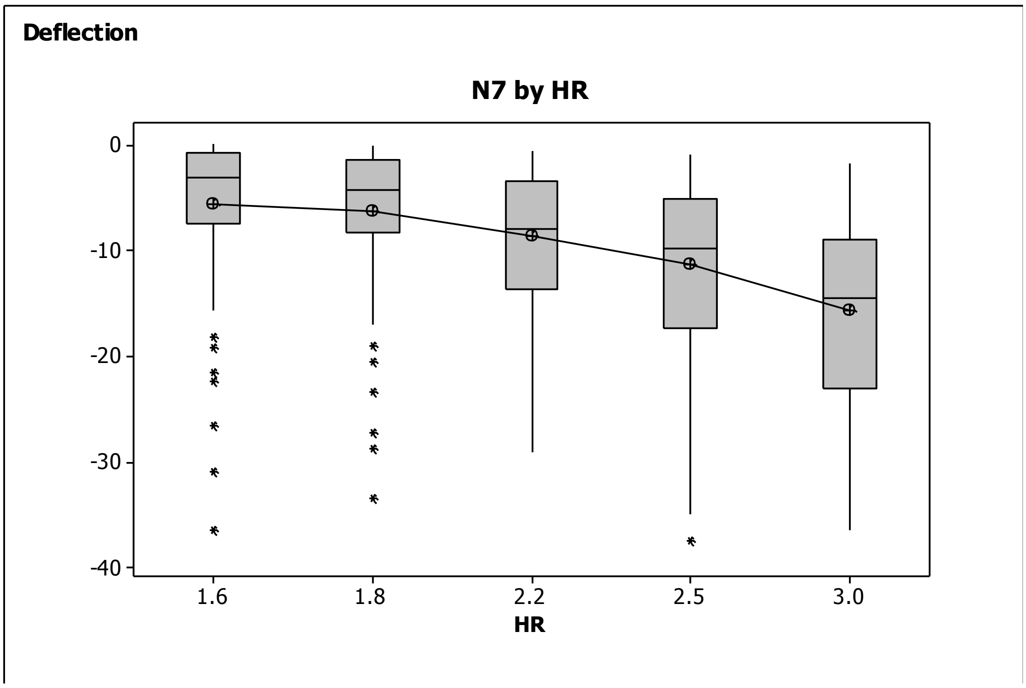

Figure 4.25 results for node N7 vs. HR

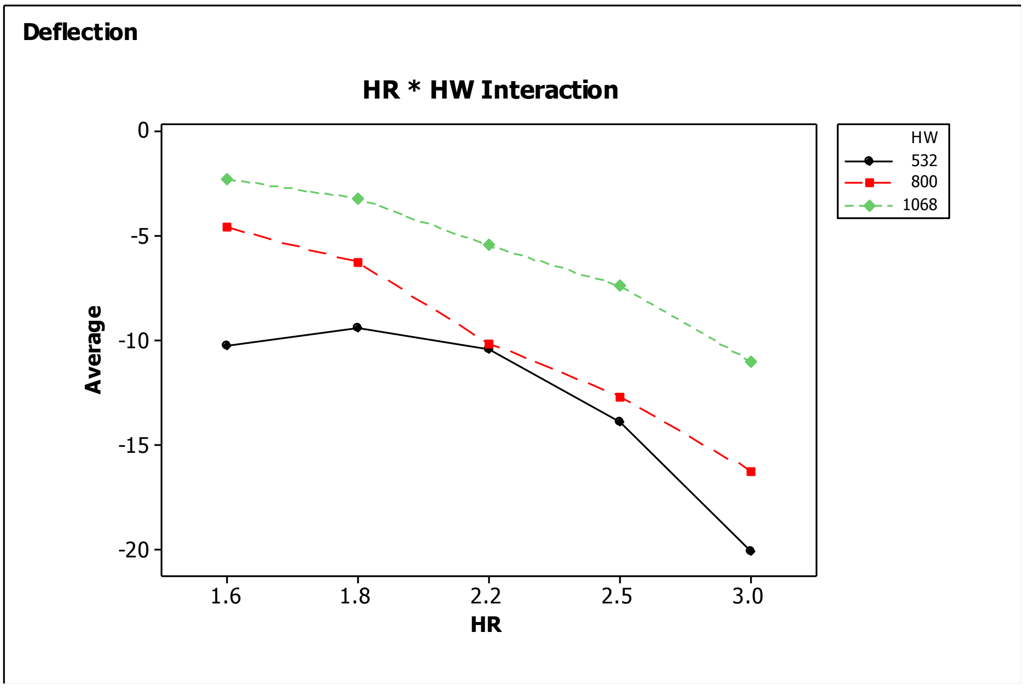

Figure 4.26 HR and HW interaction

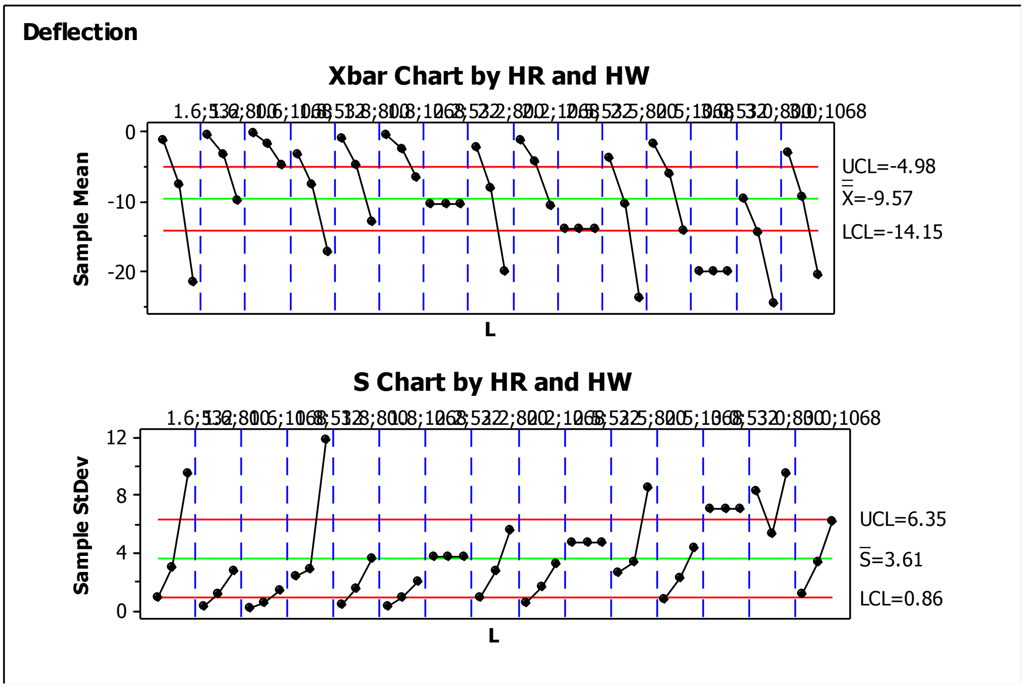

Figure 4.27 Xbar and S charts by HR and HW

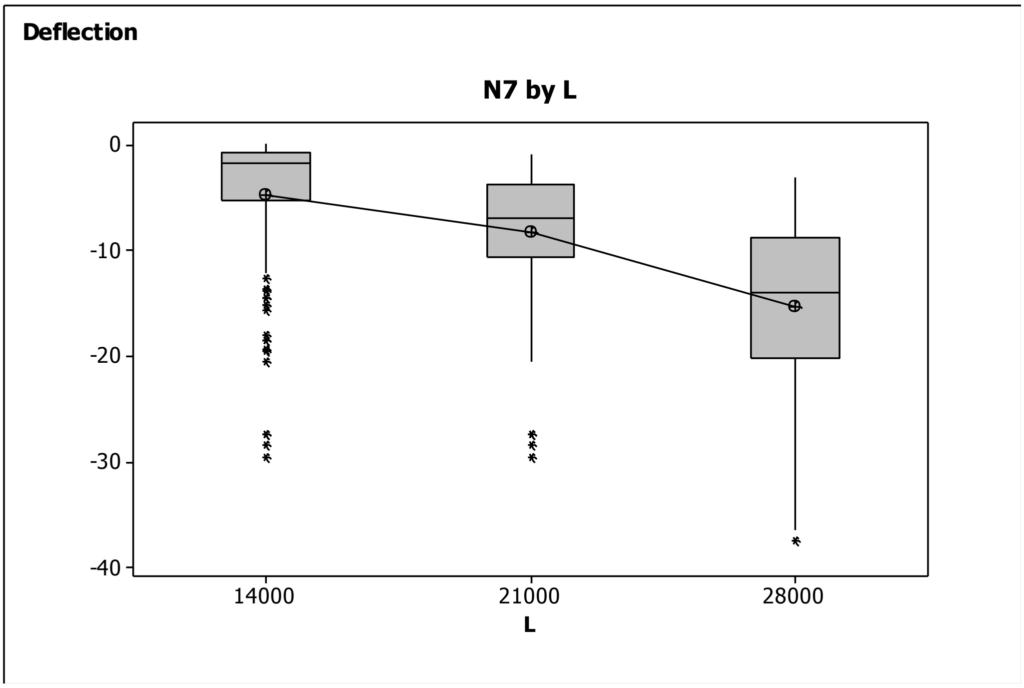

Figure 4.28 results for node N7 vs. L

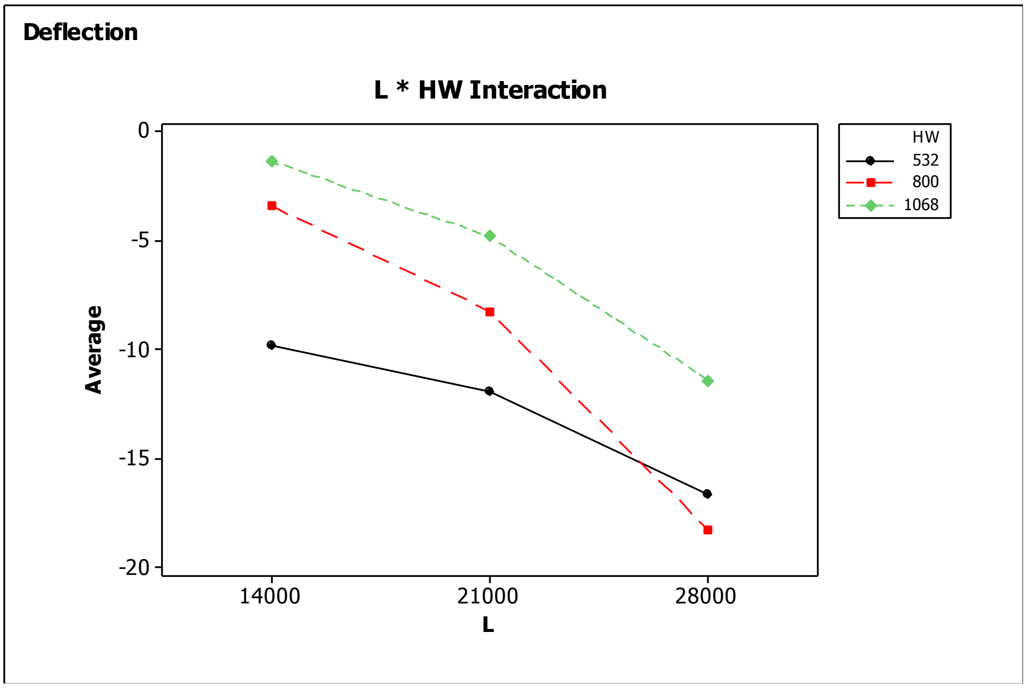

Figure 4.29 HW and L interaction

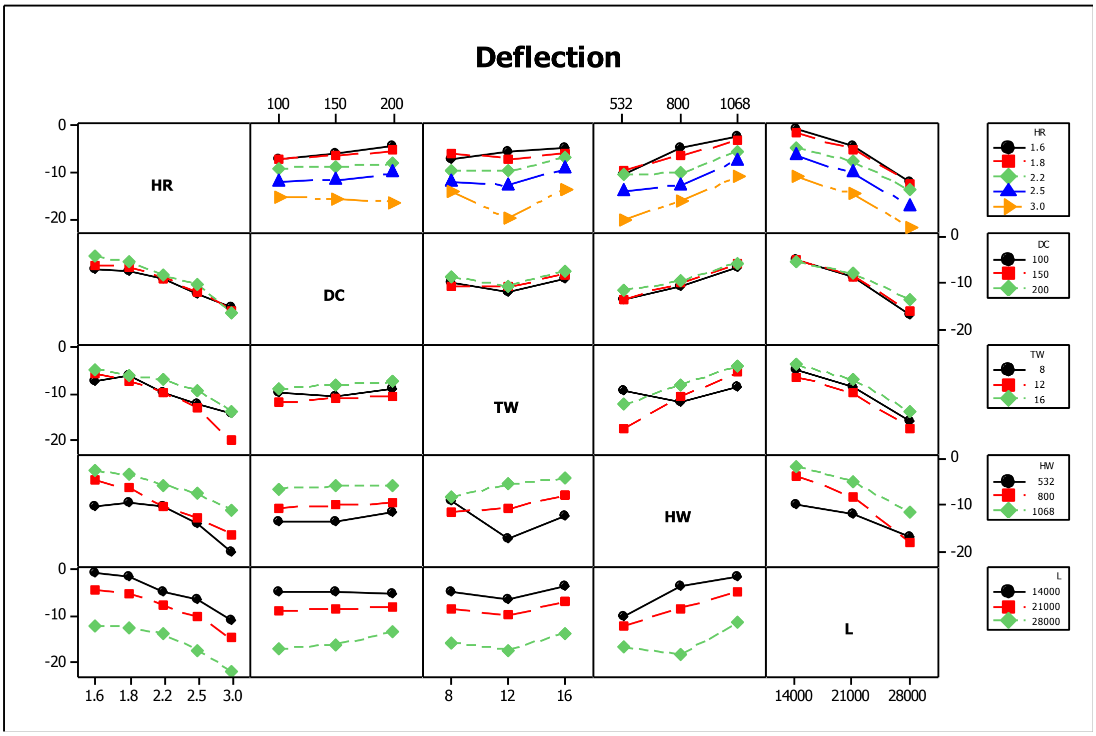

Figure 4.30 mean interaction effect between parameters for deflection results.

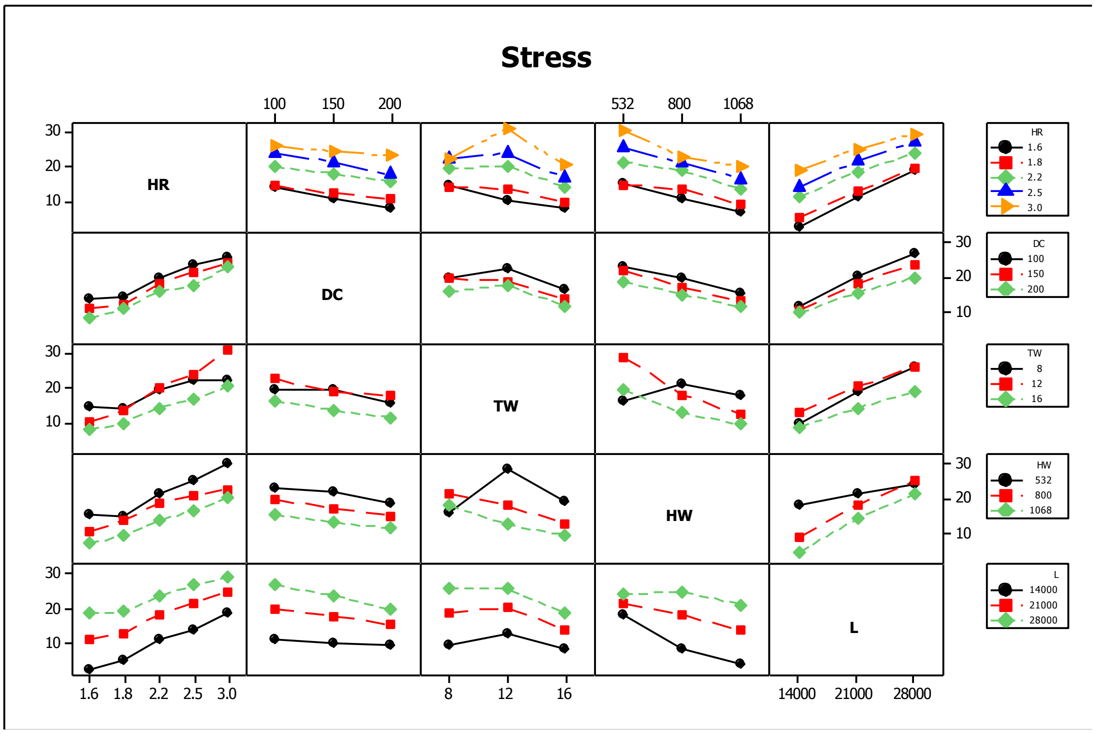

Figure 4.31 mean interaction effect between parameters for stress results.

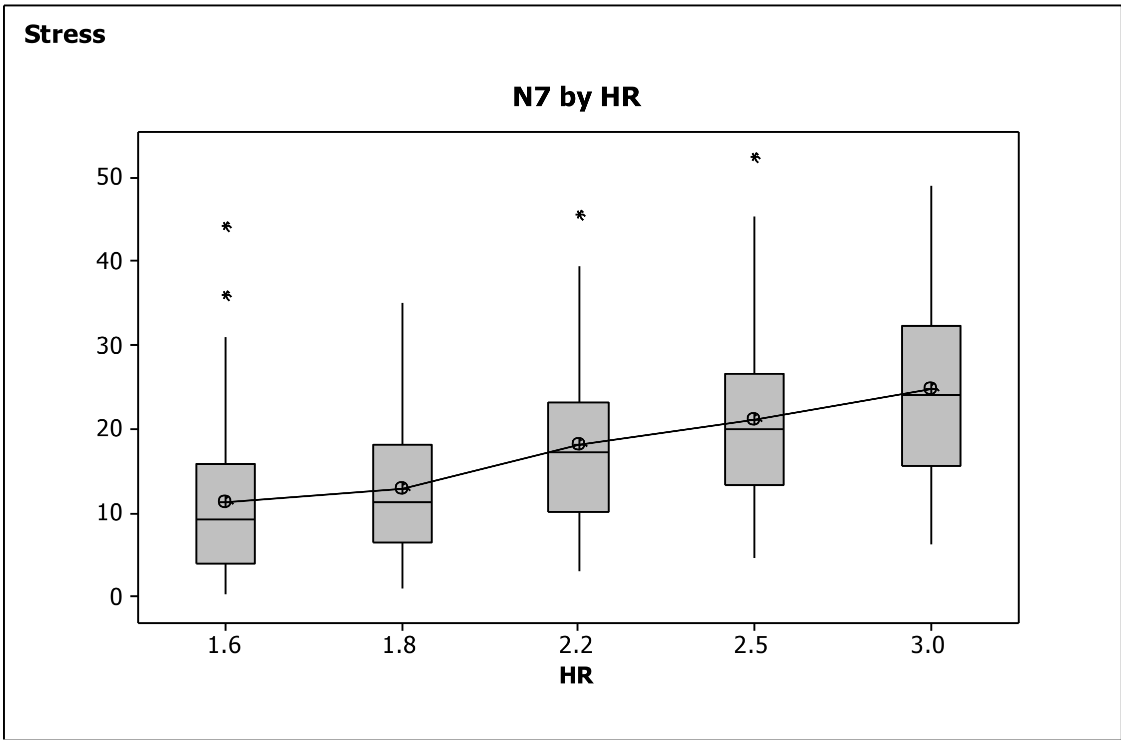

Figure 4.32 results for node N7 vs. HR

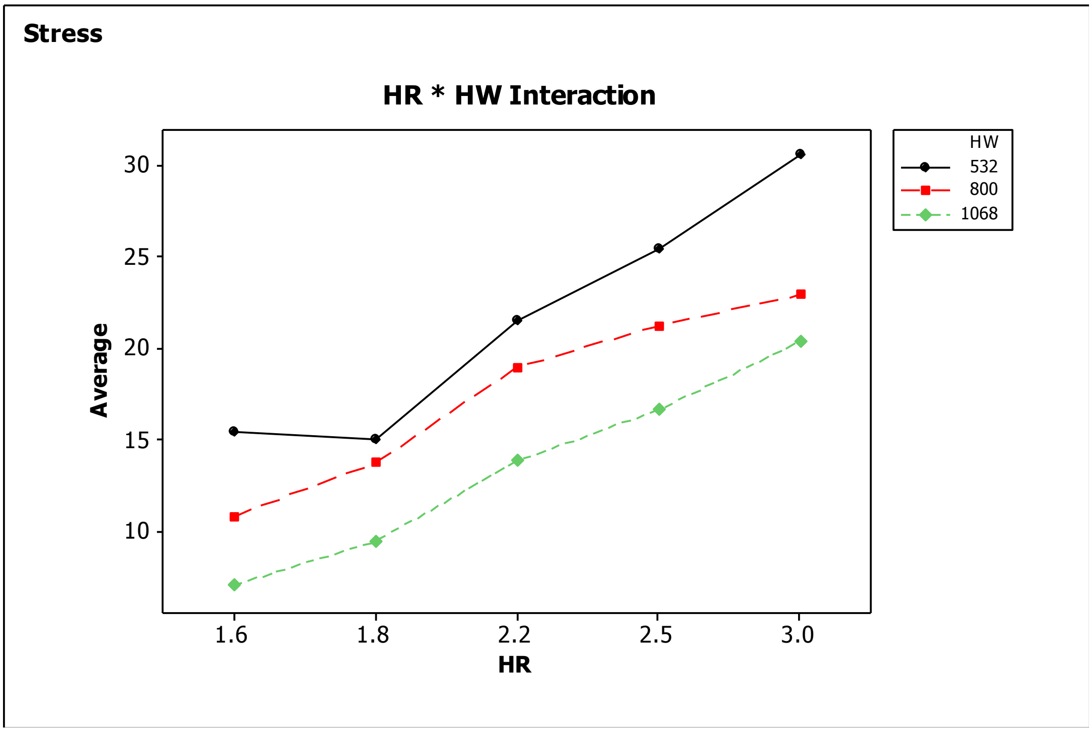

Figure 4.33 HW and HR interaction

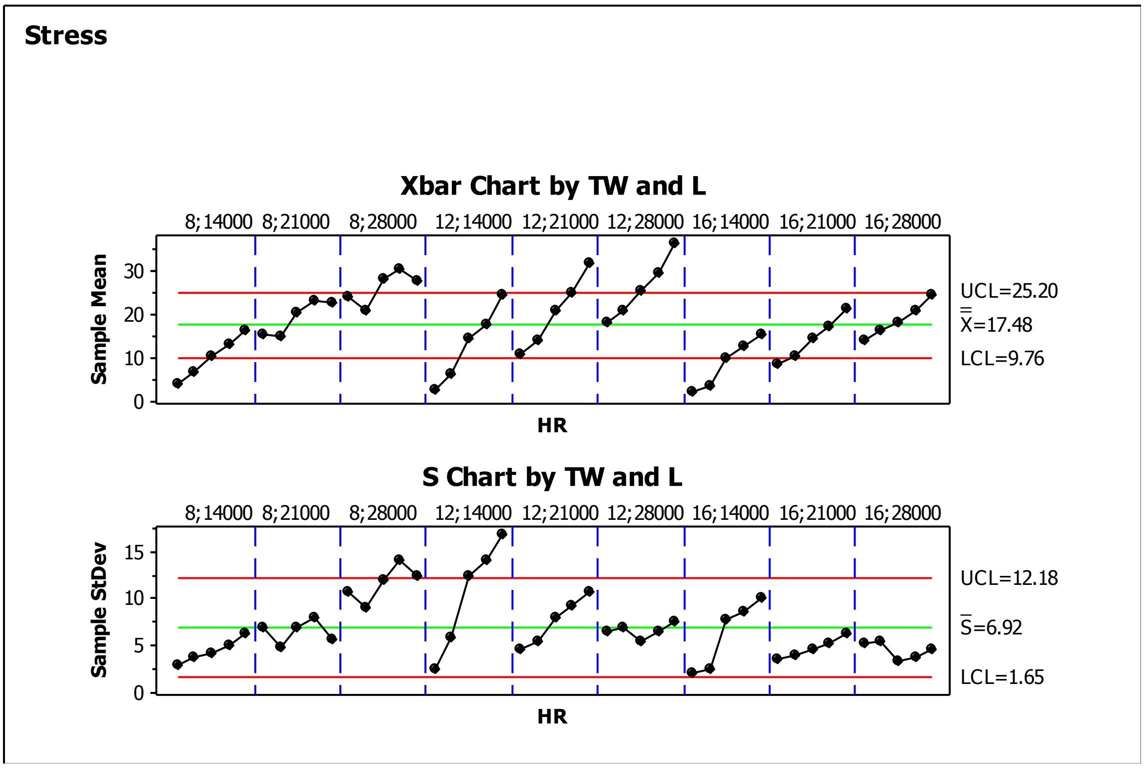

Figure 4.34 Xbar and S charts by HR and HW for stress

Figures 4.24, 4.26, 4.27 and 4.29 throw 4.34 show the interaction between the parameters. As noted from results in Appendixes C and D, that the sets of dimensions in the rows 3, 52, and 91, and 394 have special numbers. Rows 3 and 52 represent the maximum various and the minimum various value, respectively compared with the set which represents base model with percentage of difference 173.7% for row 3 and 184.7% for row 52.

At the other hand the set of dimensions in row 394 have greater values of concrete depth, and steel box web depth also the set have the nearest result to the base model. The percentage difference between a set of row 394 and base model is 0.4%. Finally, the percentage difference between base model and the set of dimension in row 91 is 1.2%, which mean that this model has the closed result to the base model. This set of dimension has a same web thickness as base model but all other values of concrete depth, web depth, and length have the lowest values 100,532 and 14000 respectively. The percentage difference between base model and row 3 for stress values is 5.7% and for row 52 is 199% and for row 394 is 101% and for row 91 is 123%. The nearest set to base model for stress is set in row 168 with 0.8% percentage difference.

The stresses in the bottom flange are plotted against the haunch ratio (HR) as shown in Figure 4.34. Figure 4.31 shows clearly that, for any haunch ratio, an increase in the

Table 4.10 Interaction Variance Components for stress results

Source	VarComp	%Contribution(of VarComp)
Total Gage R&R	44.895	28.16
Repeatability	5.259	3.30
Reproducibility	39.637	24.86
L	39.637	24.86
Part-To-Part	114.528	71.84
HR	32.239	20.22
DC	4.461	2.80
TW	0.111	0.07
HW	6.610	4.15
HR*L	0.000	0.00
HR*DC	0.000	0.00
HR*TW	1.240	0.78
HR*HW	0.000	0.00
L*DC	1.653	1.04
L*TW	1.208	0.76
L*HW	6.388	4.01
DC*TW	0.000	0.00
DC*HW	0.000	0.00
TW*HW	22.396	14.05
HR*L*DC	0.000	0.00
HR*L*TW	0.000	0.00
HR*L*HW	9.820	6.16
HR*DC*TW	0.000	0.00
HR*DC*HW	1.137	0.71
HR*TW*HW	11.091	6.96
L*DC*TW	0.134	0.08
L*DC*HW	0.000	0.00
L*TW*HW	2.735	1.72
DC*TW*HW	2.073	1.30
HR*L*DC*HW	0.714	0.45
HR*L*TW*HW	5.428	3.40
HR*DC*TW*HW	5.090	3.19
Total Variation	159.423	100

thickness of the web plate leads to a decrease of the bottom flange stresses. Increasing the girder depth at midspan, thus decreasing the haunch ratio, also results in a reduction of stresses in the bottom flange. Figure 4.31 shows the same effect of the increasing haunch ratio on bottom flange stresses for different web plate thickness. It also depicts the insignificant effect of changing web thickness. From the decreasing slope of the curves in these figures, it can be concluded that a large difference between box girder depths at midspan (that is, a large haunch ratio) is not an efficient way of achieving low stresses in the bottom flange steel plate. A moderate haunch ratio, combined with a thicker web plate and long span, is more efficient.

Table 4.10 shows the effect by %contribution for interaction variance components for stress results and as noted some combination between parameters has no effect.

4.8 Summary

A computer program depended on FE method for simulating the behaviour of composite box girders is used. The bridges are modelled as 3D structures using commercially available software. The parameters considered in the study include flange thickness, web thickness, span length, haunch ratio, concrete depth and web box depth. The aim of this study is to present a detailed description and explanation of the behaviour of composite box girder bridge at several types of models under varying conditions. Comparisons are made between stresses obtained for the composite box girder bridges according to many changes in the dimensions of the bridge. Finally, the parametric investigations are performed on the composite box girder model to evaluate the effects of several important parameters on the behaviour of the girder. The results from this study would enable bridge engineers to design composite box girder bridges more reliably and economically.

CHAPTER 5

PARTIAL INTERACTION INTERFACE CONNECTION

5.1 General

Due to advances in fabrication technology, the use of steel trapezoidal box girders for interchange structures has become popular. The rapid erection, long span capability, economics, and aesthetics of these girders make them more favorable than other structural systems. A typical box girder system consists of one or more U-shaped steel girders that act compositely with a cast-in-place concrete deck. The composite action between the steel girder and concrete deck is achieved through the use of shear studs welded to the top flanges of the girders.

In steel trapezoidal box girder bridge systems, the U-shaped steel girder is designed to act compositely with the concrete deck to form a closed box for live loading. During the construction stage, however, the behaviour is not well understood. The usual practice of assuming the system to be non-composite during construction requires substantial top flange bracing to form a quasi-closed box section. Composite construction has become more and more important in recent years. By means of an optimal use of materials resource-saving ecological floor systems can be erected. The characteristics of the connection between concrete slab and steel box girder and the number of connector elements decisively influence the load-bearing behaviour and the economic performance of a composite member. When using composite box girder in bridges the construction process often governs the size of the steel section. As a result, in many cases only little additional bending resistance from composite action is required for the final state. Therefore, only a small amount of shear force needs to be transferred through the shear interface.

For economic reasons the number of shear connectors is then often reduced to the structural minimum. This situation is called partial shear connection. With partial shear connection the shear interface governs failure of the composite beam. If slip in the interface exceeds the connector's deformation capacity the interface and thus the bridge fails. This occurs before the predicted ultimate load (according to the rigid-ideal plastic design method in Eurocode 4) is reached if the degree of partial shear connection is too low. Usually, composite box girder in bridges are designed by means of a rigid-ideal plastic design method.

The established design methods for reinforced concrete and for structural steel give no help with the basic problem of connecting steel to the concrete. The force applied to this connection is mainly, but not entirely, longitudinal shear. As with bolted and welded joints, the connection is a region of severe and complex stress that defies accurate analysis, and so methods of connection have been developed empirically and verified by tests. Other types of connectors with higher strength have been developed, primarily for use in bridges. These are bars with hoops, tees with hoops, horseshoes and channels.

5.2 Partial Interaction Theory

In studying the simple composite beam with full interaction it was assumed that slip was everywhere zero. However, the results of push tests show that, even at the smallest loads, slip is not zero. It is therefore necessary to know how the behaviour of a beam is modified by the presence of slip. This is best illustrated by an analysis

based on elastic theory. It leads to a differential equation that has to be solved afresh for each type of loading, and is therefore too complex for use in design offices. Even so, partial-interaction theory is useful, for it provides a starting point for the development of simpler methods for predicting the behaviour of beams at working load, and finds application in the calculation of interface shear forces due to shrinkage and differential thermal expansion.

Elastic analysis is relevant to situations in which the loads on connectors do not exceed about half their ultimate strength. In a composite beam, the steel section is thinner than the concrete section, and the steel has a much higher coefficient of thermal conductivity. Thus the steel responds more rapidly than the concrete to changes of temperature. In practice, it may be advantageous to use fewer connectors than the number required for full interaction, though even this may lead to an increased deflection and to a lower strength. Using fewer connectors may simplify details around the connectors, reduce the cost and provide just the required strength, since full interaction design might give excessive strength.

The maximum slip, occurring in composite beams, increases with the span of the beam; therefore, for long span beams, and particularly bridge beams which are subjected to repeat loading, it is necessary to consider the ductility and fatigue resistance of the shear connectors. For this reason, partial interaction design is generally confined to beams with spans less than approximately twenty meters, and not subjected to repeated loading. The use of partial interaction design in determining the number of shear connectors in a composite box girder bridge is now uncommon. From tests carried out on full-scale composite beam it has been found that discrete flexible connectors give rise to non-linear connection behaviour.

Partial interaction state enables the designer to reduce the number of connectors used to transmit shear between slab and beam. Consequently, the degree of connection may be designed that the size of the steel beam found as a result of construction loading will be just adequate for the composite stage loading. The ultimate load which the beam can carry in its final service condition is then dependent not on the yield strength of the steel but on the capacity of the shear connection. This has implications when considering the stiffness of the composite beam, as the reduced connection also has a reduced stiffness. In addition, as the shear connection is the critical design parameter, the strength, deformation and cumulative slip deformation along the beam become important.

5.3 Slip Calculations

Slip can be defined as the longitudinal differential displacement at the interface between concrete and steel. As the shear connectors used in this study are headed studs, which can be classified as flexible connectors, interface slips, which represent the slip between concrete and steel, cannot be completely prevented. The interaction between the steel and the concrete is therefore, incomplete producing a differential strain at the interfaces. The shear flow at the interface is related to the number and spacing of shear connectors provided between the two materials, and the properties of the shear connectors such as the shear stiffness (K). (K) Can be defined as the slop of the load-slip curve for the connectors. In the other words, (K) is the load per connector required to produce unit slip and this is assumed constant for the elastic range.

Shear connections in composite beams are obviously essential. The nature of composite action includes large shear forces at the interface between the steel and concrete. Traditionally, these shear forces have are carried by means of a shear stud welded to the steel, which is then embedded into the concrete deck. When a cast-in-place deck is used, embedding of the shear studs is simple. Shear studs are shop-welded and the deck is poured around them. However, if the deck is prefabricated, pockets are left in the precast slabs that correspond to the location of the shear studs on the steel. These pockets are then filled with a non-shrink grout, which hardens to achieve the composite action. The design of the shear studs, as well as the properties of the grout used, can have large effects on the response of the entire section.

According to Oehlers & Bradford [126] in Figure 5.1- a, before loading point B is in the concrete slab and point C is adjacent to point B in the flange of the steel beam. When the force P is applied point B moves L + Uc and point C moves L + Us. The difference in movement is called the slip, s. In the figure the slip is s = Uc - Us.

The strain in the lower edge of the concrete is denoted εc. The slip Uc in the concrete is:

$$U_c = \int_L \varepsilon_c dx \qquad 5.1$$

In the same way the slip of the upper part of the steel part is given by:

$$U_s = \int_L \varepsilon_s dx \qquad 5.2$$

The slip strain is the rate of change of slip along the beam and defined as:

$$\frac{d_s}{d_x} = \Delta\,\varepsilon = \varepsilon_c - \varepsilon_s \qquad 5.3$$

When slip is totally prevented, it is called full composite action. In practice, full composite action is very difficult to achieve and in most composite members, the type of interaction can be denoted partial composite action, which means that a certain slip is unavoidable.

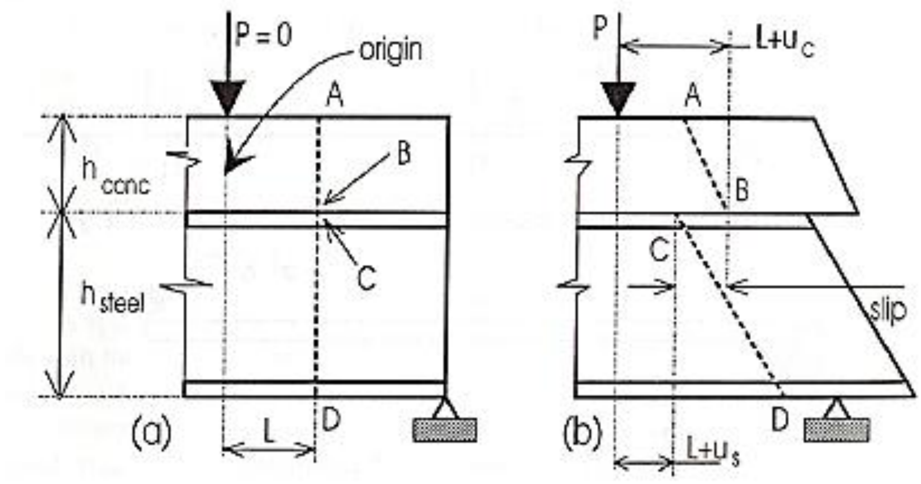

Figure 5.1 Slip calculation [126].

Yam and Chapman [127] presented a study for the inelastic behaviour of simply supported composite beams, based on Newmark's model. A nonlinear behaviour is assumed for the shear connectors, which is presented in the following exponential form:

$$Q = a.(1 - e^{-b.\gamma}) \quad \text{..5.4}$$

In which, (a) and (b) are constants of idealized load/slip function of a shear connector, (γ) is the slip at the interface, (Q) is the shear load on a shear connector.

Oehlers and Johnson [112] showed that push-specimens with a single row of studs have virtually no capacity to redistribute the force, and will thus fail at the strength of the weaker connection. Figure 5.2 show a schematic presentation of the behaviour of three brittle connectors. A, B and C. When a slip is applied, connector A will fail at a force PA. The whole force applied will then be taken by connector B and C, and they will immediately fail as their limit is reached. If the connectors are instead ductile, connector A will reach its maximum capacity and start to deform plastically. As connector A still keep the maximum force, the others will reach their maximum capacity one after one and continue to deform plastically. When all connectors have reached their maximum capacity, the structure will fail and the maximum load will thus be the mean strength of the connectors. Connectors are perfectly ductile, and so the truth is somewhere between ductile and brittle. The necessity of ductile connectors that can redistribute the force among themselves in a bridge.

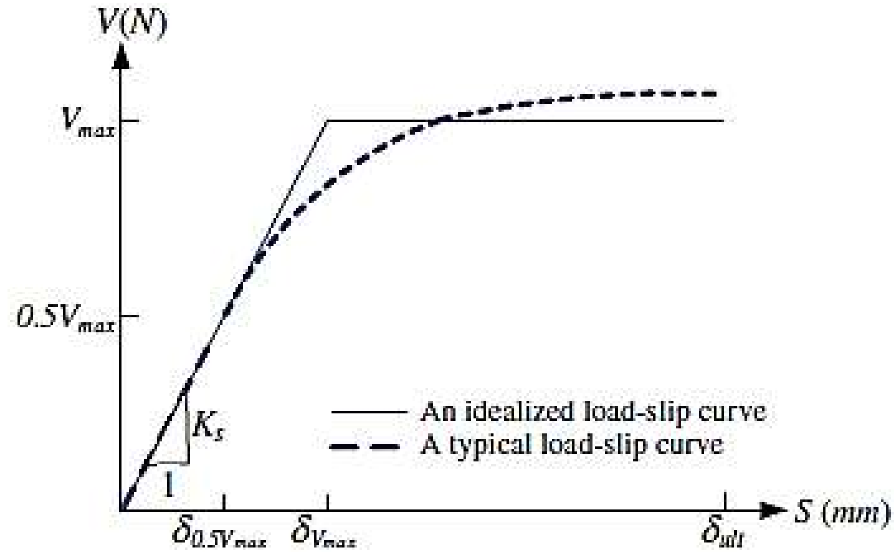

Figure 5.2 Load-Slip characteristics of shear connectors [112].

A typical load–slip curve determined from a push-out test as formulated in Eurocode [128], as shown in Figure 5.3, represents linear variation nearly up to half of the strength. When slip increases further, the stiffness are reduced gradually and finally makes the shear strength Vmax.

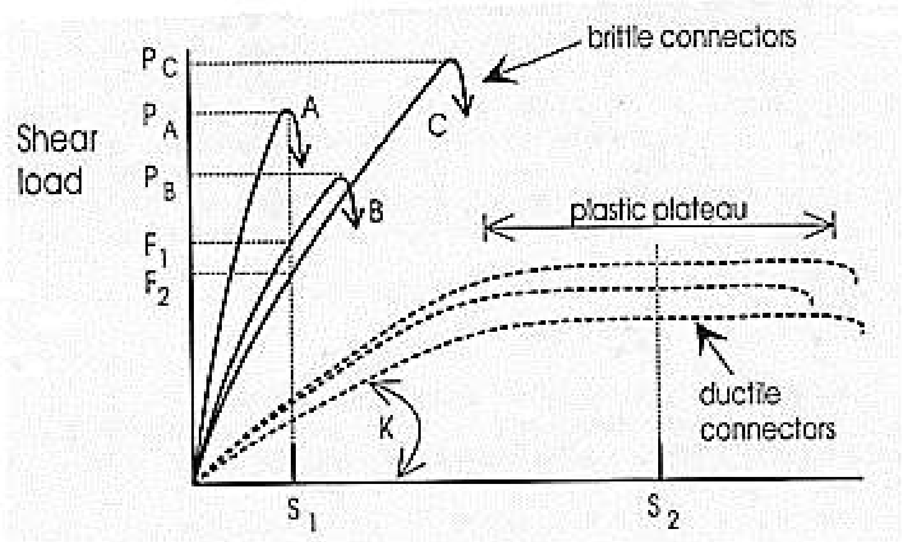

Figure 5.3 Idealized loads-slip curve of studs [128].

5.3 Shear Connectors

Headed shear connectors are the most common type of shear connector used in composite beams and bridges. Push-out tests are commonly used to determine the capacity of the shear connection and load slip behaviour of the shear connectors. The established design methods for reinforced concrete and for structural steel give no help with the basic problem of connecting steel to the concrete. The force applied to this connection is mainly, but not entirely, longitudinal shear.

As with bolted and welded joints, the connection is a region of severe and complex stress that defies accurate analysis, and so methods of connection have been developed empirically and verified by tests. The most widely used type of connector according to Johnson [129] is the headed stud as in Figure 5.4 .These range in diameter from 13 to 25 mm, and in length, from 65 to 150 mm, though longer studs are sometimes used. Studs should have an ultimate tensile strength of at least 450 N/mm2 and an elongation of at least 15%. The advantages of stud connectors are that the welding process is rapid; they provide little obstruction to reinforcement in the concrete slab, and they are equally strong and stiff in shear in all directions normal to the axis of the stud.

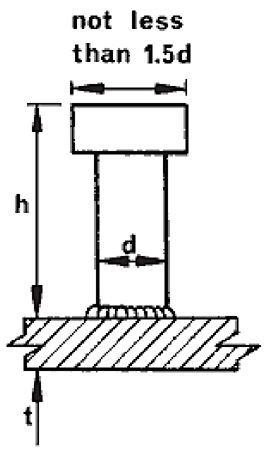

Figure 5.4 Headed shear connector [129].

There are two elements that influence the diameter of the studs. Ace is the welding process, which gets increasingly unmanageable and expensive at diameters exceeding 20 mm, and the other is the thickness, t in Figure 5.4 of the plate or flange to which the stud is welded. Johnson [129] showed that the maximum shear force which can be resisted by a 25 mm stud is relatively low, about 130 kN. Other types of connector with higher strength have been developed, primarily for use in bridges. These are bars with hoops, tees with hoops, horseshoes and channels. After this load we can see the failure mode of shear connector as shown in Figure 5.5 as mentioned by Yam [130].

Due to the complexity of the 3D stress–strain state and interaction between shear connector and concrete, there is little success in numerical modeling of the push-off test. Push-out tests are usually used to investigate the behaviour of shear connections. However, they are often costly and time consuming. FE modeling of shear connection can provide an efficient alternative to full-scale push-out tests.

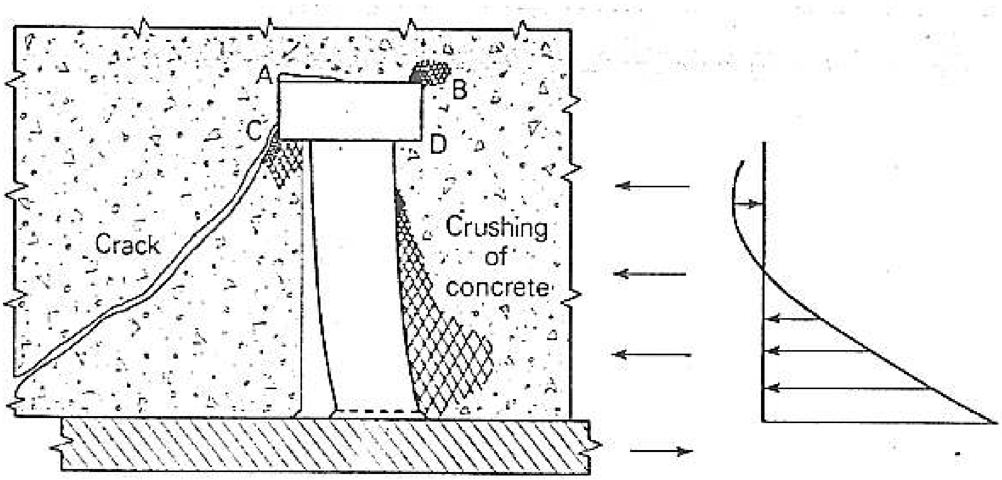

Figure 5.5 Failure Mode of Shear Connector [130].

5.4 Definitions of Stud Strength, Properties, and the Push-out Tests

There are a number of ways of providing a shear connection between the steelwork and the deck slab but by far the most common is the stud connector. This is essentially a headed dowel that is welded to the top flange using a special tool that supplies an electrical pulse sufficient to fuse the end of the dowel to the flange. Alternative forms of shear connectors include steel bars with hoops, and short lengths of channel. Although both of these provide a higher resistance per unit, they each have to b welded on manually and consequently are more expensive.

Shear connectors are welded to the steel girder and later cast inside the concrete slab. They are made of steel, are easily welded to the steel girder and establish a mechanical bond with the concrete slab. The aim of an optimal performance led investigators to study different typologies and geometries in order to define connectors with good behaviour and minimum cost. The minimum cost has to do with the total amount of material necessary to produce the connector, with the connectors production conditions, with welding conditions (at site or at an industrial unit) and with man ship time needed for the welding work [131]. The type of shear connectors studied within this work are presented in Figure 5.6, the study here presented analyses headed studs using 3D simulation with FE method.

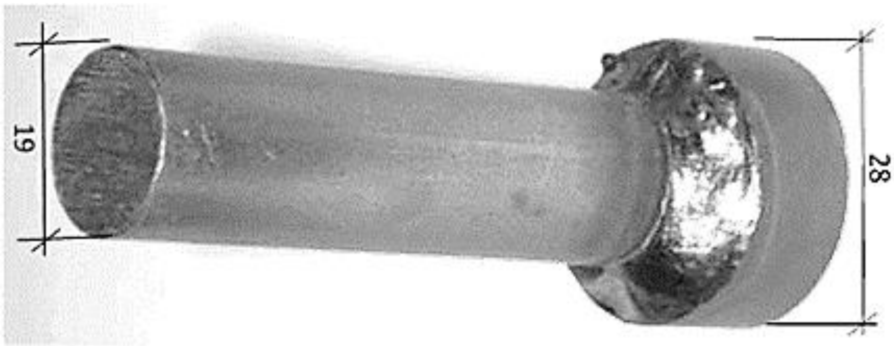

Figure 5.6 Geometry of a shear stud (unit: mm) [131].

The most important characteristics of a connector, is the capability to sustain shear forces and tension forces either separately or in a combined form. Yet standard tests are available to measure one of these forces only, which are push-out test. The property of a shear connector, most relevant to design, is the relationship between the transmitted shear force and the slip at the interface.

This load–slip curve should ideally be found from tests on composite structures, but in practice a simpler specimen is necessary. Most of the data on connectors have been obtained from various types of 'push-out' or 'push' test. The flanges of a short length of steel I-section are connected to two small concrete slabs. The slabs are bedded onto the lower platen of a compression-testing machine or frame, and load is applied to the upper end of the steel section.

In practice, designers normally specify shear connectors for which strengths have already been established, for it is an expensive matter to carry out sufficient tests to determine design strengths for a new type of connector. If reliable results are to be obtained, the test must be specified in detail, as the load–slip relationship is influenced by many variables, including number of connectors in the test specimen, and the thickness of concrete surrounding the connectors and mean longitudinal stress in the concrete slab surrounding the connectors, also the size, arrangement and strength of slab reinforcement in the vicinity of the connectors, also bond at the steel–concrete interface and strength of the concrete slab and degree of compaction of the concrete surrounding the base of each connector are very effect on the results.

5.5 Design Code Calculation Methods

5.5.1 Eurocode4

In the latest proposal of Eurocode 4[132].The shear resistance of a headed stud is determined by

$$Pu = \frac{0.29\alpha^2 \sqrt{f'c\, Ec}}{\gamma_v} \ldots\ldots\ldots\ldots\ldots\ldots\ldots\ldots 5.5$$

$$Pu = \frac{0.8\, Fu\, \pi\alpha^2/4}{\gamma_v} \ldots\ldots\ldots\ldots\ldots\ldots\ldots\ldots 5.6$$

Whichever is smaller.

5.5.2 AASHTO LRFD

In AISC (LRFD) [133]. The nominal shear resistance of one stud shear connector embedded in a concrete deck shall be taken as

$$Pu = \emptyset. 0.5. As\sqrt{f'}c. Ec \ \leq\ \emptyset\, AsFu \ldots\ldots\ldots\ldots 5.7$$

Where Ø = resistance factor for shear connectors (=0. 85)

5.5.3 BS 5950

In BS 5950 [134] the shear resistance of a headed stud is determined by

$$Pu = 0.25\ \alpha\, d^2\sqrt{0.8f'_c}\, E_c \ldots\ldots\ldots\ldots\ldots\ldots 5.8$$

$$Pu = 0.6\, f_u \frac{\pi d^2}{4} \ldots\ldots\ldots\ldots\ldots\ldots\ldots\ldots 5.9$$

Whichever is smaller.

Where the units are in mm; d=diameter of the studs; Fu = ultimate tensile strength of the stud; f c = compressive strength of concrete cylinders; Ec =elastic modulus of concrete; the partial safety factor γ_v should be taken as 1.25; α=0.2 (H/d+l) < l; and H=height of the studs.

5.6 Finite Element Models

5.6.1 General concepts

Numerical models have become a popular tool for simulating the behaviour of structures, but the majority of numerical models propose simplified forms of analysis. In this study, push-out test model was simulated using the FE program. In order to obtain accurate results from the FE analysis, all components in the shear connection must be properly modelled. Inelastic analyses was carried out with 3D FE model and non-linear geometry and materials analysis for shear connectors is done. The superstructure consisting of a concrete and steel girder and shear connector is considered as push out model. The main components influencing the behaviour of the shear connection in the composite beam are concrete slab, steel beam, and shear connectors are shown in Figure 5.7.

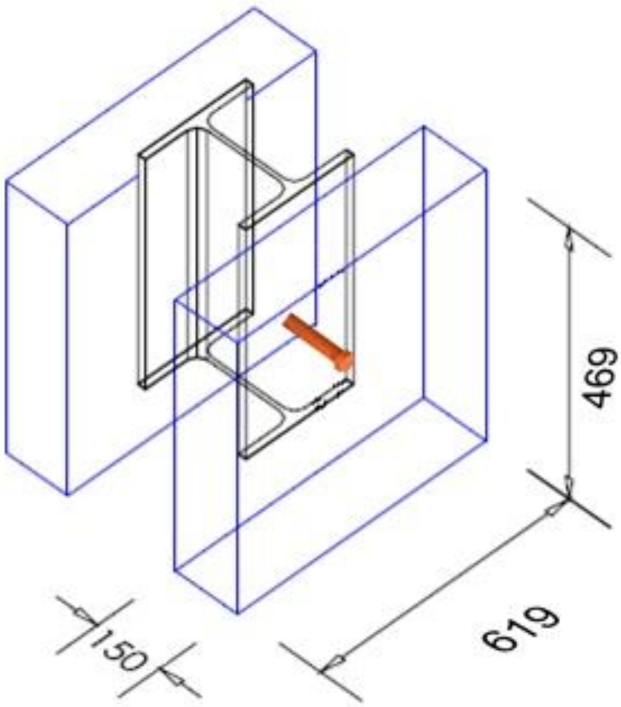

Figure 5.7 FE model (units in mm)

5.6.2 Finite element mesh

As noted in literature reviewed above illustrated FE modelling of shear connectors, most of researchers deal with push out test as experimental work, few researches contained numerical work on shear connectors, which are modelled the shear connector with single element. In this study, shear connectors modelled as 3D body with multiple elements.

Push out tests are usually made of a steel girder linked to a concrete slab by some sort of shear connection, which may allow for relative tangential displacements between the elements. A 3D model is proposed, in which the concrete slab and shear connectors are modelled with solid elements, while the steel girder is modelled with shell elements because the clear difference in thickness between these structural parts. Modelling and analysis of push out test combine many of the challenges encountered in the interaction and load sharing between structural steel and concrete components.

In this context, structural engineers involved in the analysis and design of steel–concrete composite structures have to face practical difficulties since procedures, which directly handle specific behavioural aspects of composite construction, are not generally included in available commercial software. Nevertheless, various models have been proposed in the literature to date in the effort to provide effective and robust tools for the analysis of steel–concrete composite buildings and bridges.

In this study two models are considered with two types of solid elements for concrete and shear connectors to form brick model and tetrahedral model while steel beam for both models are modelled using shell elements. For concrete and shear connectors, SOLID185 element is used to mesh these parts in brick model. It is defined by eight nodes having three degrees of freedom at each node. SOLID 285 is used for tetrahedral model. It is defined by eight nodes having six degrees of freedom at each node. The element has plasticity, stress stiffening, creep, large deflection, and large strain capabilities. It also has mixed formulation capability for simulating deformations of nearly incompressible lastoplastic materials, and fully incompressible hyperelastic materials.

Steel girder is meshed using SHELL181 which is a four-node element with six degrees of freedom at each node. It may be used for layered applications for modelling composite shells or sandwich construction. The accuracy in modelling composite shells is governed by the first-order shear-deformation theory (usually referred to as Mindlin-Reissner shell theory). The meshed numerical models of push out test are shown in Figure 5.8. The width of the head is more or 1.5 times the stud diameter and its thickness is 0.5 times the diameter as specified by Johnson [129] see Figure 5.4.

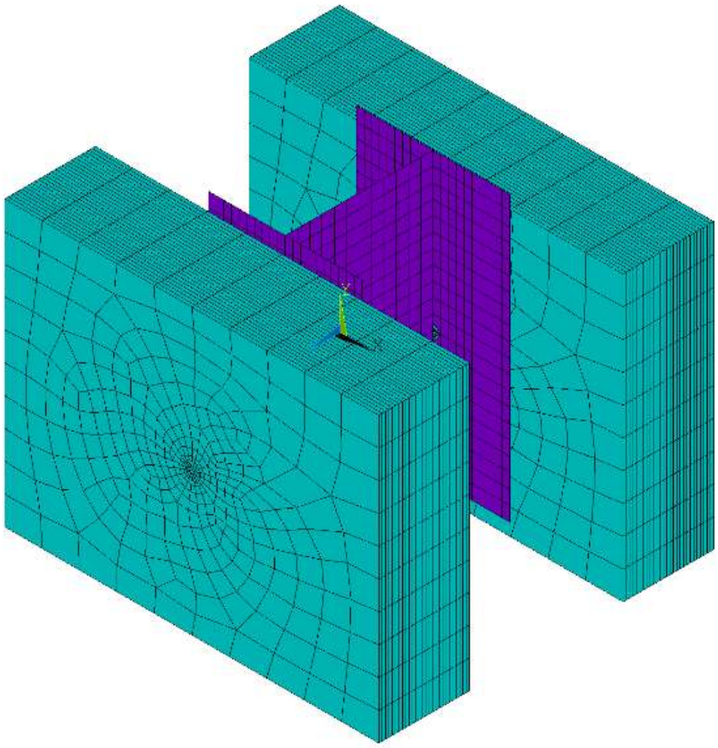

(a) Brick model

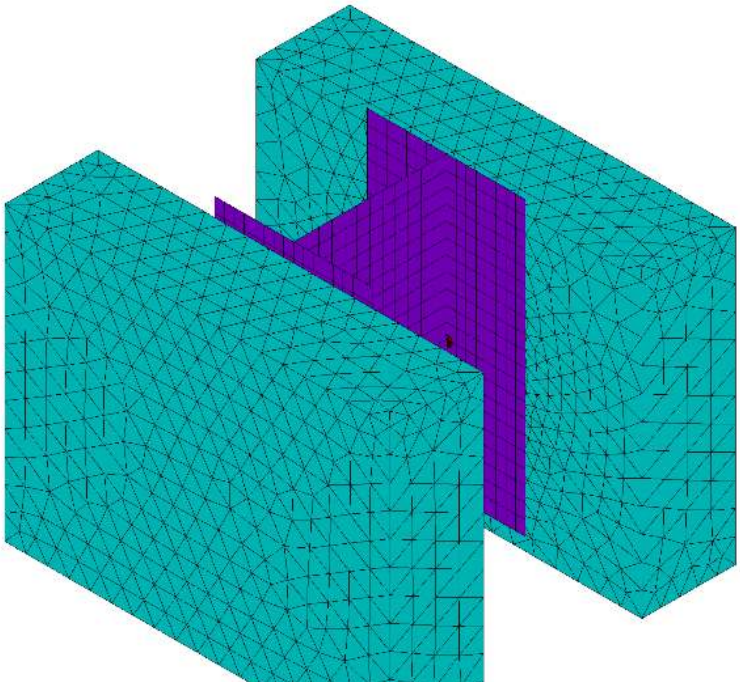

(b) Tetrahedral model

Figure 5.8 Meshed FE models of push out test

5.6.3 Description about the elements used in the model

The FE modeling and analysis performed in this study were done using a general purpose, multi-discipline FE program, ANSYS. ANSYS is a commercial FE program developed by Swanson Analysis Systems, Inc. The analyses presented in this study were performed using ANSYS version 14.0. ANSYS has an extensive library of truss, beam, shell and solid elements. The brief description of the elements used in the model is presented below: (SHELL181 and SOLID185 are submitted in section 3.6.2):

5.6.3.1 SOLID285 Eelement description

SOLID285 element is a lower-order 3-D, 4-node mixed u-P element. The element has a linear displacement and hydrostatic pressure behaviour. The element is suitable for modeling irregular meshes (such as those generated by various CAD/CAM systems) and general materials (including incompressible materials). The element is defined by four nodes having four degrees of freedom at each node: three translations in the nodal x, y, and z directions, and one hydrostatic pressure (HDSP) for all materials except nearly incompressible hyperelastic materials [124]. The following Figure 5.9 presents the geometry, node locations, and the element coordinates system for this factor.

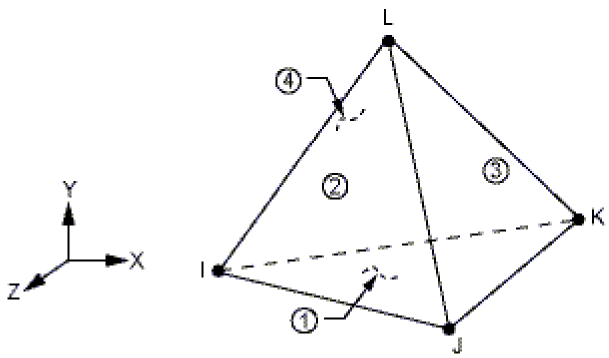

Figure 5.9 SOLID285 Geometry [124]

5.6.3.2 TARGE170 element description

TARGE170 is used to represent various 3-D "target" surfaces for the associated contact elements (CONTA173, CONTA174, CONTA175, CONTA176, and CONTA177). The contact elements themselves overlay the solid, shell, or line elements describing the boundary of a deformable body and are potentially in contact with the target surface, defined by TARGE170. This target surface is discretized by a set of target segment elements (TARGE170) and is paired with its associated contact surface via a shared real constant set [124]. The following Figure 5.10 presents the geometry, node locations, and the element coordinates system for this factor.

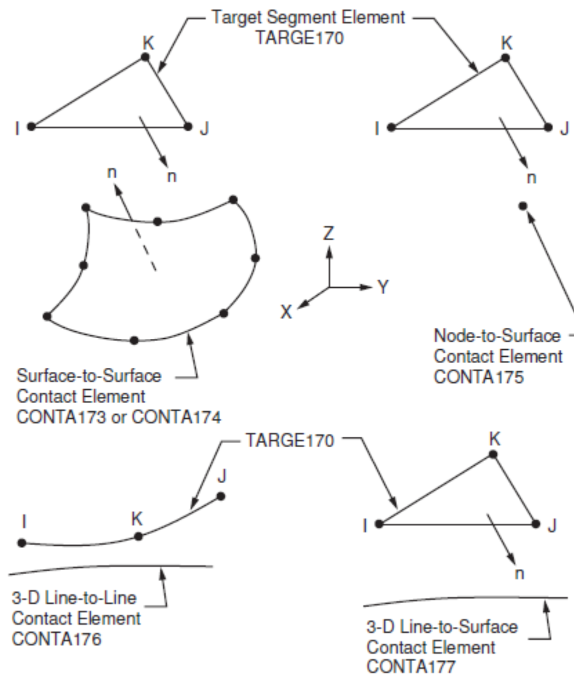

Figure 5.10 TARGE170 Geometry [124]

5.6.3.3 CONTA173 element description

CONTA173 is used to represent contact and sliding between 3-D "target" surfaces (TARGE170) and a deformable surface, defined by this element. The element is applicable to 3-D structural and coupled field contact analyses. This element is located on the surfaces of 3-D solid or shell elements without midside nodes (SOLID65, SOLID70, SOLID96, SOLID185, SOLID285, SOLSH190, SHELL28, SHELL41, SHELL131, SHELL157, SHELL181, and MATRIX50). It has the same geometric characteristics as the solid or shell element face with which it is connected. Contact occurs when the element surface penetrates one of the target segment elements (TARGE170) on a specified target surface. [124]. The following Figure 5.11 shows the geometry, node locations, and the element coordinate system for this element.

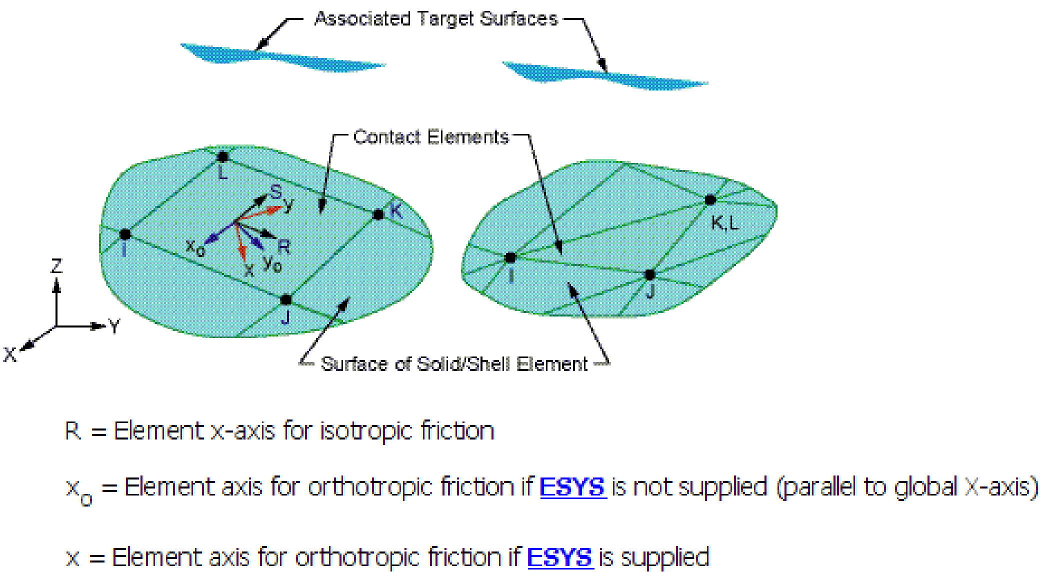

Figure 5.11 CONTA173 geometry [124]

5.6.4 Interaction between solid and shell elements

Since the sixties of the 20th century, the development of numerical methods has been the base for developing various advanced engineering simulation tools. Still nowadays, at the beginning of the 21st century, applications of numerical methods in simulation and prediction of industrial problems or technological processes become more and more important. The most popular numerical methods is the FE method with applications for simulation of biomechanics problems, elastoplasticity problems , thermal mechanic problems and contact problems , etc. Modeling these parts with standard solid elements would require a huge number of elements and leads to prohibitive computational costs.

However, for certain problems in structural analysis displacement Degrees Of Freedom (DOF) at the nodes of the element are more advantageous for analysis than displacement and rotational DOF's. For example, consider complex structures which consist of both thin and thick walls. For the sake of effectiveness, shell elements should be used for thin-walled parts and solid elements should be used for thick-walled parts. If both solid and shell elements have the same DOF's (e.g. only displacements at nodes), the analysis process exhibits one type of DOF only, no requirement on transition elements exhibiting displacement and rotational DOF.

Transverse shear locking can occur in shear deformable beam, plate and shell elements. In principle, it is also present in solid elements if these are applied to the analysis of thin-walled structures. However, with solid elements, it is simply called "shear locking", because there is no distinct "transverse" direction in a solid element. On the contrary, the solid-shell elements take the shell behaviour in thickness direction hence the transverse direction is distinct. Shear locking in the solid elements is one of the most severe locking effects because it does not only slows down the convergence but also can essentially preclude an analysis with a reasonable amount of numerical effort in practical applications.

5.6.4.1 Modelling a shell-solid a

The 3-D shell-solid assembly provides a transition from a shell element region to a solid element region. This approach is useful when local modeling requires a full 3D model with a relatively fine mesh, but other parts of the structure can be represented by shell elements. Alignment is required between the solid element mesh and the shell element mesh. The contact surface or edge must be built on the shell element side. The target surface must be built on the solid elements side. To define a shell-solid assembly using the internal MPC approach, several sets must be considered by changing the key options on the contact elements and the target elements.

5.6.4.2 Surface-to-surface contact elements

Contact problems fall into two general classes: rigid-to-flexible and flexible-to-flexible. In rigid-to-flexible contact problems, one or more of the contacting surfaces are treated as rigid (i.e., it has a much higher stiffness relative to the deformable body it contacts). In general, any time a soft material comes in contact with a hard material, the problem may be assumed to be rigid-to-flexible. Many metal forming problems fall into this category. The other class, flexible-to-flexible, is the more common type. In this case, both (or all) contacting bodies are deformable.

ANSYS supports both rigid-to-flexible and flexible-to-flexible surface-to-surface contact elements .These contact elements use a "target surface" and a "contact surface" to form a contact pair.

The target surface is modelled with TARGE170 for 3-D, the contact surface is modelled with elements CONTA173. To create a contact pair, assign the same real constant number to both the target and contact elements. These surface-to-surface elements are well-suited for applications such as interference fit assembly contact or entry contact, forging, and deep-drawing problems. Shear connectors made from solid285 elements and they connected to the pocket holes in concrete deck which meshed by solid285 also, by using contact pair type surface to surface with target170 elements to the hardest part in this case the steel shear connectors and the contact173 for the softer material in this case the concrete holes.

5.6.5 Interaction and restriction conditions

At first, a series of surface-to-surface contact elements allowed one to model rigid-to-flexible surface interaction. The augmented Lagrange method with penalty is the basis for the elements, but with a significant difference. The penalty stiffness, selected by default, is a function of many factors (including the size of adjoining elements and the properties of underlying materials). It is not necessary to provide an absolute value of stiffness, but one may override default values via a scaling non-dimensional factor. This option is necessary in bending-dominated situations. A recent update of the algorithm modifies the penalty stiffness based upon the stresses in underlying elements.

In a wide range of structural applications, bonded contact element methods are sufficient to calculate stresses between parts in assemblies in which multiple components are bolted, welded, glued or otherwise joined together. In cases such as gears, cams, levers and other assemblies with moving parts, however, the contact area between components changes during the load history. Post-processing is the most important step of any analysis, and contact problems are no exception. Always review contour plots of contact status, pressure and penetration to verify that the mesh adequately captures the contact behaviour and that results are correct. Contact penetration is in units of length, so deformation can be compared in the same direction as contact. If the penetration is a small fraction of the deformation, you can safely assume that any variation in penetration would not affect results significantly.

TARGE170 is used to represent various 3-D "target" surfaces for the associated contact elements. The contact elements themselves overlay the solid, shell, or line elements describing the boundary of a deformable body and are potentially in contact with the target surface, defined by TARGE170. This target surface is discretized by a set of target segment elements TARGE170 and is paired with its associated contact surface via a shared real constant set. CONTA173 is used to represent contact and sliding between 3-D "target" surfaces (TARGE170) and a deformable surface, defined by this element. The element is applicable to 3-D structural and coupled field contact analyses. This element is located on the surfaces of 3-D solid or shell elements without midside nodes. It has the same geometric characteristics as the solid or shell element face with which it is connected. Contact occurs when the element surface penetrates one of the target segment elements (TARGE170) on a specified target surface.[124]

The contact elements are easier to visualize and interpret. The output is in the form of stress rather than force. The numerical algorithms employed are efficient- even in large problems. contact elements provide a rich set of initial adjustment and interaction models. Besides the standard unilateral contact, it offers the options of bonded, no-separation, and rough sliding contact. The bonded contact option is especially useful.

5.7 Analysis Approach

The requirements of contact analysis are wide ranging, and there is no single approach that meets the needs of all. The concept of offering a toolkit is even more applicable here than in elements or materials. The augmented Lagrangian approach, while able to solve complex contact problems, produces a certain level of penetration (generally so small that the effect is negligible); however, options are available to make it satisfactory. Lagrange multipliers are available to enforce penetration constraints (while completely avoiding the penalty stiffness input).

The Lagrange multiplier approach of enforcing compatibility has two disadvantages, an increase in the number of degrees of freedom (DOFs) and the inability to use iterative solvers. The Lagrange multiplier approach is also susceptible to convergence difficulties (constant chattering, necessitating artificial smooth2ing or viscous-based solution heuristics).

5.7.1 Loading and boundary conditions

A static concentrated load is applied at the center of the steel web. Single point load applied for the model on the top of the steel girder for the FE model of push out test. The rigid base was assumed to be immovable so all DOF of the e nodes of the rigid base were restricted. The loading rate can be varied by using different amplitude functions. The slip was measured as the relative displacement between the nodes on the steel flange and on the concrete slab near by the stud. The load per stud was measured as the total reaction acting on the loading surface.

5.7.2 Material Model

5.7.2.1 Concrete

To model the behaviour of the reinforced concrete slab in the push out test, concrete is treated as an elastic-plastic material. The concrete behaves as a linear-elastic material is obtained. Following the BS 8110 [125], average values of yield strain, Young's modulus of concrete, and the yield stress can be calculated from the following relations:

$$\varepsilon_{yc} = 0.00024\sqrt{f_{cu}} \quad \text{.......} 5.10$$

$$f_{yc} = 0.8\, f_{cu} \quad \text{.......} 5.11$$

$$E_c = f_{yc}/\varepsilon_{yc} \quad \text{.......} 5.12$$

5.7.2.2 Steel girder

The steel beam is modeled with yield stress of 275 N/mm2 in this study. It is believed that the effect of the steel beam is insignificant in a push-off test. Its function is to allow for the transmission of applied load to the connectors and hence the characteristic load-slip characteristic in the steel concrete interface can be studied.

5.7.2.3 Shear connector

The shear connector material is of capital importance in modelling the shear interaction between steel and concrete since the area round the connector has been a region of austere and complex tensions. The shear forces are removed across the steel concrete interface by the mechanical action of shear connectors. The stud material model behaved as a linear elastic material with Young's modulus E_s up to the yield stress of stud, f_{ys}. Later on this point, it becomes fully plastic. In the present work, the following values are utilized for the study material: *Es*: 200,000 N/mm2 and f_{ys} 470.8 N/mm2.

5.8 Results and Validation of Proposed Model

The FE model acquired in this study is affirmed against push test experiments held in previous experimental studies undertaken by other sources. Two specimens, Brick and

Tetrahedral models, using the proposed FE model were analysed in this survey. The Brick model meshed with hexahedral solid elements for steel shear connector and concrete slab while the tetrahedral model meshed with tetrahedral solid elements. Steel shaft in both models meshed with shell elements.

5.8.1 Lam and el-lobody experimental results

The push-out test specimen SP1 in the experimental study of Lam and El-Lobody [92] was investigated in this study. The geometry of the specimen is shown in Figure 5.7. A push-out test specimen is formed from a short length of steel beam that is connected to two small concrete slabs by means of shear connectors as shown in Figure 5.7. The slabs are then conventionally bedded down on mortar directly onto the reaction floor with load being applied to the upper end of the steel member. Slip between the steel member and the two slabs is measured at specified load or displacement increments.

This push-out test specimen is similar to the standard push-out test specimen according to CP 117 (BSI 1995) [134], but just one connector is connected to each flange since it is taken for granted that the payload is transferred equally from the steel shaft to each shear stud. The push-off test specimen shown in Figure 5.7 consists of a 254 X 254 UC 73 (W10X49), two concrete slabs with 50 N/mm2 strength attached to the flanges of the steel beam with dimensions of 619 mm long, 469 mm wide, and 150 mm thickness for each slab, and one stud connector attached to each flange with a stem diameter of 19 mm and 100 mm in elevation. The length from the stud to the concrete limits, in the direction of loading, is taken as 200 mm with a concrete recess over the steel beam equal to 50 mm similar to CP117 [134]. In the perpendicular direction, it is taken as 300 mm with the total length of concrete slab being 619 mm similar to EC4 (BSI 1994)[132].

Out tests were extended out to ascertain the load-slip behaviour of the headed stud connector in concrete slabs. The mechanical behaviour of the materials used was determined from material tests. The concrete slab was cast horizontally according to the demands of the EC4 [132]. The steel beam used in the test was a 254 X 254 UC 73. The flanges of the steel beam were not greased so natural adhesion is not prevented. The average load slip curve derived from the test of Lam and El-Lobody [92] and the curve obtained from the proposed FE analysis are compared well in Figure 5.12. It can be seen that the Brick model curve had a good agreement with the Lam and El-

Lobody's [92] result, while the tetrahedral model curve showed a little difference until the slip reaches the maximum displacement at the failure of the elements. As a result, when the slip reached the maximum displacement at the failure of the tetrahedral elements, the force vanished. Both the experimental and Brick model results showed a similar maximum slip at failure. While the FE model proposed by Lam and El-Lobody [92] themselves show a notice deference with the experimental results as shown in Figure 5.12. Additionally, when we study the curve of idealized slip-load curve in Figure 5.2 and comparing this curve with Brick model curve, it can be detected that the FE modelling of load–slip behaviour matches the experimental load slip behaviour reasonably well.

5.8.2 Fu and Lam experimental results

Fu and Lam [135] created a special test model to study a stud shear connector of 19 mm diameters and 50 N/mm^2 of concrete strength. They performed the direct shear test under monotonic loading. The present study used the same push-out arrangement as Fu and Lam's tests. Figure 5.12 shows a good agreement between the capacities of headed stud shear connectors obtained from the tests of Fu and Lam [135] and the proposed FE analyses.

The capacity and the maximum slip at the failure of the shear connections obtained from the tests and FE analyses are presented in Table 5.1 for comparison. Good agreement has been achieved between experimental and numerical results for all of the push-out tests.

Table 5.1 Comparison of shear connection capacity and slip obtained from other results.

	Experiment Load (kN)		**FE Load P_{FEA} (kN)**		**FE max slip at fail (mm)**	
	Load (kN) P_{test} (kN)	**max slip at fail (mm)**	**Brick**	**Tetra**	**Brick**	**Tetra**
Present study	-----	-----	127.9	132.1	8.5	1.68
Lam and Ellobody	130.4	11.9	116.6	-----	7.7	-----
Fu and Lam	128.9	8.0	-----	-----	-----	-----
Maria Valente	133.6	11.2	-----	-----	-----	-----
Qian and Li	129.4	2.2	-----	-----	-----	

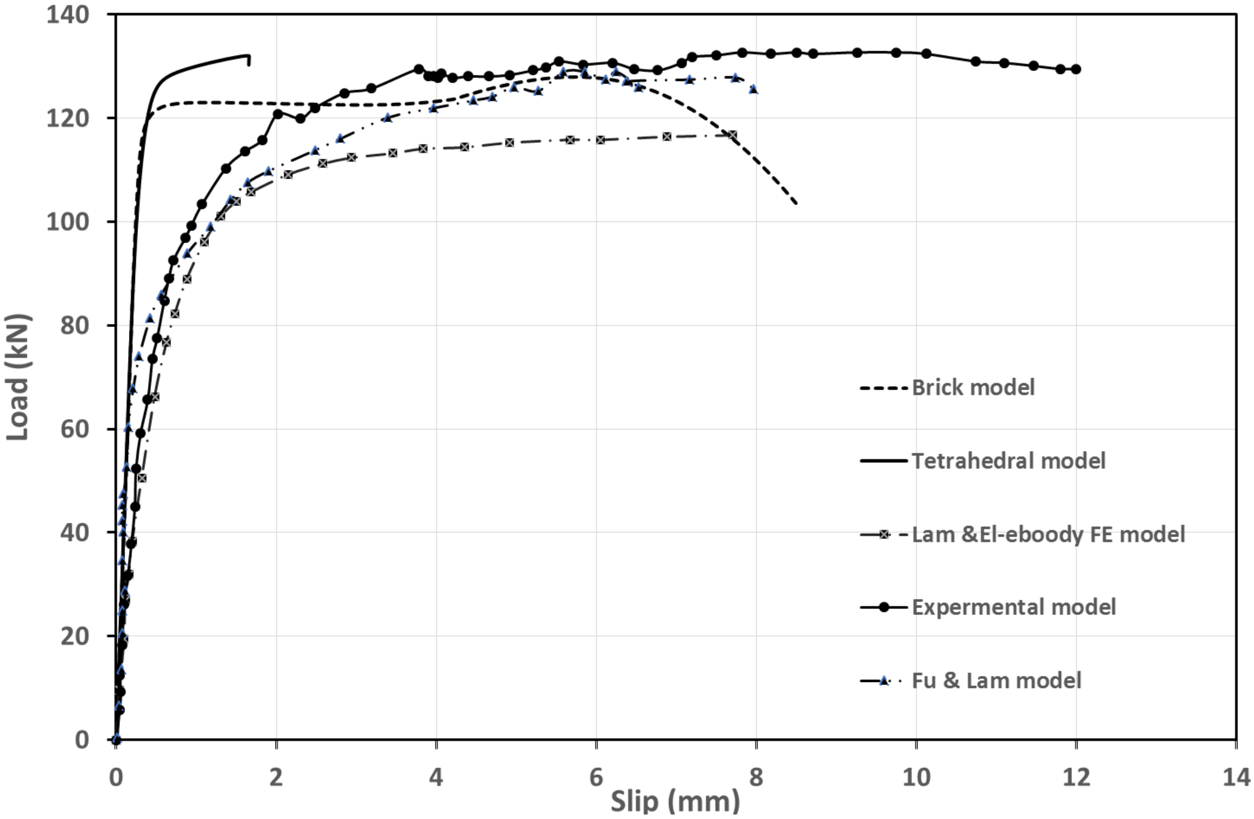

Figure 5.12 Comparison of the FE analysis result with Lam and El-Lobody's, Lam and Fu result.

Also, the shear capacity of stud shear connectors obtained from the FE study was compared in table 5.2 with the nominal design strength of shear connectors calculated by the design codes of Eurocode 4 [128] and AASHTO LRFD [122] and BS 5950[136].

Table 5.2 Comparison of shear connection capacity obtained from FE analysis and current codes of practice with 40 N/mm^2 concrete strength.

<table>
<tr><th>Model</th><th>P_{FEA} (kN)</th><th>P_{EC4} (kN)</th><th>$P_{AASHTO\text{-}LRFD}$ (kN)</th><th>P_{BS5950}</th><th>P_{FEA}/P_{EC4}</th><th>$P_{FEA}/P_{AASHTO\text{-}LRFD}$</th><th>$P_{FEA}/P_{BS5950}$</th></tr>
<tr><td>Brick</td><td>127.9</td><td rowspan="2">136.8</td><td rowspan="2">171.1</td><td rowspan="2">112.3</td><td>0.94</td><td>0.75</td><td>1.14</td></tr>
<tr><td>Tetrahedral</td><td>132.1</td><td>0.97</td><td>0.77</td><td>1.18</td></tr>
</table>

A maximum difference of 5% was observed between the experimental and numerical results for the stud of 30 mm diameter in Lee et al.'s tests. The mean value of P_{test}/P_{FEA} ratio is 0.99 with the corresponding coefficient of variation (CV) of 0.01. The maximum slip obtained from FE analysis compared well with the experiment results as shown in Table 1. As a result, the FE models successfully predicted the shear connection capacity as well as the load slip behaviour of the headed shear stud with common diameter.

Which they compared to the experimental results and the design standards - British BS5950 [136], Eurocode [132] and American AISC[133]. It was shown that EC4 [132] gave a good correlation with the experimental and numerical results, while BS5950 [136] and AISC [133] may overestimate the shear capacity of the headed studs.

5.8.4 Maria Valente Experimental Results

Valente [137] contemplated the portrayal of diverse sorts of shear joined devices to be utilized as a part of composite components of steel and concrete. Headed studs, Perfobond connectors and T connectors are investigated for static loadings and looked at. Failure modes, load limit, twisting limit, ductility and stiffness are the primary parameters in the investigation. With a specific end goal to acquire the characteristic curve for a alone shear connector, another shear test was created at the Institute of Structural Concrete.

In the Single Push-Out Test a single shear connector with 19 mm can be tested individually. Here, the structural stability does not result from the symmetrical construction but from the nearly identical straining lines of the acting forces. Since the resulting lateral force during shearing does not remain at a constant level, the experimental set-up should be capable of tracking such changes without losing its stable state of equilibrium. Figure 5.13 shows a good agreement between the capacities of headed stud shear connectors obtained from the tests of Valente [137] and the proposed FE examinations.

5.8.5 Qian and Li Experimental Results

Qian and Li [138] presented an experimental study on the influence of concrete material ductility on crucial performance of stud shear connection, including failure mode, slip capacity, and ultimate strength. A series of pushout specimens were tested for this evaluation. Figure 5.13 shows a good agreement between the capacities of headed stud shear connectors obtained from the tests of Qian and Li [138] and the proposed FE analyses.

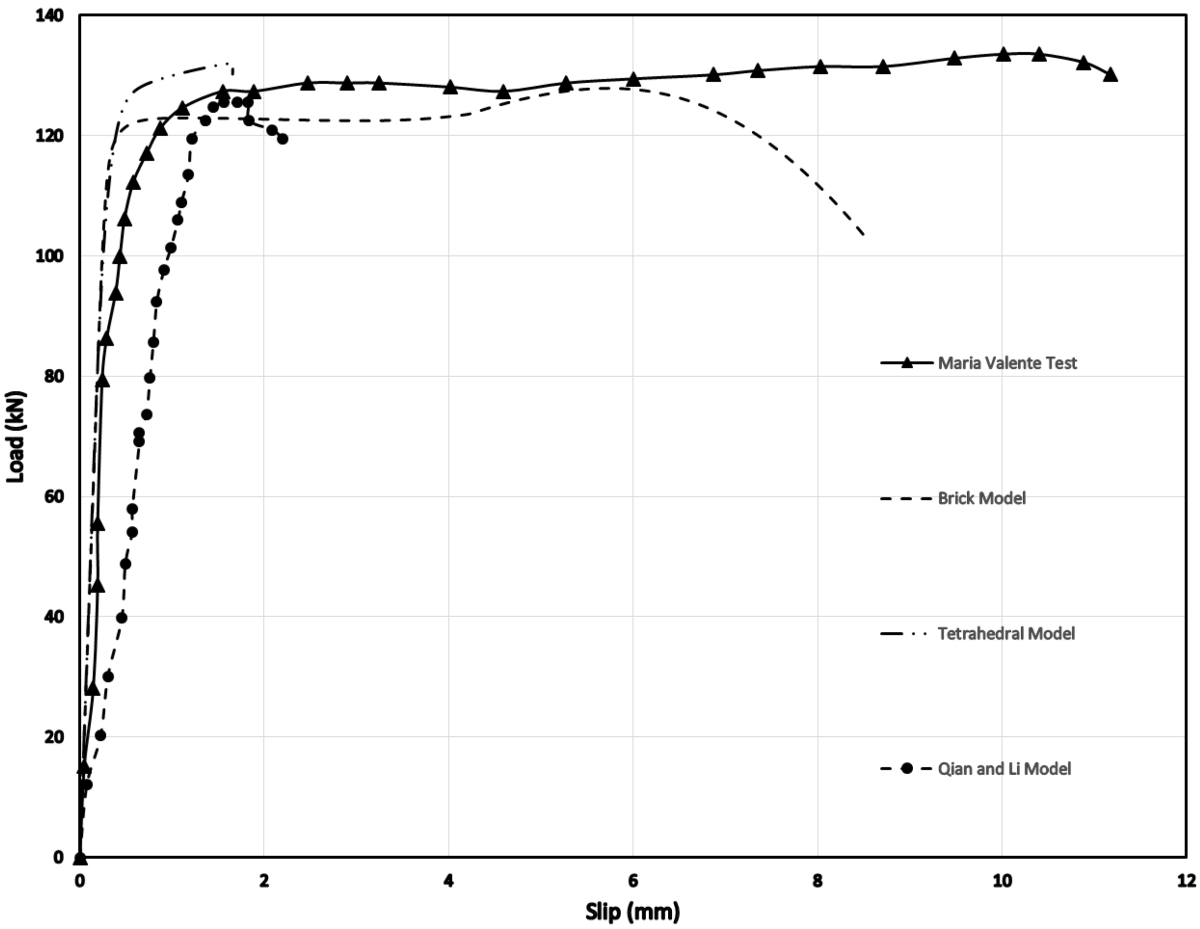

Figure 5.13 Comparison of the FE result with Valente, Qian and Li result

Mesh types considered are outlined in Figure 5.14 for the shear connectors with brick and tetrahedral elements. It can be seen from Figure 5.15 that the stresses flow in concrete is similar to the failure mode of the shear connector. As seen from Figure 5.16 below, numerical models show comparison of interface slips. It can be observed that the computed interface slip for Brick and Tetrahedral models give good agreements with test results., also von mises stresses for the shear connector are plotted in Figure 5.17. The von mises plastic strain with partial shear interaction at working load is shown in Figure 5.18. Contact status between shear connector and steel beam is shown in Figure 5.19, which show sliding between the shear connector and the concrete surrounded and the sticking between steel plate and concrete deck. Finally contact pressure and contact gap distance for the shear connector in brick and tetrahedral elements are shown in Figures 5.20 and 5.21 respectively.

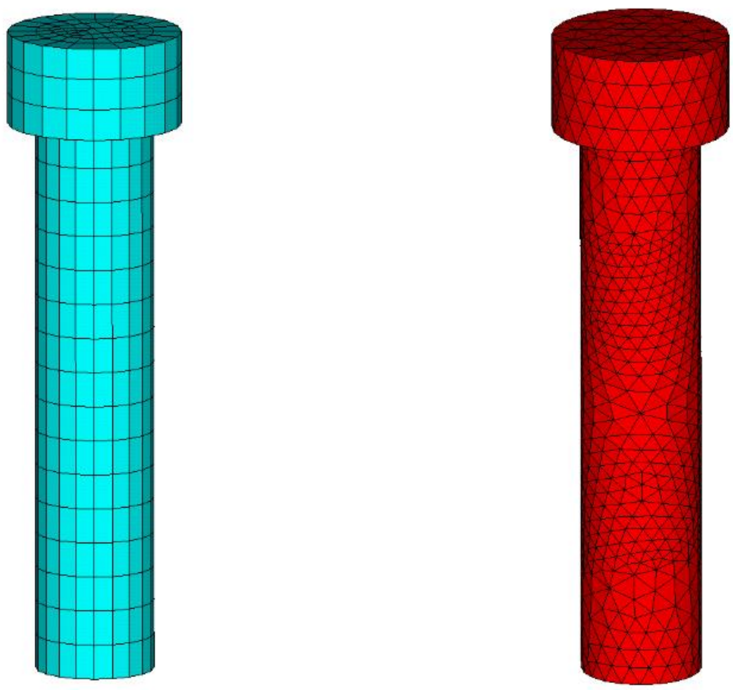

(a) Brick element (b) Tetrahedral elements

Figure 5.14 Stud Mesh Types

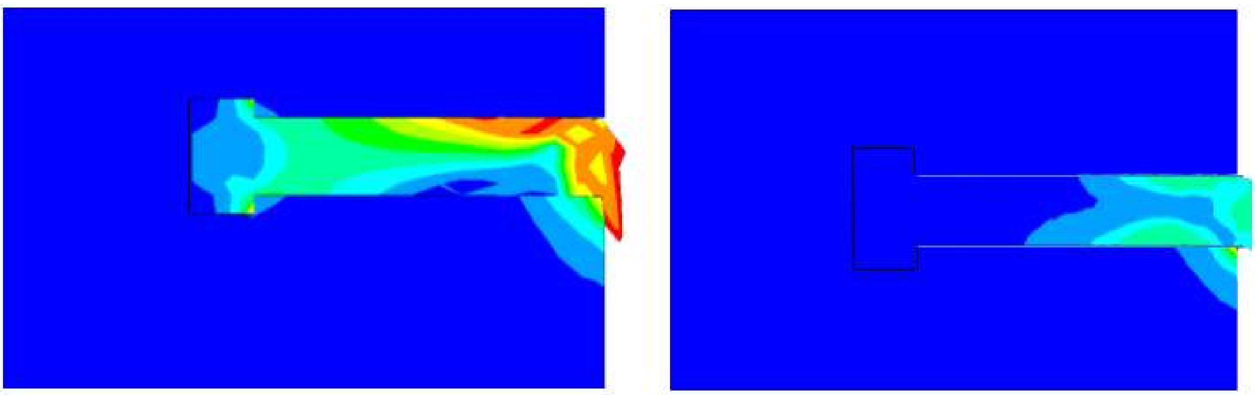

(a) Brick elements at load =127.9 kN (b) Tetrahedral elements at load =132.1 kN

Figure 5.15 Stresses Flow Section

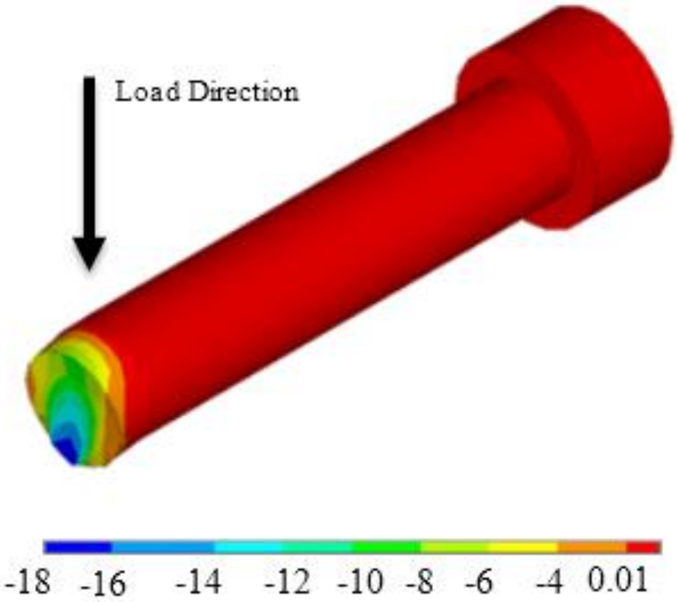

(a) Brick elements at load =127.9 kN

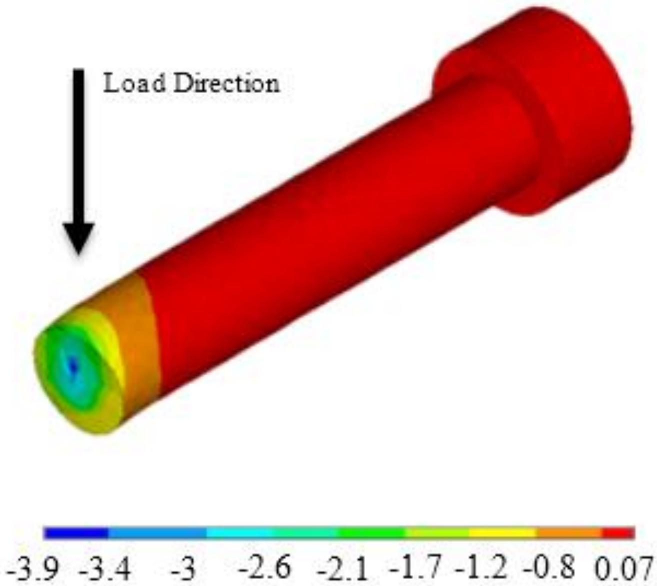

(b) Tetrahedral elements at load =132.1kN

Figure 5.16 Interface Slips

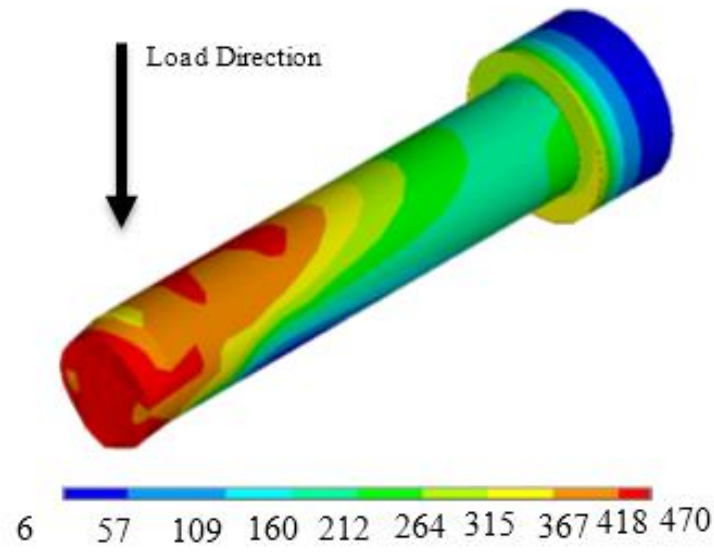

(a) Brick elements at load =127.9 kN

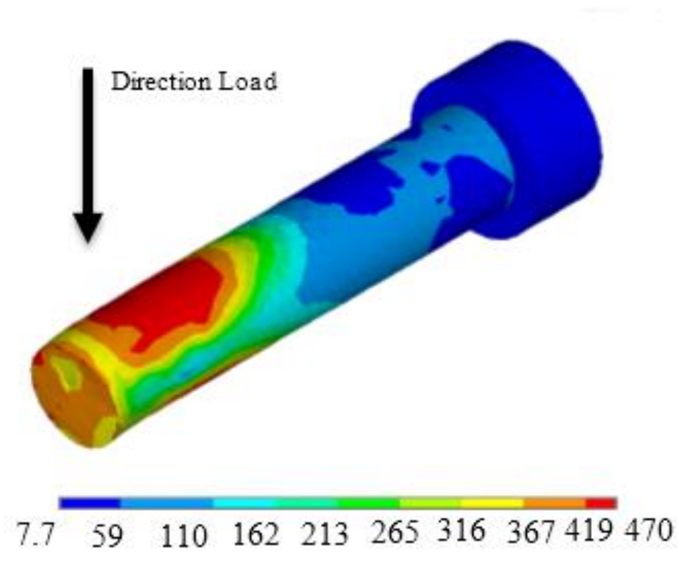

(b) Tetrahedral elements at load =132.1 kN

Figure 5.17 Von Mises Stress

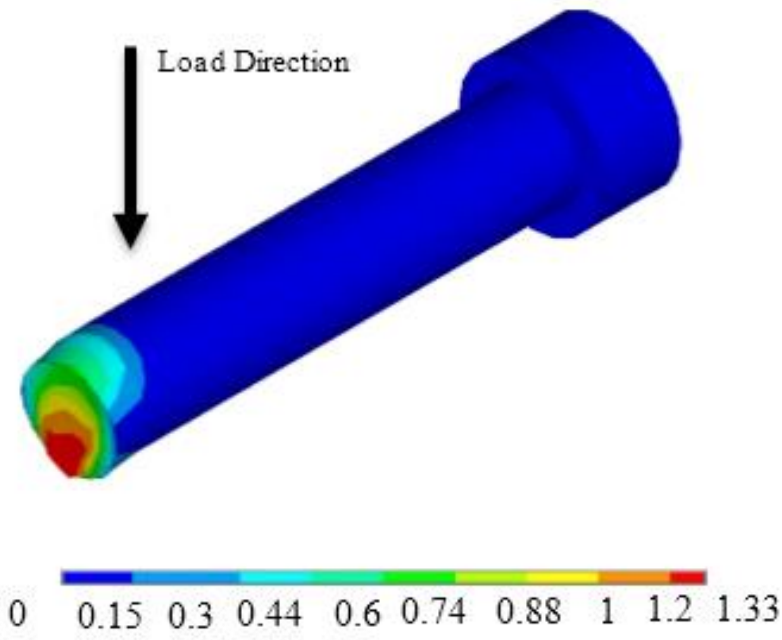

(a) Brick elements at load =127.9 kN

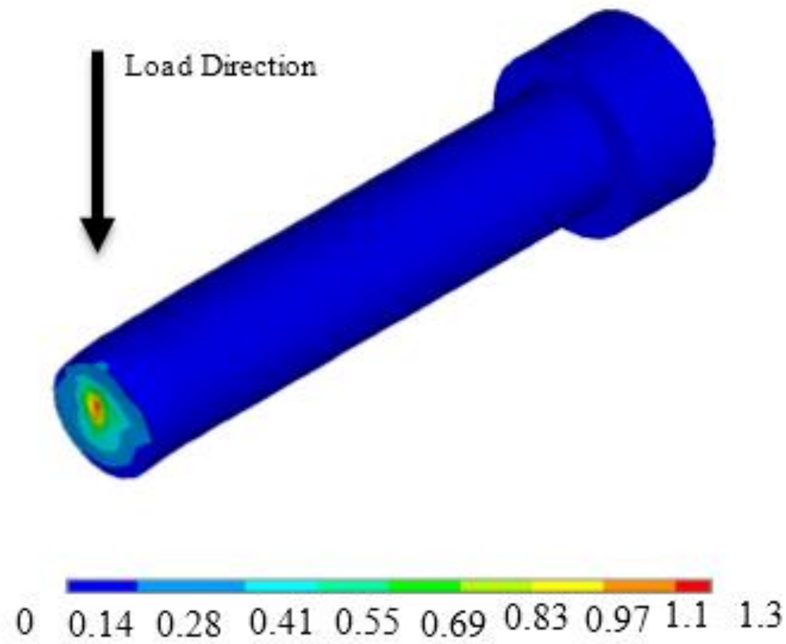

(b) Tetrahedral elements at load =132.1kN

Figure 5.18 Von Mises Plastic Strain

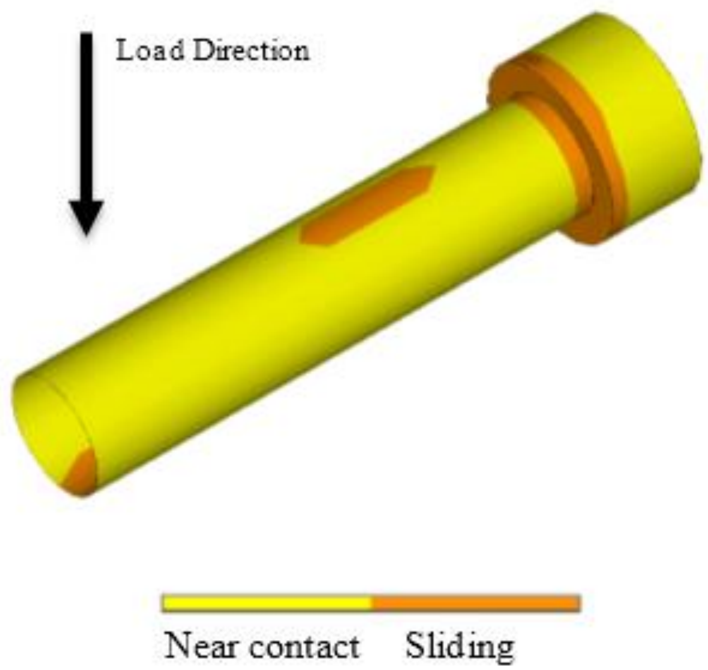

(a) Brick elements at load =127.9 kN

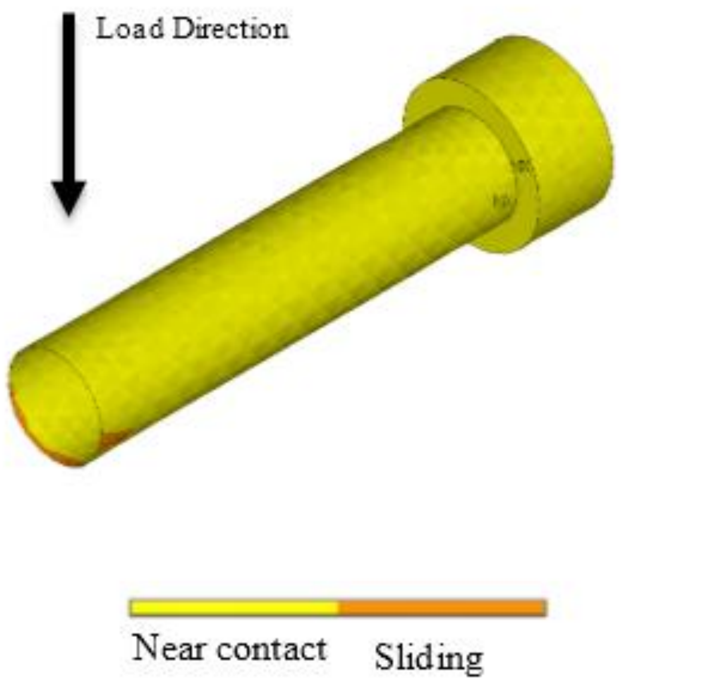

(b) Tetrahedral elements at load =132.1kN

Figure 5.19 Contact Status

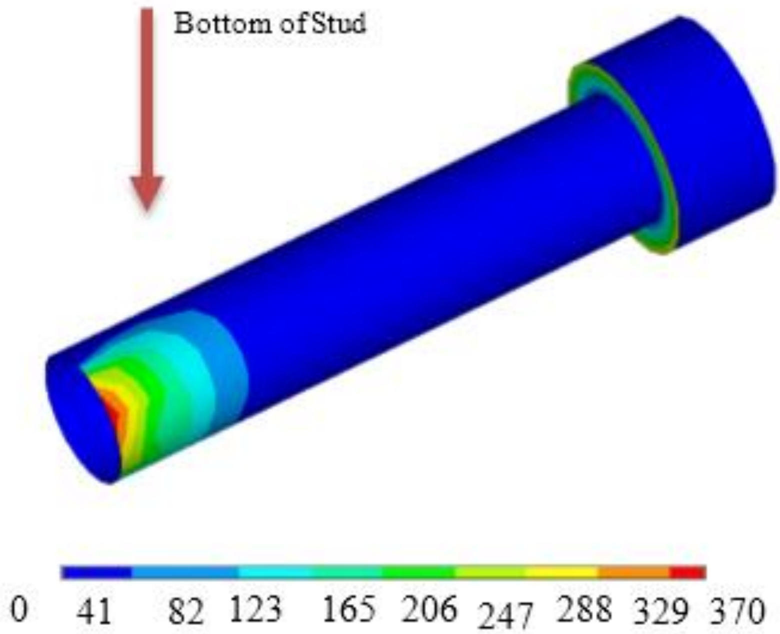

(a) Brick elements at load =127.9 kN

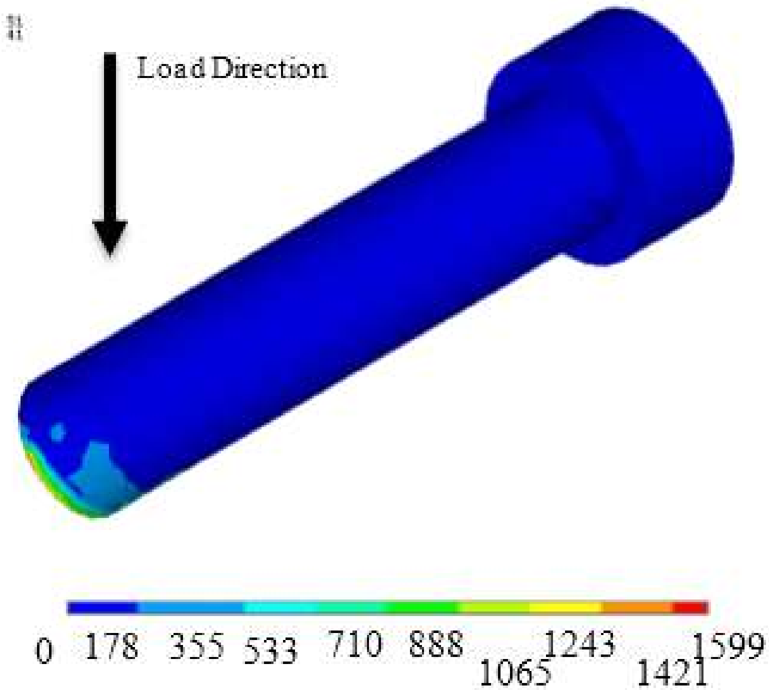

(b) Tetrahedral elements at load =132.1kN

Figure 5.20 Contact Pressure

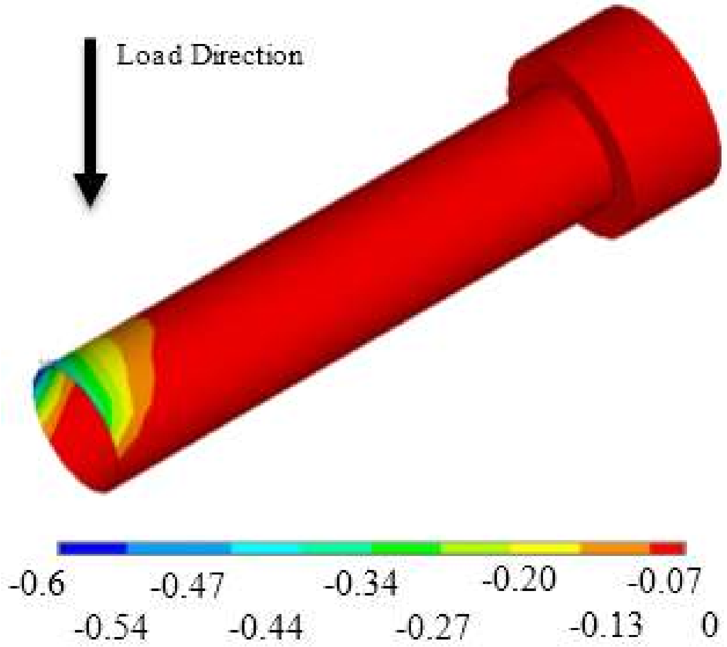

(a) Brick elements at load =127.9 kN

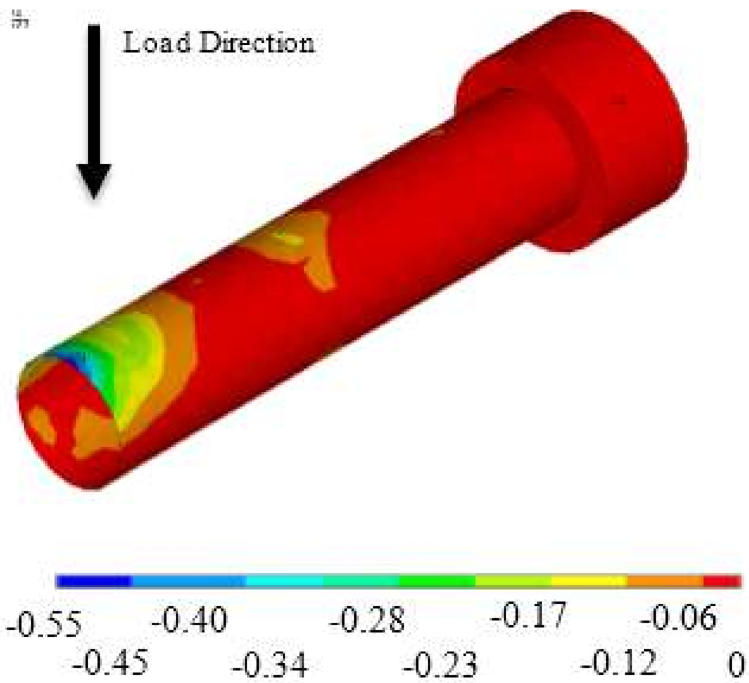

(b) Tetrahedral elements at load =132.1kN

Figure 5.21 Contact Gap distance

5.8.6 Roberts and kazemi experimental results

Roberts and Kazemi [139], performed tests on several rectangular concrete beams having steel plates attached mechanically to the tension face of beams by expanding bolts, which were either cast in during manufacture of the beams or drilled and fixed at a torque control process after curing. The parameters considered are the thickness of plates (2mm and 4mm) and the bolt length. Test results showed a significant improvement in the stiffness of the plated beams and, all beams exhibited a ductile failure followed by crushing of the concrete in the compression zone.

In this study, only model C1 is considered to validate the numerical model. All steel plates are (1750 mm.) in length and connector pitch is 140 mm. A typical composite beam is assumed with material properties as shown in Figure 5.22 and Table 5.3.

As noted in the literature reviewed most of researchers used single line elements to model shear connectors. In this study, shear connectors are modelled as a 3D body with multiple elements.

Table 5.3 Information on Robert's series.

(a): Details of test beams and concrete properties**.**

Beam No.	**Plate thickness (mm)**	**Bolt diameter (mm)**	**Elastic Modulus 10^3 (kPa)**
C1	2	8	36

(b): Average properties of steel plate and shear connector

Plate thickness (mm)	**Yield stress for Steel (MPa)**	**Elastic Modulus for Plate (Mpa)**	**Elastic Modulus for Stud (Mpa)**	**Yield stress for Stud (MPa)**
2	282	208	200	487

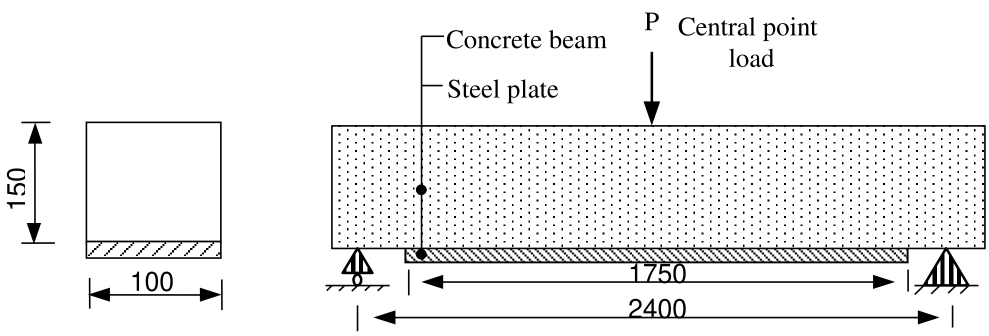

Figure 5.22 Details of Roberts’s beams series

Composite beams are usually made of a steel plate or girder linked to a concrete slab by some sort of shear connection, which may allow relative tangential displacements between the elements. A 3D model is proposed, in which the concrete slab and shear connectors are modelled with solid elements, while the steel plate is modelled with shell elements. Modelling and analysis of shear connector combines many challenges encountered in the interaction and load sharing between structural steel and concrete components.

For concrete and shear connectors, solid element is used to mesh these parts. It is defined by eight nodes having three degrees of freedom at each node. The element has plasticity, stress stiffening, creep, large deflection, and large strain capabilities. It also has the mixed formulation capability for simulating deformations of nearly incompressible elastoplastic materials, and fully incompressible hyperplastic materials. Steel plate is meshed using the shell element, which is a four-node element with six degrees of freedom at each node. It may be used for layered applications for modelling composite shells or sandwich construction. The accuracy in modelling composite shells is governed by the first-order shear-deformation theory (usually referred to as Mindlin-Reissner shell theory). All dimensions are handled in accordance with Roberts's experimental works as shown in Figure 5.22.

The program automatically constrains both translational and rotational degrees of freedom for a shell-solid assembly. However, properties of target elements may also be used to explicitly define the type of constraint. Contact properties have been specified between concrete and steel elements using surface-to-surface and embodiment techniques. Steel plate is assumed the target body, and concrete deck is considered contact surface.

5.8.6.1 Loading and boundary conditions

A static concentrated load is applied at the Midspan of the beam. Single point load applied to the model and line loading was simulated by applying coupled constrains on the top of the concrete slab for the FE model of composite beam. Simply supported boundary conditions are applied to the beam.

5.8.6.2 Material Model

Concrete has elastic properties with modulus elasticity 36 kPa for C1 model. In this study the steel plate is modelled with yield stress of 208 Mpa for 2 mm thick. In the present study, the following values are used for the stud material: E_s =200,000 MPa and f_{ys} =487 MPa.

5.8.6.3 Results and Validation of Proposed Models

It can be seen from Figure 5.23 that the stresses flow in concrete is similar to the failure mode of the shear connector shown in Figure 5.5. The maximum deflection of a composite beam with partial shear interaction at working load is shown in Figure 5.24. Interlayer slip is calculated to be 0.377 mm as a maximum value as shown in Figure 5.25, also sliding between the shear connector and the concrete surrounded clearly appears in Figure 5.26. Figure 5.27 shows the sticking between steel plate and concrete deck. In Figure 5.28 a comparison between FE model and Roberts model for deflection values is shown.

The distribution of slip along the beam is plotted in Figure 5.29. The maximum slip values are plotted against the applied load and shown in Figure 5.30. It can be seen that the initial value of slip is noticed at 12% of the service load, with the increased value at the increased loading. When the slip is increased, loss of interaction results, allowing for extra deflection, whereas, the slip is a function of the degree of connection and the properties of materials.

Table 5.4 Comparison between FE model and Roberts's solution.

Type of test	Beam No.	Loads (kN)	Experimental values (mm)	Numerical values (mm)	Experimental/ Numerical
Deflection values	C1	33	5.53	5.68	0.97

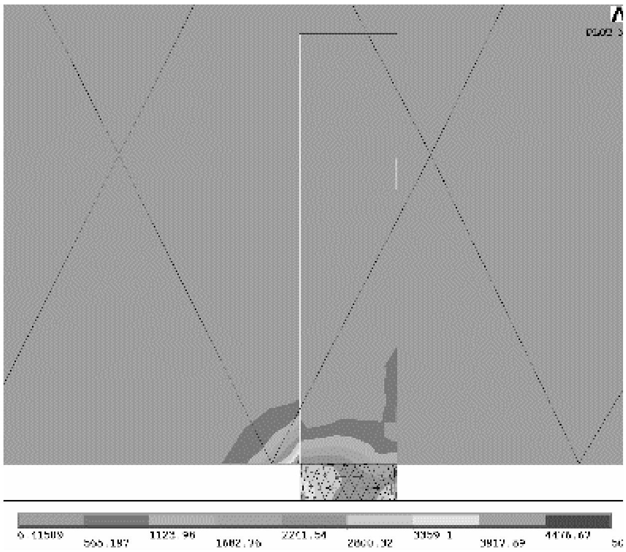

Figure 5.23 Stresses flow in both connector and concrete

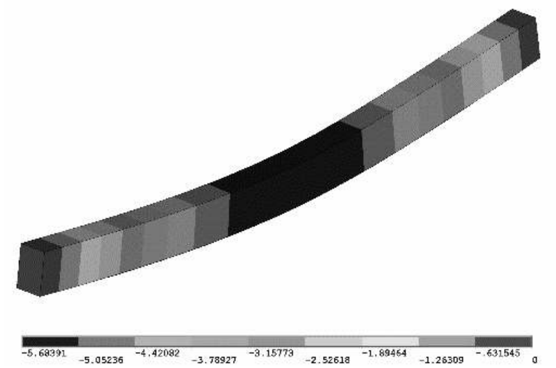

Figure 5.24 Deflections in FE model

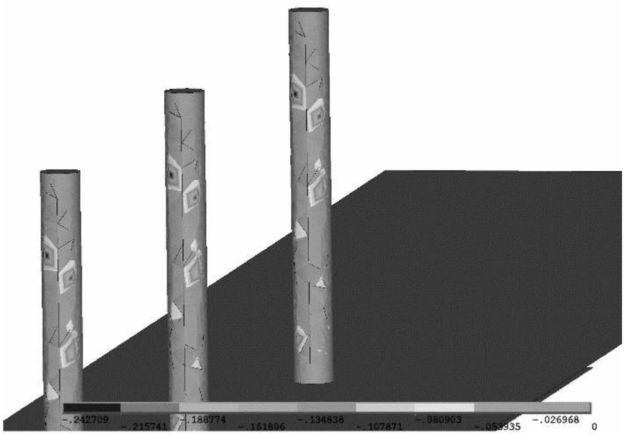

Figure 5.25 Interlayer Slip in FE model

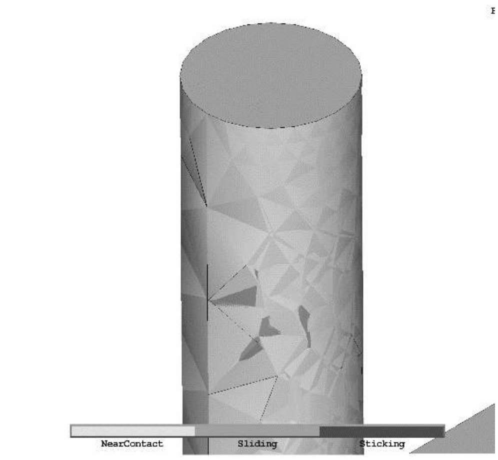

Figure 5.26 Sliding between the components

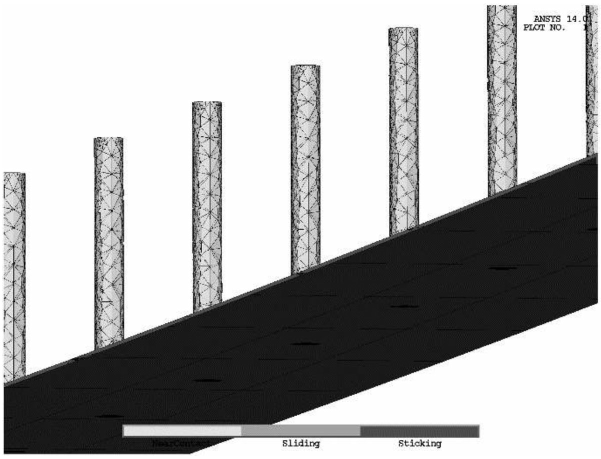

Figure 5.27 Sticking between steel plate and concrete

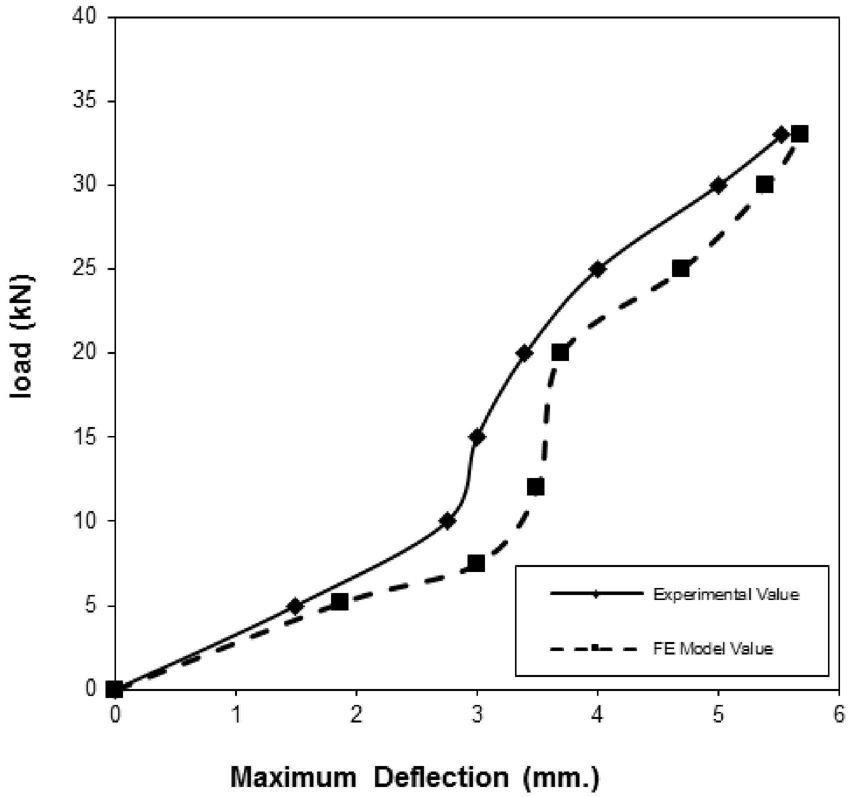

Figure 5.28 Comparison of deflections between experimental and FE values

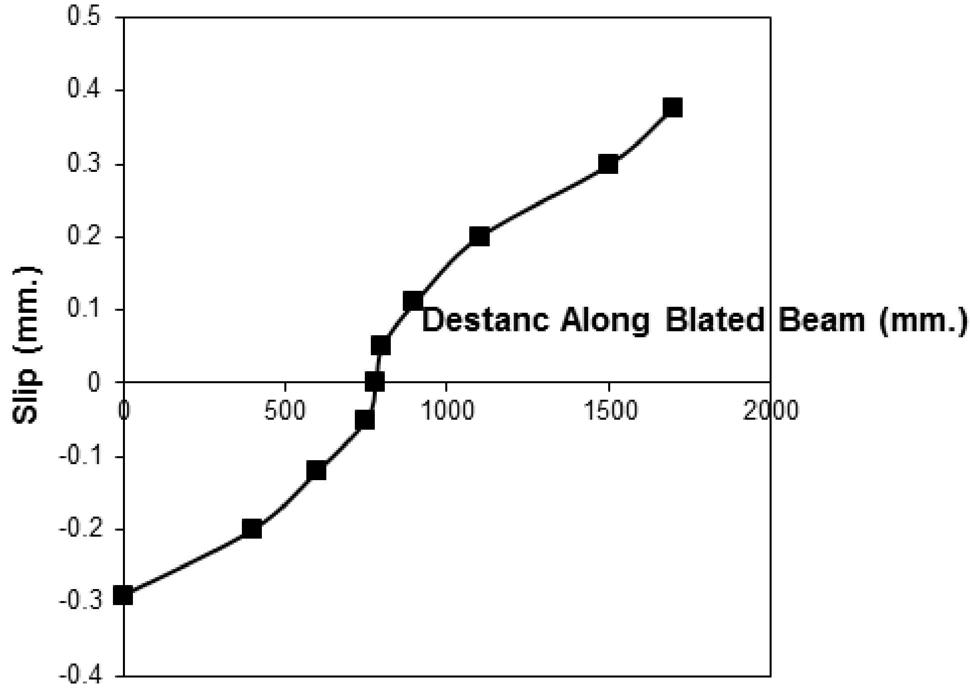

Figure 5.29 Slip along the platted part of beam

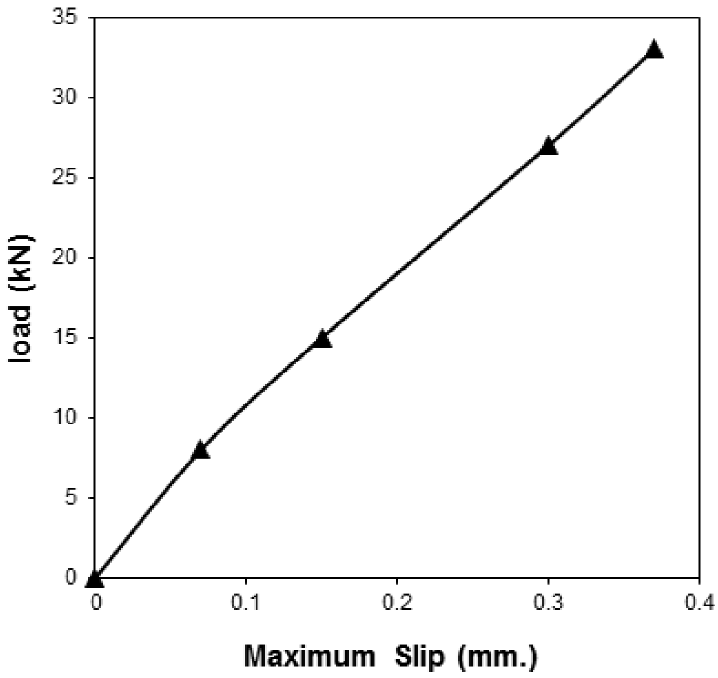

Figure 5.30 Load –Slip curve for FE model

CHAPTER 6

CONCLUSION

6.1 Conclusion

The behaviour of the composite box girder system is more complex than that of the box girder and girder system. In this study, the main objective is to investigate the static structural behaviour of composite box girder bridges. It was noted that the plurality of the experimental and analytical research pains have focused on non-composite box girder and I-girder systems, and very little on composite box girders. Therefore, for the composite box girder systems, more study to locate design criteria is needed.

The proposed model showed good congruence of the service load results obtained between the numerical and experimental results. The numerical simulations also allowed the behaviour of the composite system to be analysed from a global standpoint based on the force vs. displacement curves, and from a located standpoint, by determining the stresses in the regions of the connectors and in other components of the model. The stresses in both steel and concrete in the regions of the connections tended to be distributed along the length of the connectors, with greater concentrations at the steel-concrete interface.

The interaction between the two parts of the bridge in the analysis modelled using rigid links to give full interaction between components. Nevertheless, the bridge shear connectors actually deform and influence the structural behaviour of the bridge. The connection may be significantly more vital if an interaction is modelled as partial connected between bridge parts. In this study, the effects of rigid link simulated by a link element between shell or solid modelling for concrete deck.

The FE analysis using ANSYS can model the structural behaviour of a composite box girder bridge very well, the results would be in good agreement with those of experimental test, as long as that's a FE model takes account of all the contributing factors. The thickness of precast concrete 15 cm is big to simulate using shell elements, so noteworthy difference can be observed (about 8 %) by using 3D solid elements to model such thickness.

The coupling is realized with ANSYS CP command, the value of the degree of freedom is coincident for all the points to be coupled, was important thing effects on result of simulation of constrained point load, big difference appeared (15 %) when the loading simulated by Coupling to force a set of nodes to have the same DOF value.

Preparatory results show that number of shear studs can be fundamentally diminished to encourage appropriation of new arrangement in modelling CBGBs with full interaction. Notwithstanding, a further practicality study to explore the useful and monetary parts of such a curative is prescribed, and it may represent incomplete composition in such modelling.

A computer program depended on FE method for simulating the behaviour of composite box girders is used. The bridges are modelled as 3D structures using commercially available software. The parameters considered in the study include flange thickness, web thickness, span length, haunch ratio, concrete depth and web box depth. The aim of this study is to present a detailed description and explanation of the behaviour of composite box girder bridge at several types of models under varying conditions. Comparisons are made between stresses obtained for the composite box girder bridges according to many changes in the dimensions of the bridge. Finally, the parametric investigations are performed on the composite box girder model to evaluate the effects of several important parameters on the behaviour of the girder. The results from this study would enable bridge engineers to design composite box girder bridges more reliably and economically.

Analysis of the results of the restricted parametric study uncovered a few rules for the determination of the longitudinal profile of ceaseless steel box girder spans. Composite box girder bridges deflections are reduced by increasing the depth of concrete, depth of the web and thickness of the web but Raised by an increase in bottom steel box thickness. Thicker bottom flange plates would result in a raise of deflections. This study was extended to altering several parameters at a time and the combination between them from the base model model. However, by considering several figures together, researcher can work towards the choice of an efficient and economical profile of continuous composite box girders.

The FEA can simulate the structural behaviour of a steel-concrete composite box girder bridge very well; complicated 3D FE modelling was investigated. Nevertheless, it is included in this study in order to provide some assistance in the selection of a superstructure profile. 67.5 % of percentage difference appears from changing the depth of the steel box web, which is the largest percentage effects in the model. In addition, 0.42 % of percentage difference appears from changing the thickness of steel box bottom flange, which represents the lowest percentage effects in the model.

The nonlinearity of shear connection has a significant consequence on the conduct of continuing composite Box girder bridges. The result of nonlinearity becomes more important as the hardness of the shear connection decreases. It is important to look at the real load–slip relationship of the shear connection in order to obtain better predictions of deflections and stresses in composite box girder spans.

This work has looked into the influence of material parameter uncertainties on the nonlinear response of composite box girder bridge by means of the FE method. 3D FE models, with all elements of the composite member being modelled by means of solid and shell elements, have been carried out in the commercial software ANSYS and analysed using an explicit expression. All materials have been presumed to be nonlinear and contact properties have been specified between concrete and steel components using surface-to-surface and embodiment techniques.

This work included the interaction between solid and shell elements and also suggested an acceptable process to link each to other. A survey was carried out on the effects of partial shear connection partial interaction. It was proven that, by decreasing the level of shear connection, the composite system becomes more elastic, with reduced strength and stiffness, mainly for beams with less than 100%, for which the partial interaction effects are important and must be brought into account.

Nevertheless, the full-scale push-out test remains also the time-consuming and costly option; therefore the mathematical analysis is adopted, once the verification of the numerical model with experimental results was demonstrated. A 3D FE model was developed using the FE software to demonstrate the behaviour of headed shear stud connectors. The results of this model were compared with the experimental results.

It has shown to be efficient in terms of calculating the load–slip response for stud subjected to concentrated loads, longitudinal slip at the steel–concrete interface, shear force carried by the studs. It is also able to investigate the structure with partial shear connection. Comparisons against experimental results and against alternative numerical analyses indicate that the present model can be applied to perform extensive parametric studies.

The nonlinearity of shear connector has a huge impact on the conduct of structures. The impact of nonlinearity gets to be more critical as the firmness of the shear association diminishes. It is essential to consider the real load–slip relationship of the shear interaction in order to get better forecasts of deflections and stresses in composite structures.

This study has examined the impact of material parameter vulnerability on the nonlinear reaction of composite structure by method of FE method. 3D FE models, with all segments of the composite part being simulated by means of solid and shell elements, have been executed in the software programming and treated utilizing an explicit expresions. All materials have been thought to be nonlinear with the exception of concrete and contact properties have been indicated between concrete and steel components utilizing surface-to-surface method.

The solid stud is the most realistic simulation approach used for modelling a shear connector. It captures thermal, bending, and tensile loads. Therefore, it is the best approach to use. The solid stud simulation requires that the contact elements be used for the horizontal joint and the contact surface between the flange and the headed stud. The solid stud is the closest simulation of the actual shear connector, but there are some characteristics that are ignored to simplify the simulations. One of these characteristics is the effect of friction interaction, at the contact surfaces, which is not considered in the analysis.

6.2 Recommendations of future works

This work showed the use of a family of interface elements, which, combined with, appropriate FEs, allows the numerical simulation of composite box girder with horizontal slip, or partial interaction. The studies Shell-Solid element assembly can be extended to simulate larger composite structures.

For further study, more complex 3D FE modelling should be examined, for instance, demonstrating of bearing pad included, propping and diaphragm and more points of interest of pier establishment. Likewise, the use of a proposed model for different sorts of composite box girder bridges ought to be investigated, for example, curved bridges, high-quality concrete, pre-stressed concrete bridges.

REFERENCES

[1] Chen, W.-F. and Duan, L. (1999). Bridge Engineering Handbook. Boca Raton London New York Washington, D. C.

[2] Abbu, M. (200). Behaviour and Strength of Multi-layer Beam with Unequal Lengths Components. M.Sc. University of Al-Mustansirya.

[3] Kwak, H.-G. and Hwang, J. W. (2010). FE model to simulate bond-slip behavior in composite concrete beam bridges. *Computers & Structures*, **88**, 973-984.

[4] Kim, J. and Williamson, E. (2014). Finite-Element Modeling of Twin Steel Box-Girder Bridges for Redundancy Evaluation. *Journal of Bridge Engineering*, **0**, 04014106.

[5] Chartree Lertsima, Chaisomphob, T. and Yamaguchi, E. (2004). Three-dimensional finite element modeling of a long-span cable-stayed bridge for local stress analysis. *Structural Engineering and Mechanics*, **18**, 113-124.

[6] Eiki Yamaguchi, N.H., Takemi Kubo and Yoshinobu Kubo (2005). Numerical study of stress states near construction joint in two-plate-girder bridge with cast-in-place PC slab. *Structural Engineering and Mechanics* **19**, 173-184.

[7] Kwasniewski, L., Li, H., Wekezer, J., and Malachowski, J. (2006). Finite element analysis of vehicle–bridge interaction. *Finite Elements in Analysis and Design*, **42**, 950-959.

[8] Schlune, H., Plos, M., and Gylltoft, K. (2009). Improved bridge evaluation through finite element model updating using static and dynamic measurements. *Engineering Structures*, **31**, 1477-1485.

[9] Fan, Z. and Helwig, T. (2002). Distortional Loads and Brace Forces in Steel Box Girders. *Journal of Structural Engineering*, **128**, 710-718.

[10] Hsu, Y., Fu, C., and Schelling, D. (1995). EBEF Method for Distortional Analysis of Steel Box Girder Bridges. *Journal of Structural Engineering*, **121**, 557-566.

[11] Kim, K. and Yoo, C. (2006). Brace Forces in Steel Box Girders with Single Diagonal Lateral Bracing Systems. *Journal of Structural Engineering*, **132**, 1212-1222.

[12] Popp, D. and Williamson, E. (2005). Stability Analysis of Steel Trapezoidal Box-Girder Bridges. Structures Congress 2005.

[13] Williamson, E., Kim, J., and Frank, K. (2010). Redundancy Evaluation of Twin Steel Box-Girder Bridges Using Finite Element Analyses. Structures Congress 2010.

[14] El-Lobody, E. and Lam, D. (2003). Finite element analysis of steel-concrete composite girders. *Advances in Structural Engineering*, **6**, 267-281.

[15] Chung, W. and Sotelino, E.D. (2006). Three-dimensional finite element modeling of composite girder bridges. *Engineering Structures*, **28**, 63-71.

[16] Nie, J. and Zhu, L. (2014). Beam-Truss Model of Steel-Concrete Composite Box-Girder Bridges. *Journal of Bridge Engineering*, **19**, 04014023.

[17] Sennah, K., Kennedy, J., and Nour, S. (2003). Design for Shear in Curved Composite Multiple Steel Box Girder Bridges. *Journal of Bridge Engineering*, **8**, 144-152.

[18] Zhang, N. (2008). Analysis of External Prestressing Effect on Flexural Performance of Composite Steel Box-concrete Continuous Girder Bridge. *Journal of Highway and Transportation Research and Development (English Edition)*, **3**, 81-86.

[19] Chang, J.B.J. and Robertson, I.N. (2003). Computer Modeling of the Proposed Kealakaha Stream Bridge. Hawaii university of Hawaii.

[20] Ryu, H.-K., Shim, C.-S., and Chang, S.-P. (2004). Testing a composite box-girder bridge with precast decks. *Proceedings of the ICE - Structures and Buildings*, **157**, 243-250.

[21] Samaan, M. (2004). Dynamic and static analyses of continuous curved composite multiple-box girder bridges. Ph.D. University of Windsor.

[22] Zheng, L. (2008). Development of new distribution factor equations of live load moment and shear for steel open-box girder bridges. Ph.D. Tennessee Technological University.

[23] Zheng, Y., Robinson, D., Taylor, S., and Cleland, D. (2009). Finite element investigation of the structural behaviour of deck slabs in composite bridges. *Engineering Structures*, **31**, 1762-1776.

[24] Jianyong Song, J.L., Wanheng Li, Jinquan Zhang (2010). Finite element simulation of the composite continuous box-girder bridge with corrugated steel webs by CBCW. Proceedings of the International Conference on Computing in Civil and Building Engineering. W. TIzani. University of Nottingham.

[25] Sa-nguanmanasak, J.C., Taweep; Yamaguchi, Eiki (2010). Improvement on design analyses of composite steel-concrete bridges using elaborate finite element methods. *Songklanakarin Journal of Science & Technology*, **32**, 289-297.

[26] He, J., Liu, Y., and Chen, A. (2008). Research on Internal and External Tendon System of Composite Box Girder Bridge with Corrugated Steel Webs. *Journal of Highway and Transportation Research and Development (English Edition)*, **3**, 92-97.

[27] Samaan, M., Kennedy, J., and Sennah, K. (2007). Impact Factors for Curved Continuous Composite Multiple-Box Girder Bridges. *Journal of Bridge Engineering*, **12**, 80-88.

[28] Branco, F.A. and Green, R. (1984). Bracing for composite box girder bridges. *Canadian Journal of Civil Engineering*, **11**, 844-853.

[29] Branco, F.A. and Green, R. (1984). Bracing in completed composite box girder bridges. *Canadian Journal of Civil Engineering*, **11**, 967-977.

[30] Bradford, M.A. and Wong, T.C. (1992). Local Buckling of Composite Box Girders Under Negative Bending. *The Structural Engineer* **70**, 100-112.

[31] Hinton, E. and Rao, N.V.R. (1994). Structural shape optimization of shells and folded plates using two noded finite strips. *Computers and Structures*, **46**, pp.1055-1071.

[32] Hinton, E. and Rao, N.V.R. (1993). Analysis and shape optimization of variable thickness prismatic folded plates and curved shells. Part II: shape optimization. *Thin Walled Structures*, **17**, pp.161-183.

[33] Özakça, M., Hinton, E., and Rao, N.V.R. (1994). Free vibration analysis and shape optimization of prismatic folded plates and shells with curved planform. Part 1: finite strip formulation. *Numerical Methods in Engineering Int. J.*, **37**, pp.1713-1739.

[34] Hinton, E., Özakça, M., and Rao, N.V.R. (1995). Free vibration analysis and shape optimization of variable thickness prismatic folded plates and curved shells. Part II: shape optimization". *J. Sound and Vibration*, **181**, pp.567-581.

[35] Ghasemi, M.R. and Dizangian, B. (2010). Size, Shape and Topology Optimization of Composite Steel Box Girders Using Pso Method. *Asian Journal of Civil Engineering (Building And Housing)*, **11**, 699-715.

[36] Musa, Y. and Diaz, M. (2007). Design Optimization of Composite Steel Box Girder in Flexure. *Practice Periodical on Structural Design and Construction*, **12**, 146-152.

[37] Kaveh, A., der bridges using Cuckoo Search algorithm. . *Steel and Composite Structures*, **17**, 298-310.

[38] Surtees, J., Tordoff, D., and Merrison (1977). Optimum Design of Composite Box Girder Bridge Structures. *ICE Proceedings*, **63**, 181-198.

[39] Price, K. (2000). Design of Steel Bridges: Two Box Girder Concept—Current and Future Innovation. Advanced Technology in Structural Engineering.

[40] Samaan, M., Sennah, K., and Kennedy, J. (2005). Distribution Factors for Curved Continuous Composite Box-Girder Bridges. *Journal of Bridge Engineering*, **10**, 678-692.

[41] Sennah, K. and Kennedy, J. (1999). Load Distribution Factors for Composite Multicell Box Girder Bridges. *Journal of Bridge Engineering*, **4**, 71-78.

[42] Sennah, K. and Kennedy, J.B. (1998). Vibrations of horizontally curved continuous composite cellular bridges. *Canadian Journal of Civil Engineering*, **25**, 139-150.

[43] Cheung, M.S. and Foo, S.H.C. (1995). Design of horizontally curved composite box-girder bridges: a simplified approach. *Canadian Journal of Civil Engineering*, **22**, 93-105.

[44] Chapman, J.C., Dowling, P.J., Lim, P.T.K., and Billington, C.J. (1971). The Structural Behaviour of Steel and Concrete Box Girder Bridges. *The Structural Engineer* **49**, 150-157.

[45] Schelling, D., Galdos, N., and Sahin, M. (1992). Evaluation of Impact Factors for Horizontally Curved Steel Box Bridges. *Journal of Structural Engineering*, **118**, 3203-3221.

[46] Cheung, M.S. (1982). Impact factors for composite steel box girder bridges. IABSE.

[47] Hee-Jung Ko, J.M., Yong-Woo Shin and Hak-Eun Lee (2013). Non-linear analyses model for composite box-girders with corrugated steel webs under torsion. *Steel and Composite Structures*, **14**, 200-212.

[48] Samaras, V., Sutton, J., Williamson, E., and Frank, K. (2012). Simplified Method for Evaluating the Redundancy of Twin Steel Box-Girder Bridges. *Journal of Bridge Engineering*, **17**, 470-480.

[49] Fan, Z. and Helwig, T. (1999). Behavior of Steel Box Girders with Top Flange Bracing. *Journal of Structural Engineering*, **125**, 829-837.

[50] Gara, F., Ranzi, G., and Leoni, G. (2011). Simplified method of analysis accounting for shear-lag effects in composite bridge decks. *Journal of Constructional Steel Research*, **67**, 1684-1697.

[51] Peiretti, H.C. (1997). Behaviour of composite box girder sections at ultimate limit state. IABSE.

[52] Evans, H.R., Ahmad, M.K.H., and Kristek, V. (1993). Shear lag in composite box girders of complex cross-sections. *Journal of Constructional Steel Research*, **24**, 183-204.

[53] Kwak, H.-G., Seo, Y.-J., and Jung, C.-M. (2000). Effects of the slab casting sequences and the drying shrinkage of concrete slabs on the short-term and long-term behavior of composite steel box girder bridges. Part 1. *Engineering Structures*, **22**, 1453-1466.

[54] El-Tawil, S. and Okeil, A.M. (2002). Behavior and Design Of Curved Composite Box Girder Bridges.

[55] Alliy, G. (1976). Synopsis. The thermal behaviour of a composite box girder bridge. *ICE Proceedings*, **61**, 400-412.

[56] Kristek, V., Evans, H.R., and Ahmad, M.K.M. (1990). A shear lag analysis for composite box girders. *Journal of Constructional Steel Research*, **16**, 1-21.

[57] Lin, Z. and Zhao, J. (2012). Modeling inelastic shear lag in steel box beams. *Engineering Structures*, **41**, 90-97.

[58] Zhou, W.-b., Jiang, L.-z., Liu, Z.-j., and Liu, X.-j. (2012). Closed-form solution to thin-walled box girders considering effects of shear deformation and shear lag. *Journal of Central South University*, **19**, 2650-2655.

[59] Moffatt, K.R. and Dowling, P.J. (1975). Shear Lag in Steel Box Girder Bridges. *The Structural Engineer*, **53**, 80-87.

[60] Zhou, W.-b., Jiang, L.-z., and Yu, Z.-w. (2013). Analysis of free vibration characteristic of steel-concrete composite box-girder considering shear lag and slip. *Journal of Central South University*, **20**, 2570-2577.

[61] Hendy, C.R. and Chakrabarti, S. (2014). Fatigue management of the Midland Links, UK steel box girder decks. *Proceedings of the ICE - Bridge Engineering*, **167**, 143-154.

[62] Abbu, M., Ekmekyapar, T., and Özakça, M. (2013). 3D FE modelling of composite box Girder Bridge. Proceedings of 2nd International Balkans Conference on Challenges of Civil Engineering, BCCCE. E. University. Tirana, Albania. 487-494.

[63] Abbu, M., Özakça, M., and Ekmekyapar, T. (2014). 3D FE modeling considering shear connectors representation and number in CBGB. *Steel and Composite Structures* **17**, 237.

[64] Abbu, M., Ekmekyapar, T., and Özakça, M. (2014). FE Analysis of Stresses in Composite Box Girder Bridges. International Civil Engineering & Architecture Symposium for Academicians 2014 (ICESA2014). Side, Antalya.

[65] Abbu, M., Ekmekyapar, T., and Özakça, M. (2014). Effects of Dimensional Details on Behaviour of Composite Box Girder Bridges. Istanbul Bridge Conference 2014. Istanbul.

[66] Lu, P., Li, F., and Zhao, R. (2012). A theoretical model of deflection for composite box girder considering interface slip. *Australian Journal of Mechanical Engineering*, **9**, 47-59.

[67] Milner, H.R. and Peczkis, J. (2007). Wooden ship hulls as box girders with multiple interlayer slip. *Journal of Structural Engineering*, **133**, 855(7).

[68] Moffatt, K.R. and Dowling, P.J. (1978). The Longitudinal Bending Behaviour of Composite Box Girder Bridges Having Incomplete Interaction. *The Structural Engineer*, **56**, 134-140.

[69] Moffat, K. and Lim, P. (1976). Finite Element Analysis of Composite Box Girder Bridges Having Complete or Incomplete Interaction. *ICE Proceedings*, **61**, 1-22.

[70] Zhou, W.-b., Jiang, L.-z., Liu, Z.-j., and Liu, X.-j. (2012). Closed-form solution for shear lag effects of steel-concrete composite box beams considering shear deformation and slip. *Journal of Central South University*, **19**, 2976-2982.

[71] Abbu, M., Ekmekyapar, T., and Ozakca, M. (2014). 3D Modelling of Shear Connector behaviour with Partially Interaction. 11th International Congress on Advances in Civil Engineering, ACE2014. Istanbul.

[72] Ng, S.F., Cheung, M.S., and Hachem, H.M. (1993). Study of a curved continuous composite box girder bridge. *Canadian Journal of Civil Engineering*, **20**, 107-119.

[73] Sayed-Ahmed, E.Y. (2001). Behaviour of steel and (or) composite girders with corrugated steel webs. *Canadian Journal of Civil Engineering*, **28**, 656-672.

[74] Dalen, K.V. and Narasimham, S.V. (1980). Elastic behaviour of composite box girder bridges. *Canadian Journal of Civil Engineering*, **7**, 492-501.

[75] Branco, F. and Green, R. (1985). Composite Box Girder Bridge Behavior During Construction. *Journal of Structural Engineering*, **111**, 577-593.

[76] Dilger, W., Ghali, A., Chan, M., Cheung, M., and Maes, M. (1983). Temperature Stresses in Composite Box Girder Bridges. *Journal of Structural Engineering*, **109**, 1460-1478.

[77] Huang, D. (2004). Field Test of A Curved Steel Box Girder Bridge. Structures 2004.

[78] Shim, C., Ryu, H., Chung, C., Youn, S., and Chang, S. (2006). Inelastic Behavior of a Continuous Composite Box-Girder Bridge with Prefabricated Slabs. Composite Construction in Steel and Concrete V.

[79] Tategami, H., Ebina, T., Uehira, K., Sonoda, K., and Kitoh, H. (2002). Shear Connectors in PC Box Girder Bridge with Corrugated Steel Webs. Composite Construction in Steel and Concrete IV.

[80] Jun He, Y.L., Xiaoqing Xu, and Laibin Li (2014). Loading capacity evaluation of composite box girder with corrugated webs and steel tube slab. *Structural Engineering and Mechanics*, **50**, 57-65.

[81] Ryu, H.-K. and Chang, S.-P. (2005). Ultimate strength of continuous composite box-girder bridges with precast decks. *Journal of Constructional Steel Research*, **61**, 329 (15).

[82] Yong Ding, K.J., Fei Shao and Anzhong Deng (2013). Experimental study on ultimate torsional strength of PC composite box-girder with corrugated steel webs under pure torsion. *Structural Engineering and Mechanics*, **46**,

[83] Korol, R.M., Thimmhardy, E.G., and Cheung, M.S. (1988). An experimental investigation of the effects of imperfections on the strength of steel box girders. *Canadian Journal of Civil Engineering*, **15**, 443-449.

[84] Korol, R.M., Thimmhardy, E.G., and Cheung, M.S. (1984). Field investigation of out-of-plane deviations for steel box girder bridges. *Canadian Journal of Civil Engineering*, **11**, 377-386.

[85] Daniels, J.H., Fisher, J.W., and Yen, B.T. (1980). Fatigue of Curved Steel Bridge Elements--Design Recommendations for Fatigue of Curved Plate Girder and Box Girder Bridges. Bethlehem. Lehigh university.

[86] Daniels, J.H., Fisher, T.A., Batcheler, R.P., and Maurer, J.K. (1979). Fatigue of Curved Steel Bridge Elements-Ultimate Stength Tests Of Horizontally Curved Plate and Box Girders. Bethlehem. Lehigh University.

[87] Heins, C.P. and Humphreys, R.S. (1977). Interaction Effects of Bending and Trosion On Steel Box Girders. USA. UC Berkeley Transportation Library.

[88] Xu, C., Su, Q., Wu, C., and Sugiura, K. (2011). Experimental study on double composite action in the negative flexural region of two-span continuous composite box girder. *Journal of Constructional Steel Research*, **67**, 1636-1648.

[89] Chang, S.P. and Im, C.K. (2000). Thermal behaviour of composite box-girder bridges. *Proceedings of the ICE - Structures and Buildings*, **140**, 117-126.

[90] Androus, A. (2003). Experimental and theoretical studies of composite multiple-box girder bridges. Digital Commons @ Ryerson.

[91] Topkaya, C., Yura, J.A., Williamson, E.B., and Frank, K.H. (2005). Composite Action during Construction of Steel Trapezoidal Box Girder Bridges.

[92] Lam, D. and El-Lobody, E. (2005). Behavior of Headed Stud Shear Connectors in Composite Beam. *Journal of Structural Engineering*, **131**, 96-107.

[93] Bursi, O.S., Sun, F.-F., and Postal, S. (2005). Non-linear analysis of steel–concrete composite frames with full and partial shear connection subjected to seismic loads. *Journal of Constructional Steel Research*, **61**, 67-92.

[94] Queiroz, F.D., Vellasco, P.C.G.S., and Nethercot, D.A. (2007). Finite element modelling of composite beams with full and partial shear connection. *Journal of Constructional Steel Research*, **63**, 505-521.

[95] Wang, A.J. and Chung, K.F. (2008). Advanced finite element modelling of perforated composite beams with flexible shear connectors. *Engineering Structures*, **30**, 2724-2738.

[96] Sakr, M.A. and Sakla, S.S.S. (2008). Long-term deflection of cracked composite beams with nonlinear partial shear interaction: I — Finite element modeling. *Journal of Constructional Steel Research*, **64**, 1446-1455.

[97] Nguyen, H.T. and Kim, S.E. (2009). Finite element modeling of push-out tests for large stud shear connectors. *Journal of Constructional Steel Research*, **65**, 1909-1920.

[98] Julander, J.L. (2009). Finite Element Modelling of Full Depth Precast Concrete Transverse Bridge Deck Connections. MSc. Utah State University.

[99] Oudjene, M., Meghlat, E.M., Ait-Aider, H., and Batoz, J.L. (2013). Non-linear finite element modelling of the structural behaviour of screwed timber-to-concrete composite connections. *Composite Structures*, **102**, 20-28.

[100] Tahmasebinia, F., Ranzi, G., and Zona, A. (2013). Probabilistic three-dimensional finite element study on composite beams with steel trapezoidal decking. *Journal of Constructional Steel Research*, **80**, 394-411.

[101] Gattesco, N. and Giuriani, E. (1996). Experimental study on stud shear connectors subjected to cyclic loading. *Journal of Constructional Steel Research*, **38**, 1-21.

[102] Shim, C.-S., Lee, P.-G., and Yoon, T.-Y. (2004). Static behavior of large stud shear connectors. *Engineering Structures*, **26**, 1853-1860.

[103] Shim CS, L.P., Chang SP. (2010). Push-out tests on shear studs in high strength concrete. Proceedings of FraMCoS-7. F.M.o.C.a.C. Structures.

[104] Mirza, O. and Uy, B. (2010). Effects of the combination of axial and shear loading on the behaviour of headed stud steel anchors. *Engineering Structures*, **32**, 93-105.

[105] Pavlović, M., Marković, Z., Veljković, M., and Buđevac, D. (2013). Bolted shear connectors vs. headed studs behaviour in push-out tests. *Journal of Constructional Steel Research*, **88**, 134-149.

[106] Guezouli, S. and Lachal, A. (2012). Numerical analysis of frictional contact effects in push-out tests. *Engineering Structures*, **40**, 39-50.

[107] Shen M H, C.K. (2001). An Investigation into Shear Resistances of Headed Shear Studs in Solid Concrete Slabs with Local Aggregates in Hong Kong. Procedia Engineering 14. 1098–1105.

[108] Xue, D., Liu, Y., Yu, Z., and He, J. (2012). Static behavior of multi-stud shear connectors for steel-concrete composite bridge. *Journal of Constructional Steel Research*, **74**, 1-7.

[109] Slutter, R.G. and Fisher, J.W. (1966). Fatigue strength of shear connectors. Bethlehem, Pennsylvania. Lehigh University.

[110] Mainstone RJ, M.J. (1967). Shear connectors in steel-concrete composite beams for bridges. *Part1 and 2 concrete*, **1(9-10)**, 40-50.

[111] Ollgaard JG, S.R.a.F.J. (1971). Shear strength of stud connectors in lightweight and normal weight concrete, AISC Eng 'g Jr., April 1971 (71-10). New York. Lehigh University.

[112] Johnson, R. and Oehlers, D. (1981). Analysis and Design for Longitudinal Shear In Composite T-Beams. *ICE Proceedings*, **71**, 989-1021.

[113] Roderick, J.W. and Ansourian, P.P. (1976). Repeated loading of composite beams.

[114] Hallam, M.W., Engineering, U.o.S.S.o.C., and Laboratories, U.o.S.C.E. (1976). The behaviour of stud shear connectors under repeated loading. School of Civil Engineering, University of Sydney.

[115] Faust T, L.A., Mesinger M. (2000). Fatigue of headed studs embedded in LWAC. Second international symposium on structural lightweight aggregate concrete 2000. 212-220.

[116] Shim, C.-S., Lee, P.-G., and Chang, S.-P. (2001). Design of shear connection in composite steel and concrete bridges with precast decks. *Journal of Constructional Steel Research*, **57**, 203-219.

[117] Badie, S., Tadros, M., Kakish, H., Splittgerber, D., and Baishya, M. (2002). Large Shear Studs for Composite Action in Steel Bridge Girders. *Journal of Bridge Engineering*, **7**, 195-203.

[118] Jin-Hee Ahn, S.-H.K., and Youn-Ju Jeong (2007). Fatigue experiment of stud welded on steel plate for a new bridge deck system. *Steel and Composite Structures*, **7**, 391-404

[119] Yen, B.T.H., T.; Wang, D.; and Chuang, C. K., . (1986). Composite compression bottom flange for steel box girders. Federal Highway Administration, Fritz Laboratory Reports, Paper 2288.

[120] Huang, T., Chuang, C.K., Daniels, J.H., and B T Yen, B.T. (1984). Comparison of Haunched and Constant-Depth Steel Box Bridge Girders. International Bridge Conference. Pittsburgh, PA. Fritz Laboratory Reports. Paper 2287, 84-26.

[121] BS5400 (1979). Steel concrete and composite bridges, Part 5: Code of practice for design of composite bridges. London. BSI.

[122] AASHTO (2012). AASHTO LRFD Bridge Design Specifications. USA. American Association of State Highway and Transportation Officials.

[123] Madenci, E. and Guven, I. (2006). The Finite Element Method And Applications in Engineering Using ANSYS. New York. Springer Science Business Media.

[124] ANSYSManual (2009). Element Reference V.13. U.S.A. Swanson Analysis Systems.

[125] BS8110 (1995). Code of practice for design and construction. London. British Standards Institution (BSI).

[126] Oehlers, D.J. and Bradford., M.A. (1995). Composite steel and concrete structural members. Oxford, U.K. Pergamon Press.

[127] Yam, L., Chapman, J., RRL, and 117, C. (1968). The Inelastic Behaviour of Simply Supported Composite Beams of Steel And Concrete. *ICE Proceedings*, **41**, 651-683.

[128] Eurocode4 (2004). Design of Composite Steel and Concrete Structures. European Committee for Standardisation (CEN).

[129] RP., J. (1975). Composite Structures of Steel and Concrete Vol.1, Beams, Columns, Frames and Applications in Building. Vol.1. London. Crosby-Lock wood Staples.

[130] CP., Y. (1981). Design of Composite Steel-Concrete Structures. UK. Surrey University Press.

[131] Johnson, R.P. and Buckby, R.J. (1979). Composite Structures of Steel And Concrete, Volume 2. Bridges, with A Commentary on BS 5400: Part 5. London.

[132] EC4 (1994). Design of composite steel and concrete structures, Part 1.1, General rules and rules for buildings (with U.K. National Application Document). London. British Standards Institution (BSI).

[133] AISC (1999). Load and Resistance Factor Design Specification for Structural Steel Building. Chicago. American Institute of Steel Construction.

[134] CP117-Part5 (1995). Composite construction in structural steel and concrete. London. British Standards Institution (BSI).

[135] Fu, F. and Lam, D. (2006). Experimental study on semi-rigid composite joints with steel beams and precast hollowcore slabs. *Journal of Constructional Steel Research*, **62**, 771-782.

[136] BS5950 (1968). Code of Practice for Design of Simple and Continuous Composite Beams:Part 3: Section 3.1. London. British Standards Institution BSI.

[137] Valente, M. (2007). Experimental Studies on Shear Connection Systems in Steel and Lightweight Concrete Composite Bridges. University of Minho.

[138] Qian, S.a.V.C.L. (2006). Influence of Concrete Material Ductility on Shear Response of Stud Connections. *ACI Material Journal*, **103**, 60-66.

[139] Roberts, T.M. and Kazemi, H.H. (1989). Strengthening of Under-Reinforced Concrete Beams with Mechanically Attached Steel Plates. *The International Journal of Cement Composites and Lightweight Concrete*, **11**, 21-27.

APPENDIX A

1. Results of the deflection at nodes 1-7

No.	DC	TW	HW	L	N1	N2	N3	N4	N5	N6	N7
1	100	8	532	14000	-1.86	-1.86	-1.86	-1.85	-1.85	-1.85	-1.85
2	100	8	532	21000	-8.61	-8.60	-8.59	-8.59	-8.59	-8.58	-8.58
3	100	8	532	28000	-18.23	-18.22	-18.21	-18.21	-18.20	-18.20	-18.20
4	100	8	800	14000	-1.59	-1.59	-1.59	-1.58	-1.58	-1.58	-1.58
5	100	8	800	21000	-4.04	-4.04	-4.04	-4.03	-4.03	-4.03	-4.03
6	100	8	800	28000	-8.29	-8.28	-8.28	-8.28	-8.28	-8.28	-8.28
7	100	8	1068	14000	-1.05	-1.04	-1.04	-1.04	-1.04	-1.04	-1.04
8	100	8	1068	21000	-2.40	-2.40	-2.40	-2.39	-2.39	-2.39	-2.39
9	100	8	1068	28000	-4.69	-4.69	-4.69	-4.69	-4.69	-4.69	-4.69
10	100	12	532	14000	-2.23	-2.23	-2.22	-2.22	-2.22	-2.22	-2.22
11	100	12	532	21000	-6.34	-6.34	-6.33	-6.33	-6.33	-6.32	-6.32
12	100	12	532	28000	-13.45	-13.44	-13.43	-13.43	-13.43	-13.42	-13.42
13	100	12	800	14000	-1.14	-1.14	-1.14	-1.13	-1.13	-1.13	-1.13
14	100	12	800	21000	-2.96	-2.96	-2.96	-2.95	-2.95	-2.95	-2.95
15	100	12	800	28000	-6.12	-6.12	-6.12	-6.12	-6.11	-6.11	-6.11
16	100	12	1068	14000	-0.74	-0.74	-0.74	-0.73	-0.73	-0.73	-0.73
17	100	12	1068	21000	-1.74	-1.74	-1.74	-1.74	-1.74	-1.74	-1.74
18	100	12	1068	28000	-3.46	-3.46	-3.46	-3.46	-3.45	-3.45	-3.45
19	100	16	532	14000	-1.79	-1.79	-1.78	-1.78	-1.78	-1.78	-1.78
20	100	16	532	21000	-5.14	-5.13	-5.13	-5.13	-5.12	-5.12	-5.12
21	100	16	532	28000	10.89	-10.88	-10.88	-10.87	-10.87	-10.87	-10.87
22	100	16	800	14000	-0.90	-0.90	-0.90	-0.90	-0.90	-0.90	-0.90
23	100	16	800	21000	-2.39	-2.38	-2.38	-2.38	-2.38	-2.38	-2.38
24	100	16	800	28000	-4.96	-4.96	-4.95	-4.95	-4.95	-4.95	-4.95
25	100	16	1068	14000	-0.58	-0.58	-0.58	-0.57	-0.57	-0.57	-0.57
26	100	16	1068	21000	-1.39	-1.39	-1.39	-1.39	-1.39	-1.39	-1.39
27	100	16	1068	28000	-2.79	-2.79	-2.79	-2.79	-2.79	-2.79	-2.79
28	150	8	532	14000	-2.56	-2.55	-2.55	-2.55	-2.54	-2.54	-2.54
29	150	8	532	21000	-7.07	-7.06	-7.06	-7.05	-7.05	-7.05	-7.05
30	150	8	532	28000	14.94	-14.93	-14.92	-14.92	-14.92	-14.91	-14.91
31	150	8	800	14000	-1.40	-1.40	-1.39	-1.39	-1.39	-1.39	-1.39
32	150	8	800	21000	-3.47	-3.46	-3.46	-3.46	-3.46	-3.46	-3.46
33	150	8	800	28000	-7.04	-7.04	-7.03	-7.03	-7.03	-7.03	-7.03
34	150	8	1068	14000	-0.95	-0.95	-0.95	-0.95	-0.95	-0.95	-0.95

35	150	8	1068	21000	-2.11	-2.11	-2.11	-2.11	-2.11	-2.11	-2.11
36	150	8	1068	28000	-4.07	-4.06	-4.06	-4.06	-4.06	-4.06	-4.06
37	150	12	532	14000	-1.85	-1.85	-1.84	-1.84	-1.84	-1.84	-1.84
38	150	12	532	21000	-5.17	-5.17	-5.16	-5.16	-5.16	-5.16	-5.16
39	150	12	532	28000	-10.95	-10.94	-10.94	-10.93	-10.93	-10.93	-10.93
40	150	12	800	14000	-0.99	-0.99	-0.99	-0.99	-0.99	-0.99	-0.99
41	150	12	800	21000	-2.52	-2.52	-2.52	-2.51	-2.51	-2.51	-2.51
42	150	12	800	28000	-5.16	-5.16	-5.16	-5.15	-5.15	-5.15	-5.15
43	150	12	1068	14000	-0.67	-0.66	-0.66	-0.66	-0.66	-0.66	-0.66
44	150	12	1068	21000	-1.52	-1.52	-1.52	-1.52	-1.52	-1.52	-1.52
45	150	12	1068	28000	-2.98	-2.97	-2.97	-2.97	-2.97	-2.97	-2.97
46	150	16	532	14000	-1.48	-1.48	-1.47	-1.47	-1.47	-1.47	-1.47
47	150	16	532	21000	-4.18	-4.17	-4.17	-4.17	-4.17	-4.16	-4.16
48	150	16	532	28000	-8.84	-8.84	-8.84	-8.83	-8.83	-8.83	-8.83
49	150	16	800	14000	-0.79	-0.78	-0.78	-0.78	-0.78	-0.78	-0.78
50	150	16	800	21000	-2.02	-2.02	-2.02	-2.02	-2.02	-2.02	-2.02
51	150	16	800	28000	-4.17	-4.17	-4.17	-4.16	-4.16	-4.16	-4.16
52	150	16	1068	14000	-0.52	-0.52	-0.52	-0.52	-0.52	-0.52	-0.52
53	150	16	1068	21000	-1.22	-1.21	-1.21	-1.21	-1.21	-1.21	-1.21
54	150	16	1068	28000	-2.40	-2.40	-2.40	-2.40	-2.40	-2.40	-2.40
55	200	8	532	14000	-2.17	-2.17	-2.17	-2.16	-2.16	-2.16	-2.16
56	200	8	532	21000	-5.94	-5.94	-5.93	-5.93	-5.93	-5.93	-5.92
57	200	8	532	28000	-12.54	-12.53	-12.53	-12.52	-12.52	-12.52	-12.52
58	200	8	800	14000	-1.25	-1.25	-1.25	-1.25	-1.25	-1.25	-1.25
59	200	8	800	21000	-3.05	-3.05	-3.05	-3.05	-3.05	-3.04	-3.04
60	200	8	800	28000	-6.15	-6.15	-6.15	-6.14	-6.14	-6.14	-6.14
61	200	8	1068	14000	-0.88	-0.88	-0.87	-0.87	-0.87	-0.87	-0.87
62	200	8	1068	21000	-1.91	-1.91	-1.91	-1.90	-1.90	-1.90	-1.90
63	200	8	1068	28000	-3.63	-3.63	-3.63	-3.63	-3.62	-3.62	-3.62
64	200	12	532	14000	-1.57	-1.57	-1.57	-1.56	-1.56	-1.56	-1.56
65	200	12	532	21000	-4.34	-4.34	-4.33	-4.33	-4.33	-4.33	-4.33
66	200	12	532	28000	-9.17	-9.17	-9.16	-9.16	-9.16	-9.16	-9.16
67	200	12	800	14000	-0.89	-0.89	-0.89	-0.88	-0.88	-0.88	-0.88
68	200	12	800	21000	-2.21	-2.21	-2.20	-2.20	-2.20	-2.20	-2.20
69	200	12	800	28000	-4.48	-4.48	-4.48	-4.48	-4.48	-4.48	-4.48
70	200	12	1068	14000	-0.61	-0.61	-0.61	-0.61	-0.61	-0.61	-0.61
71	200	12	1068	21000	-1.37	-1.37	-1.37	-1.37	-1.37	-1.37	-1.36
72	200	12	1068	28000	-2.64	-2.64	-2.64	-2.64	-2.64	-2.64	-2.64
73	200	16	532	14000	-1.26	-1.25	-1.25	-1.25	-1.25	-1.25	-1.25
74	200	16	532	21000	-3.50	-3.50	-3.49	-3.49	-3.49	-3.49	-3.49
75	200	16	532	28000	-7.40	-7.39	-7.39	-7.39	-7.39	-7.39	-7.39
76	200	16	800	14000	-0.70	-0.70	-0.70	-0.70	-0.70	-0.70	-0.70
77	200	16	800	21000	-1.77	-1.77	-1.76	-1.76	-1.76	-1.76	-1.76

78	200	16	800	28000	-3.61	-3.61	-3.61	-3.61	-3.61	-3.61	-3.61
79	200	16	1068	14000	-0.48	-0.48	-0.48	-0.48	-0.48	-0.47	-0.47
80	200	16	1068	21000	-1.09	-1.09	-1.09	-1.09	-1.09	-1.09	-1.09
81	200	16	1068	28000	-2.12	-2.12	-2.12	-2.12	-2.12	-2.12	-2.12

APPENDIX B

2. Results of the stresses at nodes 1-7

No.	DC	TW	HW	L	N1	N2	N3	N4	N5	N6	N7
1	100	8	532	14000	50.77	50.96	49.65	49.03	48.90	48.56	48.24
2	100	8	532	21000	96.35	97.33	95.36	93.91	92.91	92.32	92.00
3	100	8	532	28000	125.83	127.65	125.68	124.23	123.23	122.65	122.46
4	100	8	800	14000	39.50	39.86	38.82	38.03	37.49	37.17	37.06
5	100	8	800	21000	58.28	59.21	58.17	57.39	56.84	56.52	56.41
6	100	8	800	28000	76.49	77.99	76.95	76.17	75.63	75.30	75.20
7	100	8	1068	14000	26.90	27.32	26.70	26.24	25.91	25.72	25.65
8	100	8	1068	21000	39.55	40.38	39.76	39.30	38.97	38.77	38.71
9	100	8	1068	28000	52.00	53.23	52.62	52.15	51.83	51.63	51.57
10	100	12	532	14000	44.58	44.59	43.20	42.17	41.46	41.05	40.92
11	100	12	532	21000	65.95	66.59	65.19	64.16	63.46	63.05	62.91
12	100	12	532	28000	85.90	87.11	85.72	84.70	83.99	83.58	83.45
13	100	12	800	14000	27.11	27.34	26.61	26.06	25.68	25.46	25.38
14	100	12	800	21000	40.03	40.68	39.95	39.40	39.02	38.79	38.72
15	100	12	800	28000	52.50	53.55	52.82	52.27	51.89	51.67	51.60
16	100	12	1068	14000	18.49	18.77	18.34	18.02	17.79	17.65	17.61
17	100	12	1068	21000	27.25	27.84	27.41	27.08	26.85	26.72	26.67
18	100	12	1068	28000	35.84	36.72	36.29	35.97	35.74	35.60	35.56
19	100	16	532	14000	34.05	34.00	32.91	32.12	31.57	31.25	31.14
20	100	16	532	21000	50.37	50.80	49.72	48.92	48.37	48.05	47.95
21	100	16	532	28000	65.45	66.33	65.24	64.45	63.90	63.58	63.48
22	100	16	800	14000	20.76	20.92	20.35	19.93	19.63	19.46	19.40
23	100	16	800	21000	30.69	31.18	30.61	30.18	29.89	29.71	29.66
24	100	16	800	28000	40.23	41.02	40.46	40.03	39.74	39.56	39.51
25	100	16	1068	14000	14.18	14.39	14.05	13.80	13.63	13.52	13.49
26	100	16	1068	21000	20.94	21.39	21.06	20.81	20.63	20.53	20.49
27	100	16	1068	28000	27.55	28.23	27.90	27.65	27.47	27.37	27.33
28	150	8	532	14000	57.46	57.58	56.05	54.91	54.12	53.65	53.50
29	150	8	532	21000	85.81	86.65	85.13	83.99	83.19	82.73	82.58
30	150	8	532	28000	112.79	114.31	112.79	111.66	110.87	110.41	110.25
31	150	8	800	14000	35.93	36.24	35.38	34.73	34.28	34.01	33.92
32	150	8	800	21000	53.31	54.11	53.25	52.60	52.14	51.87	51.78
33	150	8	800	28000	70.25	71.52	70.66	70.01	69.56	69.29	69.20
34	150	8	1068	14000	24.83	25.19	24.67	24.27	23.98	23.82	23.76
35	150	8	1068	21000	36.63	37.34	36.81	36.41	36.12	35.96	35.90
36	150	8	1068	28000	48.27	49.33	48.80	48.40	48.12	47.95	47.89
37	150	12	532	14000	39.61	39.63	38.53	37.71	37.14	36.80	36.69
38	150	12	532	21000	59.01	59.53	58.43	57.61	57.04	56.71	56.60

39	150	12	532	28000	77.32	78.32	77.22	76.40	75.84	75.51	75.40
40	150	12	800	14000	24.72	24.91	24.30	23.83	23.51	23.32	23.26
41	150	12	800	21000	36.65	37.19	36.57	36.11	35.79	35.60	35.54
42	150	12	800	28000	48.23	49.10	48.49	48.03	47.71	47.52	47.45
43	150	12	1068	14000	17.08	17.32	16.95	16.66	16.46	16.35	16.31
44	150	12	1068	21000	25.22	25.71	25.34	25.05	24.86	24.74	24.70
45	150	12	1068	28000	33.22	33.97	33.60	33.31	33.11	33.00	32.96
46	150	16	532	14000	30.36	30.33	29.45	28.81	28.36	28.10	28.01
47	150	16	532	21000	45.19	45.53	44.66	44.02	43.57	43.31	43.22
48	150	16	532	28000	59.06	59.77	58.90	58.26	57.82	57.55	57.47
49	150	16	800	14000	18.96	19.08	18.60	18.24	17.99	17.84	17.79
50	150	16	800	21000	28.12	28.51	28.03	27.67	27.42	27.27	27.22
51	150	16	800	28000	36.96	37.62	37.14	36.78	36.53	36.38	36.33
52	150	16	1068	14000	13.11	13.28	12.99	12.77	12.62	12.53	12.50
53	150	16	1068	21000	19.38	19.76	19.47	19.25	19.09	19.00	18.97
54	150	16	1068	28000	25.53	26.11	25.82	25.60	25.44	25.35	25.32
55	200	8	532	14000	50.59	50.73	49.52	48.61	47.98	47.61	47.48
56	200	8	532	21000	76.28	77.02	75.82	74.91	74.28	73.91	73.79
57	200	8	532	28000	100.89	102.20	101.01	100.11	99.48	99.11	98.99
58	200	8	800	14000	32.71	32.99	32.28	31.74	31.36	31.13	31.06
59	200	8	800	21000	48.90	49.60	48.89	48.34	47.96	47.74	47.66
60	200	8	800	28000	64.72	65.84	65.13	64.59	64.21	63.98	63.91
61	200	8	1068	14000	23.00	23.32	22.87	22.52	22.28	22.13	22.08
62	200	8	1068	21000	34.10	34.74	34.28	33.94	33.69	33.55	33.50
63	200	8	1068	28000	45.09	46.03	45.58	45.23	44.99	44.85	44.80
64	200	12	532	14000	35.22	35.26	34.37	33.71	33.25	32.98	32.89
65	200	12	532	21000	52.89	53.34	52.46	51.80	51.34	51.07	50.98
66	200	12	532	28000	69.70	70.55	69.67	69.01	68.55	68.28	68.19
67	200	12	800	14000	22.61	22.79	22.27	21.88	21.61	21.44	21.39
68	200	12	800	21000	33.73	34.19	33.68	33.29	33.02	32.85	32.80
69	200	12	800	28000	44.55	45.30	44.79	44.40	44.13	43.97	43.92
70	200	12	1068	14000	15.86	16.07	15.75	15.50	15.33	15.22	15.19
71	200	12	1068	21000	23.50	23.94	23.62	23.37	23.20	23.09	23.06
72	200	12	1068	28000	31.05	31.70	31.38	31.13	30.96	30.86	30.82
73	200	16	532	14000	27.14	27.12	26.41	25.89	25.52	25.30	25.23
74	200	16	532	21000	40.67	40.96	40.26	39.73	39.37	39.15	39.08
75	200	16	532	28000	53.45	54.04	53.34	52.82	52.46	52.24	52.17
76	200	16	800	14000	17.39	17.50	17.09	16.79	16.57	16.44	16.40
77	200	16	800	21000	25.91	26.26	25.85	25.54	25.33	25.20	25.16
78	200	16	800	28000	34.18	34.75	34.34	34.04	33.82	33.70	33.65
79	200	16	1068	14000	12.19	12.34	12.09	11.89	11.76	11.68	11.65
80	200	16	1068	21000	18.08	18.40	18.15	17.96	17.82	17.74	17.71
81	200	16	1068	28000	23.86	24.37	24.11	23.92	23.78	23.70	23.68

APPENDIX C

3. Results of the deflection at nodes 7-13 with HR

NO.	HR	DC	TW	HW	L	N7	N8	N9	N10	N11	N12	N13
1	1.6	100	8	532	14000	-0.89	-0.89	-0.87	-0.87	-0.89	-0.88	-0.87
2	1.6	100	8	532	21000	-13.19	-13.16	-13.06	-12.90	-12.69	-12.44	-12.17
3	1.6	100	8	532	28000	-36.59	-36.55	-36.46	-36.30	-36.10	-35.86	-35.61
4	1.6	100	8	800	14000	-1.07	-1.06	-1.03	-0.98	-0.92	-0.84	-0.76
5	1.6	100	8	800	21000	-5.42	-5.39	-5.32	-5.19	-5.03	-4.84	-4.64
6	1.6	100	8	800	28000	-14.77	-14.74	-14.66	-14.52	-14.35	-14.14	-13.92
7	1.6	100	8	1068	14000	-0.49	-0.49	-0.48	-0.46	-0.43	-0.40	-0.37
8	1.6	100	8	1068	21000	-2.73	-2.71	-2.66	-2.57	-2.46	-2.33	-2.18
9	1.6	100	8	1068	28000	-7.40	-7.37	-7.31	-7.20	-7.05	-6.89	-6.70
10	1.6	100	12	532	14000	-1.68	-1.67	-1.65	-1.62	-1.57	-1.51	-1.45
11	1.6	100	12	532	21000	-9.40	-9.39	-9.35	-9.30	-9.22	-9.14	-9.05
12	1.6	100	12	532	28000	-26.68	-26.67	-26.64	-26.59	-26.53	-26.45	-26.37
13	1.6	100	12	800	14000	-0.61	-0.60	-0.59	-0.57	-0.55	-0.52	-0.49
14	1.6	100	12	800	21000	-3.66	-3.65	-3.62	-3.58	-3.52	-3.45	-3.38
15	1.6	100	12	800	28000	-10.54	-10.53	-10.50	-10.45	-10.39	-10.32	-10.25
16	1.6	100	12	1068	14000	-0.25	-0.25	-0.25	-0.24	-0.24	-0.23	-0.22
17	1.6	100	12	1068	21000	-1.76	-1.75	-1.73	-1.70	-1.66	-1.61	-1.56
18	1.6	100	12	1068	28000	-5.16	-5.15	-5.13	-5.09	-5.04	-4.98	-4.92
19	1.6	100	16	532	14000	-1.35	-1.34	-1.33	-1.31	-1.29	-1.26	-1.23
20	1.6	100	16	532	21000	-7.62	-7.61	-7.59	-7.57	-7.54	-7.50	-7.45
21	1.6	100	16	532	28000	-21.67	-21.67	-21.65	-21.63	-21.60	-21.57	-21.54
22	1.6	100	16	800	14000	-0.47	-0.46	-0.46	-0.45	-0.43	-0.42	-0.40
23	1.6	100	16	800	21000	-2.91	-2.91	-2.89	-2.87	-2.85	-2.81	-2.78
24	1.6	100	16	800	28000	-8.50	-8.50	-8.48	-8.46	-8.44	-8.40	-8.37
25	1.6	100	16	1068	14000	-0.19	-0.19	-0.19	-0.18	-0.18	-0.17	-0.17
26	1.6	100	16	1068	21000	-1.38	-1.38	-1.37	-1.35	-1.33	-1.31	-1.28
27	1.6	100	16	1068	28000	-4.14	-4.14	-4.13	-4.11	-4.09	-4.06	-4.03
28	1.6	150	8	532	14000	-1.64	-1.63	-1.59	-1.54	-1.46	-1.37	-1.28
29	1.6	150	8	532	21000	-10.73	-10.71	-10.62	-10.48	-10.30	-10.08	-9.85
30	1.6	150	8	532	28000	-30.95	-30.92	-30.83	-30.69	-30.51	-30.29	-30.05
31	1.6	150	8	800	14000	-0.75	-0.74	-0.72	-0.69	-0.65	-0.60	-0.55
32	1.6	150	8	800	21000	-4.59	-4.57	-4.51	-4.40	-4.26	-4.09	-3.91
33	1.6	150	8	800	28000	-12.90	-12.88	-12.80	-12.67	-12.51	-12.32	-12.11
34	1.6	150	8	1068	14000	-0.35	-0.35	-0.34	-0.33	-0.32	-0.30	-0.29
35	1.6	150	8	1068	21000	-2.34	-2.33	-2.28	-2.21	-2.11	-1.99	-1.87
36	1.6	150	8	1068	28000	-6.52	-6.50	-6.44	-6.34	-6.21	-6.06	-5.89
37	1.6	150	12	532	14000	-1.06	-1.06	-1.04	-1.02	-0.99	-0.95	-0.91
38	1.6	150	12	532	21000	-7.60	-7.59	-7.56	-7.51	-7.45	-7.37	-7.30

39	1.6	150	12	532	28000	-22.49	-22.48	-22.45	-22.40	-22.34	-22.27	-22.20
40	1.6	150	12	800	14000	-0.38	-0.38	-0.37	-0.36	-0.35	-0.33	-0.32
41	1.6	150	12	800	21000	-3.03	-3.02	-2.99	-2.96	-2.91	-2.85	-2.78
42	1.6	150	12	800	28000	-9.07	-9.07	-9.04	-9.00	-8.94	-8.88	-8.81
43	1.6	150	12	1068	14000	-0.14	-0.14	-0.14	-0.14	-0.14	-0.14	-0.14
44	1.6	150	12	1068	21000	-1.45	-1.45	-1.43	-1.40	-1.37	-1.33	-1.28
45	1.6	150	12	1068	28000	-4.45	-4.44	-4.42	-4.39	-4.34	-4.29	-4.24
46	1.6	150	16	532	14000	-0.86	-0.86	-0.85	-0.84	-0.82	-0.80	-0.78
47	1.6	150	16	532	21000	-6.15	-6.15	-6.13	-6.11	-6.08	-6.05	-6.01
48	1.6	150	16	532	28000	-18.26	-18.25	-18.24	-18.22	-18.19	-18.16	-18.13
49	1.6	150	16	800	14000	-0.28	-0.28	-0.28	-0.27	-0.27	-0.26	-0.25
50	1.6	150	16	800	21000	-2.39	-2.38	-2.37	-2.35	-2.33	-2.30	-2.27
51	1.6	150	16	800	28000	-7.29	-7.28	-7.27	-7.25	-7.23	-7.20	-7.17
52	1.6	150	16	1068	14000	-0.10	-0.10	-0.10	-0.10	-0.10	-0.10	-0.10
53	1.6	150	16	1068	21000	-1.12	-1.12	-1.11	-1.10	-1.08	-1.06	-1.04
54	1.6	150	16	1068	28000	-3.55	-3.54	-3.53	-3.52	-3.50	-3.47	-3.44
55	1.6	200	8	532	14000	-3.55	-3.54	-3.53	-3.52	-3.50	-3.47	-3.44
56	1.6	200	8	532	21000	-3.55	-3.54	-3.53	-3.52	-3.50	-3.47	-3.44
57	1.6	200	8	532	28000	-3.55	-3.54	-3.53	-3.52	-3.50	-3.47	-3.44
58	1.6	200	8	800	14000	-0.51	-0.50	-0.49	-0.47	-0.45	-0.42	-0.39
59	1.6	200	8	800	21000	-4.01	-3.99	-3.93	-3.84	-3.71	-3.56	-3.40
60	1.6	200	8	800	28000	-11.57	-11.55	-11.47	-11.36	-11.21	-11.03	-10.83
61	1.6	200	8	1068	14000	-0.27	-0.27	-0.26	-0.26	-0.25	-0.24	-0.24
62	1.6	200	8	1068	21000	-2.12	-2.11	-2.07	-2.00	-1.91	-1.80	-1.69
63	1.6	200	8	1068	28000	-6.00	-5.98	-5.92	-5.82	-5.70	-5.55	-5.40
64	1.6	200	12	532	14000	-0.57	-0.57	-0.56	-0.55	-0.54	-0.52	-0.50
65	1.6	200	12	532	21000	-6.23	-6.22	-6.19	-6.15	-6.10	-6.03	-5.96
66	1.6	200	12	532	28000	-19.27	-19.26	-19.23	-19.19	-19.14	-19.07	-19.00
67	1.6	200	12	800	14000	-0.23	-0.23	-0.23	-0.22	-0.22	-0.21	-0.20
68	1.6	200	12	800	21000	-2.61	-2.60	-2.58	-2.54	-2.50	-2.45	-2.39
69	1.6	200	12	800	28000	-8.08	-8.07	-8.04	-8.01	-7.95	-7.89	-7.83
70	1.6	200	12	1068	14000	-0.08	-0.08	-0.09	-0.09	-0.09	-0.09	-0.10
71	1.6	200	12	1068	21000	-1.28	-1.27	-1.26	-1.23	-1.20	-1.16	-1.12
72	1.6	200	12	1068	28000	-4.02	-4.02	-4.00	-3.97	-3.92	-3.87	-3.82
73	1.6	200	16	532	14000	-0.49	-0.49	-0.49	-0.48	-0.47	-0.46	-0.45
74	1.6	200	16	532	21000	-5.06	-5.05	-5.04	-5.02	-5.00	-4.97	-4.94
75	1.6	200	16	532	28000	-15.68	-15.67	-15.66	-15.64	-15.62	-15.59	-15.56
76	1.6	200	16	800	14000	-0.16	-0.16	-0.16	-0.16	-0.16	-0.15	-0.15
77	1.6	200	16	800	21000	-2.04	-2.04	-2.02	-2.01	-1.99	-1.96	-1.94
78	1.6	200	16	800	28000	-6.46	-6.45	-6.44	-6.42	-6.40	-6.37	-6.34
79	1.6	200	16	1068	14000	-0.04	-0.05	-0.05	-0.05	-0.05	-0.05	-0.06
80	1.6	200	16	1068	21000	-0.97	-0.96	-0.96	-0.95	-0.93	-0.91	-0.89
81	1.6	200	16	1068	28000	-3.17	-3.17	-3.16	-3.15	-3.13	-3.11	-3.08
82	1.8	100	8	532	14000	-3.17	-3.17	-3.16	-3.15	-3.13	-3.11	-3.08
83	1.8	100	8	532	21000	-3.17	-3.17	-3.16	-3.15	-3.13	-3.11	-3.08
84	1.8	100	8	532	28000	-3.17	-3.17	-3.16	-3.15	-3.13	-3.11	-3.08
85	1.8	100	8	800	14000	-1.89	-1.87	-1.81	-1.73	-1.61	-1.47	-1.31
86	1.8	100	8	800	21000	-7.54	-7.50	-7.38	-7.19	-6.94	-6.64	-6.32

87	1.8	100	8	800	28000	-19.18	-19.14	-19.01	-18.81	-18.54	-18.22	-17.87
88	1.8	100	8	1068	14000	-0.97	-0.96	-0.94	-0.89	-0.83	-0.76	-0.68
89	1.8	100	8	1068	21000	-4.00	-3.98	-3.89	-3.75	-3.57	-3.36	-3.12
90	1.8	100	8	1068	28000	-9.93	-9.89	-9.79	-9.62	-9.39	-9.13	-8.84
91	1.8	100	12	532	14000	-2.55	-2.54	-2.50	-2.43	-2.35	-2.26	-2.15
92	1.8	100	12	532	21000	-12.22	-12.21	-12.15	-12.07	-11.96	-11.83	-11.69
93	1.8	100	12	532	28000	-33.53	-33.52	-33.47	-33.39	-33.29	-33.18	-33.06
94	1.8	100	12	800	14000	-1.06	-1.05	-1.03	-0.99	-0.94	-0.88	-0.82
95	1.8	100	12	800	21000	-4.97	-4.95	-4.91	-4.84	-4.75	-4.64	-4.52
96	1.8	100	12	800	28000	-13.54	-13.52	-13.48	-13.41	-13.32	-13.21	-13.09
97	1.8	100	12	1068	14000	-0.52	-0.52	-0.51	-0.49	-0.46	-0.43	-0.40
98	1.8	100	12	1068	21000	-2.51	-2.50	-2.47	-2.41	-2.34	-2.26	-2.17
99	1.8	100	12	1068	28000	-6.80	-6.79	-6.75	-6.69	-6.61	-6.52	-6.42
100	1.8	100	16	532	14000	-1.98	-1.97	-1.95	-1.92	-1.88	-1.83	-1.77
101	1.8	100	16	532	21000	-9.86	-9.85	-9.83	-9.79	-9.74	-9.68	-9.61
102	1.8	100	16	532	28000	-27.25	-27.24	-27.22	-27.19	-27.14	-27.09	-27.04
103	1.8	100	16	800	14000	-0.77	-0.77	-0.76	-0.74	-0.71	-0.68	-0.65
104	1.8	100	16	800	21000	-3.90	-3.89	-3.87	-3.84	-3.79	-3.74	-3.69
105	1.8	100	16	800	28000	-10.88	-10.87	-10.85	-10.82	-10.78	-10.73	-10.67
106	1.8	100	16	1068	14000	-0.37	-0.37	-0.36	-0.35	-0.33	-0.32	-0.30
107	1.8	100	16	1068	21000	-1.93	-1.92	-1.90	-1.88	-1.84	-1.80	-1.76
108	1.8	100	16	1068	28000	-5.41	-5.40	-5.38	-5.36	-5.32	-5.27	-5.23
109	1.8	150	8	532	14000	-5.41	-5.40	-5.38	-5.36	-5.32	-5.27	-5.23
110	1.8	150	8	532	21000	-5.41	-5.40	-5.38	-5.36	-5.32	-5.27	-5.23
111	1.8	150	8	532	28000	-5.41	-5.40	-5.38	-5.36	-5.32	-5.27	-5.23
112	1.8	150	8	800	14000	-1.49	-1.48	-1.44	-1.37	-1.28	-1.18	-1.06
113	1.8	150	8	800	21000	-6.59	-6.56	-6.45	-6.28	-6.06	-5.79	-5.51
114	1.8	150	8	800	28000	-17.09	-17.05	-16.93	-16.74	-16.49	-16.19	-15.87
115	1.8	150	8	1068	14000	-0.79	-0.79	-0.77	-0.73	-0.68	-0.63	-0.57
116	1.8	150	8	1068	21000	-3.55	-3.52	-3.45	-3.32	-3.16	-2.97	-2.77
117	1.8	150	8	1068	28000	-8.93	-8.90	-8.80	-8.65	-8.44	-8.19	-7.93
118	1.8	150	12	532	14000	-1.81	-1.80	-1.77	-1.72	-1.67	-1.60	-1.52
119	1.8	150	12	532	21000	-10.19	-10.17	-10.13	-10.05	-9.95	-9.84	-9.72
120	1.8	150	12	532	28000	-28.87	-28.86	-28.81	-28.74	-28.65	-28.55	-28.43
121	1.8	150	12	800	14000	-0.79	-0.78	-0.76	-0.74	-0.70	-0.66	-0.62
122	1.8	150	12	800	21000	-4.25	-4.23	-4.20	-4.13	-4.05	-3.96	-3.85
123	1.8	150	12	800	28000	-11.90	-11.89	-11.85	-11.78	-11.70	-11.60	-11.49
124	1.8	150	12	1068	14000	-0.38	-0.38	-0.37	-0.36	-0.34	-0.32	-0.30
125	1.8	150	12	1068	21000	-2.15	-2.14	-2.11	-2.06	-2.00	-1.93	-1.85
126	1.8	150	12	1068	28000	-5.99	-5.98	-5.95	-5.89	-5.82	-5.74	-5.65
127	1.8	150	16	532	14000	-1.41	-1.40	-1.39	-1.36	-1.33	-1.30	-1.26
128	1.8	150	16	532	21000	-8.22	-8.21	-8.19	-8.15	-8.11	-8.05	-8.00
129	1.8	150	16	532	28000	-23.47	-23.46	-23.44	-23.41	-23.37	-23.33	-23.28
130	1.8	150	16	800	14000	-0.55	-0.55	-0.54	-0.53	-0.51	-0.49	-0.46
131	1.8	150	16	800	21000	-3.31	-3.30	-3.28	-3.25	-3.21	-3.17	-3.12
132	1.8	150	16	800	28000	-9.52	-9.52	-9.50	-9.47	-9.43	-9.39	-9.34
133	1.8	150	16	1068	14000	-0.25	-0.25	-0.25	-0.24	-0.23	-0.22	-0.21
134	1.8	150	16	1068	21000	-1.62	-1.62	-1.60	-1.58	-1.55	-1.52	-1.48

135	1.8	150	16	1068	28000	-4.73	-4.73	-4.71	-4.68	-4.65	-4.61	-4.57
136	1.8	200	8	532	14000	-4.73	-4.73	-4.71	-4.68	-4.65	-4.61	-1.43
137	1.8	200	8	532	21000	-4.73	-4.73	-4.71	-4.68	-4.65	-4.61	-10.92
138	1.8	200	8	532	28000	-4.73	-4.73	-4.71	-4.68	-4.65	-4.61	-33.14
139	1.8	200	8	800	14000	-1.18	-1.17	-1.14	-1.09	-1.02	-0.94	-0.85
140	1.8	200	8	800	21000	-5.90	-5.86	-5.77	-5.61	-5.41	-5.17	-4.91
141	1.8	200	8	800	28000	-15.57	-15.53	-15.42	-15.24	-15.00	-14.72	-14.42
142	1.8	200	8	1068	14000	-0.68	-0.67	-0.66	-0.63	-0.59	-0.55	-0.50
143	1.8	200	8	1068	21000	-3.28	-3.26	-3.19	-3.07	-2.92	-2.75	-2.56
144	1.8	200	8	1068	28000	-8.33	-8.30	-8.21	-8.06	-7.86	-7.62	-7.37
145	1.8	200	12	532	14000	-8.33	-8.30	-8.21	-8.06	-7.86	-7.62	-7.37
146	1.8	200	12	532	21000	-8.33	-8.30	-8.21	-8.06	-7.86	-7.62	-7.37
147	1.8	200	12	532	28000	-8.33	-8.30	-8.21	-8.06	-7.86	-7.62	-7.37
148	1.8	200	12	800	14000	-0.60	-0.59	-0.58	-0.56	-0.54	-0.51	-0.47
149	1.8	200	12	800	21000	-3.76	-3.75	-3.71	-3.65	-3.58	-3.49	-3.40
150	1.8	200	12	800	28000	-10.77	-10.76	-10.72	-10.66	-10.58	-10.49	-10.39
151	1.8	200	12	1068	14000	-0.31	-0.30	-0.30	-0.29	-0.28	-0.26	-0.25
152	1.8	200	12	1068	21000	-1.94	-1.93	-1.91	-1.87	-1.81	-1.74	-1.67
153	1.8	200	12	1068	28000	-5.51	-5.50	-5.47	-5.41	-5.35	-5.27	-5.18
154	1.8	200	16	532	14000	-0.95	-0.95	-0.94	-0.92	-0.90	-0.87	-0.85
155	1.8	200	16	532	21000	-6.95	-6.94	-6.92	-6.89	-6.85	-6.80	-6.75
156	1.8	200	16	532	28000	-20.53	-20.53	-20.51	-20.48	-20.44	-20.40	-20.35
157	1.8	200	16	800	14000	-0.41	-0.40	-0.40	-0.39	-0.38	-0.36	-0.34
158	1.8	200	16	800	21000	-2.90	-2.90	-2.88	-2.85	-2.82	-2.78	-2.73
159	1.8	200	16	800	28000	-8.59	-8.58	-8.56	-8.54	-8.50	-8.46	-8.41
160	1.8	200	16	1068	14000	-0.19	-0.19	-0.18	-0.18	-0.18	-0.17	-0.16
161	1.8	200	16	1068	21000	-1.44	-1.44	-1.43	-1.41	-1.38	-1.35	-1.31
162	1.8	200	16	1068	28000	-4.31	-4.31	-4.29	-4.27	-4.24	-4.20	-4.16
163	2.2	100	8	532	14000	-4.31	-4.31	-4.29	-4.27	-4.24	-4.20	-5.78
164	2.2	100	8	532	21000	-4.31	-4.31	-4.29	-4.27	-4.24	-4.20	-24.21
165	2.2	100	8	532	28000	-4.31	-4.31	-4.29	-4.27	-4.24	-4.20	-64.69
166	2.2	100	8	800	14000	-3.85	-3.82	-3.72	-3.55	-3.32	-3.04	-2.73
167	2.2	100	8	800	21000	-12.51	-12.43	-12.23	-11.89	-11.45	-10.92	-10.35
168	2.2	100	8	800	28000	-29.23	-29.15	-28.92	-28.56	-28.09	-27.53	-26.92
169	2.2	100	8	1068	14000	-2.11	-2.09	-2.03	-1.94	-1.81	-1.64	-1.46
170	2.2	100	8	1068	21000	-7.02	-6.97	-6.82	-6.57	-6.24	-5.85	-5.43
171	2.2	100	8	1068	28000	-15.77	-15.71	-15.52	-15.21	-14.81	-14.34	-13.83
172	2.2	100	12	532	14000	-15.77	-15.71	-15.52	-15.21	-14.81	-14.34	-3.89
173	2.2	100	12	532	21000	-15.77	-15.71	-15.52	-15.21	-14.81	-14.34	-17.72
174	2.2	100	12	532	28000	-15.77	-15.71	-15.52	-15.21	-14.81	-14.34	-48.00
175	2.2	100	12	800	14000	-2.19	-2.18	-2.13	-2.05	-1.95	-1.82	-1.68
176	2.2	100	12	800	21000	-8.04	-8.01	-7.93	-7.81	-7.64	-7.44	-7.23
177	2.2	100	12	800	28000	-20.34	-20.32	-20.24	-20.11	-19.95	-19.76	-19.55
178	2.2	100	12	1068	14000	-1.20	-1.19	-1.16	-1.11	-1.05	-0.97	-0.89
179	2.2	100	12	1068	21000	-4.30	-4.28	-4.22	-4.12	-3.99	-3.83	-3.66
180	2.2	100	12	1068	28000	-10.57	-10.54	-10.48	-10.37	-10.22	-10.05	-9.87
181	2.2	100	16	532	14000	-10.57	-10.54	-10.48	-10.37	-10.22	-10.05	-3.12
182	2.2	100	16	532	21000	-10.57	-10.54	-10.48	-10.37	-10.22	-10.05	-14.55

183	2.2	100	16	532	28000	-10.57	-10.54	-10.48	-10.37	-10.22	-10.05	-39.41
184	2.2	100	16	800	14000	-1.56	-1.55	-1.52	-1.48	-1.42	-1.35	-1.28
185	2.2	100	16	800	21000	-6.21	-6.20	-6.16	-6.10	-6.02	-5.92	-5.82
186	2.2	100	16	800	28000	-16.26	-16.25	-16.22	-16.16	-16.08	-15.99	-15.90
187	2.2	100	16	1068	14000	-0.83	-0.83	-0.81	-0.78	-0.74	-0.70	-0.65
188	2.2	100	16	1068	21000	-3.23	-3.21	-3.18	-3.13	-3.06	-2.99	-2.90
189	2.2	100	16	1068	28000	-8.31	-8.29	-8.26	-8.21	-8.14	-8.06	-7.98
190	2.2	150	8	532	14000	-8.31	-8.29	-8.26	-8.21	-8.14	-8.06	-4.68
191	2.2	150	8	532	21000	-8.31	-8.29	-8.26	-8.21	-8.14	-8.06	-21.11
192	2.2	150	8	532	28000	-8.31	-8.29	-8.26	-8.21	-8.14	-8.06	-57.52
193	2.2	150	8	800	14000	-3.33	-3.30	-3.22	-3.08	-2.90	-2.66	-2.41
194	2.2	150	8	800	21000	-11.36	-11.30	-11.11	-10.81	-10.41	-9.94	-9.42
195	2.2	150	8	800	28000	-26.83	-26.76	-26.55	-26.21	-25.77	-25.24	-24.68
196	2.2	150	8	1068	14000	-1.87	-1.85	-1.81	-1.73	-1.62	-1.48	-1.32
197	2.2	150	8	1068	21000	-6.46	-6.41	-6.28	-6.05	-5.76	-5.40	-5.02
198	2.2	150	8	1068	28000	-14.61	-14.55	-14.37	-14.09	-13.71	-13.27	-12.79
199	2.2	150	12	532	14000	-14.61	-14.55	-14.37	-14.09	-13.71	-13.27	-3.12
200	2.2	150	12	532	21000	-14.61	-14.55	-14.37	-14.09	-13.71	-13.27	-15.44
201	2.2	150	12	532	28000	-14.61	-14.55	-14.37	-14.09	-13.71	-13.27	-42.77
202	2.2	150	12	800	14000	-1.85	-1.84	-1.80	-1.73	-1.65	-1.55	-1.44
203	2.2	150	12	800	21000	-7.19	-7.17	-7.10	-6.98	-6.83	-6.65	-6.46
204	2.2	150	12	800	28000	-18.49	-18.46	-18.39	-18.27	-18.12	-17.94	-17.75
205	2.2	150	12	1068	14000	-1.02	-1.01	-0.99	-0.95	-0.90	-0.84	-0.77
206	2.2	150	12	1068	21000	-3.86	-3.85	-3.79	-3.70	-3.58	-3.44	-3.29
207	2.2	150	12	1068	28000	-9.62	-9.60	-9.54	-9.44	-9.31	-9.15	-8.98
208	2.2	150	16	532	14000	-9.62	-9.60	-9.54	-9.44	-9.31	-9.15	-2.49
209	2.2	150	16	532	21000	-9.62	-9.60	-9.54	-9.44	-9.31	-9.15	-12.71
210	2.2	150	16	532	28000	-9.62	-9.60	-9.54	-9.44	-9.31	-9.15	-35.20
211	2.2	150	16	800	14000	-1.28	-1.28	-1.26	-1.22	-1.17	-1.12	-1.06
212	2.2	150	16	800	21000	-5.52	-5.51	-5.47	-5.42	-5.34	-5.26	-5.16
213	2.2	150	16	800	28000	-14.73	-14.72	-14.69	-14.64	-14.57	-14.48	-14.40
214	2.2	150	16	1068	14000	-0.69	-0.68	-0.67	-0.65	-0.62	-0.58	-0.54
215	2.2	150	16	1068	21000	-2.86	-2.85	-2.82	-2.78	-2.72	-2.65	-2.57
216	2.2	150	16	1068	28000	-7.52	-7.51	-7.48	-7.43	-7.37	-7.29	-7.21
217	2.2	200	8	532	14000	-7.52	-7.51	-7.48	-7.43	-7.37	-7.29	-3.50
218	2.2	200	8	532	21000	-7.52	-7.51	-7.48	-7.43	-7.37	-7.29	-18.12
219	2.2	200	8	532	28000	-7.52	-7.51	-7.48	-7.43	-7.37	-7.29	-50.77
220	2.2	200	8	800	14000	-2.83	-2.81	-2.74	-2.63	-2.48	-2.30	-2.09
221	2.2	200	8	800	21000	-10.43	-10.37	-10.20	-9.93	-9.57	-9.15	-8.68
222	2.2	200	8	800	28000	-24.96	-24.89	-24.70	-24.38	-23.96	-23.47	-22.94
223	2.2	200	8	1068	14000	-1.68	-1.67	-1.63	-1.56	-1.47	-1.35	-1.21
224	2.2	200	8	1068	21000	-6.11	-6.07	-5.94	-5.73	-5.46	-5.13	-4.77
225	2.2	200	8	1068	28000	-13.89	-13.83	-13.66	-13.40	-13.04	-12.62	-12.16
226	2.2	200	12	532	14000	-13.89	-13.83	-13.66	-13.40	-13.04	-12.62	-2.40
227	2.2	200	12	532	21000	-13.89	-13.83	-13.66	-13.40	-13.04	-12.62	-13.47
228	2.2	200	12	532	28000	-13.89	-13.83	-13.66	-13.40	-13.04	-12.62	-38.27
229	2.2	200	12	800	14000	-1.58	-1.57	-1.54	-1.49	-1.42	-1.34	-1.24
230	2.2	200	12	800	21000	-6.59	-6.57	-6.50	-6.40	-6.26	-6.10	-5.92

231	2.2	200	12	800	28000	-17.17	-17.15	-17.08	-16.97	-16.83	-16.66	-16.48
232	2.2	200	12	1068	14000	-0.91	-0.91	-0.89	-0.85	-0.81	-0.75	-0.69
233	2.2	200	12	1068	21000	-3.61	-3.60	-3.54	-3.46	-3.35	-3.22	-3.08
234	2.2	200	12	1068	28000	-9.06	-9.04	-8.98	-8.89	-8.76	-8.61	-8.45
235	2.2	200	16	532	14000	-9.06	-9.04	-8.98	-8.89	-8.76	-8.61	-1.95
236	2.2	200	16	532	21000	-9.06	-9.04	-8.98	-8.89	-8.76	-8.61	-11.17
237	2.2	200	16	532	28000	-9.06	-9.04	-8.98	-8.89	-8.76	-8.61	-31.71
238	2.2	200	16	800	14000	-1.09	-1.08	-1.06	-1.04	-1.00	-0.95	-0.90
239	2.2	200	16	800	21000	-5.04	-5.03	-5.00	-4.94	-4.88	-4.80	-4.71
240	2.2	200	16	800	28000	-13.67	-13.66	-13.62	-13.57	-13.51	-13.43	-13.35
241	2.2	200	16	1068	14000	-0.60	-0.59	-0.58	-0.56	-0.54	-0.51	-0.48
242	2.2	200	16	1068	21000	-2.64	-2.64	-2.61	-2.57	-2.51	-2.45	-2.38
243	2.2	200	16	1068	28000	-7.04	-7.03	-7.00	-6.95	-6.89	-6.82	-6.75
244	2.5	100	8	532	14000	-7.04	-7.03	-7.00	-6.95	-6.89	-6.82	-8.22
245	2.5	100	8	532	21000	-7.04	-7.03	-7.00	-6.95	-6.89	-6.82	-31.38
246	2.5	100	8	532	28000	-7.04	-7.03	-7.00	-6.95	-6.89	-6.82	-81.37
247	2.5	100	8	800	14000	-5.51	-5.46	-5.33	-5.11	-4.81	-4.43	-4.01
248	2.5	100	8	800	21000	-16.69	-16.60	-16.33	-15.89	-15.31	-14.61	-13.86
249	2.5	100	8	800	28000	-37.61	-37.51	-37.22	-36.74	-36.11	-35.37	-34.57
250	2.5	100	8	1068	14000	-3.07	-3.04	-2.97	-2.85	-2.67	-2.44	-2.19
251	2.5	100	8	1068	21000	-9.57	-9.51	-9.31	-8.98	-8.55	-8.03	-7.47
252	2.5	100	8	1068	28000	-20.69	-20.60	-20.35	-19.95	-19.41	-18.78	-18.10
253	2.5	100	12	532	14000	-20.69	-20.60	-20.35	-19.95	-19.41	-18.78	-5.46
254	2.5	100	12	532	21000	-20.69	-20.60	-20.35	-19.95	-19.41	-18.78	-22.88
255	2.5	100	12	532	28000	-20.69	-20.60	-20.35	-19.95	-19.41	-18.78	-60.49
256	2.5	100	12	800	14000	-3.19	-3.17	-3.10	-2.99	-2.85	-2.67	-2.48
257	2.5	100	12	800	21000	-10.67	-10.63	-10.52	-10.35	-10.13	-9.86	-9.57
258	2.5	100	12	800	28000	-26.06	-26.03	-25.92	-25.76	-25.54	-25.28	-25.01
259	2.5	100	12	1068	14000	-1.80	-1.78	-1.74	-1.67	-1.58	-1.47	-1.34
260	2.5	100	12	1068	21000	-5.85	-5.82	-5.74	-5.60	-5.42	-5.20	-4.97
261	2.5	100	12	1068	28000	-13.75	-13.72	-13.63	-13.48	-13.29	-13.06	-12.81
262	2.5	100	16	532	14000	-13.75	-13.72	-13.63	-13.48	-13.29	-13.06	-4.34
263	2.5	100	16	532	21000	-13.75	-13.72	-13.63	-13.48	-13.29	-13.06	-18.78
264	2.5	100	16	532	28000	-13.75	-13.72	-13.63	-13.48	-13.29	-13.06	-49.81
265	2.5	100	16	800	14000	-2.26	-2.25	-2.21	-2.14	-2.06	-1.96	-1.86
266	2.5	100	16	800	21000	-8.20	-8.18	-8.13	-8.04	-7.93	-7.80	-7.66
267	2.5	100	16	800	28000	-20.81	-20.79	-20.74	-20.67	-20.57	-20.45	-20.32
268	2.5	100	16	1068	14000	-1.25	-1.25	-1.22	-1.18	-1.12	-1.06	-0.98
269	2.5	100	16	1068	21000	-4.35	-4.34	-4.29	-4.22	-4.13	-4.02	-3.90
270	2.5	100	16	1068	28000	-10.76	-10.75	-10.70	-10.63	-10.54	-10.43	-10.32
271	2.5	150	8	532	14000	-10.76	-10.75	-10.70	-10.63	-10.54	-10.43	-6.93
272	2.5	150	8	532	21000	-10.76	-10.75	-10.70	-10.63	-10.54	-10.43	-27.99
273	2.5	150	8	532	28000	-10.76	-10.75	-10.70	-10.63	-10.54	-10.43	-73.68
274	2.5	150	8	800	14000	-4.90	-4.86	-4.75	-4.58	-4.32	-4.01	-3.65
275	2.5	150	8	800	21000	-15.45	-15.36	-15.12	-14.73	-14.21	-13.58	-12.91
276	2.5	150	8	800	28000	-35.11	-35.01	-34.74	-34.30	-33.71	-33.02	-32.28
277	2.5	150	8	1068	14000	-2.79	-2.77	-2.71	-2.61	-2.45	-2.26	-2.03
278	2.5	150	8	1068	21000	-8.97	-8.91	-8.73	-8.43	-8.04	-7.57	-7.06

279	2.5	150	8	1068	28000	-19.46	-19.38	-19.15	-18.77	-18.27	-17.68	-17.04
280	2.5	150	12	532	14000	-19.46	-19.38	-19.15	-18.77	-18.27	-17.68	-4.61
281	2.5	150	12	532	21000	-19.46	-19.38	-19.15	-18.77	-18.27	-17.68	-20.46
282	2.5	150	12	532	28000	-19.46	-19.38	-19.15	-18.77	-18.27	-17.68	-55.05
283	2.5	150	12	800	14000	-2.81	-2.79	-2.73	-2.64	-2.52	-2.38	-2.21
284	2.5	150	12	800	21000	-9.77	-9.74	-9.64	-9.49	-9.29	-9.04	-8.79
285	2.5	150	12	800	28000	-24.15	-24.12	-24.02	-23.87	-23.67	-23.43	-23.17
286	2.5	150	12	1068	14000	-1.60	-1.59	-1.55	-1.50	-1.42	-1.32	-1.21
287	2.5	150	12	1068	21000	-5.38	-5.35	-5.28	-5.15	-4.99	-4.80	-4.59
288	2.5	150	12	1068	28000	-12.76	-12.73	-12.65	-12.51	-12.33	-12.12	-11.89
289	2.5	150	16	532	14000	-12.76	-12.73	-12.65	-12.51	-12.33	-12.12	-3.66
290	2.5	150	16	532	21000	-12.76	-12.73	-12.65	-12.51	-12.33	-12.12	-16.86
291	2.5	150	16	532	28000	-12.76	-12.73	-12.65	-12.51	-12.33	-12.12	-45.52
292	2.5	150	16	800	14000	-1.96	-1.95	-1.92	-1.87	-1.80	-1.72	-1.63
293	2.5	150	16	800	21000	-7.47	-7.46	-7.41	-7.33	-7.23	-7.12	-6.99
294	2.5	150	16	800	28000	-19.25	-19.23	-19.19	-19.12	-19.02	-18.91	-18.79
295	2.5	150	16	1068	14000	-1.09	-1.08	-1.06	-1.03	-0.98	-0.93	-0.86
296	2.5	150	16	1068	21000	-3.96	-3.95	-3.91	-3.84	-3.76	-3.66	-3.55
297	2.5	150	16	1068	28000	-9.93	-9.92	-9.88	-9.81	-9.73	-9.63	-9.52
298	2.5	200	8	532	14000	-9.93	-9.92	-9.88	-9.81	-9.73	-9.63	-5.34
299	2.5	200	8	532	21000	-9.93	-9.92	-9.88	-9.81	-9.73	-9.63	-24.28
300	2.5	200	8	532	28000	-9.93	-9.92	-9.88	-9.81	-9.73	-9.63	-65.62
301	2.5	200	8	800	14000	-9.93	-9.92	-9.88	-9.81	-9.73	-9.63	-65.62
302	2.5	200	8	800	21000	-9.93	-9.92	-9.88	-9.81	-9.73	-9.63	-65.62
303	2.5	200	8	800	28000	-9.93	-9.92	-9.88	-9.81	-9.73	-9.63	-65.62
304	2.5	200	8	1068	14000	-2.54	-2.53	-2.48	-2.39	-2.26	-2.09	-1.89
305	2.5	200	8	1068	21000	-8.55	-8.49	-8.33	-8.06	-7.70	-7.27	-6.79
306	2.5	200	8	1068	28000	-18.68	-18.61	-18.38	-18.03	-17.56	-17.00	-16.40
307	2.5	200	12	532	14000	-18.68	-18.61	-18.38	-18.03	-17.56	-17.00	-3.72
308	2.5	200	12	532	21000	-18.68	-18.61	-18.38	-18.03	-17.56	-17.00	-18.16
309	2.5	200	12	532	28000	-18.68	-18.61	-18.38	-18.03	-17.56	-17.00	-49.94
310	2.5	200	12	800	14000	-2.48	-2.46	-2.42	-2.34	-2.24	-2.12	-1.99
311	2.5	200	12	800	21000	-9.10	-9.07	-8.98	-8.84	-8.66	-8.44	-8.21
312	2.5	200	12	800	28000	-22.76	-22.73	-22.64	-22.49	-22.30	-22.08	-21.84
313	2.5	200	12	1068	14000	-1.47	-1.46	-1.43	-1.38	-1.31	-1.23	-1.13
314	2.5	200	12	1068	21000	-5.11	-5.08	-5.01	-4.90	-4.75	-4.57	-4.37
315	2.5	200	12	1068	28000	-12.18	-12.16	-12.08	-11.95	-11.77	-11.57	-11.35
316	2.5	200	16	532	14000	-12.18	-12.16	-12.08	-11.95	-11.77	-11.57	-3.00
317	2.5	200	16	532	21000	-12.18	-12.16	-12.08	-11.95	-11.77	-11.57	-15.13
318	2.5	200	16	532	28000	-12.18	-12.16	-12.08	-11.95	-11.77	-11.57	-41.67
319	2.5	200	16	800	14000	-1.73	-1.72	-1.69	-1.65	-1.60	-1.53	-1.45
320	2.5	200	16	800	21000	-6.96	-6.94	-6.90	-6.83	-6.74	-6.63	-6.52
321	2.5	200	16	800	28000	-18.14	-18.13	-18.09	-18.02	-17.93	-17.83	-17.72
322	2.5	200	16	1068	14000	-0.99	-0.98	-0.97	-0.94	-0.90	-0.85	-0.80
323	2.5	200	16	1068	21000	-3.73	-3.72	-3.68	-3.63	-3.55	-3.46	-3.36
324	2.5	200	16	1068	28000	-9.44	-9.43	-9.39	-9.33	-9.25	-9.15	-9.05
325	3	100	8	532	14000	-9.44	-9.43	-9.39	-9.33	-9.25	-9.15	-12.77
326	3	100	8	532	21000	-9.44	-9.43	-9.39	-9.33	-9.25	-9.15	-44.49

327	3	100	8	532	28000	-9.44	-9.43	-9.39	-9.33	-9.25	-9.15	-9.15
328	3	100	8	800	14000	-9.44	-9.43	-9.39	-9.33	-9.25	-9.15	-9.33
329	3	100	8	800	21000	-9.44	-9.43	-9.39	-9.33	-9.25	-9.15	-9.43
330	3	100	8	800	28000	-9.44	-9.43	-9.39	-9.33	-9.25	-9.15	-9.25
331	3	100	8	1068	14000	-4.83	-4.80	-4.71	-4.54	-4.30	-3.97	-3.60
332	3	100	8	1068	21000	-14.24	-14.15	-13.88	-13.44	-12.85	-12.14	-11.36
333	3	100	8	1068	28000	-29.66	-29.55	-29.20	-28.64	-27.90	-27.02	-26.07
334	3	100	12	532	14000	-29.66	-29.55	-29.20	-28.64	-27.90	-27.02	-8.47
335	3	100	12	532	21000	-29.66	-29.55	-29.20	-28.64	-27.90	-27.02	-32.43
336	3	100	12	532	28000	-29.66	-29.55	-29.20	-28.64	-27.90	-27.02	-83.41
337	3	100	12	800	14000	-5.05	-5.02	-4.92	-4.77	-4.56	-4.31	-4.03
338	3	100	12	800	21000	-15.53	-15.48	-15.33	-15.09	-14.78	-14.41	-14.00
339	3	100	12	800	28000	-36.61	-36.56	-36.41	-36.18	-35.88	-35.52	-35.13
340	3	100	12	1068	14000	-2.92	-2.90	-2.84	-2.74	-2.60	-2.43	-2.24
341	3	100	12	1068	21000	-8.72	-8.68	-8.56	-8.37	-8.11	-7.81	-7.48
342	3	100	12	1068	28000	-19.64	-19.59	-19.46	-19.25	-18.98	-18.65	-18.30
343	3	100	16	532	14000	-19.64	-19.59	-19.46	-19.25	-18.98	-18.65	-6.70
344	3	100	16	532	21000	-19.64	-19.59	-19.46	-19.25	-18.98	-18.65	-26.71
345	3	100	16	532	28000	-19.64	-19.59	-19.46	-19.25	-18.98	-18.65	-69.11
346	3	100	16	800	14000	-3.59	-3.57	-3.52	-3.43	-3.30	-3.16	-3.00
347	3	100	16	800	21000	-11.92	-11.89	-11.82	-11.70	-11.54	-11.36	-11.16
348	3	100	16	800	28000	-29.25	-29.23	-29.16	-29.06	-28.91	-28.75	-28.57
349	3	100	16	1068	14000	-2.05	-2.04	-2.00	-1.94	-1.86	-1.75	-1.64
350	3	100	16	1068	21000	-6.46	-6.44	-6.38	-6.28	-6.14	-5.98	-5.81
351	3	100	16	1068	28000	-15.32	-15.30	-15.24	-15.14	-15.01	-14.85	-14.68
352	3	150	8	532	14000	-15.32	-15.30	-15.24	-15.14	-15.01	-14.85	-11.08
353	3	150	8	532	21000	-15.32	-15.30	-15.24	-15.14	-15.01	-14.85	-40.60
354	3	150	8	532	28000	-15.32	-15.30	-15.24	-15.14	-15.01	-14.85	-14.85
355	3	150	8	800	14000	-15.32	-15.30	-15.24	-15.14	-15.01	-14.85	-6.03
356	3	150	8	800	21000	-15.32	-15.30	-15.24	-15.14	-15.01	-14.85	-19.49
357	3	150	8	800	28000	-15.32	-15.30	-15.24	-15.14	-15.01	-14.85	-46.48
358	3	150	8	1068	14000	-4.52	-4.49	-4.42	-4.27	-4.06	-3.77	-3.44
359	3	150	8	1068	21000	-13.60	-13.52	-13.28	-12.88	-12.35	-11.70	-11.00
360	3	150	8	1068	28000	-28.45	-28.34	-28.02	-27.50	-26.82	-26.00	-25.12
361	3	150	12	532	14000	-28.45	-28.34	-28.02	-27.50	-26.82	-26.00	-7.51
362	3	150	12	532	21000	-28.45	-28.34	-28.02	-27.50	-26.82	-26.00	-29.95
363	3	150	12	532	28000	-28.45	-28.34	-28.02	-27.50	-26.82	-26.00	-78.00
364	3	150	12	800	14000	-4.62	-4.59	-4.52	-4.39	-4.22	-4.01	-3.76
365	3	150	12	800	21000	-14.64	-14.59	-14.46	-14.25	-13.97	-13.63	-13.25
366	3	150	12	800	28000	-34.82	-34.77	-34.64	-34.43	-34.15	-33.82	-33.44
367	3	150	12	1068	14000	-2.70	-2.69	-2.64	-2.55	-2.44	-2.29	-2.12
368	3	150	12	1068	21000	-8.24	-8.21	-8.10	-7.92	-7.69	-7.42	-7.12
369	3	150	12	1068	28000	-18.67	-18.63	-18.51	-18.31	-18.06	-17.76	-17.43
370	3	150	16	532	14000	-18.67	-18.63	-18.51	-18.31	-18.06	-17.76	-5.96
371	3	150	16	532	21000	-18.67	-18.63	-18.51	-18.31	-18.06	-17.76	-24.83
372	3	150	16	532	28000	-18.67	-18.63	-18.51	-18.31	-18.06	-17.76	-65.10
373	3	150	16	800	14000	-3.27	-3.25	-3.21	-3.13	-3.03	-2.91	-2.77
374	3	150	16	800	21000	-11.22	-11.20	-11.13	-11.03	-10.89	-10.72	-10.53

375	3	150	16	800	28000	-27.85	-27.83	-27.76	-27.66	-27.53	-27.38	-27.21
376	3	150	16	1068	14000	-1.88	-1.87	-1.84	-1.78	-1.71	-1.62	-1.53
377	3	150	16	1068	21000	-6.07	-6.05	-5.99	-5.90	-5.78	-5.64	-5.48
378	3	150	16	1068	28000	-14.52	-14.50	-14.45	-14.35	-14.23	-14.09	-13.93
379	3	200	8	532	14000	-14.52	-14.50	-14.45	-14.35	-14.23	-14.09	-8.69
380	3	200	8	532	21000	-14.52	-14.50	-14.45	-14.35	-14.23	-14.09	-35.53
381	3	200	8	532	28000	-14.52	-14.50	-14.45	-14.35	-14.23	-14.09	-92.60
382	3	200	8	800	14000	-14.52	-14.50	-14.45	-14.35	-14.23	-14.09	-5.37
383	3	200	8	800	21000	-14.52	-14.50	-14.45	-14.35	-14.23	-14.09	-18.36
384	3	200	8	800	28000	-14.52	-14.50	-14.45	-14.35	-14.23	-14.09	-44.21
385	3	200	8	1068	14000	-4.14	-4.12	-4.06	-3.94	-3.77	-3.52	-3.24
386	3	200	8	1068	21000	-13.04	-12.96	-12.75	-12.40	-11.92	-11.34	-10.70
387	3	200	8	1068	28000	-27.56	-27.46	-27.16	-26.69	-26.05	-25.30	-24.48
388	3	200	12	532	14000	-27.56	-27.46	-27.16	-26.69	-26.05	-25.30	-6.27
389	3	200	12	532	21000	-27.56	-27.46	-27.16	-26.69	-26.05	-25.30	-27.04
390	3	200	12	532	28000	-27.56	-27.46	-27.16	-26.69	-26.05	-25.30	-71.81
391	3	200	12	800	14000	-27.56	-27.46	-27.16	-26.69	-26.05	-25.30	-3.47
392	3	200	12	800	21000	-27.56	-27.46	-27.16	-26.69	-26.05	-25.30	-12.64
393	3	200	12	800	28000	-27.56	-27.46	-27.16	-26.69	-26.05	-25.30	-32.10
394	3	200	12	1068	14000	-2.53	-2.52	-2.48	-2.40	-2.30	-2.17	-2.03
395	3	200	12	1068	21000	-7.95	-7.92	-7.82	-7.66	-7.45	-7.20	-6.93
396	3	200	12	1068	28000	-18.12	-18.08	-17.97	-17.79	-17.55	-17.27	-16.97
397	3	200	16	532	14000	-18.12	-18.08	-17.97	-17.79	-17.55	-17.27	-5.10
398	3	200	16	532	21000	-18.12	-18.08	-17.97	-17.79	-17.55	-17.27	-22.77
399	3	200	16	532	28000	-18.12	-18.08	-17.97	-17.79	-17.55	-17.27	-60.71
400	3	200	16	800	14000	-2.98	-2.97	-2.93	-2.87	-2.79	-2.69	-2.58
401	3	200	16	800	21000	-10.67	-10.65	-10.60	-10.50	-10.38	-10.24	-10.07
402	3	200	16	800	28000	-26.79	-26.77	-26.71	-26.62	-26.51	-26.37	-26.22
403	3	200	16	1068	14000	-1.76	-1.76	-1.73	-1.68	-1.62	-1.54	-1.46
404	3	200	16	1068	21000	-5.85	-5.83	-5.78	-5.69	-5.58	-5.45	-5.31
405	3	200	16	1068	28000	-14.09	-14.07	-14.01	-13.93	-13.81	-13.68	-13.53

APPENDIX D

4. Results of the stresses at nodes 7-13 with HR

NO.	HR	DC	TW	HW	L	N7	N8	N9	N10	N11	N12	N13
1	1.6	100	8	532	14000	6.28	6.23	6.10	5.91	5.71	5.67	5.91
2	1.6	100	8	532	21000	29.07	28.88	28.32	27.46	26.44	25.49	23.93
3	1.6	100	8	532	28000	44.11	43.94	43.47	42.73	41.84	40.92	38.51
4	1.6	100	8	800	14000	5.28	5.23	5.10	4.91	4.71	4.67	4.91
5	1.6	100	8	800	21000	18.44	18.28	17.82	17.12	16.30	15.60	14.72
6	1.6	100	8	800	28000	29.23	29.07	28.61	27.90	27.05	26.23	24.47
7	1.6	100	8	1068	14000	2.01	2.00	1.97	1.93	1.90	1.96	2.14
8	1.6	100	8	1068	21000	11.66	11.55	11.22	10.73	10.16	9.72	9.34
9	1.6	100	8	1068	28000	20.16	20.03	19.63	19.01	18.28	17.61	16.43
10	1.6	100	12	532	14000	7.71	7.64	7.44	7.13	6.78	6.51	6.30
11	1.6	100	12	532	21000	19.88	19.79	19.52	19.12	18.64	18.16	17.24
12	1.6	100	12	532	28000	30.73	30.65	30.45	30.12	29.72	29.29	27.99
13	1.6	100	12	800	14000	3.54	3.50	3.39	3.23	3.05	2.94	2.97
14	1.6	100	12	800	21000	12.52	12.43	12.20	11.84	11.42	11.03	10.37
15	1.6	100	12	800	28000	20.18	20.11	19.91	19.58	19.19	18.79	17.69
16	1.6	100	12	1068	14000	1.17	1.15	1.11	1.05	0.99	0.98	1.07
17	1.6	100	12	1068	21000	7.97	7.91	7.72	7.45	7.12	6.84	6.46
18	1.6	100	12	1068	28000	13.88	13.81	13.63	13.34	12.99	12.64	11.83
19	1.6	100	16	532	14000	6.17	6.12	5.99	5.79	5.55	5.35	5.17
20	1.6	100	16	532	21000	15.48	15.43	15.28	15.05	14.77	14.48	13.95
21	1.6	100	16	532	28000	24.07	24.03	23.92	23.73	23.51	23.25	22.55
22	1.6	100	16	800	14000	2.89	2.86	2.78	2.66	2.52	2.42	2.41
23	1.6	100	16	800	21000	9.78	9.73	9.59	9.38	9.12	8.87	8.39
24	1.6	100	16	800	28000	15.84	15.80	15.68	15.50	15.27	15.03	14.28
25	1.6	100	16	1068	14000	0.98	0.97	0.94	0.88	0.83	0.81	0.89
26	1.6	100	16	1068	21000	6.29	6.25	6.13	5.96	5.75	5.56	5.24
27	1.6	100	16	1068	28000	10.92	10.89	10.78	10.61	10.40	10.19	9.60
28	1.6	150	8	532	14000	6.42	6.36	6.18	5.91	5.62	5.45	5.46
29	1.6	150	8	532	21000	22.73	22.57	22.09	21.35	20.48	19.70	18.52
30	1.6	150	8	532	28000	35.76	35.61	35.17	34.50	33.68	32.86	30.93
31	1.6	150	8	800	14000	3.23	3.21	3.14	3.03	2.93	2.93	3.11
32	1.6	150	8	800	21000	15.13	14.99	14.60	14.00	13.31	12.73	12.05
33	1.6	150	8	800	28000	24.86	24.71	24.29	23.64	22.87	22.12	20.65
34	1.6	150	8	1068	14000	1.04	1.04	1.02	1.01	1.00	1.04	1.15
35	1.6	150	8	1068	21000	9.65	9.56	9.29	8.87	8.40	8.04	7.75
36	1.6	150	8	1068	28000	17.40	17.28	16.92	16.36	15.70	15.10	14.10

37	1.6	150	12	532	14000	4.50	4.46	4.34	4.15	3.94	3.78	3.68
38	1.6	150	12	532	21000	15.39	15.31	15.08	14.73	14.31	13.91	13.23
39	1.6	150	12	532	28000	24.69	24.62	24.43	24.13	23.77	23.38	22.37
40	1.6	150	12	800	14000	1.88	1.86	1.80	1.71	1.62	1.57	1.59
41	1.6	150	12	800	21000	10.04	9.97	9.77	9.46	9.10	8.77	8.26
42	1.6	150	12	800	28000	16.88	16.82	16.63	16.33	15.98	15.62	14.70
43	1.6	150	12	1068	14000	0.21	0.21	0.20	0.18	0.17	0.18	0.22
44	1.6	150	12	1068	21000	6.35	6.30	6.15	5.92	5.65	5.42	5.12
45	1.6	150	12	1068	28000	11.71	11.65	11.49	11.23	10.91	10.60	9.93
46	1.6	150	16	532	14000	3.68	3.65	3.57	3.43	3.28	3.16	3.06
47	1.6	150	16	532	21000	11.92	11.88	11.74	11.54	11.30	11.06	10.67
48	1.6	150	16	532	28000	19.26	19.22	19.12	18.95	18.74	18.51	18.00
49	1.6	150	16	800	14000	1.50	1.48	1.44	1.37	1.30	1.25	1.25
50	1.6	150	16	800	21000	7.76	7.72	7.60	7.42	7.20	6.99	6.61
51	1.6	150	16	800	28000	13.16	13.12	13.01	12.85	12.64	12.43	11.81
52	1.6	150	16	1068	14000	0.11	0.11	0.10	0.10	0.10	0.12	0.16
53	1.6	150	16	1068	21000	4.93	4.90	4.81	4.66	4.49	4.34	4.09
54	1.6	150	16	1068	28000	9.13	9.10	9.00	8.85	8.67	8.48	7.99
55	1.6	200	8	532	14000	9.13	9.10	9.00	8.85	8.67	8.48	7.99
56	1.6	200	8	532	21000	9.13	9.10	9.00	8.85	8.67	8.48	7.99
57	1.6	200	8	532	28000	9.13	9.10	9.00	8.85	8.67	8.48	7.99
58	1.6	200	8	800	14000	1.80	1.78	1.75	1.70	1.66	1.67	1.79
59	1.6	200	8	800	21000	12.77	12.65	12.31	11.79	11.19	10.70	10.16
60	1.6	200	8	800	28000	21.69	21.55	21.16	20.55	19.83	19.15	17.88
61	1.6	200	8	1068	14000	0.51	0.51	0.51	0.50	0.50	0.53	0.59
62	1.6	200	8	1068	21000	8.45	8.37	8.13	7.76	7.35	7.05	6.82
63	1.6	200	8	1068	28000	15.66	15.54	15.20	14.68	14.06	13.50	12.62
64	1.6	200	12	532	14000	2.13	2.11	2.05	1.96	1.86	1.78	1.75
65	1.6	200	12	532	21000	12.04	11.97	11.77	11.46	11.10	10.76	10.25
66	1.6	200	12	532	28000	20.11	20.05	19.87	19.60	19.26	18.91	18.12
67	1.6	200	12	800	14000	0.82	0.81	0.78	0.74	0.70	0.68	0.71
68	1.6	200	12	800	21000	8.37	8.31	8.13	7.86	7.54	7.26	6.84
69	1.6	200	12	800	28000	14.58	14.52	14.34	14.06	13.73	13.40	12.62
70	1.6	200	12	1068	14000	0.26	0.26	0.26	0.25	0.25	0.25	0.24
71	1.6	200	12	1068	21000	5.41	5.37	5.23	5.03	4.80	4.59	4.35
72	1.6	200	12	1068	28000	10.36	10.30	10.14	9.90	9.61	9.32	8.73
73	1.6	200	16	532	14000	1.89	1.88	1.83	1.76	1.68	1.61	1.57
74	1.6	200	16	532	21000	9.32	9.28	9.16	8.98	8.77	8.56	8.29
75	1.6	200	16	532	28000	15.65	15.62	15.52	15.37	15.18	14.97	14.59
76	1.6	200	16	800	14000	0.61	0.61	0.59	0.56	0.53	0.51	0.52
77	1.6	200	16	800	21000	6.41	6.37	6.26	6.10	5.91	5.73	5.42
78	1.6	200	16	800	28000	11.28	11.25	11.15	10.99	10.80	10.61	10.08
79	1.6	200	16	1068	14000	0.37	0.36	0.36	0.35	0.34	0.33	0.30
80	1.6	200	16	1068	21000	4.12	4.10	4.01	3.89	3.74	3.60	3.40
81	1.6	200	16	1068	28000	7.99	7.96	7.87	7.73	7.56	7.38	6.96

82	1.8	100	8	532	14000	7.99	7.96	7.87	7.73	7.56	7.38	6.96
83	1.8	100	8	532	21000	7.99	7.96	7.87	7.73	7.56	7.38	6.96
84	1.8	100	8	532	28000	7.99	7.96	7.87	7.73	7.56	7.38	6.96
85	1.8	100	8	800	14000	8.47	8.43	8.33	8.19	8.09	8.30	8.94
86	1.8	100	8	800	21000	23.48	23.26	22.62	21.64	20.51	19.61	18.71
87	1.8	100	8	800	28000	34.86	34.62	33.93	32.88	31.62	30.45	28.44
88	1.8	100	8	1068	14000	4.17	4.19	4.22	4.29	4.42	4.73	5.31
89	1.8	100	8	1068	21000	15.61	15.46	15.02	14.36	13.61	13.12	12.82
90	1.8	100	8	1068	28000	25.02	24.82	24.23	23.32	22.25	21.30	19.95
91	1.8	100	12	532	14000	10.74	10.64	10.33	9.87	9.35	8.98	8.84
92	1.8	100	12	532	21000	23.42	23.28	22.87	22.26	21.53	20.84	19.87
93	1.8	100	12	532	28000	34.38	34.27	33.96	33.47	32.87	32.24	30.91
94	1.8	100	12	800	14000	5.89	5.84	5.68	5.44	5.18	5.06	5.18
95	1.8	100	12	800	21000	15.67	15.55	15.19	14.65	14.01	13.45	12.70
96	1.8	100	12	800	28000	23.58	23.47	23.15	22.66	22.07	21.48	20.23
97	1.8	100	12	1068	14000	2.94	2.91	2.85	2.75	2.65	2.67	2.87
98	1.8	100	12	1068	21000	10.60	10.51	10.23	9.80	9.31	8.91	8.48
99	1.8	100	12	1068	28000	16.87	16.77	16.48	16.03	15.49	14.98	14.03
100	1.8	100	16	532	14000	8.37	8.29	8.08	7.75	7.37	7.07	6.92
101	1.8	100	16	532	21000	17.93	17.85	17.61	17.26	16.82	16.41	15.90
102	1.8	100	16	532	28000	26.65	26.59	26.41	26.14	25.80	25.43	24.81
103	1.8	100	16	800	14000	4.67	4.62	4.49	4.28	4.05	3.90	3.90
104	1.8	100	16	800	21000	12.01	11.93	11.71	11.38	10.98	10.62	10.07
105	1.8	100	16	800	28000	18.26	18.20	18.02	17.74	17.39	17.04	16.21
106	1.8	100	16	1068	14000	2.37	2.34	2.27	2.16	2.04	2.00	2.10
107	1.8	100	16	1068	21000	8.20	8.13	7.95	7.67	7.35	7.06	6.68
108	1.8	100	16	1068	28000	13.07	13.01	12.84	12.57	12.25	11.94	11.25
109	1.8	150	8	532	14000	13.07	13.01	12.84	12.57	12.25	11.94	11.25
110	1.8	150	8	532	21000	13.07	13.01	12.84	12.57	12.25	11.94	11.25
111	1.8	150	8	532	28000	13.07	13.01	12.84	12.57	12.25	11.94	11.25
112	1.8	150	8	800	14000	6.10	6.09	6.06	6.01	6.02	6.26	6.80
113	1.8	150	8	800	21000	19.66	19.47	18.93	18.10	17.14	16.42	15.74
114	1.8	150	8	800	28000	29.96	29.74	29.11	28.15	27.00	25.95	24.26
115	1.8	150	8	1068	14000	3.04	3.06	3.11	3.19	3.34	3.61	4.07
116	1.8	150	8	1068	21000	13.27	13.14	12.78	12.23	11.61	11.23	11.04
117	1.8	150	8	1068	28000	21.89	21.70	21.17	20.34	19.38	18.53	17.39
118	1.8	150	12	532	14000	7.04	6.97	6.77	6.47	6.13	5.91	5.87
119	1.8	150	12	532	21000	18.40	18.28	17.93	17.39	16.75	16.16	15.47
120	1.8	150	12	532	28000	27.72	27.62	27.33	26.88	26.33	25.77	24.77
121	1.8	150	12	800	14000	3.99	3.96	3.86	3.70	3.55	3.49	3.60
122	1.8	150	12	800	21000	12.88	12.77	12.46	11.99	11.44	10.96	10.38
123	1.8	150	12	800	28000	19.94	19.84	19.55	19.10	18.55	18.02	16.98
124	1.8	150	12	1068	14000	1.85	1.83	1.80	1.75	1.70	1.72	1.85
125	1.8	150	12	1068	21000	8.76	8.67	8.44	8.08	7.67	7.34	7.00
126	1.8	150	12	1068	28000	14.46	14.37	14.10	13.70	13.21	12.76	11.96

127	1.8	150	16	532	14000	5.53	5.48	5.33	5.10	4.84	4.64	4.58
128	1.8	150	16	532	21000	14.00	13.93	13.72	13.40	13.02	12.66	12.33
129	1.8	150	16	532	28000	21.37	21.31	21.15	20.89	20.58	20.25	19.84
130	1.8	150	16	800	14000	3.08	3.04	2.96	2.82	2.67	2.58	2.59
131	1.8	150	16	800	21000	9.77	9.70	9.51	9.22	8.87	8.56	8.13
132	1.8	150	16	800	28000	15.33	15.27	15.10	14.85	14.53	14.21	13.54
133	1.8	150	16	1068	14000	1.35	1.34	1.30	1.24	1.18	1.15	1.21
134	1.8	150	16	1068	21000	6.67	6.62	6.46	6.23	5.95	5.71	5.41
135	1.8	150	16	1068	28000	11.10	11.04	10.89	10.65	10.36	10.08	9.50
136	1.8	200	8	532	14000	11.10	11.04	10.89	10.65	10.36	10.08	5.10
137	1.8	200	8	532	21000	11.10	11.04	10.89	10.65	10.36	10.08	14.45
138	1.8	200	8	532	28000	11.10	11.04	10.89	10.65	10.36	10.08	22.53
139	1.8	200	8	800	14000	4.32	4.32	4.32	4.34	4.40	4.64	5.08
140	1.8	200	8	800	21000	16.79	16.63	16.16	15.45	14.64	14.05	13.55
141	1.8	200	8	800	28000	26.27	26.07	25.48	24.58	23.52	22.56	21.13
142	1.8	200	8	1068	14000	2.31	2.33	2.39	2.49	2.64	2.88	3.27
143	1.8	200	8	1068	21000	11.77	11.66	11.35	10.87	10.35	10.04	9.93
144	1.8	200	8	1068	28000	19.83	19.65	19.15	18.38	17.48	16.71	15.70
145	1.8	200	12	532	14000	19.83	19.65	19.15	18.38	17.48	16.71	15.70
146	1.8	200	12	532	21000	19.83	19.65	19.15	18.38	17.48	16.71	15.70
147	1.8	200	12	532	28000	19.83	19.65	19.15	18.38	17.48	16.71	15.70
148	1.8	200	12	800	14000	2.71	2.69	2.63	2.54	2.44	2.42	2.52
149	1.8	200	12	800	21000	10.93	10.83	10.56	10.14	9.65	9.24	8.78
150	1.8	200	12	800	28000	17.33	17.23	16.95	16.53	16.02	15.53	14.65
151	1.8	200	12	1068	14000	1.25	1.25	1.23	1.20	1.18	1.20	1.30
152	1.8	200	12	1068	21000	7.64	7.57	7.36	7.04	6.67	6.38	6.11
153	1.8	200	12	1068	28000	12.91	12.82	12.57	12.19	11.73	11.31	10.61
154	1.8	200	16	532	14000	3.42	3.39	3.29	3.14	2.97	2.85	2.84
155	1.8	200	16	532	21000	11.02	10.96	10.77	10.49	10.15	9.84	9.65
156	1.8	200	16	532	28000	17.28	17.23	17.08	16.84	16.55	16.25	16.02
157	1.8	200	16	800	14000	2.03	2.01	1.95	1.86	1.77	1.71	1.73
158	1.8	200	16	800	21000	8.22	8.16	7.99	7.72	7.41	7.14	6.80
159	1.8	200	16	800	28000	13.22	13.17	13.01	12.77	12.47	12.18	11.61
160	1.8	200	16	1068	14000	0.80	0.79	0.77	0.73	0.70	0.69	0.73
161	1.8	200	16	1068	21000	5.73	5.68	5.55	5.34	5.09	4.88	4.64
162	1.8	200	16	1068	28000	9.80	9.75	9.61	9.38	9.11	8.85	8.35
163	2.2	100	8	532	14000	9.80	9.75	9.61	9.38	9.11	8.85	21.75
164	2.2	100	8	532	21000	9.80	9.75	9.61	9.38	9.11	8.85	30.71
165	2.2	100	8	532	28000	9.80	9.75	9.61	9.38	9.11	8.85	41.22
166	2.2	100	8	800	14000	13.39	13.47	13.73	14.18	14.87	16.11	17.94
167	2.2	100	8	800	21000	32.63	32.33	31.46	30.12	28.63	27.66	27.08
168	2.2	100	8	800	28000	45.40	45.01	43.89	42.18	40.16	38.41	36.13
169	2.2	100	8	1068	14000	7.23	7.36	7.80	8.52	9.48	10.74	12.36
170	2.2	100	8	1068	21000	22.59	22.42	21.93	21.19	20.41	20.14	20.33
171	2.2	100	8	1068	28000	34.17	33.85	32.92	31.50	29.85	28.52	27.03

172	2.2	100	12	532	14000	34.17	33.85	32.92	31.50	29.85	28.52	12.73
173	2.2	100	12	532	21000	34.17	33.85	32.92	31.50	29.85	28.52	20.76
174	2.2	100	12	532	28000	34.17	33.85	32.92	31.50	29.85	28.52	29.71
175	2.2	100	12	800	14000	10.16	10.10	9.94	9.70	9.50	9.61	10.19
176	2.2	100	12	800	21000	21.65	21.45	20.87	19.98	18.94	18.11	17.37
177	2.2	100	12	800	28000	29.90	29.71	29.15	28.30	27.28	26.34	24.92
178	2.2	100	12	1068	14000	5.99	5.98	5.98	5.99	6.07	6.39	7.04
179	2.2	100	12	1068	21000	15.62	15.47	15.04	14.37	13.62	13.08	12.69
180	2.2	100	12	1068	28000	22.59	22.42	21.91	21.13	20.21	19.39	18.26
181	2.2	100	16	532	14000	22.59	22.42	21.91	21.13	20.21	19.39	9.36
182	2.2	100	16	532	21000	22.59	22.42	21.91	21.13	20.21	19.39	16.53
183	2.2	100	16	532	28000	22.59	22.42	21.91	21.13	20.21	19.39	24.20
184	2.2	100	16	800	14000	8.10	8.02	7.81	7.49	7.15	7.01	7.22
185	2.2	100	16	800	21000	16.24	16.11	15.73	15.14	14.45	13.86	13.31
186	2.2	100	16	800	28000	22.67	22.56	22.23	21.73	21.13	20.56	19.68
187	2.2	100	16	1068	14000	5.00	4.96	4.87	4.72	4.59	4.62	4.92
188	2.2	100	16	1068	21000	11.91	11.80	11.48	11.00	10.44	9.99	9.58
189	2.2	100	16	1068	28000	17.11	17.01	16.70	16.23	15.66	15.14	14.32
190	2.2	150	8	532	14000	17.11	17.01	16.70	16.23	15.66	15.14	16.59
191	2.2	150	8	532	21000	17.11	17.01	16.70	16.23	15.66	15.14	24.84
192	2.2	150	8	532	28000	17.11	17.01	16.70	16.23	15.66	15.14	33.20
193	2.2	150	8	800	14000	10.38	10.48	10.80	11.36	12.15	13.38	15.03
194	2.2	150	8	800	21000	27.65	27.41	26.70	25.62	24.43	23.74	23.47
195	2.2	150	8	800	28000	39.30	38.95	37.94	36.38	34.56	33.01	31.19
196	2.2	150	8	1068	14000	5.81	5.94	6.37	7.11	8.05	9.23	10.67
197	2.2	150	8	1068	21000	19.58	19.45	19.08	18.51	17.92	17.83	18.14
198	2.2	150	8	1068	28000	30.25	29.96	29.13	27.86	26.38	25.22	24.01
199	2.2	150	12	532	14000	30.25	29.96	29.13	27.86	26.38	25.22	9.57
200	2.2	150	12	532	21000	30.25	29.96	29.13	27.86	26.38	25.22	16.52
201	2.2	150	12	532	28000	30.25	29.96	29.13	27.86	26.38	25.22	23.79
202	2.2	150	12	800	14000	7.79	7.76	7.67	7.55	7.47	7.66	8.22
203	2.2	150	12	800	21000	18.19	18.01	17.51	16.74	15.85	15.16	14.64
204	2.2	150	12	800	28000	25.54	25.36	24.84	24.05	23.12	22.27	21.13
205	2.2	150	12	1068	14000	4.66	4.67	4.70	4.76	4.88	5.20	5.76
206	2.2	150	12	1068	21000	13.33	13.20	12.84	12.27	11.63	11.20	10.94
207	2.2	150	12	1068	28000	19.69	19.53	19.07	18.36	17.52	16.79	15.85
208	2.2	150	16	532	14000	19.69	19.53	19.07	18.36	17.52	16.79	6.96
209	2.2	150	16	532	21000	19.69	19.53	19.07	18.36	17.52	16.79	13.08
210	2.2	150	16	532	28000	19.69	19.53	19.07	18.36	17.52	16.79	19.38
211	2.2	150	16	800	14000	6.13	6.08	5.93	5.70	5.47	5.41	5.63
212	2.2	150	16	800	21000	13.54	13.42	13.08	12.56	11.95	11.45	11.06
213	2.2	150	16	800	28000	19.20	19.09	18.79	18.33	17.77	17.25	16.57
214	2.2	150	16	1068	14000	3.77	3.75	3.69	3.60	3.53	3.58	3.84
215	2.2	150	16	1068	21000	10.06	9.96	9.69	9.27	8.79	8.41	8.10
216	2.2	150	16	1068	28000	14.79	14.69	14.41	13.97	13.46	12.99	12.31

217	2.2	200	8	532	14000	14.79	14.69	14.41	13.97	13.46	12.99	11.44
218	2.2	200	8	532	21000	14.79	14.69	14.41	13.97	13.46	12.99	19.59
219	2.2	200	8	532	28000	14.79	14.69	14.41	13.97	13.46	12.99	26.26
220	2.2	200	8	800	14000	7.83	7.94	8.28	8.88	9.70	10.84	12.28
221	2.2	200	8	800	21000	23.49	23.30	22.74	21.88	20.95	20.49	20.48
222	2.2	200	8	800	28000	34.25	33.94	33.02	31.61	29.97	28.61	27.17
223	2.2	200	8	1068	14000	4.72	4.85	5.27	6.00	6.92	8.01	9.31
224	2.2	200	8	1068	21000	17.38	17.28	16.99	16.56	16.15	16.19	16.62
225	2.2	200	8	1068	28000	27.40	27.14	26.38	25.22	23.88	22.86	21.87
226	2.2	200	12	532	14000	27.40	27.14	26.38	25.22	23.88	22.86	6.82
227	2.2	200	12	532	21000	27.40	27.14	26.38	25.22	23.88	22.86	13.03
228	2.2	200	12	532	28000	27.40	27.14	26.38	25.22	23.88	22.86	18.90
229	2.2	200	12	800	14000	6.01	6.00	5.96	5.92	5.93	6.16	6.69
230	2.2	200	12	800	21000	15.54	15.39	14.95	14.28	13.50	12.93	12.59
231	2.2	200	12	800	28000	22.15	21.98	21.50	20.77	19.90	19.12	18.22
232	2.2	200	12	1068	14000	3.80	3.82	3.87	3.96	4.12	4.44	4.95
233	2.2	200	12	1068	21000	11.81	11.70	11.38	10.88	10.33	9.97	9.81
234	2.2	200	12	1068	28000	17.70	17.55	17.11	16.45	15.67	14.99	14.19
235	2.2	200	16	532	14000	17.70	17.55	17.11	16.45	15.67	14.99	5.00
236	2.2	200	16	532	21000	17.70	17.55	17.11	16.45	15.67	14.99	10.32
237	2.2	200	16	532	28000	17.70	17.55	17.11	16.45	15.67	14.99	15.46
238	2.2	200	16	800	14000	4.72	4.69	4.58	4.43	4.27	4.25	4.50
239	2.2	200	16	800	21000	11.51	11.41	11.10	10.64	10.10	9.65	9.40
240	2.2	200	16	800	28000	16.53	16.43	16.14	15.71	15.19	14.70	14.20
241	2.2	200	16	1068	14000	3.02	3.00	2.97	2.91	2.88	2.95	3.19
242	2.2	200	16	1068	21000	8.84	8.75	8.51	8.13	7.70	7.37	7.14
243	2.2	200	16	1068	28000	13.18	13.08	12.82	12.41	11.92	11.48	10.92
244	2.5	100	8	532	14000	13.18	13.08	12.82	12.41	11.92	11.48	29.04
245	2.5	100	8	532	21000	13.18	13.08	12.82	12.41	11.92	11.48	36.21
246	2.5	100	8	532	28000	13.18	13.08	12.82	12.41	11.92	11.48	45.66
247	2.5	100	8	800	14000	16.06	16.27	16.93	18.09	19.68	21.93	24.83
248	2.5	100	8	800	21000	38.40	38.08	37.15	35.73	34.18	33.39	33.30
249	2.5	100	8	800	28000	52.40	51.92	50.52	48.38	45.89	43.81	41.55
250	2.5	100	8	1068	14000	8.82	9.08	9.92	11.37	13.21	15.35	17.86
251	2.5	100	8	1068	21000	26.94	26.80	26.38	25.76	25.18	25.32	26.05
252	2.5	100	8	1068	28000	40.27	39.89	38.77	37.07	35.10	33.61	32.21
253	2.5	100	12	532	14000	40.27	39.89	38.77	37.07	35.10	33.61	16.70
254	2.5	100	12	532	21000	40.27	39.89	38.77	37.07	35.10	33.61	23.86
255	2.5	100	12	532	28000	40.27	39.89	38.77	37.07	35.10	33.61	32.58
256	2.5	100	12	800	14000	12.80	12.76	12.67	12.56	12.55	13.01	14.10
257	2.5	100	12	800	21000	25.64	25.39	24.67	23.56	22.29	21.33	20.75
258	2.5	100	12	800	28000	34.12	33.87	33.13	32.02	30.70	29.51	28.09
259	2.5	100	12	1068	14000	7.82	7.86	7.98	8.20	8.56	9.26	10.36
260	2.5	100	12	1068	21000	18.99	18.81	18.30	17.51	16.63	16.08	15.86
261	2.5	100	12	1068	28000	26.51	26.28	25.62	24.61	23.43	22.41	21.24

262	2.5	100	16	532	14000	26.51	26.28	25.62	24.61	23.43	22.41	12.00
263	2.5	100	16	532	21000	26.51	26.28	25.62	24.61	23.43	22.41	18.79
264	2.5	100	16	532	28000	26.51	26.28	25.62	24.61	23.43	22.41	26.50
265	2.5	100	16	800	14000	10.35	10.27	10.03	9.68	9.34	9.29	9.79
266	2.5	100	16	800	21000	19.10	18.92	18.42	17.65	16.77	16.03	15.58
267	2.5	100	16	800	28000	25.55	25.40	24.96	24.30	23.51	22.77	21.96
268	2.5	100	16	1068	14000	6.70	6.68	6.60	6.50	6.43	6.62	7.18
269	2.5	100	16	1068	21000	14.46	14.32	13.92	13.30	12.59	12.05	11.70
270	2.5	100	16	1068	28000	19.87	19.73	19.32	18.69	17.95	17.27	16.43
271	2.5	150	8	532	14000	19.87	19.73	19.32	18.69	17.95	17.27	22.48
272	2.5	150	8	532	21000	19.87	19.73	19.32	18.69	17.95	17.27	29.30
273	2.5	150	8	532	28000	19.87	19.73	19.32	18.69	17.95	17.27	36.47
274	2.5	150	8	800	14000	12.56	12.77	13.48	14.72	16.38	18.55	21.20
275	2.5	150	8	800	21000	32.42	32.17	31.45	30.36	29.20	28.77	29.07
276	2.5	150	8	800	28000	45.19	44.76	43.52	41.61	39.39	37.60	35.91
277	2.5	150	8	1068	14000	7.21	7.46	8.28	9.71	11.51	13.52	15.81
278	2.5	150	8	1068	21000	23.41	23.31	23.03	22.63	22.29	22.64	23.52
279	2.5	150	8	1068	28000	35.69	35.35	34.36	32.85	31.13	29.87	28.80
280	2.5	150	12	532	14000	35.69	35.35	34.36	32.85	31.13	29.87	12.92
281	2.5	150	12	532	21000	35.69	35.35	34.36	32.85	31.13	29.87	19.02
282	2.5	150	12	532	28000	35.69	35.35	34.36	32.85	31.13	29.87	25.87
283	2.5	150	12	800	14000	10.05	10.05	10.04	10.06	10.19	10.71	11.78
284	2.5	150	12	800	21000	21.59	21.37	20.75	19.81	18.73	17.95	17.65
285	2.5	150	12	800	28000	29.09	28.86	28.19	27.17	25.96	24.89	23.84
286	2.5	150	12	1068	14000	6.33	6.37	6.52	6.79	7.20	7.88	8.89
287	2.5	150	12	1068	21000	16.35	16.20	15.77	15.11	14.38	13.96	13.89
288	2.5	150	12	1068	28000	23.21	23.00	22.40	21.48	20.41	19.51	18.56
289	2.5	150	16	532	14000	23.21	23.00	22.40	21.48	20.41	19.51	9.22
290	2.5	150	16	532	21000	23.21	23.00	22.40	21.48	20.41	19.51	14.90
291	2.5	150	16	532	28000	23.21	23.00	22.40	21.48	20.41	19.51	21.08
292	2.5	150	16	800	14000	8.08	8.03	7.87	7.63	7.41	7.44	7.98
293	2.5	150	16	800	21000	15.98	15.82	15.38	14.70	13.92	13.30	13.06
294	2.5	150	16	800	28000	21.59	21.45	21.05	20.43	19.70	19.03	18.48
295	2.5	150	16	1068	14000	5.33	5.32	5.28	5.23	5.24	5.44	5.96
296	2.5	150	16	1068	21000	12.36	12.23	11.88	11.35	10.73	10.28	10.07
297	2.5	150	16	1068	28000	17.26	17.13	16.75	16.17	15.49	14.89	14.21
298	2.5	200	8	532	14000	17.26	17.13	16.75	16.17	15.49	14.89	11.87
299	2.5	200	8	532	21000	17.26	17.13	16.75	16.17	15.49	14.89	15.35
300	2.5	200	8	532	28000	17.26	17.13	16.75	16.17	15.49	14.89	17.16
301	2.5	200	8	800	14000	17.26	17.13	16.75	16.17	15.49	14.89	17.16
302	2.5	200	8	800	21000	17.26	17.13	16.75	16.17	15.49	14.89	17.16
303	2.5	200	8	800	28000	17.26	17.13	16.75	16.17	15.49	14.89	17.16
304	2.5	200	8	1068	14000	5.88	6.10	6.88	8.26	9.98	11.84	13.91
305	2.5	200	8	1068	21000	20.59	20.53	20.36	20.14	20.02	20.53	21.54
306	2.5	200	8	1068	28000	32.09	31.79	30.91	29.57	28.04	26.98	26.20

307	2.5	200	12	532	14000	32.09	31.79	30.91	29.57	28.04	26.98	6.87
308	2.5	200	12	532	21000	32.09	31.79	30.91	29.57	28.04	26.98	9.45
309	2.5	200	12	532	28000	32.09	31.79	30.91	29.57	28.04	26.98	11.92
310	2.5	200	12	800	14000	7.84	7.85	7.89	7.99	8.21	8.76	9.79
311	2.5	200	12	800	21000	18.25	18.07	17.54	16.73	15.82	15.20	15.15
312	2.5	200	12	800	28000	24.92	24.71	24.09	23.15	22.05	21.10	20.36
313	2.5	200	12	1068	14000	5.26	5.31	5.48	5.78	6.22	6.88	7.83
314	2.5	200	12	1068	21000	14.45	14.33	13.96	13.40	12.79	12.47	12.53
315	2.5	200	12	1068	28000	20.79	20.60	20.05	19.19	18.20	17.38	16.62
316	2.5	200	16	532	14000	20.79	20.60	20.05	19.19	18.20	17.38	4.80
317	2.5	200	16	532	21000	20.79	20.60	20.05	19.19	18.20	17.38	7.25
318	2.5	200	16	532	28000	20.79	20.60	20.05	19.19	18.20	17.38	9.77
319	2.5	200	16	800	14000	6.35	6.31	6.20	6.04	5.91	6.00	6.56
320	2.5	200	16	800	21000	13.48	13.34	12.95	12.35	11.66	11.13	11.08
321	2.5	200	16	800	28000	18.35	18.22	17.84	17.27	16.59	15.98	15.67
322	2.5	200	16	1068	14000	4.41	4.41	4.39	4.39	4.44	4.66	5.16
323	2.5	200	16	1068	21000	10.88	10.77	10.46	9.98	9.44	9.05	8.94
324	2.5	200	16	1068	28000	15.35	15.23	14.87	14.33	13.69	13.13	12.60
325	3	100	8	532	14000	15.35	15.23	14.87	14.33	13.69	13.13	30.71
326	3	100	8	532	21000	15.35	15.23	14.87	14.33	13.69	13.13	30.14
327	3	100	8	532	28000	15.35	15.23	14.87	14.33	13.69	13.13	32.00
328	3	100	8	800	14000	15.35	15.23	14.87	14.33	13.69	13.13	32.00
329	3	100	8	800	21000	15.35	15.23	14.87	14.33	13.69	13.13	32.00
330	3	100	8	800	28000	15.35	15.23	14.87	14.33	13.69	13.13	32.00
331	3	100	8	1068	14000	10.85	11.29	12.86	15.67	19.15	22.85	26.92
332	3	100	8	1068	21000	32.84	32.77	32.59	32.38	32.37	33.41	35.26
333	3	100	8	1068	28000	48.98	48.52	47.20	45.17	42.87	41.34	40.32
334	3	100	12	532	14000	48.98	48.52	47.20	45.17	42.87	41.34	16.83
335	3	100	12	532	21000	48.98	48.52	47.20	45.17	42.87	41.34	18.29
336	3	100	12	532	28000	48.98	48.52	47.20	45.17	42.87	41.34	22.00
337	3	100	12	800	14000	16.30	16.32	16.41	16.62	17.08	18.23	20.38
338	3	100	12	800	21000	31.24	30.93	30.02	28.64	27.08	26.03	25.94
339	3	100	12	800	28000	40.07	39.72	38.73	37.22	35.44	33.90	32.72
340	3	100	12	1068	14000	10.28	10.39	10.78	11.46	12.44	13.87	15.87
341	3	100	12	1068	21000	23.78	23.58	22.99	22.10	21.13	20.68	20.90
342	3	100	12	1068	28000	32.24	31.93	31.06	29.71	28.15	26.87	25.78
343	3	100	16	532	14000	32.24	31.93	31.06	29.71	28.15	26.87	16.27
344	3	100	16	532	21000	32.24	31.93	31.06	29.71	28.15	26.87	22.27
345	3	100	16	532	28000	32.24	31.93	31.06	29.71	28.15	26.87	29.94
346	3	100	16	800	14000	13.45	13.37	13.14	12.81	12.53	12.73	13.92
347	3	100	16	800	21000	23.13	22.89	22.22	21.19	20.00	19.09	19.00
348	3	100	16	800	28000	29.52	29.31	28.70	27.77	26.68	25.69	25.20
349	3	100	16	1068	14000	9.08	9.08	9.08	9.12	9.27	9.80	10.93
350	3	100	16	1068	21000	18.18	18.00	17.47	16.67	15.77	15.14	15.04
351	3	100	16	1068	28000	23.90	23.70	23.13	22.26	21.23	20.34	19.57

352	3	150	8	532	14000	23.90	23.70	23.13	22.26	21.23	20.34	16.49
353	3	150	8	532	21000	23.90	23.70	23.13	22.26	21.23	20.34	12.90
354	3	150	8	532	28000	23.90	23.70	23.13	22.26	21.23	20.34	9.11
355	3	150	8	800	14000	23.90	23.70	23.13	22.26	21.23	20.34	29.12
356	3	150	8	800	21000	23.90	23.70	23.13	22.26	21.23	20.34	33.31
357	3	150	8	800	28000	23.90	23.70	23.13	22.26	21.23	20.34	35.76
358	3	150	8	1068	14000	8.95	9.36	10.84	13.54	16.89	20.35	24.11
359	3	150	8	1068	21000	28.34	28.33	28.32	28.37	28.67	29.93	31.95
360	3	150	8	1068	28000	43.09	42.70	41.57	39.83	37.88	36.67	36.11
361	3	150	12	532	14000	43.09	42.70	41.57	39.83	37.88	36.67	13.15
362	3	150	12	532	21000	43.09	42.70	41.57	39.83	37.88	36.67	14.40
363	3	150	12	532	28000	43.09	42.70	41.57	39.83	37.88	36.67	16.83
364	3	150	12	800	14000	12.85	12.89	13.05	13.37	13.96	15.13	16.41
365	3	150	12	800	21000	25.94	25.68	24.92	23.77	22.49	21.69	19.35
366	3	150	12	800	28000	33.62	33.31	32.41	31.05	29.45	28.10	23.00
367	3	150	12	1068	14000	8.49	8.61	9.01	9.73	10.73	12.11	13.99
368	3	150	12	1068	21000	20.49	20.32	19.84	19.12	18.35	18.07	18.50
369	3	150	12	1068	28000	28.15	27.88	27.09	25.88	24.48	23.36	22.58
370	3	150	16	532	14000	28.15	27.88	27.09	25.88	24.48	23.36	9.01
371	3	150	16	532	21000	28.15	27.88	27.09	25.88	24.48	23.36	10.93
372	3	150	16	532	28000	28.15	27.88	27.09	25.88	24.48	23.36	13.80
373	3	150	16	800	14000	10.61	10.56	10.40	10.19	10.05	10.34	11.02
374	3	150	16	800	21000	19.12	18.91	18.32	17.42	16.39	15.63	13.96
375	3	150	16	800	28000	24.49	24.30	23.74	22.88	21.88	20.99	17.78
376	3	150	16	1068	14000	7.45	7.46	7.50	7.59	7.81	8.35	9.44
377	3	150	16	1068	21000	15.59	15.43	14.98	14.29	13.52	13.01	13.08
378	3	150	16	1068	28000	20.73	20.54	20.02	19.22	18.28	17.48	16.95
379	3	200	8	532	14000	20.73	20.54	20.02	19.22	18.28	17.48	6.62
380	3	200	8	532	21000	20.73	20.54	20.02	19.22	18.28	17.48	2.18
381	3	200	8	532	28000	20.73	20.54	20.02	19.22	18.28	17.48	5.19
382	3	200	8	800	14000	20.73	20.54	20.02	19.22	18.28	17.48	23.24
383	3	200	8	800	21000	20.73	20.54	20.02	19.22	18.28	17.48	28.24
384	3	200	8	800	28000	20.73	20.54	20.02	19.22	18.28	17.48	30.15
385	3	200	8	1068	14000	7.22	7.56	8.88	11.37	14.46	17.58	20.97
386	3	200	8	1068	21000	24.28	24.32	24.44	24.69	25.24	26.66	28.80
387	3	200	8	1068	28000	37.86	37.53	36.56	35.08	33.45	32.54	32.38
388	3	200	12	532	14000	37.86	37.53	36.56	35.08	33.45	32.54	3.20
389	3	200	12	532	21000	37.86	37.53	36.56	35.08	33.45	32.54	1.38
390	3	200	12	532	28000	37.86	37.53	36.56	35.08	33.45	32.54	5.10
391	3	200	12	800	14000	37.86	37.53	36.56	35.08	33.45	32.54	13.57
392	3	200	12	800	21000	37.86	37.53	36.56	35.08	33.45	32.54	16.45
393	3	200	12	800	28000	37.86	37.53	36.56	35.08	33.45	32.54	19.26
394	3	200	12	1068	14000	7.04	7.16	7.55	8.26	9.26	10.57	12.35
395	3	200	12	1068	21000	17.81	17.67	17.28	16.69	16.09	15.96	16.56
396	3	200	12	1068	28000	24.79	24.55	23.83	22.73	21.47	20.49	19.99

397	3	200	16	532	14000	24.79	24.55	23.83	22.73	21.47	20.49	5.48
398	3	200	16	532	21000	24.79	24.55	23.83	22.73	21.47	20.49	1.69
399	3	200	16	532	28000	24.79	24.55	23.83	22.73	21.47	20.49	4.06
400	3	200	16	800	14000	8.17	8.14	8.03	7.89	7.84	8.15	9.17
401	3	200	16	800	21000	15.48	15.31	14.80	14.02	13.13	12.50	11.78
402	3	200	16	800	28000	19.85	19.68	19.17	18.39	17.48	16.69	14.82
403	3	200	16	1068	14000	6.21	6.23	6.29	6.42	6.67	7.22	8.28
404	3	200	16	1068	21000	13.55	13.41	13.02	12.41	11.74	11.34	11.56
405	3	200	16	1068	28000	18.14	17.97	17.49	16.75	15.89	15.16	14.84